Transgenic mice as a tool for depression research:

examples from the endocannabinoid and the corticotropin-releasing hormone system

Dissertation
zur Erlangung des Grades

"Doktor der Naturwissenschaften"

im Promotionsfach Biochemie
am Fachbereich Chemie, Pharmazie und Geowissenschaften
der Johannes Gutenberg-Universität
in Mainz

Michel-Alexander Steiner
geboren am 10.11.1976 in Wiesbaden

Mainz, Oktober 2007

(Akakus, Libya, 2006)

„Nur wer den Weg verliert, lernt ihn kennen."
(Afrikanisches Sprichwort)

Table of contents

II

Table of illustrations

Tables   **Page**

SUMMARY

Major depression belongs to the most serious and widespread psychiatric disorders in today's society. There is a great need for the delineation of the underlying molecular mechanisms as well as for the identification of novel targets for its treatment. In this thesis, transgenic mice of the endocannabinoid and the corticotropin-releasing hormone (CRH) system were investigated to determine the putative role of these systems for depression-like phenotypes in mice.

In the first part of the thesis, we found that the endocannabinoid system was prominently involved in a brain region-specific and temporally controlled manner in acute as well as in chronic stress processing. Genetic deletion in combination with pharmacological intervention revealed the importance of a fully functional endocannabinoid system for efficient neuroendocrine and behavioral stress coping. Accordingly, cannabinoid type 1 (CB1) receptor-deficient mice displayed several depression-like symptoms and molecular alterations, including "behavioral despair", stress hormone hypersecretion and decreased glucocorticoid receptor and brain-derived neurotrophic factor expression in the hippocampus. However, the endocannabinoid system was dispensable for the efficacy of currently used antidepressant drugs. To facilitate future endocannabinoid research, a transgenic mouse was generated, which overexpressed the CB1 receptor protein fused to a fluorescent protein.

In the second part of the thesis, conditional brain region-specific CRH overexpressing mice were evaluated as a model for pathological chronic CRH hyperactivation. Mutant mice showed aberrant neuroendocrine and behavioral stress coping and hyperarousal due to CRH-induced activation of the noradrenergic system in the brain. Mutant mice appeared to share similarities with naturally occurring endogenous CRH activation in wild-type mice and were sensitive to acute pharmacological blockade of CRH receptor type 1 (CRH-R1). Thus, CRH overexpressing mice serve as an ideal *in vivo* tool to evaluate the efficacy of novel CRH-R1 antagonists.

Together, these findings highlight the potential of transgenic mice for the understanding of certain endo-phenotypes (isolated symptoms) of depression and their molecular correlates.

ZUSAMMENFASSUNG

Depressionen gehören zu den schwerwiegendsten und am weitesten verbreiteten psychiatrischen Erkrankungen in unserer heutigen Gesellschaft. Die Erfoschung der zu Grunde liegenden molekularen Mechanismen und die Identifizierung neuer Zielmoleküle für die Behandlung ist unbedingt erforderlich. In dieser Doktorarbeit wurden transgene Mäuse des Endocannabinoid- und des „Corticotropin-releasing hormone" (Corticotropin freisetzendes Hormon) (CRH)-Systems eingehend untersucht, um die Rolle dieser Systeme für die Ausbildung depressionsähnlicher Phänotypen in der Maus zu charakterisieren.

Im ersten Teil der Arbeit konnte gezeigt werden, dass das Endocannabinoid-System in einer hirnregionspezifischen und zeitlich kontrollierten Weise von herausragender Bedeutung für die akute und chronische Stressprozessierung ist. Mit Hilfe von genetischer Deletion in Kombination mit pharmakologischer Intervention wurde die Wichtigkeit eines einwandfrei funktionierenden Endocannabinoid-Systems für die ungestörte neuroendokrine und verhaltensbezogene Stressbewältigung nachgewiesen. Dementsprechend zeigten Cannabinoid-Rezeptor Typ 1 (CB1-Rezeptor)-defiziente Mäuse depressionsähnliche Symptome und molekulare Veränderungen, wie z.B. „behavioral despair" (verhaltenbezogene Hoffnungslosigkeit oder Aufgabe), erhöhte Stresshormonsekretion und reduzierte Glucocorticoid-Rezeptor- und „brain-derived neurotrophic factor" (endogen im Gehirn produzierter neurotropher Faktor)-Expression im Hippocampus. Für die Wirkung klassischer Antidepressiva hingegen war das Endocannabinoid-System ohne Bedeutung. Um die Endocannabinoidforschung in Zukunft zu erleichtern, wurde eine transgene Maus generiert, welche das CB1-Rezeptor-Protein, fusioniert mit einem fluoreszierenden Protein, überexprimiert.

Im zweiten Teil der Arbeit wurden konditionale, hirnregionspezifisch CRH-überexprimierende Mäuse als Modell für eine pathologische, chronische Überaktivierung des CRH Systems untersucht. Mutierte Mäuse wiesen sowohl eine gestörte neuroendokrine und verhaltensbezogene Stressprozessierung, als auch einen erhöhten Erregungszustand auf. Dies war auf eine CRH induzierte Aktivierung des noradrenergen Systems im Gehirn zurückzuführen. Die mutierten Mäuse imitierten die natürlicherweise vorkommende Aktivierung des endogenen

CRH Systems in Wildtyp-Mäusen und waren sensitiv gegenüber akuter pharmakologischer Blockade des CRH-Rezeptors Typ 1. Somit dienen CRH-überexprimierende Mäuse als ein ideales *in vivo* Modell für die Evaluierung der Effektivität neuer CRH-Rezeptor Typ 1 Antagonisten.

Zusammenfassend zeigen diese Ergebnisse das Potential von transgenen Mausmodellen, um spezielle Endophänotypen (einzelne Symptome) von Depression und deren molekulare Korrelate besser verstehen zu können.

List of abbreviations

2-AG	2-arachidonoyl glycerol
5-HIAA	5-hydroxyindoleacetic acid
5-HT	Serotonin
5-HTT	Serotonin transporter
ACh	Acetylcholin
ACTH	Adrenocorticotropic hormone
AEA	Anandamide
AMPT	α-methyl-*para*-tyrosine methyl ester
BAC	Bacterial artificial chromosome
BDNF	Brain-derived neurotrophic factor
BLA	Basolateral nucleus of the amygdala
BMA	Basomedial nucleus of the amygdala
BNST	Bed nucleus of the stria terminalis
cAMP	Cyclic andenosine monophosphate
CB1 receptor	Cannabinoid type 1 receptor
CB1$^{-/-}$	CB1 receptor knockout
CB1$^{+/+}$	CB1 receptor wild-type
CeA	Central nucleus of the amygdala
CNS	Central nervous system
CPU	Caudate putamen
CREB	cAMP response element binding protein
CRH	Corticotropin-releasing hormone
CRH-R1	Corticotropin-releasing hormone receptor type 1
CRH-R2	Corticotropin-releasing hormone receptor type 2
CX	Cortex
DA	Dopamin
Dex	Dexamethasone
DH	Dorsal hippocampus
DOPAC	3,4-dihydroxyphenylacetic acid
DRN	Dorsal raphe nucleus
EGFP	Enhanced green fluorescent protein
EPM	Elevated-Plus-Maze test
FAAH	Fatty acid amide hydrolase
FKBP5	FK506 binding protein 5
FST	Forced swim test
GABA	Gamma-amino butyric acid

GPCR	G-protein-coupled receptor
GR	Glucocorticoid receptor
HIP	Hippocampus
HPA	Hypothalamic-pituitary-adrenocortical
HVA	Homovanillic acid
IEG	Immediate early gene
ISH	*In situ* hybridization
LC	Locus coeruleus
LD	Light-Dark test
MAGL	Monoacyl glycerol lipase
MAO	Monoamine oxidase
MAOI	Monoamine oxidase inhibitor
MHPG	3-methoxy-4-hydroxyphenylglycol
MR	Mineralocorticoid receptor
mRNA	Messenger RNA
NA	Noradrenaline
NAC	Nucleus accumbens
NGF	Nerve growth factor
NST	Nucleus of the solitary tract
NT-3	Neurotrophin-3
OB	Olfactory bulb
OF	Open field test
PCPA	*Para*-chlorophenylalanine methyl ester
pCREB	Phosphorylated CREB
POMC	Proopiomelanocortin
PVN	Paraventricular nucleus of the hypothalamus
RN	Raphe nuclei
SN	Substantia nigra
SNRI	Selective noradrenaline reuptake inhibitor
SSRI	Selective serotonin reuptake inhibitor
TrkB	Tyrosin kinase receptor type 2
TST	Tail suspension test
VEGF	Vascular endothelial growth factor
VGLUT1	Vesicular glutamate transporter type 1
VPC	Ventromedial prefrontal cortex
VTA	Ventral tegmental area

CHAPTER 1

GENERAL INTRODUCTION

THEORIES FOR AND ANIMAL MODELS OF DEPRESSION

1.1 The invention of genetically engineered mice

After groundbreaking work of Jon Gordon, who introduced the method of DNA injections into the pronucleus of one-cell mouse embryos, one of the first transgenic mice, the giant mouse of Richard Palmiter and co-workers, which overexpressed the rat growth hormone, made the cover of *Nature* in 1982 (Brinster et al., 1982). Shortly after the works of Mario Capecchi, Martin Evans and Oliver Smithies, who established the introduction of targeted mutations into the mouse germ line by homologous recombination in embryonic stem cells, for which they were awarded the *Lasker* prize in 2001, laid the foundation for the first generation of knockout mice during the late eighties and early nineties. Ever since the ability to precisely tailor the mouse genome has revolutionized our understanding of gene-phenotype relations and has thereby greatly facilitated biomedical research. Several thousand genetically engineered mice have been created until today, and about 80 different lines have been reported so far to show abnormal behavior interpreted as depression- or anxiety-related (Cryan and Holmes, 2005). This has greatly enhanced our view of the complexity of the gene environment that regulates emotion and has put an early and inevitable end to the naive idea to find "the gene" whose malfunction could be the "one" reason underlying such multi-factorial and diverse psychiatric disorders like depression or anxiety. However, transgenic mouse research has enabled the research community to gain important insights into molecular correlates of certain endo-phenotypes of these diseases and has greatly helped to understand their respective neurochemical basis. In particular, the use of sophisticated molecular tools such as the Cre-loxP or the tetracycline transactivator systems (Gaveriaux-Ruff and Kieffer, 2007; Morozov et

al., 2003; Davey and MacLean, 2006) has rendered the investigation of the specific spatial and temporal function of a certain gene product and its molecular and behavioral effects on the organism possible. Thus, transgenic mice, especially when combined with traditional pharmacology, have a great potential for the search and understanding of molecular correlates of psychiatric disorders. They can help to evaluate the effects of a human candidate gene mutation on an endophenotype of a disease, to identify new candidate genes, to study gene-environment interactions and to understand the interplay of a specific gene in a particular molecular pathway (Seong et al., 2002).

1.2 Pathophysiology of depression

Major depression belongs to one of the most devastating and costly brain diseases of today's society. In the last two main epidemiology studies conducted in the United States, major depression had an overall lifetime prevalence rate of about 17 % with almost double as much women being affected than men (21% vs. 13% respectively) (Kessler et al., 1994; Kessler et al., 2003). Moreover, the prevalence of depression is rapidly increasing (Crown et al., 2002) and the economic burden of depression in lost productive work time is immense (Wang et al., 2003). The mean age of onset of depression has markedly decreased from the 40-50-year-old range noted several decades ago to the 25- to 35-year range (Klerman and Weissman, 1985). In addition, depression is associated with a high risk of suicide accounting for a considerable cause of death worldwide (Wang et al., 2003).

Major depression is very heterogeneous in its manifestation including such diverse symptoms as depressed mood, feelings of guilt, low self-esteem, high anxiety, anhedonia and decreased pleasure. Alterations in memory and concentration, and disturbances in homeostatic systems such as feeding, sleeping and reproductive function as well as vegetative symptoms including increased sweating, heart rate and gastrointestinal disturbances are also frequently encountered. Based on a certain combination of the above mentioned symptoms major depression can be further differentiated in specific subtypes including melancholic and atypical depression (Antonijevic, 2006; Ayuso-Gutierrez, 2005).

Although some patients develop chronic depression [10-15%; (Fagiolini and Kupfer, 2003)], in the majority of patients the disease is of episodic nature, lasting from a few weeks to several months. However, these depressive episodes may reoccur one or several times during the lifetime of the patient.

Major depression is a complex disease with a strong hereditary component (Kessler et al., 2003). Heritability based on twin studies is 40-50% (Levinson, 2006). Nevertheless, the gene variances conferring increased disease susceptibility still remain to be discovered. In addition, the outcome of the disease seems to be strongly dependent on potent environmental risk factors including childhood abuse and neglect, and life stress (Caspi and Moffitt, 2006). People with a functional polymorphism in the promoter region of the serotonin transporter (5-HTT) gene, for instance, bearing one or two copies of the so called "5-HTT short allele" exhibited more depressive symptoms following stressful life events than individuals with two copies of the "long allele" (Caspi et al., 2003). In addition, depression is often associated with comorbid psychiatric disorders, most notably anxiety disorders [panic disorder, social anxiety disorder, post-traumatic stress disorder and others; (Nemeroff and Owens, 2002)], thereby complicating diagnosis and treatment.

Until today three forms of treatment for depression have demonstrated clinical effectiveness: antidepressants, certain forms of psychotherapy and electroconvulsive therapy [ECT; (Nemeroff and Owens, 2002)]. Because of the high prevalence of the disease, antidepressants have been among the best-selling drugs on the market for the past decades. Nevertheless, drugs with a novel mechanism of action for the treatment of depression have not yet been invented basically since their first discovery in the 1950s (compare Chapter 1.4.1, The monamine theory of depression) illustrating the tremendous need for novel, more efficient therapeutics.

1.3 Tests of depression- and anxiety-related behavior in rodents

It goes without saying that rodents are not small human beings and that we can never hope to fully recapitulate human depression or anxiety in an animal model. It is, for instance, impossible to decide whether a mouse can feel

"depressed" at all. Accordingly, the rodent cerebral cortex is much less elaborated than the human and, thus, very likely incapable of processing complex psychological concepts such as, for instance, feelings of guilt or low self esteem. Nevertheless, the cortex is interconnected with a variety of subcortical structures, which are well conserved across mammalian species. Therefore, a number of fundamental physiological and behavioral responses appear to be evolutionary conserved. This can allow us, by deduction, to study these responses and to investigate behaviors and their underlying genetic factors and neural circuits. By this means, lower species such as mice can serve to better understand the neurochemical basis of human behaviors and diseases.

Researchers have proposed certain criteria for animal models in order to have validity for modeling psychiatric diseases in humans: the model should have "face validity", which means being reasonably analogous to the human disorder in its manifestation or symptomatology; it should have "predictive validity", in the sense that only specific treatments, which ameliorate the human disease, are also effective in the animal model; it should further have "construct validity", which means the involvement of similar neurochemical processes in the animal model and the human disorder; and it should have "etiological validity" in the meaning that behaviors can be provoked by events thought to be important in eliciting the human disorder (Cryan and Mombereau, 2004; McArthur and Borsini, 2006; Anisman and Matheson, 2005). Certainly, construct validity and etiological validity are most difficult to proof for an animal model. Thus, most models aim at providing at least face and predictive validity and aim at involving a behavioral change that can be objectively measured and that is reproducible between different investigators and laboratories (Cryan and Holmes, 2005).

During the past century a high number of different animal models for depression and anxiety have been developed, which tried to model one or more of the different endo-phenotypes [defined as isolated symptoms of behavioral or biochemical nature, which are associated with the disease, and part of a complex disease phenotype; for a detailed definition see (Gottesman and Gould, 2003)] of these diseases. For brevity reasons, a short introduction is provided below only to the most widely employed models, most of which have been used in the present study.

1.3.1 Animal tests and models of depression

Stress is regarded as one of the major risk factors to develop major depression and the disease is often viewed as a manifestation of an inability to cope with stress (De Kloet et al., 2005; Holsboer, 2000). Therefore, most common behavioral models of depression-like behavior in rodents are based on the exposure of the animal to different kinds and episodes of stress and assessing the differential active or passive coping strategies of the animal. These models have been validated primarily because the effects of stress are reversed by different classes of antidepressants.

Whereas stressful events undoubtedly precipitate or exacerbate depressive illness, remarkable individual variability exists with regard to behavioral and physiological responses to stressors. For instance, the intensity of a stressor might be differentially perceived by different individuals and the coping strategies as well as the neurochemical processes elicited by the stressor may vary extensively between individuals. Accordingly, although genetic factors determine a high proportion of the variability associated with depression disorders, they interact with experimental and environmental factors to determine the manifestation of the disease (Anisman and Matheson, 2005).

Thus, similar difficulties are experienced with animal models, where the genetic background strain, the type and duration of the stressor and the experimental conditions all impact on the behavioral and neurochemical response of an animal to the stressor, resulting in considerable variability.

1.3.1.1 The Forced Swim Test (FST)

The FST certainly belongs to the most widely applied tests for depression-related behavior in rodents (Cryan and Holmes, 2005). Originally devised for the rat (Porsolt et al., 1977), the test has long been translated to the mouse as well (Porsolt et al., 1978). The mouse FST is based on the exposure of the animal to water forcing it to swim for 6 min, usually within a round glass beaker filled to a height, where the animal is unable to touch the bottom with the feet or tail (Fig. 1.3.1.1). Exposed to such a situation, the mouse first engages in vigorous escape movements, breaking the surface of the water with the front paws, referred to as

Figure 1.3.1.1 The Forced Swim Test (FST)

"struggling". Usually after 1-2 min the mouse switches its behavior over to less vigorous swimming movements and, over the time course of the experiment (6 min in total), towards the end starts to engage more and more in immobile "floating" postures, which don't involve any other movements of the paws than the ones necessary to stay afloat.

The test owes its popularity to the fact that in particular antidepressants cause mice to stay longer engaged in escape oriented behavior, thereby showing a decrease of floating. Therefore, the test has gained much value as a fast and reliable screening test for novel antidepressants (Cryan and Mombereau, 2004; Petit-Demouliere et al., 2005). Furthermore, the test has also widely been employed as a phenotypic screening test for depression-related behavior in mutant mice as the FST has proven sensitive to a number of factors that also influence depression in humans, such as previous chronic stress exposure, genetic pre-disposition, sleep disturbances and changes in food intake (Cryan and Holmes, 2005).

Nevertheless, despite its common application, reasonable concerns about the validity of the test have also been expressed: first: the test is sensitive to the acute application of antidepressants, but treatment in humans usually takes several weeks before clinical improvement is seen. This suggests that forced swim behavior might not be a suitable outcome measure of long term adaptive changes in response to antidepressants which are necessary for their clinical efficacy (Petit-Demouliere et al., 2005); second: floating was originally interpreted as "behavioral despair" as it rather refers to reluctance to maintain effort than to general hypoactivity of the animal (many antidepressants, for example, reduce floating behavior in the FST without inducing general locomotor activation). Thus, the test has certain face validity with regard to psychomotor impairments and an "inability to sustain expenditure of effort", symptoms which are often seen in depressed human patients. Nevertheless, this interpretation has been challenged in view of other reasonable explanations for immobility in the FST such as a reduced arousal state, memory processes or a positive coping strategy in order to conserve energy

(West, 1990; Borsini et al., 1986; Borsini and Meli, 1988); third: as the test is specifically sensitive to antidepressants, which up-regulate the synaptic serotonin and/or noradrenaline content, it might be impossible to find novel antidepressants, which act through non-monoamine-based mechanisms.

It remains to be mentioned that the last point is one current major drawback not only for the FST, but for all current animal models of depression. As there is no "non-monoamine-based" antidepressant on the market, which has been adequately validated in humans, it is currently unknown, whether our animal models of depression would respond to such a drug at all (Berton and Nestler, 2006), thus questioning the current validation of these models, which is purely based on currently available monoaminergic antidepressants.

1.3.1.2 The Tail Suspension Test (TST)

The tail suspension test is based on a similar principle as the FST. The mouse is suspended upside down by the tail above the ground, forcing the animal to actively struggle against this unnatural condition and to engage in escape-oriented movements (Steru et al., 1985). The test duration is usually 6 min and over the time-course of the experiment the mouse ceases to struggle against the situation and exhibits passive immobility postures, according to the behavioral adaptations that are seen in the mouse FST. Although the test circumvents possible confounds of the FST due to body cooling because of cold water exposure (Arai et al., 2000; Taltavull et al., 2003), the TST might be confounded by varying pain sensitivity due to tail suspension. Whereas antidepressant effects of the class of selective serotonin reuptake inhibitors (SSRIs), which are often not detected in the mouse FST (only the rat FST), are frequently detected in the TST, C57BL/6 mice, one of the most frequently used mouse strains, are known to climb their tail during the test rendering behavioral analysis difficult (Mayorga and Lucki, 2001). In addition, it has to be noted that both tests are similar but not synonymous. Whereas many antidepressants exert antidepressant-like effects in both tests, the biological substrates which underlie the observed behaviors may differ significantly (Cryan et al., 2005).

1.3.1.3 Learned Helplessness

Learned helplessness is based on the observation that animals, when exposed to a number of uncontrollable electric footshocks in an inescapable environment, loose their ability to actively escape the threatening stimulus later, even when they are allowed to flee. The effect was originally observed in dogs, but the paradigm was later translated to the rat and mouse, where it was demonstrated that escape deficits can be reversed by antidepressant treatment (Seligman, 1978). One confound of the test is that only a certain percentage of animals, depending on the genetic background, develop learned helplessness at all, and that of those that do, animals loose this phenotype already after 2-3 days (Cryan and Mombereau, 2004).

1.3.1.4 Chronic Mild Stress

During the chronic mild stress paradigm the rodent is daily exposed to a variety of randomly alternating mild stressors over a longer period of time, usually at least four weeks (Katz, 1982; Willner, 1997). As mild stressors serve, for example, forced swimming, cold stress, tilted cage stress, constant lighting, wet bedding or food deprivation. This chronic unpredictable stress procedure induces a number of neuroendocrine, neuroimmune, neurochemical and behavioral alterations, which resemble symptoms of depressed patients, and which are reversible by chronic antidepressant treatment. Two major confound of the paradigm so far are its poor reproducibility between different laboratories and its practical difficulties as it is very labor intensive and requires a lot of time and space (Willner, 1997).

1.3.1.5 Chronic Social Defeat

The social defeat paradigm was originally developed in tree shrews (Fuchs and Flugge, 2002) and has emerged as a powerful model to study social stress in rodents. Rats exposed to chronic social defeat demonstrate marked behavioral alterations, including social aversion, anxiety, hypoactivity, disrupted circadian and sleep rhythms, as well as changes in neurochemical characteristics,

neuroendocrine responses and compromised immune functions (Buwalda et al., 2005). Recently, the social defeat model has also been adopted and validated for mice (Berton et al., 2006). Mice were subjected to daily bouts of social defeat, followed by continuous protected sensory contact with their aggressor. This procedure lasted for 10 days with exposure to a different aggressor each day. Mice defeated in such a manner show severe social aversion to new unfamiliar mice that were physically distinct from the previous aggressors. This acquired deficit in social interaction is long lasting (at least 4 weeks) and reversible by chronic, but not acute, antidepressant treatment (Berton et al., 2006). Importantly, this model has a strong psychological component as it is based on social stress, being also a predominant form of stress encountered by humans (Bjorkqvist, 2001).

1.3.2 Animal tests of anxiety

Anxiety and depression disorders are, from a historical point of view, regarded as different entities, as their treatment can be achieved by different classes of drugs (benzodiazepines vs. tricyclic antidepressants). However, a considerable co-morbidity between both diseases exists, and treatments, which have the potential to ameliorate aspects of both diseases, such as SSRIs, are preferentially used in today's clinical daily routine.

Many animal models of anxiety are based on exploratory based "approach-avoidance conflict" tests. They have primarily been established because of their predictive validity with regards to classical anxiolytics (Cryan and Holmes, 2005). Probably because of their innate fear of predators, mice and rats naturally try to avoid open, exposed or well-lit spaces and try to hide in dark, enclosed areas. However, due to their foraging, exploratory nature, small rodents are also curious and inclined to explore novel spaces. Many anxiety tests make use of this conflicting tendency of an animal to either approach or avoid a potentially dangerous area (Rodgers, 1997). This "dangerous area" has different forms in a number of different anxiety tests: In the "**Light-Dark**" paradigm it consists of a well lit compartment, which can be approached through a tunnel or opening from a dark compartment. In the "**Elevated-Plus-Maze**" paradigm, it consists of open arm areas, which are elevated above the ground and can be reached via leaving

enclosed "safe" arms. In the "**Open Field**" test animals are place in a relatively big, lit, open space, usually a quadrant enclosed by walls, where the animals tend to stay close to the walls as protective compartment.

Nevertheless, due to the approach-avoidance ambiguity of these paradigms one major confound is the impossibility to differentiate between less anxious or more explorative, novelty seeking behavior. Furthermore, the locomotor activity of the animals has to be carefully controlled and possibly an intact sensory function of the tested animals ensured in order to correctly interpret the behavior.

1.4 The three major theories for the development of depression

1.4.1 The monoamine theory of depression

The first drugs to treat major depression were discovered by mere serendipity in the 1950s. Iproniazid belonged to the class of monoamine oxidase inhibitors and was originally introduced as an antitubercular drug. Imipramine, which belongs to the classes of tricyclic antidepressants, was originally developed as an antihistaminic/antipsychotic drug. Both drugs were recorded to have antidepressant actions by empirical discoveries in treated patients and were soon after approved of as antidepressants (Ban, 2001). Shortly after, in the 1960s researchers discovered that both drugs increased levels of noradrenaline (NA) and serotonin (5-HT) in the brain (Nutt, 2006) by blocking their presynaptic re-uptake or by inhibiting their main metabolizing enzyme, monoamine oxidase (MAO), respectively. These discoveries led to the design of second generation drugs such as subtype specific monoamine oxidase inhibitors (pargyline, selegiline) and tricyclics specific for either NA or 5-HT (desipramine, zimelidine), followed by third generation drugs such as selective serotonin reuptake inhibitors (SSRIs; paroxetine, fluoxetine, citalopram), selective noradrenaline reuptake inhibitors (SNRIs; reboxetine) and selective serotonin-noradrenaline reuptake inhibitors (venlaflaxine, duloxine) (Nutt, 2006). However, despite fewer side effects due to enhanced specificity for the molecular target the newer drugs are not more efficient and are based on the same mechanism of action: they increase the

availability of monoamines in the synaptic cleft by either blocking their reuptake or their degradation.

Based on those findings emerged the so called "**monoamine theory of depression**" (Ban, 2001), which has tried to explain depression by an impairment of serotonergic and noradrenergic, more recently also dopaminergic, neurotransmission. Although most research in the field of depression, also with regards to the creation of genetically engineered mice, has so far focused on this theory, it could neither provide an explanation for the number of non-responsive patients to current antidepressants nor for the lag period of several weeks of treatment often needed for the onset of therapeutic effects. Ultimately, it seems that alterations of monoaminergic neurotransmission only represent the initial spark needed for the induction of more slowly developing plasticity changes that may be required for the reversal of depressive episodes. A prominent example to support this hypothesis is the outcome of a recently employed clinical trial, which compared the antidepressant efficacy of paroxetine with that of tianeptine (Nickel et al., 2003). Both drugs were similarly effective in achieving clinical improvement of depression symptoms although they have an exactly opposite mechanism of action. Whereas paroxetine as a classical SSRI enhances serotonin neurotransmission at the synaptic cleft, tianeptine, which increases the presynaptic neuronal reuptake of serotonin, decreases the availability of the transmitter at postsynaptic 5-HT receptors.

1.4.2 The neurotrophin theory of depression

The above mentioned considerations guided the area of depression research to second-messenger pathways that cause long-term changes of gene expression, which can ultimately lead to changes in synaptic circuitry and connectivity. The "**neurotrophin hypothesis of depression**" evolved.

Many antidepressants activate the cyclic adenosine monophosphate (cAMP) pathway and/or raise intracellular calcium levels and thereby induce the phosphorylation of the transcription factor cAMP response element binding protein (CREB). Thus, chronic antidepressant treatment in rodents was found to up-regulate both pCREB as well as total CREB mRNA and protein in hippocampus and frontal cortex (Blendy, 2006). Furthermore, patients that were under

antidepressant treatment at the time of death showed increased levels of CREB (Dowlatshahi et al., 1998) in comparison to non-medicated patients, and a reduction of pCREB and CREB was found in the orbitofrontal cortex of antidepressant-free patients with major depression (Yamada et al., 2003).

CREB binds to a variety of target genes, among them a number of trophic factors that have been implicated in synaptic plasticity. So far, brain-derived neurotrophic factor (BDNF) has emerged as the most promising target gene of antidepressant-induced CREB activation. Accordingly, chronic antidepressant treatment, for instance, was shown to counteract stress and/or depression induced neuronal atrophy and cell loss in key limbic brain regions implicated in depression such as the hippocampus and prefrontal cortex. A considerable part of the underlying mechanism could be the antidepressant-induced upregulation of trophic factors including BDNF, which might influence neuronal connectivity. A high number of preclinical and clinical research studies strengthen this hypothesis. Exposure to various stressors has been repeatedly shown to downregulate BDNF in the rodent brain (Duman and Monteggia, 2006). In addition, also other neurotrophic factors such as nerve growth factor (NGF), neurotrophin-3 (NT-3) and lately also vascular endothelial growth factor (VEGF) are reduced in response to stress (Ueyama et al., 1997; Heine et al., 2005). Antidepressant treatments in rodents, in particular electroconvulsive seizures and administration of monoamine oxidase inhibitors, have been consistently demonstrated to upregulate BDNF in limbic brain regions such as hippocampus (Nibuya et al., 1995; Duman and Monteggia, 2006). Postmortem studies of depressed patients also demonstrated a downregulation of BDNF in the hippocampus, which was not observable in patients receiving antidepressant medication at the time of death (Chen et al., 2001; Karege et al., 2005). In conclusion, clinical and pre-clinical findings strongly suggest that a deficiency of neurotrophic factors, most importantly of BDNF, may contribute to the pathophysiology of depression and that antidepressants mediate their therapeutic effect, at least in part, via the upregulation of such proteins (Duman et al., 1997; Duman and Monteggia, 2006).

1.4.3 The HPA axis theory of depression

The third major theory about the pathophysiology of depression favors dysregulations of the hypothalamic-pituitary-adrenocortical (HPA) axis, the major neuroendocrine stress system in mammals, as a major risk factor for major depression. The HPA axis is activated in response to external and internal stressors in order to meet particular needs of the body (release of glucose, degradation of fat and protein, immune suppression, anti-inflammation) in critical situations. Various stress-related inputs of the brain converge in the paraventricular neurons of the hypothalamus, where they stimulate the release of stress-related neuropeptides such as corticotropin-releasing factor (CRH) and vasopressin. These peptides are released via the median eminence into the portal blood circulation and stimulate the synthesis of adrenocorticotropic hormone (ACTH) in anterior pituitary corticotrophs. ACTH, in turn, is released in the blood stream and induces corticosterone secretion from the zona fasciculata of the adrenal cortex. Corticosterone exerts feedback regulation on HPA axis activity via binding to glucocorticoid receptors (GRs) at the level of the hippocampus, PVN and pituitary.

The HPA axis hypothesis of depression is based on the observation that stressful life events function as important pathogenetic factors for the development of the disease, and it is believed that depressed patients suffer from a disturbed capacity of the central nervous system to appropriately adapt the stress hormone system to external demands. Accordingly, many patients suffering from depression show a dysregulated circadian cortisol secretion with significantly elevated blood levels as compared to healthy controls (Gold et al., 2002; Wong et al., 2000). Furthermore, they show abnormal stress hormone responses to a variety of HPA axis challenge tests (dexamethasone suppression test, CRH challenge test, combined dexamethasone-CRH test) (Ising et al., 2007; Holsboer, 2000; Nemeroff and Evans, 1984). Interestingly, many of these HPA axis abnormalities are reversed by antidepressant treatment and effective treatment has been associated with HPA axis normalization (Holsboer, 2000; Holsboer, 2001). Furthermore, depressed patients had increased CRH concentrations in the cerebrospinal fluid (Nemeroff et al., 1984) and showed increased levels of CRH mRNA and protein levels in the paraventricular nucleus (PVN) (Nemeroff, 1996;Raadsheer et al.,

1994b;Raadsheer et al., 1994a). Recently single-nucleotide polymorphisms in a glucocorticoid receptor regulating co-chaperone of hsp-90, FKBP5, were found to confer faster response to antidepressant treatment because of enhanced glucocorticoid receptor mediated HPA axis feedback regulation (Binder et al., 2004). Finally, the first CRH-R1 antagonist, R121919, has recently proven clinical efficacy in depression treatment (Zobel et al., 2000).

These clinical observations have been supported by a wide variety of preclinical observations in conventional and conditional transgenic animals with various alterations in genes implicated in HPA axis functioning such as CRH, CRH receptor 1 and 2, glucocorticoid and mineralocorticoid receptor (MR) (Muller and Holsboer, 2006; De Kloet et al., 2005). Many clinical findings could be mimicked in these animal models, and they have helped to further understand the exact roles of specific factors in HPA axis modulating pathways.

1.5 Future directions of depression research

Although today's antidepressants are generally safe and effective, four main areas in antidepressant pharmacotherapy need improvement:

(i) Efficacy. After 6-8 weeks of treatment, only 35-45% of patients achieve full remission, meaning the patient fully recovers psychosocial functioning with a minimal burden of residual effects (Entsuah et al., 2001; Thase et al., 2001). The remainder are improved, but not well, or even do not respond at all.

(ii) Relapse and treatment resistance. About one third of the patients is not, or only marginally responding to antidepressants during the first 6 weeks of treatment (Souery et al., 2006) and in a majority of cases a very high proportion of these patients will also be resistant to future treatment. In addition, a high percentage of patients show relapse after treatment of one depression episode and develop treatment resistance to previously effective medications (Muller and Holsboer, 2006).

(iii) Tolerability. Even though novel classes of antidepressants are clearly superior to the tricyclic antidepressants in terms of tolerability, they have their own problematic long-term side effects such as sexual dysfunction, weight gain and drug interactions (Masand and Gupta, 2002).

(iv) Slow response to treatment. As mentioned above, the slow response to treatment poses a considerable risk of suicide to the patient as well as it tremendously increases general costs of patient care taking and costs due to non-productive work time. A more rapid onset of action is clearly a desirable attribute for novel medications in the field.

Until today, despite about 50 years of research, the research community has not yet managed the task of developing antidepressants with novel mechanisms of action to improve the above mentioned drawbacks of today's medications. In addition to current antidepressants, which target the monoaminergic system, the development of drugs that modulate the two other major systems implicated in the pathophysiology of depression have been hampered by pharmacokinetic and hepatotoxicity issues in the case of HPA axis targets and by difficulties to design small molecule agonists that activate the receptor for BDNF, the tyrosine kinase receptor type 2 (TrkB), in the case of the neurotrophin system.

Furthermore, it has to be noted that our knowledge of the exact molecular pathways underlying the pathophysiology of depression is still very limited mainly due to the lack of progress in identifying validated depression vulnerability genes in humans. Furthermore, the particular role of genes and pathways that we know of being potentially involved in depression, seems to vary considerably depending on the specific brain region and neural circuit they are involved in.

Nevertheless, current research does progress and several new interesting fields of depression research have begun to emerge, including, for instance, the neurokinin, opioid and endocannabinoid systems, cytokines, neuopeptide Y, galanin, phosphodiesterases and histone deacetylases (Berton and Nestler, 2006; Slattery et al., 2004).

1.6 Objective

It is the objective of this study to explore the roles of the endocannabinoid and the CRH system in the pathophysiology of depression. Several genetically engineered mouse lines serve as models, displaying certain alterations in both systems, such as ubiquitous and brain region-specific knockout of the CB1

receptor or brain region-specific overexpression of CRH. These genetic models are complemented by pharmacological interventions. The aim of the study is the behavioral, neuroendocrine and neurochemical characterization of these mutant mice in relation to depression-like endo-phenotypes. Furthermore, a novel transgenic mouse shall be generated, expressing the functional CB1 receptor fused to a fluorescent protein in order to facilitate future endocannabinoid research.

CHAPTER 2

THE ENDOCANNABINOID SYSTEM AND DEPRESSION

2.1 Introduction to the role of endocannabinoid signaling in stress processing

For a detailed introduction to the pharmacology of the endocannabinoid system and its general function in the nervous system, the reader is referred to Chapters 1 and 2 of the recently published book "Das Endocannabinoid System – Physiologie und klinische Bedeutung" (UNI-MED Science; Editor Prof. V. Schusdziarra; first edition, 2006), which were written by M.A. Steiner and B. Lutz and can be found with permission of the publisher as a copy in the Appendix, Chapter 6.5.

Endocannabinoids, including anandamide and 2-arachidonoyl glycerol (2-AG), act as retrograde messengers in the brain that are released from the postsynapse, travel backwards over the synaptic cleft and bind to presynaptic cannabinoid type 1 (CB1) receptors (Piomelli, 2003). Here, they activate CB1 receptors and thereby decrease the excitability of the presynapse, which ultimately results in reduced neurotransmitter release. CB1 receptors are present both on glutamatergic and GABAergic neurons (Marsicano and Lutz, 1999) and, hence, its activation is able to constrain either the excitation or the inhibition of neuronal circuits (Marsicano and Lutz, 2006). In addition to glutamate and GABA, CB1 receptor activation is also known to constrain the release of a variety of other neurotransmitters, including acetylcholin (ACh) (Tzavara et al., 2003a), noradrenaline (Tzavara et al., 2001), serotonin and dopamine (Tzavara et al., 2003b; Hungund et al., 2003). However, whether this is ultimately achieved via a direct inhibition of their release at the respective neuronal terminals (for instance via inhibiting ACh release from a cholinergic synapse), or via influencing GABAergic or glutamatergic innervations of the respective neurons (for instance

the innervations of a cholinergic neuron), remains to be investigated. Nevertheless, by the above means the endocannabinoid system of the brain functions as a major neuro-modulatory system, which can, by the selective influence of either gluatamatergic or GABAergic synapses, increase or decrease neuronal activity (Marsicano and Lutz, 2006).

Given the above functions, and knowing that CB1 receptors belong to the most abundant G-protein-coupled receptors (GPCRs) of the brain, which are found in almost all brain regions, including the limbic forebrain (Piomelli, 2003), it is not astonishing that endocannabinoid signaling is able to influence emotional processing both in men and mice. In particular, preclinical research during the last decade has taken the first step forward to unravel the role of CB1 receptor signaling for anxiety and depression-like behavior in rodents. Whereas it has become gradually accepted that increasing endocannabinoid signaling by pharmacological means has anxiolytic and antidepressant-like effects (Viveros et al., 2005; Hill and Gorzalka, 2005a), strangely enough, also decreasing endocannabinoid signaling via the pharmacological blockade of CB1 receptors has sometimes been observed to confer similar effects (Witkin et al., 2005a; Witkin et al., 2005b). Comparably, discrepant findings were reported with CB1 receptor-deficient knockout mice, which had either depression- and anxiety-like symptoms or behaved less "anxious" and less "depressed" than their wild-type littermates (Wotjak, 2005). Therefore, it was the first goal of the following studies to further investigate this apparent bi-directional role of CB1 receptor signaling with regard to emotional stress processing in mice.

As mentioned in the Introduction, animal tests of anxiety and depression invariably deals with the exposure of the test animal to acute or chronic stress. Therefore, different behavioral performances in those tests can ultimately be seen as a difference in the ability to cope with stress, be it on the behavioral, neurochemical, or neuroendocrine level. Accordingly, a number of recent publications have related differences in behavioral stress coping, induced by interfering with the endocannabinoid system, to an interaction between endocannabinoid signaling and stress-perceptive molecular pathways of the brain (Viveros et al., 2005). One of the major neuroendocrine pathways that constitute the immediate reaction to any kind of stress is the HPA axis. Thus, latest studies have paid increasing attention to the role of endocannabinoid signaling for stress

hormone secretion (Pagotto et al., 2006), and it was the second goal of the following studies to further explore the impact of impaired CB1 receptor signaling, by pharmacological and genetic means, on neuroendocrine stress processing.

2.2 Cannabinoid type 1 receptors are required for the basal modulation of the HPA axis

The work described in this Chapter was accomplished in close shared collaboration with Dr. D. Cota from the Clinical Neuroendocrinology group of Prof. G.K. Stalla of the Max Planck Institute of Psychiatry in Munich. Dr. D. Cota performed the primary pituitary culture experiments (Fig. 2.2.2) and the double *in situ* hybridization (ISH) experiments with CB1 receptors and CRH (Fig. 2.2.4, Table 2.2.1). I analyzed stress hormone secretion of mutant mice (Fig. 2.2.1) and performed the ISH experiments for CRH, GR and MR (Figs. 2.2.3 and 2.2.5).

2.2.1 Summary

The endocannabinoid system affects the neuroendocrine regulation of hormone secretion, including the activity of the hypothalamus-pituitary-adrenocortical (HPA) axis. However, the mechanisms by which endocannabinoids regulate HPA axis function have remained unclear. Here, we demonstrate that mice lacking cannabinoid receptor type 1 ($CB1^{-/-}$) display a significant dysregulation of the HPA axis. Although circadian HPA axis responsiveness is preserved, $CB1^{-/-}$ mice are characterized by an enhanced circadian drive on the HPA axis, resulting in elevated plasma corticosterone concentrations at the onset of the dark as compared to wild-type ($CB1^{+/+}$) littermates. Moreover, $CB1^{-/-}$-derived pituitary cells respond with a significantly higher corticotropin (ACTH) secretion to corticotropin-releasing hormone (CRH) and forskolin challenges as compared to pituitary cells derived from $CB1^{+/+}$ mice. Both $CB1^{-/-}$ and $CB1^{+/+}$ mice properly respond to a high dose dexamethasone test, but response to low dose dexamethasone is influenced by genotype. In addition, $CB1^{-/-}$ mice show increased CRH mRNA levels in the paraventricular nucleus (PVN) of the hypothalamus, but not in other extra-hypothalamic areas, such as the amygdala and the piriform cortex, where CB1 receptor and CRH mRNA have been co-localized. Finally, $CB1^{-/-}$ mice have selective glucocorticoid receptor (GR) mRNA down-regulation in the CA1 region of the hippocampus, but not in the dentate gyrus or PVN. Conversely, mineralocorticoid receptor (MR) mRNA expression levels were found

unchanged in these brain areas. In conclusion, our findings indicate that CB1 receptor deficiency enhances the circadian HPA axis activity peak and leads to central impairment of glucocorticoid feedback, thus further outlining the essential role of the endocannabinoid system in the modulation of neuroendocrine functions.

2.2.2 Introduction

CRH, which is synthesized in the paraventricular nucleus (PVN) of the hypothalamus, represents the main driving force controlling HPA axis activation, the major hormone system responsible to maintain homeostatic balance in response to stressful stimuli (De Kloet, 1995; Tsigos and Chrousos, 2002). Appropriate regulatory control of the HPA axis is critical for health and survival and several limbic brain structures, such as the hippocampus, the amygdala and the prefrontal cortex, are involved in the integration of the HPA hormonal response (Herman et al., 2003).

Several lines of evidence support a role for the endocannabinoid system as a modulator of the HPA axis (Murphy et al., 1998; Pagotto et al., 2006). CB1 receptors and its endogenous ligands (endocannabinoids) are widely present in brain areas regulating HPA axis function (Herkenham et al., 1991; Marsicano and Lutz, 1999; Bisogno et al., 1999). Recent studies have reported that endocannabinoids are involved in mediating the acute negative fast-feedback effect of glucocorticoids on the HPA axis at the level of the PVN (Di et al., 2003). Moreover, both glucocorticoids and endocannabinoids increase appetite and body weight, and an important link exists between stress and obesity (Dallman, 2003; Dallman et al., 2003). Interestingly, it has been suggested that endocannabinoid signaling negatively modulates HPA axis activation induced by stress in a context-dependent manner (Patel et al., 2004). In line with this latest finding, previous studies have described the involvement of endocannabinoids in the regulation of anxiety-related behaviors, which represent part of the physiological responses to stressful stimuli (Navarro et al., 1997; Kathuria et al., 2003; Wotjak, 2005). However, the differential contribution of CB1 receptors in the regulation of extra-hypothalamic, hypothalamic and pituitary activity is still under debate (Pagotto et al., 2006).

Pharmacological studies using animal models have shown that the administration of endocannabinoids or CB1 receptor agonists increases circulating ACTH and glucocorticoid levels as well as hypothalamic mRNA expression levels of CRH and proopiomelanocortin (POMC) (Weidenfeld et al., 1994; Wenger et al., 1997; Corchero et al., 1999). A role for CB1 receptors in HPA axis activation has been established by the ability of the CB1 receptor antagonist SR141716 to

reduce the stimulation of ACTH release induced by Δ^9-tetrahydrocannabinol (the main component of marijuana) (Manzanares et al., 1999). However, it has also been described that the administration of SR141716 is able *per se* to increase the secretion of both ACTH and corticosterone (Patel et al., 2004; Navarro et al., 1997; Manzanares et al., 1999; Wade et al., 2006). Therefore, depending on a set of variables such as drug doses, environmental context and genetic background of the animals used, cannabinoid compounds might differently affect HPA axis activity (Gaetani et al., 2003).

In the current study, we used mice lacking CB1 receptors (CB1$^{-/-}$) as a model to determine, under basal conditions, the role of the endocannabinoid system in the regulation of the HPA axis at extra-hypothalamic, hypothalamic and pituitary levels, in order to highlight the potential existence of a HPA axis-modulating endocannabinoid tone.

2.2.3 Materials and Methods

Animals

Female mice deficient for CB1 receptors (CB1$^{-/-}$) and wild-type littermates (CB1$^{+/+}$) were used. The mice were in a mixed genetic background, with a predominant C57BL/6N contribution (6 back-crossings) as described earlier (Cota et al., 2003; Marsicano et al., 2002). The animals were housed in groups of five in the animal facility of the Max Planck Institute of Psychiatry, Munich, Germany, under standard conditions with a 12 : 12 h light : dark cycle (light on, 0600 h) at 22°C. After monitoring the stage of the ovarian cycle, 16-week-old mice were sacrificed in the diestrus phase. Particular care was taken to sacrifice the animals in unstressed conditions. All animal procedures complied with the *Guidelines for the care and use of laboratory animals of the Governments of the State of Bavaria*, Germany.

Hormone measurements and dexamethasone suppression test

Twenty-one CB1$^{+/+}$ and 21 CB$^{-/-}$ mice were used to measure circadian basal plasma corticosterone and ACTH. To verify whether the normal circadian activity of the HPA axis was preserved in the two genotypes, the hormones were measured both at the onset of the light (0600h) and of the dark (1800h) phase. Trunk blood was collected in 1.5-ml ice-cold EDTA-coated tubes containing trasylol (10,000 Kallikrein-Inhibitor-Unit (KIU)/ml, Bayer, Germany). After 15 min of centrifugation at 2,000 x g at 4°C, plasma samples were stored at −80°C. Measurements of plasmatic levels of ACTH and corticosterone were performed using commercial RIA kits (MP Biomedichals, Eschwege, Germany; ICN, Meckenheim, Germany) as described elsewhere (Karanth et al., 1997), according to manufacturer's instructions. For the dexamethasone suppression test, 32 CB1$^{+/+}$ and 23 CB1$^{-/-}$ mice were injected intraperitoneally (i.p.) with saline or dexamethasone 21-phosphate disodium salt (0.02, or 0.1 mg/kg) (ICN, Meckenheim, Germany) during the light phase (1200h). Six hours later (1800h), mice were rapidly decapitated in an adjacent room, trunk blood was collected and hormones were measured as described above.

Morphological analysis of adrenal glands

Adrenals from 11 CB1$^{+/+}$ and 11 CB1$^{-/-}$ mice were rapidly dissected, weighed, post-fixed in a 10% formalin solution (Sigma-Aldrich, Schnelldorf, Germany), dehydrated and embedded in paraffin for microtome sections (12 μm). Haematoxylin-eosin staining was performed and glands histology analyzed under the microscope.

Primary pituitary cell culture

Unless stated otherwise, materials and reagents were obtained from Sigma-Aldrich, Life Technologies, Inc. (Eggenstein, Germany), NUNC (Wiesbaden, Germany), and Falcon

(Heidelberg, Germany). To establish primary pituitary cell cultures, 10 CB1$^{+/+}$ and 10 CB1$^{-/-}$ mice were sacrificed and pituitaries were rapidly removed and immediately collected in HDB buffer (Hepes 25 mM, NaCl 137 mM, KCl 5 mM, Na$_2$HPO$_4$ 0.7 mM, glucose 10 mM, amphotericin B 10 ml/L, penicillin/streptomycin 10 ml/L). After mechanical and enzymatic dispersions, as described in (Timpl et al., 1998), cells were washed by repetitive centrifugation and finally resuspended in DMEM (pH 7.3) supplemented as described in (Pagotto et al., 2001). Cell viability was consistently more than 90%, as assessed by acridine orange/ethidium bromide staining. Cells were plated in 48-well plates (100,000 cells/well in 0.5 ml culture medium) and incubated in a 5% CO$_2$ atmosphere at 37°C. After the cells had attached to the plate (48 h), the culture medium was replaced by stimulation medium (Pagotto et al., 2001). After a washout period of 24 h, fresh stimulation medium was added to the cells together with the drug treatment.

Pituitary hormone stimulation and measurement

CRH (Bachem, Heidelberg, Germany) was used at a concentration of 10^{-7} and 10^{-8} Mol/L, and forskolin (a direct activator of the catalytic subunit of adenylate cyclase) was used at a concentration of 5 x 10^{-6} Mol/L. The final volume of the stimulation medium was 0.5 ml/well. After 4 h of incubation period, the supernatant was removed and the hormone content was determined. Mouse ACTH was measured by RIA as previously described (Karanth et al., 1997). Cell number was counted at the end of the stimulation experiments using the Cell Proliferation Reagent Kit WST-1 (Roche), following the manufacturer's instructions. Values obtained for hormone secretion were normalized to cell number. All the experiments were performed in triplicate.

In situ hybridization (ISH) for CRH, mineralocorticoid receptors (MR) and glucocorticoid receptors (GR).

For the single ISH experiments, 6 CB1$^{+/+}$ and 7 CB1$^{-/-}$ mice were sacrificed at the onset of the dark phase and their brains were quickly removed and flash frozen. Coronal sections (20 μm) were cut on a cryostat (Microtome HM560, Walldorf, Germany), mounted onto frozen SuperFrost/Plus slides (Menzer-Glaser, Braunschweig, Germany), dried and stored at –20°C, until further processed. CRH cDNA and correspondent riboprobe were obtained and ISH for CRH were performed as described (Cota et al., 2003). MR cDNA was a 742 bp fragment (nucleotides 1004-1745) of mouse MR coding sequence, and GR cDNA was a 610 bp fragment (nucleotides 1654-2263) of mouse GR coding sequence, cloned into the pPCRII-TOPO vector (Invitrogen, Karlsruhe, Germany), both kindly provided by J. Deussing, Max Planck Institute of Psychiatry, Munich, Germany. Restriction enzymes (New England Biolabs, MA, USA) used for linearization and RNA polymerases (Roche, Mannheim, Germany) used for the generation of each riboprobe were as follows: MR sense, SP6 polymerase and XbaI; MR antisense, T7 polymerase and BamHI; GR sense, SP6 polymerase and XbaI; GR antisense, T7 polymerase and BamHI. According to protocol design, riboprobes were labelled with ^{35}S and ISH was carried out as described in (Cota et al., 2003). In ISH experiments, sense RNA probes did not give any detectable signals (data not

shown). Standards were included during film exposure to assure that the level of the analyzed signal was within the linear range.

Quantification of CRH, MR, and GR mRNA expression was performed on autoradiographic films, using NIH Image program Scion Image (http://rsb.info.nih.gov/nih-image/). For the area analyzed (for CRH mRNA: PVN of the hypothalamus and amygdala complex; for MR and GR mRNAs: PVN of the hypothalamus, CA1, CA3 and dentate gyrus of the hippocampus), at least 3 sections/animal were quantified after background subtraction.

For CRH and CB1 receptor double ISH experiments, coronal sections of CB1$^{+/+}$ brains were used. CB1 receptor cDNAs and the correspondent riboprobes were obtained as described (Cota et al., 2003). According to the protocol design, riboprobe for CRH was labeled with ^{35}S and CB1 receptor riboprobe was labeled with digoxigenin (DIG), and double ISH for CRH and CB1 receptor mRNA co-localization was performed as described (Hermann et al., 2002). Different brain regions were chosen for numerical evaluation of co-expression based on the published distribution patterns of CB1 receptor and CRH (Herkenham et al., 1991; Olschowka et al., 1982). CB1 receptor-positive cells and CRH-positive cells were chosen in these regions on at least 4 different brain sections and co-expression values were calculated as percentage of CB1 receptor-expressing cells per number of cells positive for CRH, as described in (Cota et al., 2003).

Statistical analysis

All values are reported as means ± SEM. Hormonal measurements were evaluated by one- or two-way analysis of variance (ANOVA), with *Genotype* or *Genotype* and *Treatment* as factors, depending on the experimental conditions examined. ANOVAs were followed by Newman-Keuls Multiple Comparisons *post-hoc* test to identify significant differences. Unpaired Student's *t*-test was used for the analysis of ISH performed for CRH, MR and GR. *p* values less than 0.05 denote statistical significance.

2.2.4 Results

Lack of CB1 receptors increases circadian drive on the HPA axis

To examine the basal activity of the HPA axis as well as the circadian changes in corticosterone and ACTH levels, plasma corticosterone and ACTH were measured both at the beginning of the light and of the dark phase. The circadian hormonal variation was maintained in both CB1$^{+/+}$ and CB1$^{-/-}$ mice and differed significantly between morning and evening in both genotypes (Figs. 2.2.1a,b). However, at the onset of the dark, CB1$^{-/-}$ mice showed higher circulating
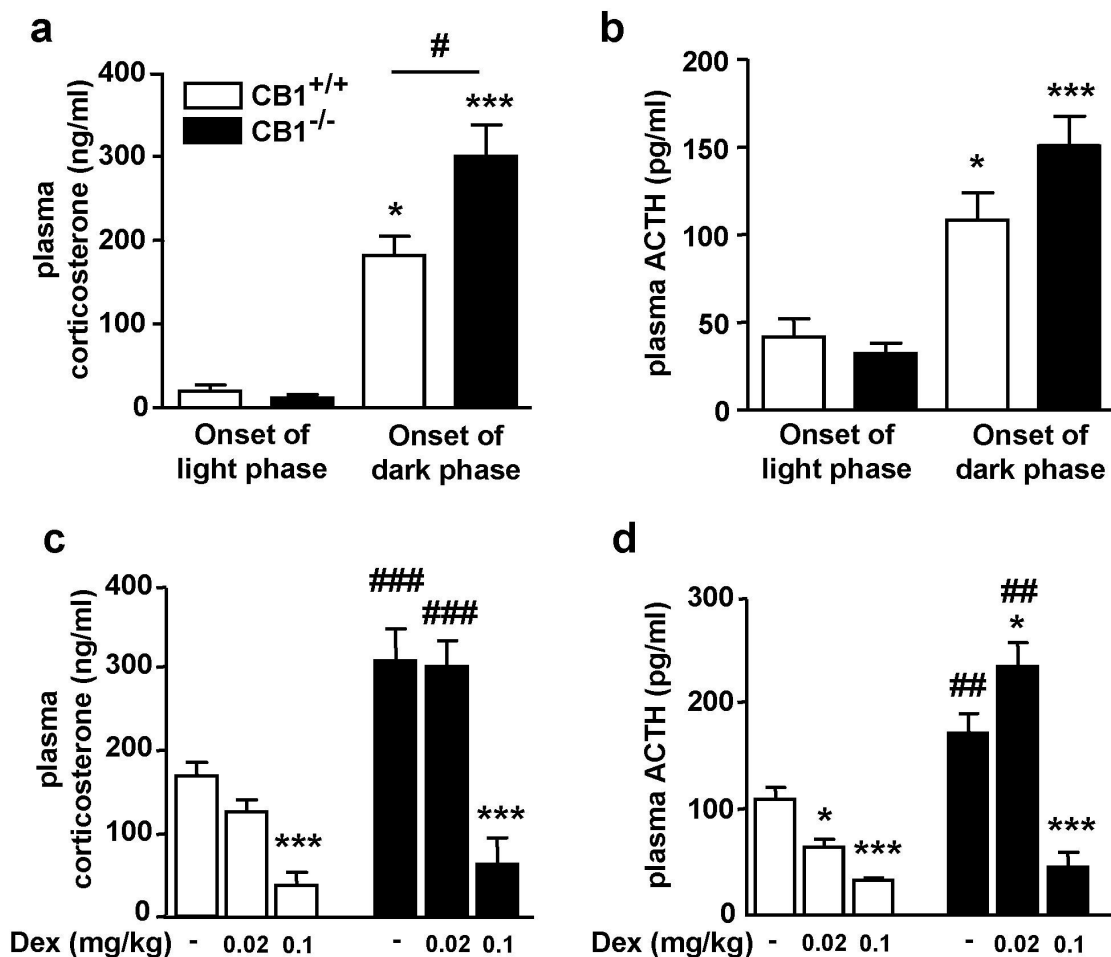
Figure 2.2.1 Plasma corticosterone and ACTH levels in CB1$^{+/+}$ and CB1$^{-/-}$ mice. (**a**) Circadian changes of corticosterone levels. Values are mean ± SEM of 8-13 animals per group. ***, $p < 0.001$ and *, $p < 0.05$ light phase vs. dark phase; #, $p < 0.05$ CB1$^{-/-}$ vs. CB1$^{+/+}$. (**b**), circadian changes of ACTH levels. Values are mean ± SEM of 8-13 animals per group. ***, $p < 0.001$ and *, $p < 0.05$ light phase vs. dark phase. (**c**) and (**d**), Corticosterone (**c**) and ACTH (**d**) levels before and after Dex test. Values are mean ± SEM of 8-15 animals per group. ***, $p < 0.001$ and *, $p < 0.05$ Dex vs. saline; ###, $p < 0.001$ and ##, $p < 0.01$ CB1$^{-/-}$ vs. CB1$^{+/+}$ in the same treatment condition.

corticosterone (Fig. 2.2.1a, $p < 0.05$) and a trend towards increased ACTH levels (Fig. 2.2.1b) as compared to CB1^{+/+} controls.

Thus, to test the responsiveness of the HPA axis to corticosteroid feedback, animals were treated with a low (0.02 mg/kg), or high dose (0.1 mg/kg) of dexamethasone (Dex). Statistical analysis of the Dex test response by two-way ANOVA revealed significant main effects of *Genotype* ($p < 0.001$, for both corticosterone and ACTH levels) and drug *Treatment* ($p < 0.001$, for both corticosterone and ACTH levels) and a significant interaction between the two factors ($p = 0.01$ for corticosterone levels; $p < 0.001$ for ACTH levels). In all the conditions but the high Dex dose, CB1^{-/-} mice had significantly higher plasma corticosterone and ACTH levels as compared to the CB1^{+/+} littermates (Figs. 2.2.1c,d). At the lowest Dex dose tested, CB1^{+/+} littermates showed a non significant trend to decreased circulating corticosterone and ACTH levels (Figs. 2.2.1c,d). In contrast, corticosterone levels in CB1^{-/-} mice did not respond to 0.02 mg/kg Dex. Furthermore, at this dose of Dex, a surprising significant increase was observed in ACTH levels of CB1^{-/-} mice (Fig. 2.2.1d, $p < 0.05$). However, when animals received the highest Dex dose, both CB1^{-/-} and CB1^{+/+} mice responded with a significant suppression in circulating levels of corticosterone and ACTH (Figs. 2.2.1c,d).

To determine whether possible chronic hyperactivity of the HPA axis with increased circulating corticosterone levels affected the structure of the adrenal glands, we investigated their morphology in CB1^{+/+} and in CB1^{-/-} mice. However, no difference in adrenal weight (CB1^{+/+}, 9.1 mg ± 0.5 versus CB1^{-/-}, 8.5 mg ± 0.7, $p = 0.451$) and no apparent alterations in the histology of the adrenal cortex were observed (data not shown).

Modulation of pituitary ACTH secretion in CB1^{-/-} mice

Steroids such as dexamethasone penetrate the brain poorly and predominantly induce feedback regulatory mechanisms at the pituitary level (De Kloet et al., 1998). Notably, both rodent and human pituitary express CB1 receptors and synthesize endocannabinoids (Pagotto et al., 2001; Gonzalez et al., 1999). Thus, to further elucidate whether the hyperactivity of the HPA axis observed in CB1^{-/-} mice could be directly related to the lack of pituitary CB1
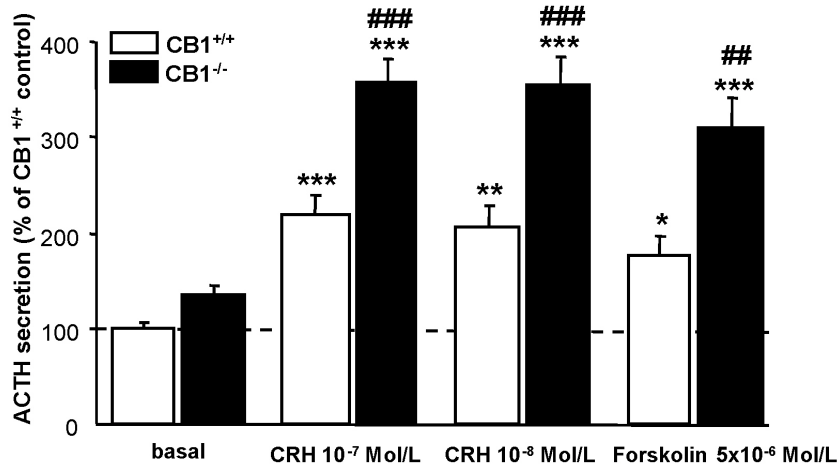
Figure 2.2.2 ACTH secretion in primary pituitary cell cultures from CB1$^{+/+}$ and CB1$^{-/-}$ mice. ***, $p < 0.001$, **, $p < 0.01$ and *, $p < 0.05$ vs. respective basal control; ###, $p < 0.001$ and ##, $p < 0.01$ vs. CB1$^{+/+}$ in the same treatment condition. The Figure was kindly provided by Dr. D. Cota.

receptors, we decided to perform *in vitro* experiments to study basal and stimulated ACTH secretion, using primary pituitary cell cultures derived from CB1$^{+/+}$ and CB1$^{-/-}$ littermates.

Statistical analysis by two-way ANOVA revealed significant main effects of *Genotype* ($p < 0.001$) and drug *Treatment* ($p < 0.001$), and a significant interaction between the two factors ($p < 0.05$). We found that cells from pituitaries of CB1$^{-/-}$ mice were characterized by a basal, though not significant, ACTH hypersecretion as compared to pituitary cultures from CB1$^{+/+}$ mice (Fig. 2.2.2). CB1$^{+/+}$-derived cells treated with CRH 10^{-7} Mol/L, CRH 10^{-8} Mol/L or forskolin 5 x 10^{-6} Mol/L were characterized by the expected significant increase in the secretion of ACTH (Fig. 2.2.2). Similarly, after the stimulation with either CRH or forskolin, CB1$^{-/-}$-derived cells showed a significant increase of ACTH secretion as compared to basal CB1$^{-/-}$ ACTH values (Fig. 2.2.2). Remarkably, however, the CRH- or forskolin-induced ACTH secretion in CB1$^{-/-}$-derived cells was much higher than that one observed in CB1$^{+/+}$ cultures in the same experimental conditions (Fig. 2.2.2), thus suggesting an increased responsiveness of pituitary cells in absence of CB1 receptors.

Lack of CB1 receptor affects CRH mRNA expression in the PVN, but not in other brain areas regulating HPA axis activity

The PVN of the hypothalamus and the CRH synthesized therein represent an essential driving force for the regulation of pituitary function. We recently

a

b

Figure 2.2.3 Levels of CRH mRNA expression in the PVN of female CB1$^{+/+}$ and CB1$^{-/-}$ mice. (**a**) Representative autoradiographic images showing the CRH mRNA expression in the PVN. (**b**) Densitometric quantification by image analysis of CRH mRNA expression in the PVN. Values are mean ± SEM of 6 CB1$^{+/+}$ and 7 CB1$^{-/-}$ mice.*, $p < 0.05$.
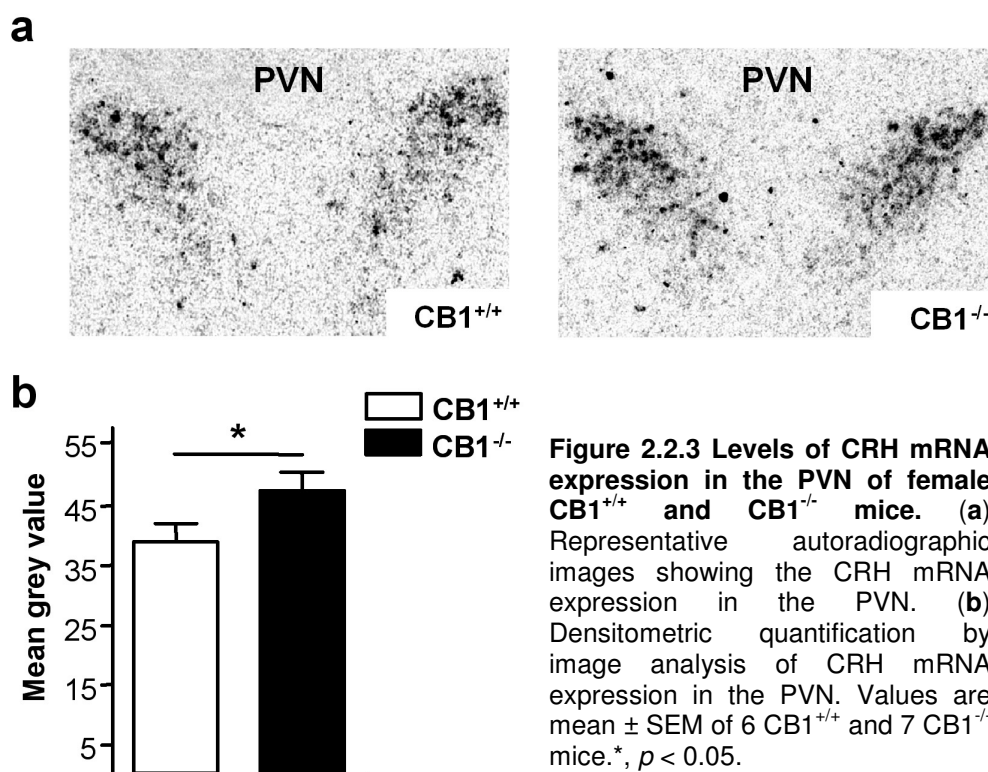
described that male CB1$^{-/-}$ mice show, among other neuroendocrine modifications, higher CRH mRNA levels in the PVN (Cota et al., 2003). Female CB1$^{-/-}$ mice used in the current study also have significantly increased CRH mRNA expression in the PVN as compared to their CB1$^{+/+}$ littermates (Figs. 2.2.3a,b, $p < 0.05$, one-tailed t-test).

To further investigate the involvement of extra-hypothalamic areas that could possibly affect HPA axis activity, ISH experiments were performed on brain tissue samples from CB1$^{+/+}$ mice to co-localize CB1 receptor transcript with CRH mRNA. CB1 receptor was found to be co-localized with CRH in several extra-hypothalamic brain areas known to integrate the overall stress response, such as in the baso-lateral (BLA), in the baso-medial (BMA), and in the central (CeA) nuclei of the amygdala, in the bed nucleus of the stria terminalis (BNST), in the piriform cortex and in the prefrontal cortex (Fig. 2.2.4). In particular, as shown in Table 2.2.1, a large percentage of CRH neurons expressed CB1 receptor mRNA in the amygdala (64.8% of CRH-positive cells in the BLA, 34.7% of CRH-positive cells in the BMA and 32.3% of CRH-positive cells in the CeA expressed CB1 receptor mRNA, respectively). In the BNST and in the piriform cortex, 22.1% of CRH-positive cells and 19.0% of CRH-positive cells co-localized with CB1 receptor
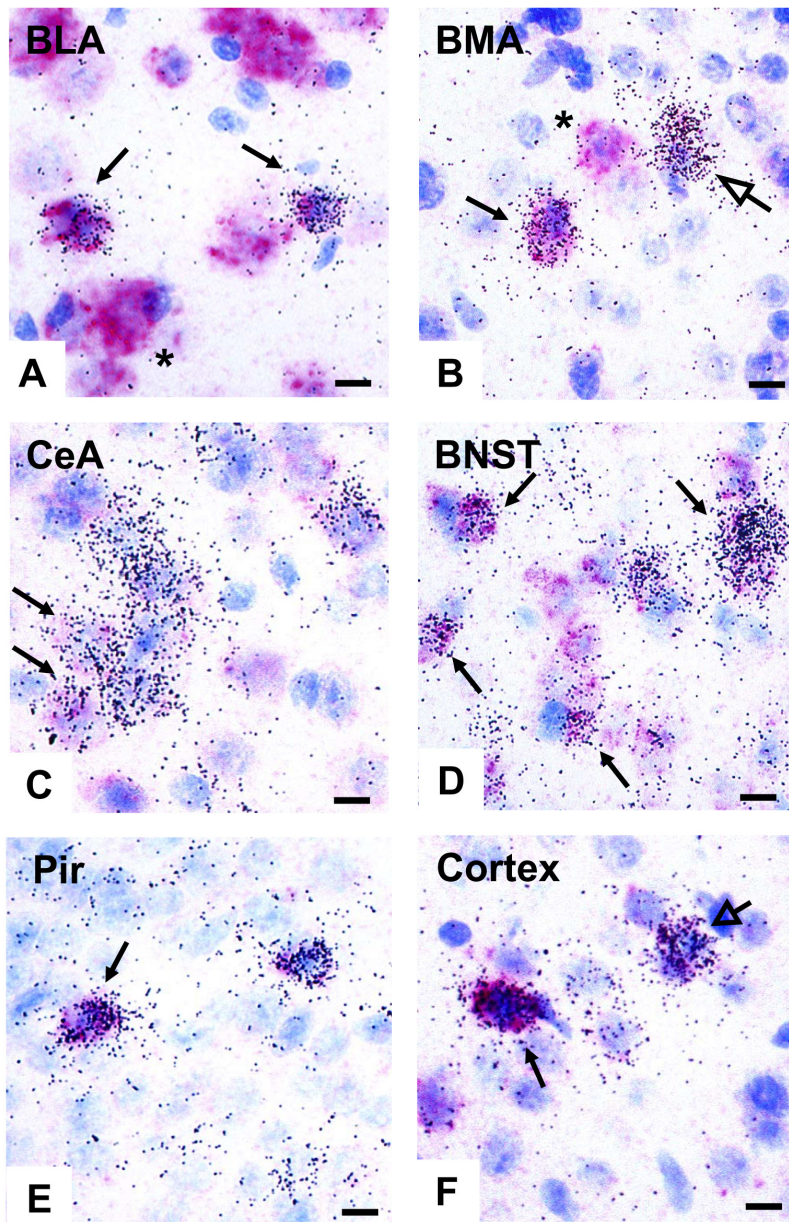
Figure 2.2.4 Co-localization of CB1 receptor and CRH mRNA in several extra-hypothalamic brain regions. Bright field micrographs. Vector red staining, CB1 receptor; silver grains, CRH. Co-localization of CB1 receptor and CRH mRNA in the baso-lateral (BLA) (A), in the baso-medial (BMA) (B) and in the central (CeA) (C) nucleus of the amygdala; co-localization of CB1 receptor and CRH mRNA in the bed nucleus stria terminalis (BNST) (D), piriform cortex (E) and prefrontal cortex (F). Filled arrow, cell co-expressing CB1 receptor and CRH; open arrow, cell expressing only CRH mRNA; asterisk, cell expressing only CB1 receptor mRNA. Scale bars, 10µm. The Figure was kindly provided by Dr. D. Cota.

mRNA, respectively. In the prefrontal cortex, 67.9% of CRH neurons expressed CB1 receptor transcript. Therefore, we investigated the levels of expression of CRH mRNA in CB1$^{-/-}$ and CB1$^{+/+}$ mice focusing on the CeA, a structure considered to be a very important relay station in the stress response network (Makino et al., 1999) and known to have the highest CRH localization among the amygdaloid nuclei (Olschowka et al., 1982). However, we found no differences in the levels of expression of CRH between the two genotypes (data not shown). Similarly, no alterations in CRH mRNA levels were noticed in the other extra-hypothalamic brain areas examined during the studies of co-localization (data not shown).

Table 2.2.1 Co-expression of CB1 receptor and CRH mRNA in extra-hypothalamic brain regions.

Area of the brain	Cells co-expressing CRH and CB1 receptors (%)*	NC
Amygdala-BLA	64.8	871
Amygdala-BMA	34.7	106
Amygdala-CeA	32.3	320
BNST	22.1	590
Piriform cortex	19.0	466
Prefrontal cortex	67.9	3553

NC, number of CRH-positive cells counted; BLA, baso-lateral nucleus of the amygdala; BMA, baso-medial nucleus of the amygdala; CeA, central nucleus of the amygdala; BNST, bed nucleus stria terminalis. *Co-expression values were calculated as percentage of CB1 receptor-expressing cells per number of cells positive for CRH. The Table was kindly provided by Dr. D. Cota.

CB1$^{-/-}$ mice have glucocorticoid receptor mRNA down-regulation in the CA1 region of the hippocampus

Corticosterone actions in the brain are mediated by glucocorticoid receptors (GR) and mineralocorticoid receptors (MR) (De Kloet et al., 1998). Given the high circulating levels of corticosterone in CB1$^{-/-}$ mice at circadian peak, we investigated the possible dysregulation of GR and MR expression.

No differences in MR mRNA levels were observed between CB1$^{+/+}$ and CB1$^{-/-}$ mice in either the PVN (Fig. 2.2.5a) or hippocampus (Fig. 2.2.5c). Interestingly, CB1$^{-/-}$ mice were characterized by a significant decrease in GR mRNA expression in the CA1 region of the hippocampus (Figs. 2.2.5d,e, $p < 0.05$) and by a slight, non-significant, downregulation of GR mRNA in the dentate gyrus (Fig. 2.2.5e). No differences in GR mRNA levels were noticed between genotypes at the level of the PVN (Fig. 2.2.5b).
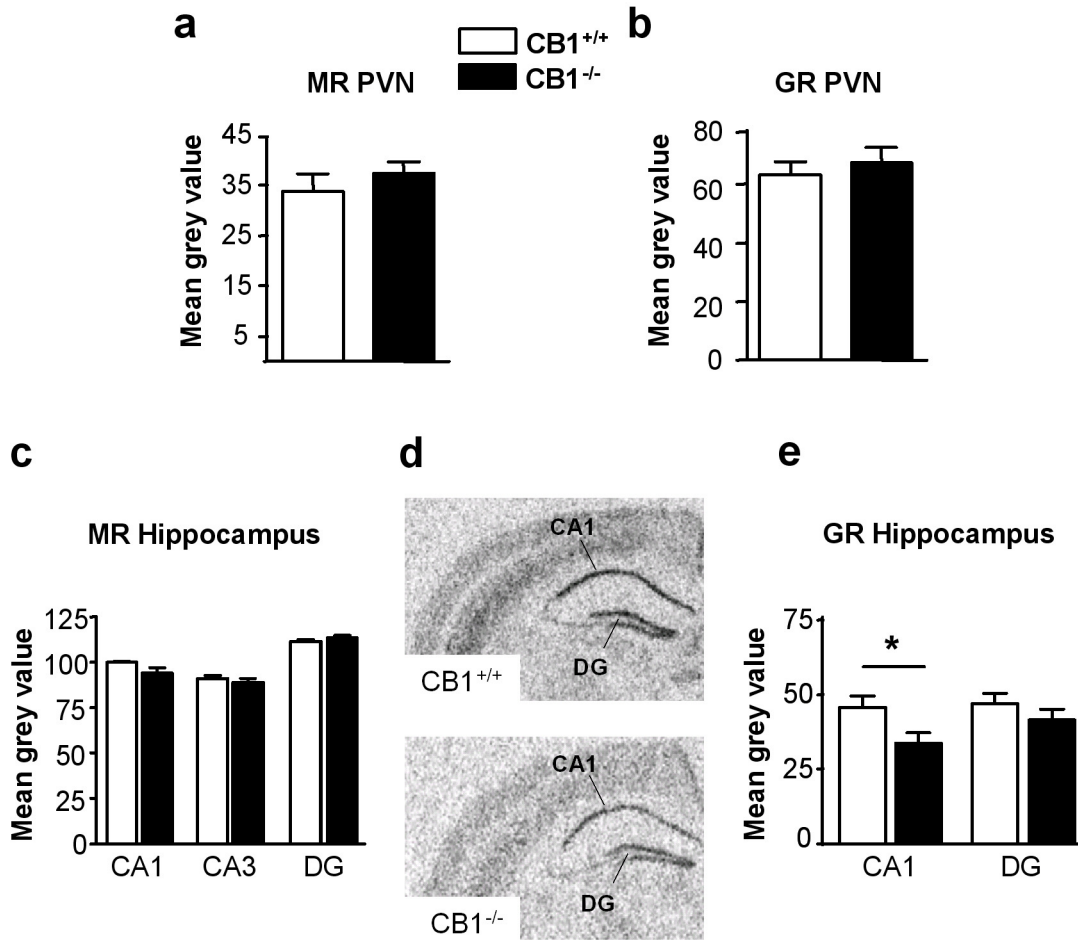
Figure 2.2.5 Levels of MR and GR mRNA expression in the PVN and hippocampus of CB1^{+/+} and CB1^{-/-} mice. (**a**,**b**) Densitometric quantification by image analysis of MR and GR mRNA expression in the PVN. (**c**) Densitometric quantification by image analysis of MR mRNA expression in the CA1, CA3 and dentate gyrus (DG) of the hippocampus. (**d**) Representative autoradiographic images showing the GR mRNA expression in the CA1 of the hippocampus. (**e**) Densitometric quantification by image analysis of GR mRNA expression in the CA1 and DG of the hippocampus. Values are mean ± SEM of 6 CB1^{+/+} and 7 CB1^{-/-} mice.*, $p < 0.05$.

2.2.5 Discussion

The appropriate regulation of the HPA axis is fundamental for the adequate response to internal and external challenges in order to maintain balance of homeostatic systems. While the short-term activation of the HPA axis is highly adaptive for the survival of the organism, long-term HPA activity is often deleterious, leading to alterations of metabolic, cognitive and behavioral functions, and being also associated with body weight disorders (Dallman et al., 2003) and neuropsychiatric diseases, such as anxiety and depression (Chrousos and Gold, 1992; De Kloet et al., 2005; Arborelius et al., 1999).

Here we describe that CB1$^{-/-}$ mice have increased circulating corticosterone levels at the circadian peak, increased *in vitro* responsiveness of their pituitary cells to CRH- and forskolin-induced ACTH secretion, dose-dependent responsiveness to dexamethasone suppression test, increased CRH mRNA expression in the PVN and decreased GR mRNA levels in the CA1 region of the hippocampus.

The present findings thus support the hypothesis that CB1 receptor signaling plays a critical role in regulating basal HPA axis activity, as a reduced inhibitory tone on the HPA axis, particularly evident at the circadian peak, occurs in the absence of CB1 receptor signaling.

In the central nervous system, endocannabinoids work as retrograde modulators of synaptic function and generally act as stress-recovery factors, produced in response to stressful stimuli re-establishing the steady state of neuropeptides, hormones and neurotransmitters (Di Marzo et al., 1998; Piomelli, 2003). For instance, several lines of evidence suggest that hypothalamic endocannabinoid levels change in response to acute and chronic stress (Pagotto et al., 2006; Patel et al., 2004). Moreover, endocannabinoids mediate the negative fast-feedback actions of glucocorticoids on CRH-containing neurons in the PVN, by retrograde inhibition of glutamatergic transmission (Di et al., 2003). Despite the fact that we did not test fast feedback mechanisms, the CB1$^{-/-}$ phenotype described in our study supports the hypothesis that CB1 receptor signaling is a critical component of the regulatory glucocorticoid feedback that modulates HPA axis function.

Interestingly, the endocannabinoid system seems to be able to regulate the HPA axis not only by modulating the function of CRH-producing neurons at the hypothalamic level, but also by directly affecting ACTH secretion at the pituitary level. Indeed, the data obtained from our pituitary culture experiments clearly point to a direct involvement of CB1 receptors in the modulation of ACTH secretion, suggesting that the absence of endocannabinoid signaling at the pituitary level may affect responsiveness to CRH. CB1$^{-/-}$-derived cells are hyper-responsive to stimuli, such as CRH and forskolin, which classically promote hypophyseal ACTH secretion. CRH stimulates ACTH secretion via a well known G stimulating (G$_s$)-protein-coupled receptor pathway that leads to the activation of the adenylate cyclase enzyme and to the increase of intracellular cAMP levels (Chalmers et al., 1996). The CB1 receptor is a seven-transmembrane G-protein-coupled receptor whose effects are primarily due to the activation of the G$_i$ subunit, resulting in reduced adenylate cyclase activity and decreased intracellular cAMP (Howlett et al., 2002). Therefore, in the corticotrope cells of the pituitary, the lack of CB1 receptors might interfere with the normal regulation of adenylate cyclase activity, thus affecting ACTH secretion. However, in contrast to our results, a previous investigation on CB1$^{-/-}$ mice reported no alteration in the modulation of pituitary ACTH secretion (Barna et al., 2004), possibly because of differences in the inbred strains or, more likely, in the experimental procedure used.

CB1$^{-/-}$ mice respond properly with a decrease in ACTH and corticosterone secretion after the high dose dexamethasone treatment, thus suggesting that the feedback control on the HPA axis is still preserved. Nevertheless, it is worth mentioning that, while CB1$^{+/+}$ mice tend to decrease both corticosterone and ACTH levels after a low dose of dexamethasone, CB1$^{-/-}$ mice do actually show a further increase in ACTH levels and no reduction of corticosterone. The reasons for the paradoxical increase in ACTH levels found in CB1$^{-/-}$ mice after treatment with a low dose of dexamethasone are currently unknown. Nevertheless, our findings suggest that the response to dexamethasone treatment seems to be in part influenced by the lack of CB1 receptors.

GR and MR mediate corticosterone actions in the brain. Under low corticosterone levels only the high affinity MR in the hippocampus is predominantly occupied. The low affinity GR can be activated additionally to MR only when corticosterone levels are high, such as at the circadian peak or during stress (De

Kloet et al., 1998). Thus, corticosterone action via MR exerts a tonic, permissive influence on hippocampus-associated functions, while occupancy of GR in this brain region mediates feedback actions aimed to terminate stress-induced HPA activation (De Kloet et al., 1998). Hence, corticosterone responses modulated by MR activation are themselves subject to feedback action via GR (De Kloet et al., 1998). In CB1^{-/-} mice, levels of GR and MR mRNA are unchanged in the PVN, and MR mRNA levels appear normal in various subregions of the hippocampus. However, GR mRNA is significantly decreased in the CA1 region of the hippocampus, possibly as a result of increased circulating glucocorticoids levels that may downregulate hippocampal GR expression.

Since CB1 receptors are highly expressed in CA1, CA3 and DG of the hippocampus (Herkenham et al., 1991; Marsicano and Lutz, 1999), a question that remains unaddressed by the present findings is whether the prominent effects of glucocorticoids in this brain region also involve a CB1 receptor-dependent signal. Moreover, it is not known whether an interaction between CB1 receptors and GR exists. Further experiments will be needed to clarify the possible role of the endocannabinoid system in the modulation of brain GR function.

CB1 receptors and endocannabinoids are also present in limbic brain regions considered to be part of the emotional stress response circuitry and known to influence the HPA axis activity (Herman et al., 2003). Our double ISH experiments demonstrate that CB1 receptors and CRH mRNA co-localize in several brain structures, such as the amygdala, the BNST and the prefrontal cortex. Nevertheless, under unstressed condition, the genetic deletion of CB1 receptors does not affect the levels of CRH mRNA expression in these extra-hypothalamic areas. On the other hand, it is well known that the exposure to psychological stress increases CRH mRNA levels in the amygdala, specifically in the CeA (Makino et al., 1999). Thus, it seems reasonable to hypothesize that CRH levels in the limbic system could be altered in CB1^{-/-} mice exposed to psychological stress. In support of this hypothesis, CB1^{-/-} mice evaluated under different behavioral paradigms, exhibit increased aggressive, anxiogenic-like and depressive-like responses (Martin et al., 2002; Uriguen et al., 2004; Fride et al., 2005), suggesting that absence of CB1 receptors results in a greater vulnerability to stress (Fride et al., 2005).

Finally, caution should be used in administering weight-reducing CB1 receptor antagonists to obese patients displaying an anxiety or depressive trait. In agreement with our conclusions, recent published trials indicate that a low but significant number of obese patients treated with the CB1 receptor antagonist rimonabant discontinued the treatment due to increased occurrence of anxiety and depressed mood disorders (Van Gaal et al., 2005; Despres et al., 2005; Pi-Sunyer et al., 2006).

Our current findings highlight an important role for the endocannabinoid system in the neuroendocrine network that regulates both ACTH and glucocorticoid secretion, implying that alterations of the central endogenous cannabinoid tone might be involved in the pathophysiology of stress-related diseases.

2.3 Impaired cannabinoid receptor type 1 signaling interferes with stress coping behavior in mice

In the previous Chapter 2.2 we demonstrated that CB1 receptor-deficient mice display depression-like symptoms of HPA axis hyperactivity under non-stress conditions, including increased corticosterone secretion, attenuated dexamethasone suppression, elevated CRH expression in the PVN and reduced GR expression in the hippocampus. In the present Chapter 2.3, we focused on the behavioral stress coping abilities of CB1 receptor-deficient mice and investigated potential disturbances of the monoamine and neurotrophin systems.

The work described in this chapter was accomplished in collaboration with Dr. H. Bächli from the Department of Neurosurgery, University Hospital Basel, Switzerland, and in collaboration with Dr. E. Borroni from F. Hoffmann-La Roche, Pharma Division, Basel, Switzerland. Dr. H. Bächli analyzed the monoamine and metabolite concentrations (Table 2.3.2), and Dr. E. Borroni analyzed the monoamine oxidase A and -B enzymatic activities in tissue from the hippocampus (Table 2.3.1). I did the behavioral and pharmacological analyses and performed the in situ hybridization experiments (Figs. 2.3.1-7).

2.3.1 Summary

Dysregulation of the endocannabinoid system is known to interfere with emotional processing of stressful events. Here we studied the role of CB1 receptor signaling in stress coping behaviors using the forced swim test (FST) with repeated exposures. We compared effects of genetic inactivation with pharmacological blockade of CB1 receptors both in male and female mice. In addition, we investigated potential interactions of the endocannabinoid system with monoaminergic and neurotrophin systems of the brain. Naïve CB1 receptor-deficient mice (CB1$^{-/-}$) showed increased passive stress coping behaviors as compared to wild-type littermates (CB1$^{+/+}$) in the FST, independent of sex. These findings were partially reproduced in C57BL/6N animals and fully reproduced in female CB1$^{+/+}$ mice by pharmacological blockade of CB1 receptors with the CB1

receptor antagonist SR141716. The specificity of SR141716 was confirmed in female CB1$^{-/-}$ mice, where it failed to affect behavioral performance. Sensitivity to the antidepressants desipramine and paroxetine was preserved, but slightly altered in female CB1$^{-/-}$ mice. There were no genotype differences between CB1$^{+/+}$ and CB1$^{-/-}$ mice in monoamine oxidase A and B activities under basal conditions, nor in monoamine content of hippocampal tissue after FST exposure. mRNA expression of vesicular glutamate transporter type 1 (VGLUT1) was unaffected in CB1$^{-/-}$ mice, but mRNA expression of brain-derived neurotrophic factor (BDNF) was reduced in the hippocampus. Our results suggest that impaired CB1 receptor function promotes passive stress coping behavior, which, at least in part, might relate to alterations in BDNF function.

2.3.2 Introduction

Preclinical research in rodents during the last decade has helped to elucidate the role of the endocannabinoid system in fear and anxiety. For instance, the importance of endocannabinoid signaling for the extinction of aversive memories was recently demonstrated in our laboratory (Marsicano et al., 2002; Kamprath et al., 2006). Endocannabinoid signaling seems to be indispensable for the adequate coping of the organism with aversive and stressful situations. These findings fit well with the observations that pharmacologically increased endocannabinoid signaling exerts anxiolytic effects in rodents (Kathuria et al., 2003; Patel and Hillard, 2006) and, thus, could represent an important lead for the development of new anti-anxiety drugs (Kathuria et al., 2003; Viveros et al., 2005; Hill and Gorzalka, 2005a). In agreement with these findings, pharmacological blockade or genetic inactivation of CB1 receptors led to anxiogenic responses (Patel and Hillard, 2006; Haller et al., 2002; Haller et al., 2004a; Martin et al., 2002). Nevertheless, there are some studies which have failed to show an effect on anxiety measures (Marsicano et al., 2002) or even demonstrated anxiolytic effects (Griebel et al., 2005). These discrepancies might be ascribed to differences in the genetic background of the rodent (Marsicano et al., 2002; Haller et al., 2002; Martin et al., 2002) or in the test conditions (Rodgers et al., 2005), especially regarding the averseness of the test situation (Haller et al., 2004b).

Given the high comorbidity between anxiety and major depression (Merikangas et al., 2003), recent research has also focused on a potential role of the endocannabinoid system in the pathology of major depression (Hill and Gorzalka, 2005a; Witkin et al., 2005a), particularly of the melancholic subtype (Hill and Gorzalka, 2005a). CB1 receptor-deficient mice share several symptoms with patients suffering from melancholic depression such as, for example, altered responsiveness to reward stimuli (Sanchis-Segura et al., 2004), altered neurovegetative functions (Cota et al., 2003), a predominance and persistence of aversive memories (Kamprath et al., 2006; Marsicano et al., 2002), and possibly neurodegeneration (Bilkei-Gorzo et al., 2005). Furthermore, it was shown by us and others that impaired endocannabinoid signaling can lead to sustained HPA axis hyperactivity (Cota et al., 2003; and results from Chapter 2.2) and might also

interfere with the proliferation of neural progenitor cells (Aguado et al., 2005). Human post-mortem studies of depressed suicide victims, which have revealed dysregulations of the endocannabinoid system in the prefrontal cortex (Hungund et al., 2004; Vinod et al., 2005), further strengthen the notion of a potential role of the endocannabinoid system in depression. In this context, it is also worthwhile to note that the most frequently encountered side effects during the recently conducted phase-III trials of the CB1 receptor antagonist rimonabant (SR141716) as an anti-obesity treatment included anxiety and mood disturbances (Despres et al., 2005; Pi-Sunyer et al., 2006; Van Gaal et al., 2005).

Studies on the function of endocannabinoids in classic animal models of depression or antidepressant-like behavior, however, have so far been sparse and revealed contradictory results in rats and mice. The forced swim test (FST) represents one of the most widely used tests to detect antidepressant-like activities of drugs as well as depression-like behavior in genetically engineered mice (Cryan and Holmes, 2005). Drugs, which elevate the endocannabinoid tone such as the fatty acid amide hydrolase inhibitor URB597 or the endocannabinoid re-uptake inhibitor AM404 were demonstrated to exert antidepressant-like effects (Gobbi et al., 2005; Hill and Gorzalka, 2005b) in the rat FST in terms of reduced immobility. Surprisingly, however, also CB1 receptor antagonists such as SR141716 given in a higher dose range (3 -10 mg/kg) were able to produce similar antidepressant-like effects in this test in rats and mice (Griebel et al., 2005; Tzavara et al., 2003b). CB1 receptor-deficient mice, though, on a different genetic background (CD1) than our mice (C57BL/6N) have failed so far to show any behavioral alterations in the FST (Jardinaud et al., 2005). Consequently, the issue of whether or not the blockade of endocannabinoid signaling could actually be of advantage or disadvantage for the potential treatment of depression is from the preclinical view still under debate (Hill and Gorzalka, 2005a; Witkin et al., 2005b). Given the higher prevalence of females to develop depression (Kessler et al., 1994), systematic investigations of the interaction between sex and endocannabinoid signaling in animal models of depression are still missing. In addition, little is known about the neural substrates underlying the potential antidepressant-like effects of drugs interfering with endocannabinoid signaling (Tzavara et al., 2003b; Gobbi et al., 2005).

In the present study we investigated the effects of impaired CB1 receptor signaling on stress coping behaviors in both male and female mice using the FST with repeated exposures. Effects of the genetic inactivation of CB1 receptors were compared to effects of the pharmacological blockade by the selective CB1 receptor antagonist SR141716. Potential links between the endocannabinoid system and monoaminergic systems of the brain were assessed by analyzing (i) sensitivity to different classes of antidepressants in the FST, (ii) basal monoamine oxidase A and B activities, and (iii) hippocampus tissue content of catecholamines and serotonin after FST in CB1 receptor-deficient mice (CB1$^{-/-}$) and wild-type littermates (CB1$^{+/+}$). Furthermore, mRNA levels of the vesicular glutamate transporter type 1 (VGLUT1), a marker of antidepressant activity (Moutsimilli et al., 2005), were evaluated, as well as mRNA levels of brain derived neurotrophic factor (BDNF), a neurotrophic factor strongly implicated in depression as well as in the behavioral response to forced swimming (Shirayama et al., 2002).

2.3.3 Materials and Methods

Animals

Mice were kept under standard conditions with food and water *ad libitum*. They were housed in groups with a 12 h : 12 h inverted light/dark schedule (lights off at 09:00 am). Animals were separated and single housed two weeks prior to experiments. C57BL/6N mice were purchased from Charles River (Germany). CB1 receptor-deficient mice (CB1$^{-/-}$) and their wild-type littermates (CB1$^{+/+}$) were maintained on a predominant C57BL/6N background (6 backcrossings) and generated and genotyped as described (Marsicano et al., 2002). The age of the animals during testing ranged between 3 and 6 months. Female mice were not controlled for the estrus cycle, because preliminary experiments failed to reveal any correlation between behavioral performance in the FST and estrus cycle phase as determined by vaginal smears at the experimental day (data not shown). Animal experiments were conducted in accordance with the *Guide for the Care and Use of Laboratory Animals* of the local Government of Bavaria, Germany. Experiments were performed during the second half of the dark, active phase of the animals under red-light conditions.

Forced swim test (FST)

Each mouse was placed into a 5-l glass beaker (height 23.5 cm; diameter 16.5 cm) containing water up to a height of 15 cm at 25 ± 1 °C for 6 min. The water was changed between subjects. During each trial, floating (immobility) and struggling time was scored by pressing preset keys on a computer keyboard, using customized freeware software (EVENTLOG; Robert Hendersen 1986). The remaining time of the 6 min that the mice did not spend floating or struggling was assigned to swimming. Time spent swimming was not reported to avoid redundancy. The resulting two-channel ethogram was further processed by customized software (Winrat Vers. 2.31; Heinz Barthelmes, MPI Munich). A mouse was judged floating when it stopped any movements except those that were necessary to keep its head above water. Vigorous swimming movements involving all 4 limbs of the mouse with the front paws breaking the surface of the water, usually at the walls of the cylinder, were regarded as struggling. Although struggling is more prominent in rats and commonly scored only in the rat FST, we have found that struggling can also be precisely defined in mice and have found it worthwhile analyzing. As struggling in mice almost exclusively occurs during the first 1-2 minutes of the first exposure to the FST on day 1, it very likely refers to arousal of the animals upon first encounter with water exposure. We have previously found that, in addition to floating, also struggling can be specifically influenced by certain factors (for instance by certain antidepressants or corticotropin releasing hormone). Animals' behavior was analyzed on-line by trained observers who were blind to treatment and genotype. Animals were tested three times, on day 1, on day 2 and on day 21.

Pharmacology

SR141716 (NIMH Chemical Synthesis and Drug Supply Program, U.S.A.) was dissolved in vehicle solution (1 drop of Tween-80 in 3 ml of 2.5% dimethylsulfoxide in 0.9% saline) and injected at a dose of 10 mg/kg in a volume of 10 ml/kg body weight i.p. 2 h prior to the forced swim test on day 1, once again 12 h later, and 2 h prior to forced swimming on day 2. Desipramine hydrochloride (Sigma-Aldrich, Steinheim, Germany) and paroxetine hydrochloride (Dongyang Pharmaceutical Chemical Co., LTD., Dongyang City, Zhejiang, China) were dissolved in vehicle solution (2% dimethylsulfoxide in saline) and injected at a dose of 20 mg/kg (an effective dose in male C57BL/6N mice as evaluated in preliminary experiments) in a volume of 10 ml/kg body weight i.p. 30 min prior to the forced swim test on day 1 and day 2 and once in between, 12 h after the first injection.

In situ hybridization

Naïve male CB1$^{+/+}$ and CB1$^{-/-}$ mice were killed by decapitation during the second half of the dark phase. Brains were quickly removed, frozen on dry ice and stored at -80ºC. Brains were mounted on Tissue Tek (Polysciences, Eppelheim, Germany), and 20 µm thick coronal sections were cut on a cryostat Microtome HM560 (Microm). Sections were mounted onto frozen SuperFrost/Plus slides (Fisher Scientific), dried on a 35ºC warming plate and stored at -20ºC. *In situ* hybridizations for BDNF and VGLUT1 mRNA were performed as previously described (Marsicano et al., 2002;Monory et al., 2006). Densitometric analyses were performed on autoradiographic films using the NIH Image software (http://rsb.info.nih.gov/nih-image/Default.html).

Determination of monoamine oxidase (MAO) enzymatic activity

Naïve female CB1$^{+/+}$ and CB1$^{-/-}$ mice were sacrificed by decapitation during the second half of the dark phase and the cortex, hippocampus and striatum were rapidly dissected, frozen and stored at -80 ℃ until assay. The enzymatic activity of MAO-A and MAO–B was measured according to a previous protocol (Zhou and PanchukVoloshina, 1997). Briefly, brain regions were homogenized in 20 volumes of ice-cold 20 mM Na-phosphate buffer containing 0.2% Triton-X 100 (w/w). For the assay of MAO-A and MAO–B the homogenates were further diluted 1/12.5 and 1/25, respectively, with 20 mM phosphate buffer 0.2% Triton-X 100. Since the mouse brain contains both MAO isoforms, homogenate aliquots destined to MAO-A assay were pre-incubated with the selective MAO-B inhibitor L-deprenyl (10 µM), whereas those destined to the MAO-B assay were pre-incubated with the selective MAO-A inhibitor clorgyline (1 µM). Serotonin (100 µM) was used as a substrate for MAO-A assay, whereas phenylethylamine (20 µM) was used for MAO-B assay. Blanks were prepared by addition of both clorgyline and L-deprenyl to the homogenates. The progress of the enzymatic reaction was monitored fluorometrically (excitation 544 nm and emission 590 nm) at room temperature in a PolarStar Galaxy microplate reader (BMG Labtech, Aylesbury,

UK). Data were expressed in nmoles of substrate metabolized/hour/mg protein. Protein content was measured with the Pierce BCA protein assay reagent (Perbio Science, Bonn, Germany).

Determination of monoamine concentrations

Ten minutes after the beginning of the forced swim test on day 2, subchronically vehicle and SR141716 treated female CB1$^{+/+}$ and CB1$^{-/-}$ animals were sacrificed by decapitation and hippocampi freshly dissected on an ice-cold plate. Tissue samples were weighed and stored at –80 °C until further processing. Concentrations of the monoamines noradrenaline (NA), dopamine (DA), serotonin (5-HT) as well as of their metabolites 3,4-dihydrophenylacetic acid (DOPAC), homovanillic acid (HVA) and 5-hydroxyindoleacetic acid (5-HIAA) were measured by high-performance liquid chromatography coupled with electrochemical detection. Brain tissues were homogenized on ice in 0.1 M ice cold perchloric acid (Sigma-Aldrich, Steinheim, Germany) containing 50 nmol/L 3,4-dihydroxybenzylamine (Sigma-Aldrich, Steinheim, Germany) as internal standard. Samples were centrifuged at 16 000 g for 10 min and supernatants filtered through 0.45 µm Millipore type HV filters (Millipore, Schwalbach, Germany). 10 µl of each sample were automatically injected into a liquid chromatographic system, which consisted of a Dionex P680 isocratic pump (Dionex, Idstein, Germany), a refrigerated (4°C) Dionex ASI-100 microsampler (Dionex, Idstein, Germany) and an amperometric Decade detector (cell potential set at + 0.85 V) equipped with a VT-03 flow cell (Antec, Leyden, The Netherlands). Chromatographic separation of catecholamines, 5-HT and metabolites was achieved on a Gemini C18 analytical column, 2 mm i.d. x 25-cm length, with 5-µm particle size (Phenomenex, Aschaffenburg, Germany). The mobile phase consisted of 0.1 M potassium phosphate buffer, 100 mg/l 1-octanesulfonic acid sodium salt, 50 mg/l EDTA and methanol 4.5 % (v/v), and was adjusted to pH 2.2 with H_3PO_4 (all chemicals from Sigma-Aldrich, Steinheim, Germany). The flow cell and the analytical column were maintained at a temperature of 40°C. The flow rate was 0.18 ml/min. The chromatograms were analyzed and integrated using a computerized data acquisition system equipped with Chromeleon chromatographic software (Dionex, Idstein, Germany). Compound identification and peak quantification were achieved by comparison with known standards. All samples were measured in duplicate and average values were expressed as pmol/mg of fresh weight of brain tissue.

Statistical analysis

For multiple comparisons data were analyzed using two- or three-way analysis of variance (ANOVA) for repeated measures where appropriate, followed by *post-hoc* Newman-Keuls Multiple Comparison Test. For two-group comparisons unpaired Student's *t*-test was used. Differences were considered statistically significant if $p < 0.05$. FST data (mean ± SEM) are presented either as the total behavioral performance shown during the entire 6-min observation period or as the behavioral performance shown during each of the six 1 min intervals of a single exposure.

2.3.4 Results

Genetic deletion of CB1 receptors increases passive coping behavior in the forced swim test (FST)

CB1$^{+/+}$ and CB1$^{-/-}$ mice of both sexes were subjected to forced swimming in three consecutive sessions on day 1, on day 2 and on day 21 (Fig. 2.3.1) in order to study the persistence of alterations in behavioral stress coping strategies over repeated testing.

With respect to long-term changes in struggling from day 1 to day 21, animals showed decreased struggling on day 2 and on day 21 as compared to the first exposure on day 1 [*Day*: $F_{2,140}$ = 71.4, $p < 0.001$; 3-way ANOVA (*Genotype, Sex, Day*) for repeated measures (*Day*); Figs. 2.3.1a,d], independent of genotype and sex. Moreover, there was a significant *Genotype x Day* interaction ($F_{2,140}$ = 6.0, p = 0.003), reflecting decreased struggling of CB1$^{-/-}$ mice of both sexes on day 1 and increased struggling of male CB1$^{-/-}$ mice on day 2 and on day 21 as compared to their CB1$^{+/+}$ littermates. Male mice of both genotypes generally struggled more than their female littermates (*Sex*: $F_{1,70}$ = 7.0, p = 0.01, *Sex x Day*: $F_{2,140}$ = 3.4, p = 0.038).

With respect to long-term changes in floating from day 1 to day 21, animals showed increased floating on day 2 and on day 21 as compared to the first exposure on day 1 [*Day*: $F_{2,140}$ = 52.8, $p < 0.001$; 3-way ANOVA (*Genotype, Sex, Day*) for repeated measures (*Day*); Figs. 2.3.1b,e], independent of genotype and sex. Moreover, there was a significant *Genotype x Day* interaction ($F_{2,140}$ = 4.1, p = 0.018), reflecting increased floating of CB1$^{-/-}$ mice of both sexes on day 1.

Integration of the behavioral performance over the entire 6-min observation period may cause information loss about the development of behavioral stress coping over the course of the stressor exposure. Therefore, we additionally analyzed the data in 1-min intervals in order to assess short-term (i.e. within-session) changes in floating (Figs. 2.3.1c,f). In general, there were significant *Genotype x Interval* interactions for each of the testing days [$F_{5,355}$ > 3.2, $p < 0.008$; 3-way ANOVAs (*Genotype, Sex, Interval*) for repeated measures (*Interval*)], independent of the sex, reflecting the fact that CB1$^{-/-}$ animals showed a more pronouncedincrease in floating than their CB1$^{+/+}$ littermates with ongoing stressor
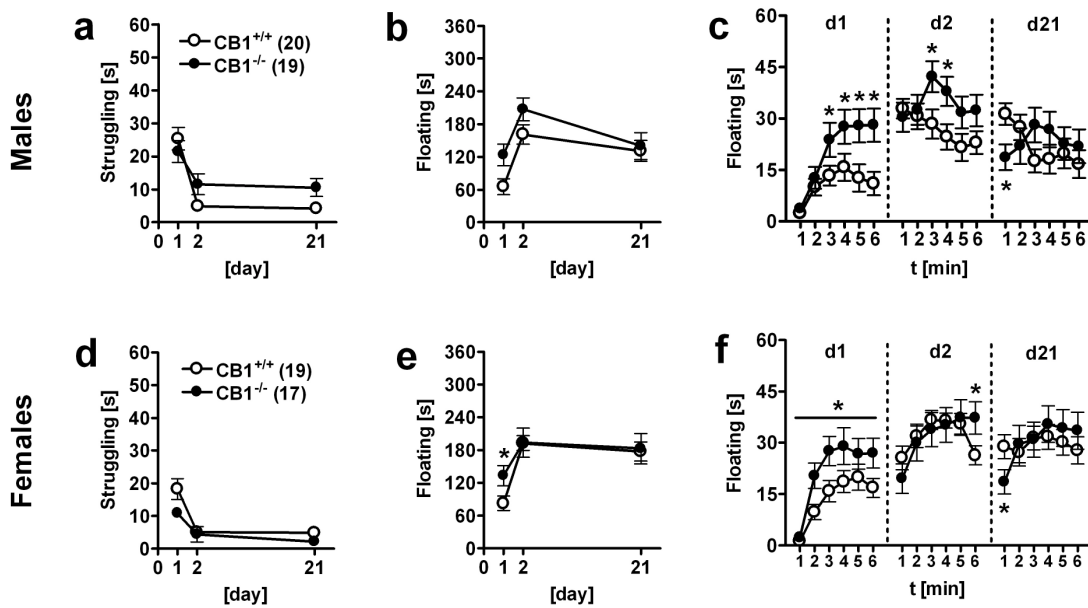
Figure 2.3.1 Behavioral response of CB1$^{+/+}$ and CB1$^{-/-}$ mice in the forced swim test. Male (**a,b,c**) and female (**d,e,f**) CB1 receptor wild-type (CB1$^{+/+}$) and null-mutant (CB1$^{-/-}$) mice were exposed to the forced swim test on day 1 (d1), day 2 (d2) and day 21 (d21). The total duration of struggling and floating time per 6 min exposure, respectively, is depicted in (**a**) and (**b**) for males and in (**d**) and (**e**) for females. The within-session floating time per 1 min interval is depicted in (**c**) for males and (**f**) for females, respectively. Data are presented as mean ± SEM for n = 17-20, each. Data of two independent experimental batches with essentially the same behavioral outcome were combined. $^{*}p < 0.05$ vs. CB1$^{+/+}$.

exposure. The higher susceptibility of CB1$^{-/-}$ mice to acquire passive stress coping strategies was substantiated by a significant *Genotype* effect for day 1 ($F_{1,71}$ = 10.7, p = 0.001). Although females and males differed in the course of floating on day 2 and day 21 (*Sex x Interval*: $F_{5,355}$ > 4.2, p < 0.001), the effects of CB1 receptor deletion on the development of floating were similar for both males and females (*Genotype x Sex x Interval*: $F_{5,355}$ < 1.9, p > 0.089). Nevertheless, we additionally analyzed floating behavior separately per sex. On day 1, male CB1$^{-/-}$ mice showed a significantly higher increase in floating over the course of the 6-min exposure than their CB1$^{+/+}$ littermates [*Genotype*: $F_{1,37}$ = 5.7, p = 0.022, *Genotype x Interval*: $F_{5,185}$ = 3.3, p = 0.007; 2-way ANOVA (*Genotype, Interval*) for repeated measures (*Interval*); Fig. 2.3.1c]. The same was the case on day 2 (*Genotype x Interval*: $F_{5,185}$ = 3.0, p = 0.013). On day 21, male CB1$^{-/-}$ mice floated less than CB1$^{+/+}$ mice during the first minute but increased their floating behavior until the end of the test, whereas CB$^{+/+}$ mice decreased their floating behavior over time (*Genotype x Interval*: $F_{5,180}$ = 6.2, p < 0.001). The phenotype of female CB1$^{-/-}$ and CB1$^{+/+}$ mice was essentially the same as that of males on day 1 (*Genotype*: $F_{1,34}$ =

5.1, $p = 0.029$), day 2 (*Genotype x Interval*: $F_{5,170} = 3.3$, $p = 0.007$) and day 21 (*Genotype x Interval*: $F_{5,170} = 2.8$, $p = 0.018$; Fig. 2.3.1f). It has to be noted, that independent of sex, CB1$^{+/+}$ but not CB1$^{-/-}$ mice usually spent more time floating during the first minute of the following FST exposure than during the last minute of the previous FST exposure.

Pharmacological blockade of CB1 receptors alters coping behavior in the FST

To assess whether the pharmacological blockade of CB1 receptors leads to similar behavioral responses in the FST as the genetic inactivation, we applied the selective CB1 receptor antagonist SR141716 to male and female C57BL/6N mice. To mimic the situation in CB1$^{-/-}$ mice, where the receptor is permanently lost, animals were injected before the FST on day 1, once again approximately 12 h later and finally before the FST on day 2 (compare Wei et al., 2004). In order to minimize acute stress responses due to the injection procedure, animals were injected 2 h before the FST.

Struggling was differently affected by pharmacological blockade than by genetic inactivation, because SR141716 treatment led to a significant increase in struggling on day 1 in both male and female mice [*Treatment*:$F_{1,44} = 20.2$, $p < 0.001$, *Treatment x Day*: $F_{1,44} = 23.8$, $p < 0.001$; 3-way ANOVA (*Treatment, Sex, Day*) for repeated measures (*Day*); Figs. 2.3.2a,d)]. Besides, female C57BL/6N mice struggled generally more than males (*Sex*: $F_{1,44} = 11.7$, $p = 0.001$), in particular on day 1 (*Sex x Day*: $F_{1,44} = 10.4$, $p = 0.002$). Independent of sex and genotype, struggling behavior was very pronounced on day 1 but almost absent on day 2 (*Day*: $F_{1,44} = 98.6$, $p < 0.001$).

Similar to the situation in CB1$^{-/-}$ mice, SR141716 treatment tended to increase total floating time at day 1 as compared to vehicle treated mice (Figs. 2.3.2b,e). Nevertheless, independent of sex, antagonist treatment altered the development of total floating time from day 1 to day 2 [*Treatment x Day*: $F_{1,44} = 12.4$, $p = 0.001$; 3-way ANOVA (*Treatment, Sex, Day*) for repeated measures (*Day*); Figs. 2.3.2b,e] reflecting the fact that SR141716 treated mice did not show a further increase of floating on day 2 as compared to day 1.
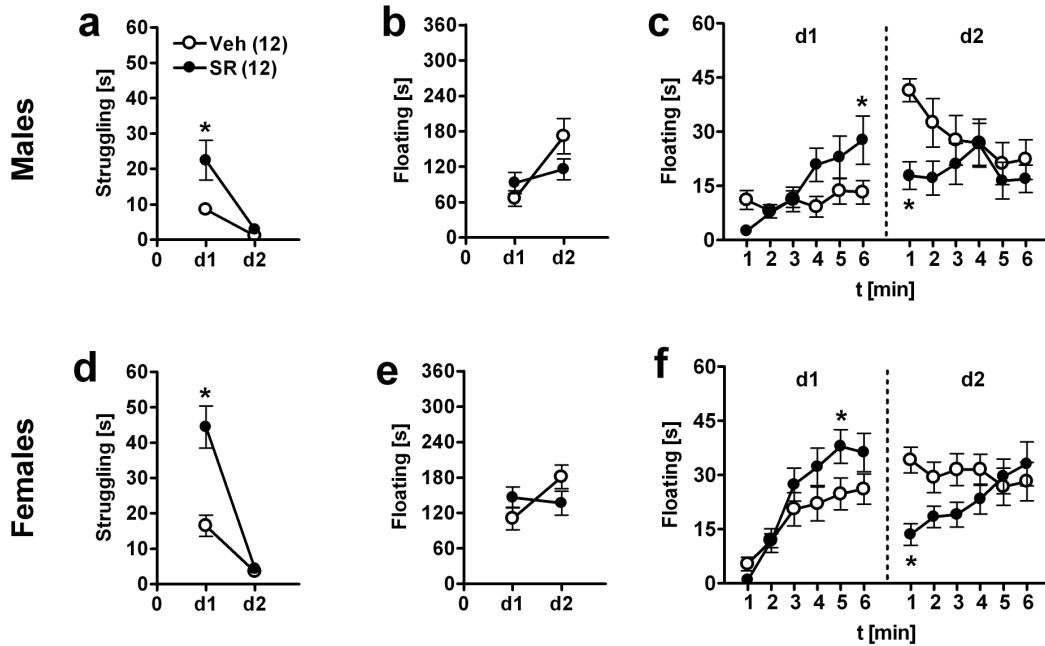
Figure 2.3.2 Effects of the CB1 receptor antagonist SR141716 on forced swimming behavior in C57BL/6N mice. Males (**a,b,c**) and females (**d,e,f**), treated with vehicle (Veh) or SR141716 (SR) (10 mg/kg i.p.), were exposed to the forced swim test on day 1 (d1) and day 2 (d2). The total duration of struggling and floating time per 6 min exposure is depicted in (**a**) and (**b**) for males and in (**d**) and (**e**) for females, respectively. The within-session floating time per 1 min interval is depicted in panel (**c**) for males and (**f**) for females, respectively. Data are presented as mean ± SEM for n = 12, each. $^{*}p < 0.05$ vs. vehicle.

Analysis of the within-session development of floating on day 1 (Figs. 2.3.2c,f) revealed that acute pharmacological blockade by SR141716 led to essentially the same phenotype as observed previously in mice with genetic deletion of CB1 receptors. There was a slight, but not significant effect of *Treatment* on day 1 [$F_{1,44} = 3.4$, $p = 0.073$; 3-way ANOVA (*Treatment x Sex x Interval*) for repeated measures (*Interval*)], a significant *Treatment x Interval* interaction ($F_{5,220} = 6.9$, $p < 0.001$) but no significant *Treatment x Sex x Interval* interaction (Figs. 2.3.2c,f). The floating response following treatment with SR141716 was more pronounced than in vehicle treated controls, especially towards the end of the stressor exposure, similar to CB1$^{-/-}$ mice. These conclusions could be confirmed in subsequent separate statistical analyses for both male [*Treatment x Interval*: $F_{5,110} = 4.7$, $p < 0.001$; 2-way ANOVA (*Treatment, Interval*) for repeated measures (*Interval*); Fig. 2.3.2c] and female mice (*Treatment x Interval*: $F_{5,110} = 2.7$, $p = 0.024$; Fig. 2f) on day 1. On day 2 floating was less pronounced following antagonist treatment, especially during the first minutes of the stressor exposure, in both male [*Treatment x Interval*: $F_{5,110} = 2.4$, $p = 0.042$; 2-

way ANOVA (*Treatment, Interval*) for repeated measures (*Interval*); Fig. 2.3.2c] and female mice (*Treatment x Interval*: $F_{5,110} = 4.7$, $p < 0.001$; Fig. 2.3.2f). This effect on day 2 was different to the situation in CB1$^{-/-}$ mice.

Apart from these discrepancies, another striking similarity between SR141716 treated animals and CB1$^{-/-}$ mice was the fact that, independent of sex, vehicle treated, but not SR141716 treated animals spent more time floating during the first minute of the FST on day 2 than during the last minute of the FST on day 1.

Effects of SR141716 on FST behavior are specific for CB1 receptors

The partial discrepancies observed between genetic inactivation and pharmacological blockade of CB1 receptors could either be due to potential developmental changes because of the life-long absence of the receptor in CB1 receptor knock-out mice, or due to influences of different environmental factors (animal housing, injection stress) between C57BL/6N mice (shipped from a commercial supplier) and CB1$^{+/+}$ and CB1$^{-/-}$ mice (housed in our own animal facility). Therefore, we repeated the antagonist experiment with a new batch of naive female CB1$^{+/+}$ and CB1$^{-/-}$ mice (Fig. 2.3.3).

In contrast to the situation in C57BL/6N mice, SR141716 failed to significantly affect struggling behavior of either CB1$^{+/+}$ or CB1$^{-/-}$ mice [*Treatment*: $F_{1,11} < 3.5$, $p > 0.09$; 2-way ANOVA (*Treatment, Day*) for repeated measures (*Day*)]. Furthermore, also in contrast to the situation in C57BL/6N mice, SR141716 treatment of CB1$^{+/+}$ mice did not result in reduced floating on day 2 as indicated by a non-significant *Treatment x Day* interaction [$F_{1,12} = 0.1$, $p = 0.73$; 2-way ANOVA (*Treatment, Day*) for repeated measures (*Day*)]. Instead, SR141716 treatment of CB1$^{+/+}$ resulted in similar increases of total floating behavior on both days similar to the situation in untreated CB1$^{-/-}$ mice.

Analyzing within-session floating behavior revealed a more pronounced floating response in SR141716 treated CB1$^{+/+}$ mice as compared to vehicle treated CB1$^{+/+}$ mice on both day 1 [*Treatment x Interval*: $F_{5,60} = 4.6$, $p = 0.001$; 2-way ANOVA (*Treatment, Interval*) for repeated measures (*Interval*); Fig. 2.3.3c] and day 2 (*Treatment x Interval*: $F_{5,60} = 3.6$, $p = 0.006$). In CB1$^{-/-}$ mice, in contrast, SR141716 failed to affect floating on either day (*Treatment x Interval*: $F_{5,55} < 0.7$, p
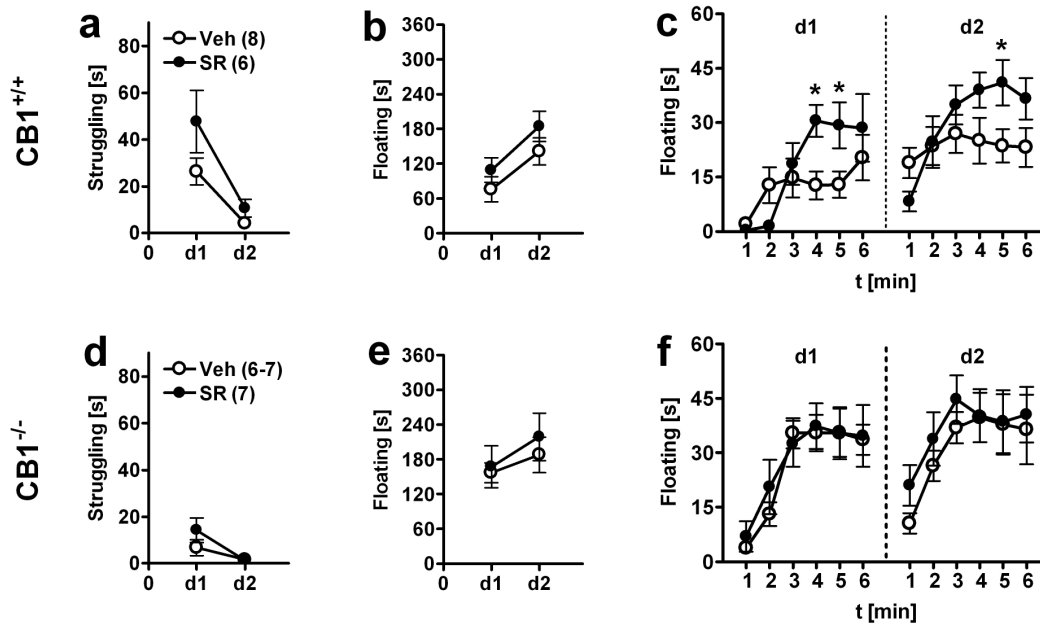
Figure 2.3.3 Effects of the CB1 receptor antagonist SR141716 on forced swimming behavior in CB1$^{+/+}$ and CB1$^{-/-}$ mice. Female CB1$^{+/+}$ (**a,b,c**) and CB1$^{-/-}$ (**d,e,f**) littermates, treated with vehicle (Veh) or SR141716 (SR) (10 mg/kg i.p.), were exposed to the forced swim test on day 1 (d1) and day 2 (d2). The total duration of struggling and floating time per 6 min exposure is depicted in (**a**) and (**b**) for CB1$^{+/+}$ mice and in (**d**) and (**e**) for CB1$^{-/-}$ mice, respectively. The within-session floating time per 1 min interval is depicted in (**c**) for CB1$^{+/+}$ mice and (**f**) for CB1$^{-/-}$ mice, respectively. Data are presented as mean ± SEM for n = 6-8, each. $^{*}p < 0.05$ vs. vehicle.

> 0.6; Fig. 2.3.3f). Accordingly, three-way ANOVA (*Genotype, Treatment, Interval*) for repeated measures (*Interval*) revealed significant interactions among all three factors both on day 1 ($F_{5,115} = 2.7$, $p = 0.026$) and on day 2 ($F_{5,115} = 3.7$, $p = 0.003$). This confirmed our observation that CB1$^{-/-}$ mice develop a more pronounced floating response than CB1$^{+/+}$ mice and demonstrated that SR141716 mediates its effects on behavioral stress coping in a highly specific manner via the CB1 receptor. Unlike the situation in C57BL/6N mice, SR141716 treatment of CB1$^{+/+}$ wild-type mice revealed essentially the same phenotype as observed previously in untreated CB1$^{-/-}$ mice on all testing days (compare Figs. 2.3.1d,e,f).

Sensitivity of FST behavior to desipramine treatment is slightly altered in CB1$^{-/-}$ mice

The effects of anxiolytic drugs have been shown to be impaired in CB1$^{-/-}$ mice (Uriguen et al., 2004), and only little is known about the interaction of the endocannabinoid system with antidepressants (Gobshtis et al., 2007). To examine if the genetic knockout of CB1 receptors leads to a different reaction or sensitivity

Figure 2.3.4 Effects of desipramine on forced swimming behavior in CB1$^{+/+}$ and CB1$^{-/-}$ mice. Female CB1$^{+/+}$ (**a,b,c**) and CB1$^{-/-}$ (**d,e,f**) littermates, treated with vehicle (Veh) or desipramine (Des) (20 mg/kg i.p.), were exposed to the forced swim test on day 1 (d1) and day 2 (d2). The total duration of struggling and floating time per 6 min exposure is depicted in (**a**) and (**b**) for CB1$^{+/+}$ mice and in (**d**) and (**e**) for CB1$^{-/-}$ mice, respectively. The within-session floating time per 1 min interval is depicted in (**c**) for CB1$^{+/+}$ mice and (**f**) for CB1$^{-/-}$ mice, respectively. Data are presented as mean ± SEM for n = 7-9, each. $^*p < 0.05$ vs. desipramine.

to antidepressants in the FST, female CB1$^{+/+}$ and CB1$^{-/-}$ mice were treated with the noradrenaline reuptake inhibitor desipramine (Fig. 2.3.4).

Desipramine treatment failed to reveal a statistically significant effect on struggling in either genotype [*Treatment*: $F_{1,28} = 3.0$, $p = 0.093$; *Genotype x Treatment*: $F_{1,28} = 0.6$, $p = 0.46$; 3-way ANOVA (*Treatment, Day, Genotype*) for repeated measures (*Day*); Figs. 2.3.4a,d]. However, desipramine treatment significantly reduced floating of both CB1$^{+/+}$ and CB1$^{-/-}$ mice [*Treatment*: $F_{1,28} = 10.9$, $p = 0.003$; 3-way ANOVA (*Treatment, Day, Genotype*) for repeated measures (*Day*) Figs. 2.3.4b,e], in particular on day 2 (*Day x Treatment*: $F_{1,28} = 16.8$, $p < 0.001$).

Analyzing within-session floating behavior on both days revealed that desipramine treatment did not affect floating of CB1$^{+/+}$ mice on day 1 (statistics not shown), but led to a significant decrease of floating on day 2 as compared to vehicle treated CB1$^{+/+}$ mice [*Treatment*: $F_{1,12} = 5.9$, $p = 0.032$, *Interval x Treatment*: $F_{5,60} = 2.5$, $p = 0.044$; 2-way ANOVA (*Treatment, Interval*) for repeated measures (*Interval*); Fig. 2.3.4c]. CB1$^{-/-}$ mice showed a slightly higher sensitivity to

desipramine treatment than their CB1$^{+/+}$ littermates. They reacted with a decrease of floating as compared to vehicle treated controls both on day 1 (*Interval x Treatment*: $F_{5,80}$ = 2.4, p = 0.045) and on day 2 (*Treatment*: $F_{1,15}$ = 9.8, p = 0.007; Fig. 2.3.4f). Treatment affected both CB1$^{+/+}$ and CB1$^{-/-}$ mice in a similar way on day 2 as illustrated by a non-significant *Genotype x Interval x Treatment* effect [$F_{5,140}$ = 1.4, p = 0.219; 3-way ANOVA (*Genotype x Interval x Treatment*) for repeated measures (*Interval*)].

Sensitivity of FST behavior to paroxetine treatment is slightly altered in CB1$^{-/-}$ mice

Treatment with the selective serotonin reuptake inhibitor paroxetine significantly increased struggling of female CB1$^{+/+}$ mice [*Treatment*: $F_{1,14}$ = 8.6, p = 0.011; 2-way ANOVA (*Treatment, Day*) for repeated measures (*Day*); Fig. 2.3.5a]. Treatment affected female CB1$^{-/-}$ mice in a similar way ($F_{1,12}$ = 4.2, p = 0.062; Fig. 2.3.5d), but this effect did not reach statistical significance.

Paroxetine treatment significantly reduced total floating time of CB1$^{+/+}$ mice [*Treatment*: $F_{1,14}$ = 15.6, p = 0.001; 2-way ANOVA (*Treatment, Day*) for repeated measures (*Day*); Fig. 2.3.5b], whereas it had no significant effect on total floating time of CB1$^{-/-}$ mice (*Treatment*: $F_{1,12}$ = 2.2, p = 0.167; *Day x Treatment*: $F_{1,12}$ = 4.2, p = 0.063; Fig. 2.3.5e).

Analysis of within-session floating behavior revealed that paroxetine treatment significantly attenuated the increase of floating in CB1$^{+/+}$ mice over the time course of the stressor exposure on day 1 [*Treatment*: $F_{1,14}$ = 8.2, p = 0.012; 2-way ANOVA (*Treatment, Interval*) for repeated measures (*Interval*); Fig. 2.3.5c]. In contrary, in CB1$^{-/-}$ mice paroxetine treatment reduced the increase of floating behavior on day 1 only during the first half of the stressor exposure, while it resulted in increased floating during the second half as compared to untreated controls (*Interval x Treatment*: $F_{5,60}$ = 9.5, p < 0.001; Fig. 2.3.5f). This discrepancy in the development of the floating response to paroxetine between treated CB1$^{+/+}$ and CB1$^{-/-}$ mice was further substantiated by a significant *Interval x Treatment x Genotype* interaction [$F_{5,130}$ = 6.8, p < 0.001; 3-way ANOVA (*Genotype x Treatment x Interval*) for repeated measures (*Interval*)]. On day 2 paroxetine treatment affected floating behavior of CB1$^{+/+}$ and CB1$^{-/-}$ mice in a similar manner
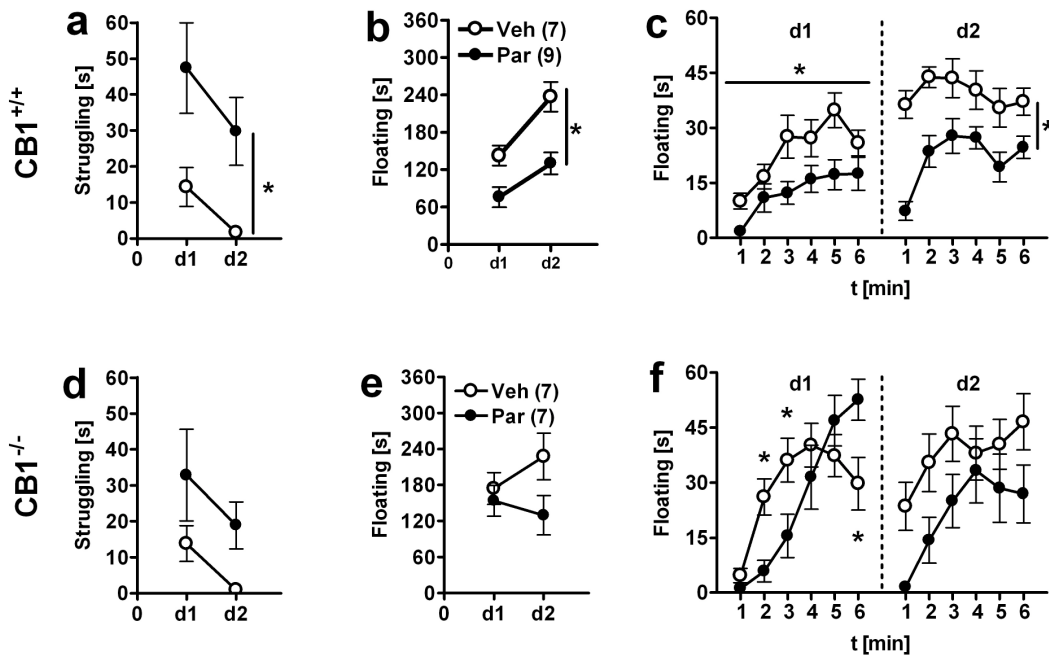
Figure 2.3.5 Effects of paroxetine on forced swimming behavior in CB1$^{+/+}$ and CB1$^{-/-}$ mice. Female CB1$^{+/+}$ (**a,b,c**) and CB1$^{-/-}$ (**d,e,f**) littermates, treated with vehicle (Veh) or paroxetine (Par) (20 mg/kg i.p.), were exposed to the forced swim test on day 1 (d1) and day 2 (d2). The total duration of struggling and floating time per 6 min exposure is depicted in (**a**) and (**b**) for CB1$^{+/+}$ mice and in (**d**) and (**e**) for CB1$^{-/-}$ mice, respectively. The within-session floating time per 1 min interval is depicted in (**c**) for CB1$^{+/+}$ mice and (**f**) for CB1$^{-/-}$ mice, respectively. Data are presented as mean ± SEM for n = 7-9, each. $^*p < 0.05$ vs. paroxetine.

[*Treatment*: $F_{1,26}$ = 13.1, p = 0.001; *Interval x Treatment x Genotype*: $F_{5,130}$ = 0.7, p = 0.617; 3-way ANOVA (*Genotype x Interval x Treatment*); Figs. 2.3.5c,f), although, if analyzed separately per genotype, paroxetine treatment significantly reduced floating of CB1$^{+/+}$ mice [*Treatment*: $F_{1,14}$ = 13.7, p = 0.002; 2-way ANOVA (*Treatment, Interval*) for repeated measures (*Interval*); Fig. 2.3.5c], whereas this effect failed to reach statistical significance in CB1$^{-/-}$ mice (*Treatment*: $F_{1,12}$ = 3.7, p = 0.078; Fig. 2.3.5f).

Basal brain monoamine oxidase (MAO) A and B enzymatic activity is not altered in CB1$^{-/-}$ mice

Behavior in the FST is known to be strongly affected by monoamine neurotransmission in the brain (Lucki and O'Leary, 2004), and the endocannabinoid system has been suggested to influence monoaminergic transmission (Tzavara et al., 2003b; Gobbi et al., 2005). Therefore, we assessed potential dysregulations of monoaminergic metabolism under basal conditions in

female $CB1^{-/-}$ mice by measuring the enzymatic activity of two major enzymes involved in the catabolism of catecholamines and serotonin, MAO-A and MAO-B (Shih et al., 2004). However, no significant genotype differences could be observed in any of the brain regions analyzed, namely cortex, striatum, hippocampus and the rest of the brain (Table 2.3.1; statistics not shown).

Table 2.3.1 Enzymatic activity of monoamine oxidase (MAO) A and B in various brain areas of female $CB1^{+/+}$ and $CB1^{-/-}$ mice under basal conditions.

	MAO-A				MAO-B			
	n	$CB1^{+/+}$	n	$CB1^{-/-}$	n	$CB1^{+/+}$	n	$CB1^{-/-}$
Cortex	7	1.19 ± 0.07	5	1.30 ± 0.09	7	8.20 ± 0.48	5	8.04 ± 0.33
Striatum	7	1.66 ± 0.08	5	1.75 ± 0.10	7	9.03 ± 0.25	5	8.92 ± 0.52
Hippocampus	13	1.59 ± 0.05	10	1.54 ± 0.06	13	8.88 ± 0.22	10	8.96 ± 0.44
Rest	7	2.17 ± 0.04	5	2.20 ± 0.05	7	7.59 ± 0.26	5	8.06 ± 0.15

Mean $\pm$ SEM [nmol/h/mg protein] Data of this Table were kindly provided by Dr. E. Borroni.

Hippocampal monoamine levels after FST are not significantly affected by the genetic deletion or by the pharmacological blockade of CB1 receptors

To further address the hypothesis that the observed phenotype of $CB1^{-/-}$ mice in the FST might be due to dysregulations of brain monoaminergic systems during activation, we measured hippocampus tissue contents of NA, 5-HT, DA and of their metabolites HVA, DOPAC and 5-HIAA of subchronically SR141716 and vehicle treated female $CB1^{-/-}$ and $CB1^{+/+}$ mice, killed 10 min after onset of the second FST exposure on day 2 (compare Fig. 2.3.3). Two-way ANOVA (*Genotype, Treatment*) revealed neither any significant *Genotype* or *Treatment* effects, nor any significant *Genotype x Treatment* interaction (Table 2.3.2; statistics not shown).

Table 2.3.2 Monoamine and metabolite concentrations in hippocampus tissue of subchronically vehicle- or SR141716-treated female CB1$^{+/+}$ and CB1$^{-/-}$ mice 10 min after FST on day 2.

		CB1$^{+/+}$				CB1$^{-/-}$		
	n	Veh	n	SR	n	Veh	n	SR
NA	8	1.75 ± 0.06	6	1.61 ± 0.12	6	1.46 ± 0.15	7	1.49 ± 0.16
DA	8	0.41 ± 0.07	6	0.40 ± 0.05	6	0.47 ± 0.08	7	0.39 ± 0.06
DOPAC	8	0.14 ± 0.02	6	0.15 ± 0.02	5	0.15 ± 0.02	7	0.16 ± 0.03
HVA	8	0.25 ± 0.03	6	0.34 ± 0.05	6	0.50 ± 0.20	6	0.36 ± 0.06
5-HT	8	10.83 ± 1.68	6	8.08 ± 2.61	6	5.98 ± 2.59	7	6.46 ± 0.87
5-HIAA	8	3.92 ± 0.6	6	3.34 ± 0.52	6	3.05 ± 0.52	7	3.66 ± 0.23

Mean ± SEM [pmol/mg tissue] Data of this table were kindly provided by Dr. H. Bächli.

Genetic deletion of CB1 receptors does not alter basal VGLUT1 mRNA expression levels

Recently, the expression level of the vesicular glutamate transporter type 1 (VGLUT1) has been demonstrated to act as a potential marker for the activity of antidepressants after chronic treatment (Moutsimilli et al., 2005). Furthermore, VGLUT1 has been shown to be co-expressed with CB1 receptors in glutamatergic neurons of the cortex and hippocampus (Monory et al., 2006). Therefore, we evaluated male CB1$^{+/+}$ and CB1$^{-/-}$ mice for their VGLUT1 mRNA expression levels under basal conditions in order to assess if a downregulation of VGLUT1 coincides with the depression-like FST phenotype in CB1$^{-/-}$ mice. However, no significant genotype differences in VGLUT1 mRNA expression could be detected in the cortex or any sub-field of the dorsal or ventral hippocampus (Fig. 2.3.6; statistics not shown).

Genetic deletion of CB1 receptors causes a downregulation of basal BDNF mRNA levels in the CA3 sub-region of the hippocampus

Downregulations of brain derived neurotrophic factor (BDNF) in the hippocampus have been associated with depression-like behavior in the FST

(Shirayama et al., 2002), and we have shown that CB1 receptor signaling influences BDNF expression (Marsicano et al., 2003; Khaspekov et al., 2004). Therefore, we evaluated male CB1^{+/+} and CB1^{-/-} mice for their BDNF mRNA expression in the hippocampus under basal conditions. Quantification of in situ hybridization signals revealed no genotype differences in the CA1 and dentate gyrus sub-fields of the hippocampus, but decreased levels of BDNF mRNA in the CA3 region of the hippocampus in CB1^{-/-} mice as compared to their CB1^{+/+} littermates. This downregulation was apparent, but not statistically significant in the dorsal hippocampus ($t_8 = 2.0$, p = 0.079; Student's t-test; Fig. 2.3.7a), and reached statistical significance in the ventral hippocampus ($t_8 = 2.5$, p = 0.037; Student's t-test; Figs. 2.3.7b,c).
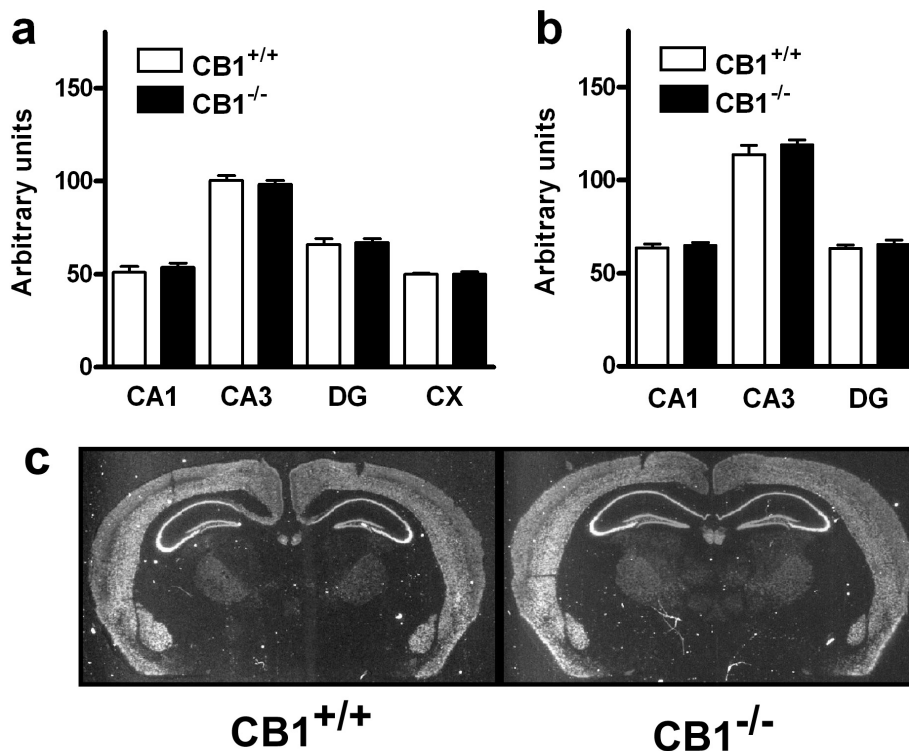
Figure 2.3.6 VGLUT1 mRNA expression levels in CB1^{+/+} and CB1^{-/-} mice. Densiometric quantification of mRNA expression levels of vesicular glutamate transporter type 1 (VGLUT1) in naïve male CB1^{+/+} and CB1^{-/-} mice for the sub-fields CA1, CA3 and dentate gyrus (DG) of the dorsal hippocampus (**a**), the cortex (CX; **a**), and the ventral hippocampus (**b**). Representative dark-field micrographs are depicted in (**c**). Data are presented as mean + SEM for n = 5, each.
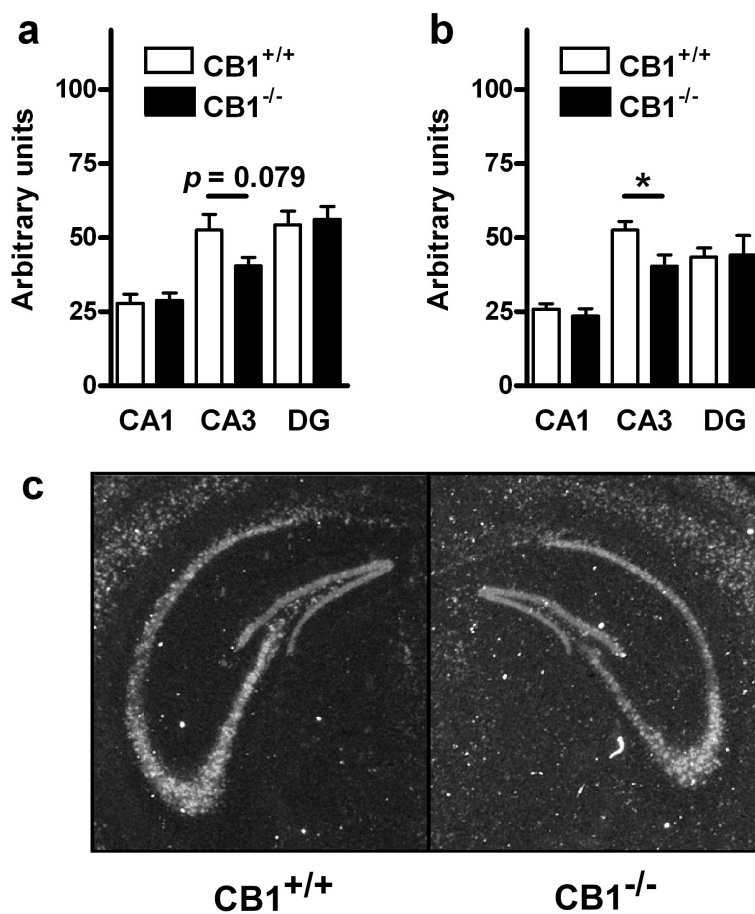
Figure 2.3.7 BDNF mRNA expression levels in CB1^{+/+} and CB1^{-/-} mice. Densiometric quantification of mRNA expression levels of brain-derived neurotrophic factor (BDNF) in naïve male CB1^{+/+} and CB1^{-/-} mice for the sub-fields CA1, CA3 and dentate gyrus (DG) of the dorsal (**a**) and ventral hippocampus (**b**). Representative dark-field micrographs of the ventral hippocampus are depicted in **c**. Data are presented as mean + SEM for n = 5, each. $^{*}p < 0.05$.

2.3.5 Discussion

We combined genetic inactivation with pharmacological blockade of CB1 receptors to elucidate the role of the endocannabinoid system in stress coping behaviors using the FST as an animal model, which is sensitive to antidepressant-like activity. The major results can be summarized as follows: (1) Impaired CB1 receptor signaling, by genetic or pharmacological means, led to increased passive stress coping behavior in the forced swim test (FST) in both male and female mice. (2) Sensitivity to the antidepressants desipramine and paroxetine in the FST was preserved in CB1$^{-/-}$ mice, although slightly altered as compared to CB1$^{+/+}$ mice. (3) CB1$^{-/-}$ mice showed no alterations of basal MAO-A and MAO-B activity, of hippocampal monoamine content after FST or of basal VGLUT1 expression. (4) CB1$^{-/-}$ mice showed reduced BDNF expression in the hippocampus. CB1$^{-/-}$ mice demonstrated increased passive coping behavior in the FST, illustrated by decreased struggling and increased floating as compared to CB1$^{+/+}$ mice (Figs. 2.3.1, 2.3.3-5). This phenotype was most prominent during the first exposure (day 1; Fig. 2.3.1) and vanished towards the third exposure (day 21), likely because of interplay between stress coping and long-term memory (West, 1990). These findings of increased floating, especially on day one, were substantiated by the pharmacological blockade of CB1 receptors in C57BL/6N mice (Fig. 2.3.2) and in CB1$^{+/+}$ mice (Fig. 2.3.3). Thus, our behavioral data implies that the blockade of CB1 receptors in mice leads to depressive-like symptoms in the FST.

We have recently shown that the CB1 receptor knockout strain generated by us shows no alterations of locomotor activity, a result, which has several times been consistently repeated in our laboratory (Marsicano et al., 2002). SR141716 administration in mice at the dose used by us was repeatedly shown not to affect locomotor activity, e.g. (Tzavara et al., 2003b; Patel and Hillard, 2006); only if applied in extremely high doses, SR141716 has been, in very rare cases, demonstrated to even increase locomotor activity [for review see (Wotjak, 2005)]. Altogether, these findings argue against locomotor effects being responsible for the increased immobility in the FST observed by us.

Our findings are in agreement with other studies in rats and mice, which have demonstrated antidepressant-like effects in the FST (i.e., reduced floating) by endocannabinoid signaling enhancing drugs, such as URB597 or AM404 (Gobbi et al., 2005; Hill and Gorzalka, 2005b). Nevertheless, these studies and others have failed so far to demonstrate any behavioral effects of either pharmacological (Gobbi et al., 2005; Hill and Gorzalka, 2005b) or genetic (Jardinaud et al., 2005) blockade of CB1 receptors in the FST. Jardinaud and co-workers, for instance, did not observe any genotype difference between CB1 receptor wild-type and deficient mice (Jardinaud et al., 2005). In contrast to our study, FST experiments were carried out under bright light by using a smaller cylinder and slightly colder water temperature. Such experimental parameters are known to influence swimming behavior (Petit-Demouliere et al., 2005). Furthermore, genetic background belongs to the most important parameters in the FST (Lucki et al., 2001), and, thus, could also account for the lack of phenotype as the knockout mice were on a different genetic background than the mice used in the present study (CD1 vs. C57BL/6N). The behavioral ineffectiveness of CB1 receptor antagonists described in the other two studies might be due to the relatively low doses used [1 mg/kg of SR141716, (Gobbi et al., 2005); 1 and 5 mg/kg of AM251; (Hill and Gorzalka, 2005b)]. Nevertheless, there are also reports which even showed decreased floating (i.e. antidepressant-like effects) in response to SR141716 treatment in rats (3 mg/kg and 10 mg/kg) (Griebel et al., 2005) and NIH Swiss mice (3 mg/kg) (Tzavara et al., 2003b). These discrepancies demonstrate the complexity of the endocannabinoid system. It seems that the effects of endocannabinoid signaling can vary significantly depending on genetic, experimental and environmental conditions. Accordingly, we also observed slightly different effects of SR141716 on struggling and floating behavior in C57BL/6N animals, which were shipped from a commercial supplier, as compared to CB1$^{+/+}$ mice, which had been backcrossed for more than six generations to C57BL/6N, but were maintained in our own animal facility (see Figs. 2.3.2-3). Furthermore, the efficiency of blocking endocannabinoid signaling, determined by the dose of antagonist used, might influence the behavioral outcome. In this context, it is worthwhile to note that SR141716 in the relatively high dose used by us (10 mg/kg) did not show any effect in CB1$^{-/-}$ mice, which excluded potential unspecific effects of the drug in the FST. Moreover, this

finding precludes a contribution of potential SR141716 sensitive non-CB1 cannabinoid receptors (Haller et al., 2002).

Regarding the fact that women are known to be more susceptible to develop depression than men (Kessler et al., 1994), we also compared male and female mice concerning their stress coping abilities in the FST. Male and female mice generally showed very similar behavioral reactions to repeated FST exposure. Furthermore, also the genetic inactivation and pharmacological blockade of CB1 receptors had similar effects on coping behavior in the FST in both sexes. This suggests that sex differences in mice appeared to be of minor biological significance in this paradigm (Figs. 2.3.1-2).

The FST is highly sensitive to elevations in monoaminergic neurotransmission as exerted by current antidepressants (Lucki and O'Leary, 2004). In this context, it is of interest that the endocannabinoid system has recently been suggested to modulate monoaminergic transmission (Gobbi et al., 2005; Tzavara et al., 2003b). Enhancing anandamide signaling via administration of URB597 was shown to increase spontaneous firing of serotonergic and noradrenergic neurons in the midbrain of rats, accompanied by increased 5-HT outflow in the hippocampus (Gobbi et al., 2005). This effect was blocked by 1 mg/kg SR141716. Surprisingly, however, treating rats with higher doses of the antagonist (3 mg/kg and 10 mg/kg) was also shown to dose dependently increase 5-HT and noradrenaline efflux in various brain regions (Tzavara et al., 2003b). Thus, in order to investigate this potential link between endocannabinoid and monoaminergic systems, we undertook two pharmacological experiments assessing the behavioral response of CB1$^{+/+}$ and CB1$^{-/-}$ mice to two different classes of antidepressants in the FST. Interestingly, CB1$^{-/-}$ mice reacted more sensitively than their wild-type littermates to desipramine (Fig. 2.3.4), a noradrenaline reuptake inhibitor, but less sensitively to paroxetine (Fig. 2.3.5), a selective serotonin reuptake inhibitor. Detailed analysis of within-session floating behavior of CB1$^{-/-}$ mice on day 1, furthermore, revealed a significant *Genotype x Treatment* interaction for paroxetine over the time course of the 6 min FST exposure (Fig. 2.3.5f). This suggested a time-dependent biphasic influence of endocannabinoid signaling on the behavioral effects exerted by the blockade of 5-HT transporters during FST on day 1. Thus, the blockade of endocannabinoid signaling seems to interfere to some extent with the actions of different kinds of

antidepressants, although CB1 receptors, in general, seem to be dispensable for the acute behavioral effects of these antidepressants. Very recently, another study with a similar rationale as ours explored the interaction between SR141716 and fluoxetine or desipramine, respectively, in the FST using female Sabra mice (Gobshtis et al., 2007). Yet, Gobshtis and co-workers could neither demonstrate an interaction between SR141716 and the antidepressant drugs, nor an effect of SR141716 (5 mg/kg) alone. Future studies have to elucidate whether the independence of antidepressant actions from endocannabinoid signaling also holds true for male mice and other kinds or different doses of antidepressants.

Our behavioral results concerning the partly different behavioral effects of antidepressants in CB1$^{-/-}$ mice prompted us to explore the function of monoaminergic systems in CB1$^{-/-}$ mice further. Dysregulations of monoaminergic transmission could become manifest in altered enzymatic activity of major catabolic enzymes for monoamines, such as monoamine oxidase (MAO) A and B (Shih, 2004). However, we found no evidence for a differential activity of MAO-A or MAO-B in various brain regions of CB1$^{-/-}$ mice under basal conditions (Table 2.3.1). Still, it is conceivable that altered monoaminergic transmission could only become apparent after strong neuronal activation and, thus, might not necessarily result in up- or downregulation of degrading enzymes such as MAO. Therefore, we also assessed monoamine contents and their metabolites in hippocampi of vehicle and SR141716 treated CB1$^{+/+}$ and CB1$^{-/-}$ mice in an activated state, after forced swimming (from the experiment depicted in Fig. 2.3.3). We did not find any statistically significant changes of monoamines or their metabolite contents between vehicle or SR141716 treated CB1$^{-/-}$ and CB1$^{+/+}$ mice (Table 2.3.2). However, alterations of synaptic monoaminergic transmission could be masked by tissue homogenization and measurement of the total content of intra- and extracellular monoamines. To help clarifying this issue in detail, it will be necessary to apply high resolution methods that are able to detect extracellular monoamine release, such as microdialysis, in the future.

Apart from the monoamine theory of depression, dysregulation of neurotrophic factors in the brain are also held responsible for the development of depression (Urani et al., 2005). A downregulation of BDNF in the hippocampus, for example, is believed to correlate with depression-like behavior, and injections of BDNF into the hippocampus have been demonstrated to lead to decreased

floating in the FST (Shirayama et al., 2002). Because we could recently demonstrate that endocannabinoid signaling via CB1 receptors regulates BDNF expression (Khaspekov et al., 2004; Marsicano et al., 2003), we aimed at investigating BDNF mRNA expression in the hippocampus of CB1$^{-/-}$ and CB1$^{+/+}$ mice. *In situ* hybridization revealed a specific downregulation of BDNF mRNA in the CA3 region of the hippocampus of CB1$^{-/-}$ mice (Fig. 2.3.7), which might, thus, be related to the depression-like FST phenotype in CB1$^{-/-}$ mice.

An up-regulation of vesicular glutamate transporter 1 (VGLUT1) mRNA expression has recently been proposed as a marker for antidepressant activity (Moutsimilli et al., 2005). This finding appears particularly interesting in light of the compelling evidence that glutamatergic dysfunction can be related to psychiatric disorders [for review see (Javitt, 2004)]. Taking into account recently accumulating evidence that CB1 receptors are, in addition to GABAergic terminals, as well prominently present on glutamatergic synapses (Monory et al., 2006; Marsicano et al., 2003), where they co-localize with VGLUT1 and influence glutamatergic transmission (Monory et al., 2006), it was reasonable to hypothesize a potential dysregulation of VGLUT1 expression in CB1$^{-/-}$ mice. Nevertheless, *in situ* hybridization of VGLUT1 mRNA in the brain revealed no alterations in CB1$^{-/-}$ mice (Fig. 2.3.6). However, this result rules out that the differences in BDNF mRNA levels simply relate to an age dependent decline in the number of neurons in CB1$^{-/-}$ mice (Bilkei-Gorzo et al., 2005).

In summary, we propose that impaired CB1 receptor signaling, which seems to compromise BDNF expression in the hippocampus, can lead to increased passive stress coping behaviors in the FST and slightly altered behavioral responses to acute antidepressant treatment. Thus, our results generally support the findings from the human rimonabant phase-III trials reporting a slightly increased percentage of patients with anxiety and depressed mood as compared to placebo controls (Despres et al., 2005; Pi-Sunyer et al., 2006; Van Gaal et al., 2005). However, in order to help define a clear pro- or anti-depressant effect of CB1 receptor blockade in rodents, it is certainly necessary to further evaluate these effects in the future in a number of additional depression-related animal paradigms.

2.4 Antidepressant-like behavioral effects of impaired cannabinoid receptor type 1 signaling coincide with exaggerated corticosterone secretion in mice

In Chapter 2.2 we have demonstrated that female CB1 receptor knockout mice display HPA axis hyperactivity under non-stress conditions. In the present Chapter we investigated whether genetically impaired CB1 receptor signaling also leads to FST stress-induced HPA axis hyperactivity and whether HPA axis disturbances in CB1 receptor knockout animals can be mimicked by the acute, subchronic or chronic pharmacological blockade of CB1 receptors. Furthermore, in Chapter 2.3 we have shown that naïve CB1 receptor knockout animals show increased floating in the FST (i.e. a pro-depressive like phenotype) and that female CB1$^{-/-}$ mice were slightly more sensitive to desipramine. In the present study, we repeated the desipramine experiment in male CB1$^{+/+}$ mice, and we compared the behavioral and neuroendocrine desipramine effects in CB1$^{-/-}$ mice to effects of the drug in mice, where CB1 receptors were blocked pharmacologically. Finally, we also investigated effects of chronic pharmacological CB1 receptor blockade on the behavioral and neuroendocrine response to the FST.

2.4.1 Summary

Hypothalamic-pituitary-adrenocortical (HPA) axis hyperactivity is associated with major depressive disorders, and treatment with classical antidepressants ameliorates not only psychopathological symptoms, but also the dysregulation of the HPA axis. Here, we further elucidated the role of impaired cannabinoid type 1 (CB1) receptor signaling for neuroendocrine and behavioral stress coping in the mouse forced swim test (FST). We demonstrate that the genetic inactivation of CB1 receptors is accompanied by increased plasma corticosterone levels both under basal conditions and at different time points following exposure to the FST. The latter effect could be mimicked in C57BL/6N mice by acute, subchronic and chronic administration of the selective CB1 receptor antagonist SR141716. Further experiments demonstrated dose-dependency of these neuroendocrine effects and

confirmed the specificity of SR1417116 actions for CB1 receptors in CB1 receptor-deficient mice. Subchronic and chronic pharmacological blockade of CB1 receptors, but not its genetic deletion, induced antidepressant-like behavioral responses in the FST that were characterized by decreased floating and/or increased struggling behavior. The antidepressant-like behavioral effects of acute desipramine treatment in the FST and the dampening effects on FST stress-induced corticosterone secretion were slightly compromised or intact in CB1 receptor-deficient mice and completely unaffected in C57BL/6N mice pre-treated with SR141716, thus indicating their independence from CB1 receptor signaling. We conclude that pharmacological blockade of CB1 receptor signaling shares antidepressant-like behavioral effects with desipramine, but reveals opposite effects on HPA axis activity.

2.4.2 Introduction

Endocannabinoids act as retrograde messengers in the brain that control the release of several neurotransmitters, including glutamate and GABA, by binding to presynaptic cannabinoid receptor type 1 (CB1) receptors (Marsicano and Lutz, 2006; Chevaleyre et al., 2006). In this manner, the endocannabinoid system functions as a neuromodulatory system to maintain the homeostasis of the brain, which is constantly challenged by physical and psychological stressors. One major neuroendocrine response to stress is the secretion of corticosterone via activation of the hypothalamic-pituitary-adrenocortical (HPA) axis. Expression of CB1 receptors occurs at different levels controlling HPA axis function. These include limbic brain regions such as the hippocampus and amygdala (Marsicano and Lutz, 1999; Mackie, 2005), the paraventricular nucleus of the hypothalamus (PVN) (Cota et al., 2003), the pituitary (Wenger et al., 1999; Pagotto et al., 2001) and the adrenal glands (Galiegue et al., 1995; Buckley et al., 1998), suggesting a multiple role of the endocannabinoid system in the regulation of the hormonal stress response. Indeed, pharmacological blockade of CB1 receptors by the selective antagonist SR141716 (rimonabant) in rodents or inactivation via gene knockout in mice resulted in increased basal and stress-induced ACTH and corticosterone levels (Manzanares et al., 1999; Uriguen et al., 2004; Barna et al., 2004; Haller et al., 2004b; Patel et al., 2004; Wade et al., 2006). However, several contradictory results have been reported, in particular with CB1 receptor null mutants (CB1$^{-/-}$), showing increased stress hormone secretion after novelty stress (Barna et al., 2004; Haller et al., 2004b), but not after saline injection (Wenger et al., 2003) or auditory stress (Fride et al., 2005). Similarly, CB1$^{-/-}$ mice were found to have either increased (Barna et al., 2004) (Chapter 2.2, Fig. 2.2.1), decreased (Uriguen et al., 2004) or similar basal corticosterone levels (Fride et al., 2005; Wade et al., 2006) as compared to wild-type mice. Important factors determining these differences could include the nature of the stressor and the genetic background. Also potential compensatory mechanisms in CB1$^{-/-}$ mice due to the life-long absence of CB1 receptors in these animals have to be considered as recent work from Wade and co-workers suggested (Wade et al., 2006). Thus, in order to establish a general role of endocannabinoid signaling for HPA axis

function, it seems essential to substantiate findings in CB1$^{-/-}$ mice with those following pharmacological blockade of CB1 receptors in the respective background strain to exclude potential developmental adaptations.

Increased HPA axis activity is known as a risk factor for depression in humans (Holsboer, 2000; De Kloet et al., 2005). Accordingly, normalization of heightened HPA axis activity seems to be linked to the clinical efficacy of antidepressant treatment (Holsboer, 2000; Ising et al., 2007). CB1 receptor deficient mice display a variety of behavioral and neurovegetative symptoms, which are reminiscent of the melancholic subtype of depression (Hill and Gorzalka, 2005a). These include, among others, hyperactivity of the HPA axis as evidenced by increased CRH expression in the PVN (Cota et al., 2003) (Chapter 2.2, Fig. 2.2.3), increased corticosterone and ACTH release (Barna et al., 2004; Haller et al., 2004b) (Chapter 2.2, Fig. 2.2.1), attenuated low-dose dexamethasone suppression (Chapter 2.2, Fig. 2.2.1) and diminished glucocorticoid receptor (GR) expression in the hippocampus (Chapter 2.2, Fig. 2.2.5). On the other hand, pharmacological blockade of CB1 receptors exerted antidepressant-like effects in mice in the tail suspension and forced swim tests (Shearman et al., 2003; Tzavara et al., 2003b; Griebel et al., 2005), which suggested that despite unfavorable neuroendocrine effects, CB1 receptor antagonists could actually have certain antidepressant-like potential (Witkin et al., 2005b). This discrepancy between behavioral and neuroendocrine effects of CB1 receptor blockade or deficiency has not yet been thoroughly investigated, particularly not under a chronic treatment schedule, which best relates to the usual long-term application of antidepressants in humans.

To better characterize the potential benefits or costs of CB1 receptor impairment in terms of antidepressant-like behavioral effects and concomitant hyperactivity of the HPA axis, we investigated the consequences of acute, subchronic and chronic SR141716 treatment in combination with the genetic inactivation of CB1 receptors on behavioral and neuroendocrine measures in the forced swim test (FST), a standard test for assessing antidepressant-like effects in rodents (Cryan and Holmes, 2005), and we evaluated the results in relation to those of desipramine treatment.

2.4.3 Materials and Methods

Animals

Mice were kept under standard conditions with food and water *ad libitum*. They were housed in groups, either in the animal facility of the University of Texas Southwestern Medical Center under a regular 12 h : 12 h light/dark schedule (lights on at 07:00 am), or in the animal facility of the Max Planck Institute of Psychiatry under a 12 h : 12 h inverted light/dark schedule (lights on at 09:00 pm). C57BL/6N mice were purchased from Charles River (Germany or USA). Cannabinoid receptor type 1 null-mutant (CB1$^{-/-}$) mice and their wild-type (CB1$^{+/+}$) littermates derived from heterozygous breeding pairs, which were backcrossed to the C57BL/6N background for at least 6 generations. They were generated and genotyped as described (Marsicano et al., 2002). Age of tested animals ranged between 2 and 4 months. Female mice were not controlled for their estrus cycle. Initial experiments, where the estrus cycle phase had been determined by vaginal smears, revealed a similar distribution between the different phases in female CB1$^{+/+}$ and CB1$^{-/-}$ mice (data not shown). Animal experiments were conducted in accordance with the *Guide for the Care and Use of Laboratory Animals* of the Government of Bavaria (Germany) or were approved by the UT Southwestern's Institutional Animal Care and Use Committee (TX, USA). Two weeks before the experiments, animals were separated and singly housed.

Treatment of blood samples and hormone analysis

Trunk blood was collected and plasma corticosterone levels measured as previously described in the Materials and Methods section of Chapter 2.2.

Drugs

Drugs were prepared and injected as previously described in the Materials and Methods section of Chapter 2.3.

Forced swim test (FST)

The FST was carried out as previously described in the Materials and Methods section of Chapter 2.3. After the FST, animals were placed in their home cages and were left undisturbed until 10 min, 20 min, 30 min or 120 min after the onset of the stressor, when they were killed by decapitation after short isoflurane anesthesia within 45 sec after touching the home cage.

Statistical analysis

Data were analyzed for multiple comparisons using one-, two- or three-way analysis of variance (ANOVA) followed by *post-hoc* Newman-Keuls Multiple Comparison Test. Homogeneity of

variance in independent groups was analyzed using the Levene test and data were subjected to logarithmic or square-root transformation, where required. For two-group comparisons unpaired Student's *t*-test was used. Differences were considered statistically significant if $p < 0.05$. Data are presented as mean ± SEM. Sample sizes are reported in figure legends.

Experiments

All experiments were performed during the second half of the dark phase of the circadian rhythm of the animals under red-light conditions. Each time-point assessed represented an independent batch of male or female animals. Experiments and sample analysis were performed blind to the animals' treatment or genotype. Experimental graphic charts of the following experiments, depicting the respective time-points of treatment, blood sampling and FST exposure, are shown schematically in the corresponding figures.

Experiment 1: Corticosterone secretion following the pharmacological blockade of CB1 receptors

Male C57BL/6N mice (Charles River, USA) were randomly assigned to one out of four treatment groups, which were injected with vehicle or SR141716 (0.5, 2, 10 mg/kg i.p) and returned to their home cages. One hour later animals were either killed directly to obtain injection stress-induced control corticosterone levels or exposed to the FST for 6 min and killed 10 min after stressor onset in order to assess the acute effects of SR141716 on immediate FST stress-induced corticosterone levels (compare corresponding Fig. 2.4.1). The dose of 10 mg/kg SR141716 was classified as the most potent dose with respect to injection stress- and FST stress-induced corticosterone secretion and was applied in all further experiments.

Experiment 2: CB1 receptor specificity of SR141716 effects

One hour after injection with vehicle or SR141716 (10 mg/kg i.p.) male and female CB1$^{+/+}$ and CB1$^{-/-}$ mice were subjected to the FST and killed 10 min after stressor onset (compare the corresponding Fig. 2.4.2).

Experiment 3: Time course of FST stress-induced corticosterone secretion in CB1 receptor mutant mice

Because of ethical reasons and because of the shortage of genetically altered CB1$^{+/+}$ and CB1$^{-/-}$ mice, in *Experiment 3* we determined stress hormone levels of animals that had previously undergone repeated forced swimming and whose behavior had previously been reported (Chapter 2.3, Fig. 2.3.1). In *Experiment 3* male and female CB1$^{+/+}$ and CB1$^{-/-}$ mice that had been repeatedly exposed to the FST (day 1, FST-1; day 2, FST-2; and day 21, FST-3) were killed 30 min or 120 min after the last stressor onset (FST-3 on day 21; compare corresponding Fig. 2.4.3). All time-point groups (basal, 30 min after FST-3 and 120 min after FST-3) represent independent batches of

mutant mice, which were bred and exposed to experiments within a time-period of 6 months. They were all housed identically and care was taken to expose all 3 independent batches of mice to identical environmental and experimental conditions.

Two *control experiments* were performed in order to evaluate whether or not repeated FST exposure leads to an adaptation of the corticosterone response following the stressor. In the *first control experiment* three groups of male C57BL/6N mice (Charles River, USA) were either once (day 1), twice (day 1 and day 2), or repeatedly (day 1, day 2 and day 21) exposed to the FST and killed 10 min after the last stressor onset, on day 1, day 2 or day 21. In the *second control experiment* naive male CB1$^{+/+}$ and CB1$^{-/-}$ mice were exposed to the FST on day 1 and were killed 30 min after stressor onset for assessment of corticosterone and later comparison with corticosterone levels derived from CB1$^{+/+}$ and CB1$^{-/-}$ mice following repeated FST exposure (*Experiment 3*).

Experiment 4: Time course of FST stress-induced corticosterone secretion following pharmacological blockade of CB1 receptors

Male and female C57BL/6N animals (Charles River, Germany) were exposed twice to the FST on two consecutive days (day 1, FST-1; and day 2, FST-2) and were injected with vehicle or SR141716 (10 mg/kg i.p.) three times, 2 h before FST-1 on day 1, again 12 h later, and last 2 h before FST-2 on day 2 (compare corresponding Fig. 2.4.4), according to an established treatment schedule for the detection of antidepressant-like effects in mice (Wei et al., 2004). Mice were killed 30 or 120 min after the last stressor onset (FST-2, day 2). For baseline stress hormone levels, male and female C57BL/6N mice were repeatedly injected with vehicle or SR141716 according to the same treatment schedule as mentioned above (three injections: once on day 1, again 12 h later, and last on day 2). They were killed 2 h after the last injection on day 2. The time-point of SR141716 injection (2 h before FST, instead of 1 h before FST used in *Experiments 1* and *2*) was chosen because we wanted to minimize residual effects of injection stress on later blood sampling or later FST exposure. Accordingly, we had recently found that this injection schedule most accurately mimicked behavior of CB1$^{-/-}$ mice in the FST (compare Fig. 2.3.3, Chapter 2.3).

Experiment 5: Behavioral and neuroendocrine effects of desipramine treatment in CB1 receptor mutant mice in response to the FST

Male CB1$^{+/+}$ and CB1$^{-/-}$ mice were exposed twice to the FST on two consecutive days (day 1, FST-1; day 2, FST-2) and were injected with vehicle or desipramine (20 mg/kg i.p.) three times, 1 h before FST-1 on day 1, once again 12 h later, and last 1 h before FST-2 on day 2 (compare corresponding Fig. 2.4.5), according to an established treatment schedule for detecting antidepressant-like behavioral effects in the FST (Wei et al., 2004). Mice were killed 20 min after the last stressor onset (FST-2 on day 2) because we wanted to investigate desipramine suppressing effects on forced swim stress-induced corticosterone secretion, and these effects had previously been demonstrated for exactly this time-point after FST stress (Conti et al., 2002).

Experiment 6: Effects of pharmacological blockade of CB1 receptors on behavioral and neuroendocrine consequences of desipramine treatment in response to the FST

Male C57BL/6N mice (Charles River, Germany) were exposed twice to the FST on two consecutive days (day 1, FST-1; day 2, FST-2) and injected with vehicle or desipramine (20 mg/kg i.p.) three times, 1 h before FST-1 on day 1, once again 12 h later, and last 1 h before FST-2 on day 2. In addition, mice were pre-treated with vehicle or SR141716 (10 mg/kg; i.p.) three times, 1 h before each vehicle or desipramine treatment (i.e., 2 h before FST-1 on day 1, once again 12 h later, and last 2 h before FST-2 on day 2) resulting in four treatment groups (Veh-Veh, Veh-DMI, SR-Veh, SR-DMI; compare corresponding Fig. 2.4.6). Mice were killed 20 min after the last stressor onset (FST-2 on day 2) in order to determine desipramine suppressing effects on corticosterone secretion (compare *Experiment 5*).

Experiment 7: Neuroendocrine consequences of chronic pharmacological blockade of CB1 receptors

Male C57BL/6N mice (Charles River, Germany) were chronically pre-treated with vehicle or SR141716 (10 mg/kg; i.p.) with one injection per day for 10 days (*Inj-1-10*). Towards the end of that period, at day 10, mice were injected twice (with 12 h in between), in order to maintain the same injection schedule during these last two days as that used for the subchronic SR141716 experiments described in *Experiments 4* and *6.* Mice were killed 2 h after the last injection (*Inj-11*) at day 10 for corticosterone assessment and direct comparison with injection stress-induced corticosterone secretion after subchronic SR141716 treatment from *Experiment 4*. For the last injection both pre-treated groups (vehicle and SR141716) were randomly assigned to one out of two treatment groups, which we acutely challenged with either vehicle or SR141716 (10 mg/kg i.p.) injection, thus resulting in a total of four groups (Veh-Veh, Veh-SR, SR-Veh, SR-SR; compare corresponding Fig. 2.4.7).

Experiment 8: Behavioral and neuroendocrine consequences of chronic pharmacological blockade of CB1 receptors in response to the FST

Male C57BL/6N mice (Charles River, Germany) were chronically injected with vehicle or SR141716 (10 mg/kg i.p.) daily for 10 days (*Inj-1-11*) as described for *Experiment 7*. Towards the end of that period mice were exposed twice to the FST, on day 9 (FST-1) and again on day 10 (FST-2; compare corresponding Fig. 2.4.8). The injection schedule with three injections during these last two days was the same as that used for the subchronic SR141716 experiments described in *Experiment 4* and *6*. Animals were killed 30 min after the last stressor onset on day 10 (FST-2) in order to allow for a direct comparison with the corticosterone secretion levels after subchronic dosing from *Experiment 4*, which had shown that SR141716 exerted its strongest corticosterone elevated effect at this time-point after FST stress.

2.4.4 Results

Experiment 1: Pharmacological blockade of CB1 receptors by SR141716 results in increased corticosterone secretion in male C57BL/6N mice

Pharmacological blockade of CB1 receptors with SR141716 (0.5, 2, 10 mg/kg) dose-dependently increased plasma corticosterone levels following injection stress without or with subsequent FST exposure [*Treatment*: $F_{3,44}$ = 15, *p* < 0.001; 2-way ANOVA (*Stress, Treatment*); Fig. 2.4.1]. *Post hoc* analyses revealed that 2 mg/kg (*p* < 0.01) and 10 mg/kg (*p* < 0.001) were effective in elevating injection stress-induced corticosterone levels, whereas only the highest dose of 10 mg/kg was able to further elevate FST stress-induced corticosterone secretion as compared to the respective vehicle-treated group (*p* < 0.05). As compared to respective injection stress-induced control levels, FST stress itself led to a further increase in corticosterone secretion (*Stress*: $F_{1,44}$ = 97.1, *p* < 0.001) in
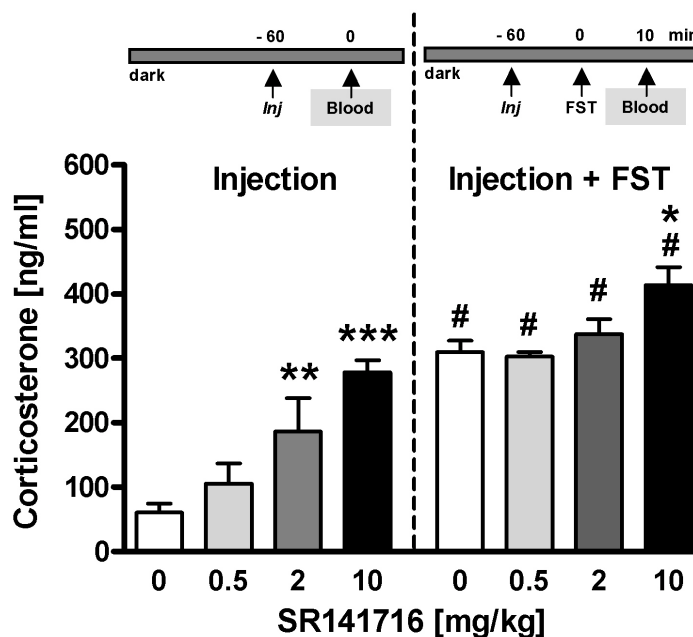
Figure 2.4.1 Acute pharmacological blockade of CB1 receptors dose-dependently increases injection stress- and forced swim test (FST) stress-induced corticosterone secretion. Experiment 1: Male C57BL/6N mice were acutely treated (Injection = *Inj*) with vehicle (0 mg/kg i.p.) or SR141716 (0.5, 2, 10 mg/kg i.p.). One hour later, half of the animals were killed for blood sampling (Blood) without further stressor exposure (Injection), the other half was exposed to the FST and killed 10 min after FST stressor onset (Injection + FST). n = 6-7 per group; [*]*p* < 0.05, [**]*p* < 0.01, [***]*p* < 0.001 vs. respective vehicle group (0 mg/kg). [#]*p* < 0.05 vs. respective injection stress control group (Injection).

all groups, independent of treatment (*Treatment x Stress*: $F_{3,44}$ = 1.9, *p* = 0.147).

Experiment 2: Effects of SR141716 on FST stress-induced corticosterone secretion in male and female CB1 receptor-deficient mice

In order to determine the specificity of SR141716 for CB1 receptors and to compare pharmacological effects with the effects of genetic deletion of CB1 receptors on stress-induced corticosterone secretion, we injected CB1$^{+/+}$ and CB1$^{-/-}$ mice with vehicle or the most potent dose of SR141716 (10 mg/kg) before exposure to the FST. Additionally, we conducted the experiment in male and female mice, to assess whether neuroendocrine CB1 receptor effects were sex-dependent. Three-way ANOVA (*Genotype, Treatment, Sex*) revealed a significant effect of *Genotype* ($F_{1,88}$ = 4.27, *p* < 0.05) reflecting the fact that CB1$^{-/-}$ mice in general showed higher corticosterone secretion than their CB1$^{+/+}$ littermates (Figs.

Figure 2.4.2 Acute pharmacological blockade of CB1 receptors increases forced swim test (FST) stress-induced corticosterone secretion in CB1$^{+/+}$ but not in CB1$^{-/-}$ mice. Experiment 2: Male (**a**) and female (**b**) CB1 receptor wild-type (CB1$^{+/+}$) and knockout (CB1$^{-/-}$) mice (n = 8-16 per group) were treated (Injection = *Inj*) with vehicle (Veh) or SR141716 (SR; 10 mg/kg i.p.) 1 h before FST exposure. Mice were killed 10 min after stressor onset, and trunk blood was collected for measurements of plasma corticosterone levels. Note that SR141716 caused a significant increase in corticosterone in CB1$^{+/+}$ mice without affecting the already elevated corticosterone levels in CB1$^{-/-}$ mice. *p* < 0.05 vs. vehicle-treated CB1$^{+/+}$ mice.

2.4.2a,b) following FST exposure. These effects were virtually identical to the effects of the pharmacological blockade of CB1 receptors in CB1$^{+/+}$ mice (*Treatment*: $F_{1,88}$= 5.78, *p* < 0.05; Figs. 2.4.2a,b). A significant *Treatment x Genotype* interaction ($F_{1,88}$= 5.32, *p* < 0.05) reflects the fact that SR141716 exerted its effects only in CB1$^{+/+}$ mice, while it had no effect in CB1$^{-/-}$ mice, thus demonstrating the specificity of SR141716 for CB1 receptors. Corticosterone elevation was similar in male and female mice, underlined by a non-significant *Treatment x Genotype x Sex* interaction ($F_{1,88}$= 0.78, *p* = 0.38), but in general, females showed higher corticosterone levels than males (*Sex*: $F_{1,88}$= 24.1, *p* < 0.001).

Experiment 3: Time course of FST stress-induced corticosterone secretion in male and female CB1 receptor mutant mice

Having confirmed the specificity of SR141716 and the effect of CB1 receptor blockade on the immediate FST stress-induced corticosterone secretion 10 min after onset of the stressor, we also wanted to investigate the effects of genetic inactivation on the time course of FST stress-induced corticosterone secretion. In addition, we also determined basal corticosterone levels in unstressed CB1 receptor mutant mice at the same time of the circadian rhythm at which the stress experiments had been performed.

In general, FST exposure of CB1$^{+/+}$ and CB1$^{-/-}$ mice led to a significant rise in corticosterone secretion 30 min after stressor onset, which returned to baseline levels after 120 min [*Time*: $F_{2,101}$ = 110.1, *p* < 0.001; 3-way ANOVA (*Genotype, Sex, Time*); Figs. 2.4.3a,b]. The genetic deletion of CB1 receptors increased corticosterone secretion 30 min after stressor onset as compared to wild-type controls (*Genotype*: $F_{1,101}$ = 26.3, *p* < 0.001; *Genotype x Time*: $F_{2,101}$ = 18.1, *p* < 0.001), similarly to what we previously observed 10 min after FST stressor onset (Fig. 2.4.2). Males and females showed similar levels of corticosterone secretion (*Sex*: $F_{1,101}$ = 0.006, *p* = 0.938), independent of genotype (*Genotype x Sex*: $F_{1,101}$ = 0.05, *p* = 0.823) and time point after stressor exposure (*Genotype x Time x Sex*: $F_{2,101}$ = 0.568, *p* = 0.569).
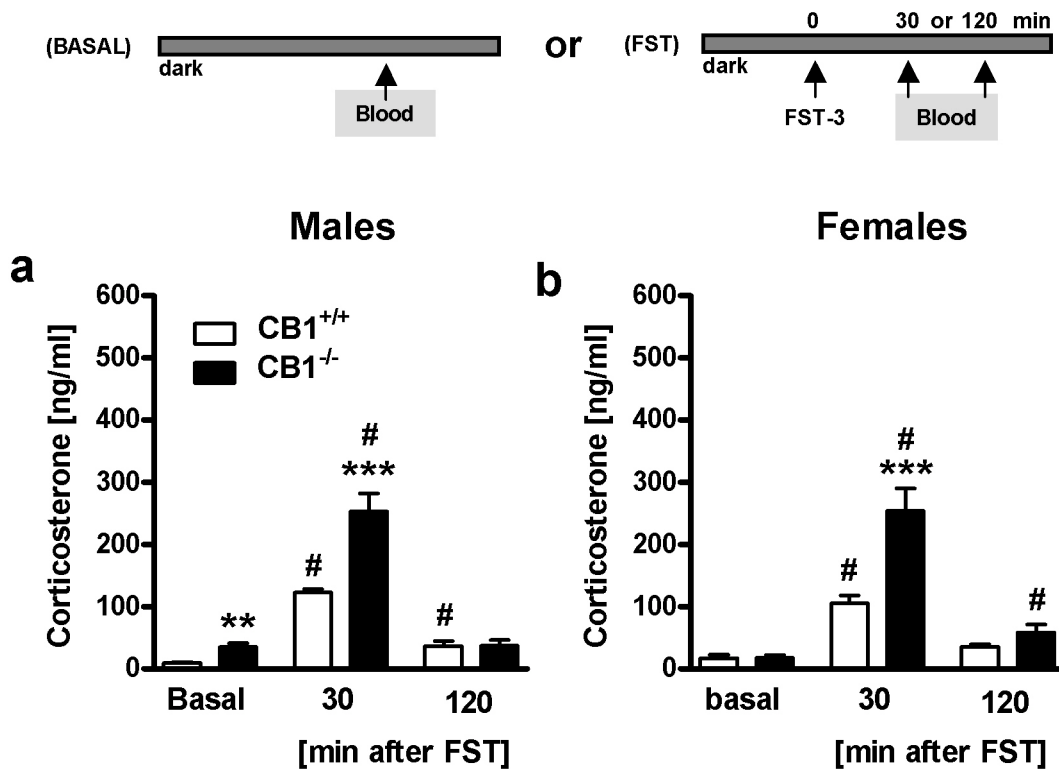
Figure 2.4.3 Genetic deletion of CB1 receptors enhances basal and forced swim test (FST) stress-induced corticosterone secretion in a time-dependent manner. Experiment 3: Male (**a**) and female (**b**) CB1 receptor wild-type (CB1$^{+/+}$) and knockout (CB1$^{-/-}$) mice (n = 7-13 per group) were either killed under basal conditions (Basal) or were exposed to the FST (FST-3; for details see Methods) and were killed 30 min or 120 min after onset of the stressor for plasma corticosterone measurements. $^{**}p < 0.01$, $^{***}p < 0.001$ vs. respective CB1$^{+/+}$ group; $^{#}p < 0.05$ vs. respective basal group.

If analyzed separately for male and female mice, *post hoc* analyses following two-way ANOVA (*Genotype, Time*) revealed that only male, but not female, CB1$^{-/-}$ mice displayed elevated corticosterone levels as compared to their wild-type littermates under basal conditions ($p < 0.01$), whereas both male and female CB1$^{-/-}$ mice displayed elevated corticosterone levels 30 min after stressor onset ($p < 0.001$; Figs. 2.4.3a,b), but not 120 min after stressor onset as compared to their CB1$^{+/+}$ littermates at the respective time point. Furthermore, while both male and female mice showed generally elevated corticosterone levels as compared to basal conditions 30 min after stressor onset ($p < 0.001$; Figs. 2.4.3a,b), only male CB1$^{+/+}$ and female CB1$^{-/-}$ mice still showed elevated corticosterone levels 120 min after stressor onset as compared to their respective baseline controls ($p < 0.05$).

As mentioned in the Methods section, above data derived from animals

which have been exposed to the FST already twice before. Therefore, we conducted two control experiments in order to ensure that repeated FST exposure did not confound the data due to occurring habituation of the corticosterone in response to repeated FST exposure. In the first *control experiment* we could demonstrate that repeated FST exposure of male C57BL/6N mice on day 1 (FST-1), day 2 (FST-2) and day 21 (FST-3) led to an adaptation of floating behavior, but not of corticosterone secretion. Mice floated significantly longer on day 2 (219.8 ± 22.33 s) and day 21 (164.2 ± 24.12 s) than on day 1 (109.4 ± 21.35 s) [*Day*: $F_{2,24}$ = 5.9, $p < 0.01$; one-way ANOVA (*Day*); n = 8-9 per group]. However, these behavioral adaptations were not paralleled by similar changes in corticosterone secretion assessed 10 min after stressor onset [day 1: 246.3 ± 17.62 ng/ml; day 2: 228.3 ± 9.97 ng/ml; day 21: 206.5 ± 12.95 ng/ml; *Day*: $F_{2,23}$ = 2.1, $p = 0.15$; one-way ANOVA (*Day*); n = 8 per group]. The *second control experiment* confirmed that the increased corticosterone levels 30 min after FST stress (FST-3) observed in CB1 receptor mutant mice were not due to a potential deficit in habituation at this later time-point after repeated stressor exposure. Acute FST exposure (FST-1) revealed a significantly stronger increase in corticosterone secretion in CB1$^{-/-}$ mice than in CB1$^{+/+}$ mice 30 min after FST-1 (265.2 ± 27.56 ng/ml vs. 135.6 ± 11.18 ng/ml; n = 10 per group; t_{18} = 4.4, $p < 0.001$; Student's t-test), which resembles our findings obtained 30 min after repeated FST (FST-3). Furthermore, neither CB1$^{+/+}$ nor CB1$^{-/-}$ mice from *Experiment 3* showed any habituation of the corticosterone response following repeated FST, because the corticosterone response of both CB1$^{+/+}$ mice (t_{20} = 1.1, $p = 0.29$) and CB1$^{-/-}$ mice (t_{18} = 0.3, $p = 0.76$) did not differ between plasma taken from mice after acute FST-1 (*second control experiment*) or repeated FST-3 (*Experiment 3*).

Experiment 4: Time course of FST stress-induced corticosterone secretion in male C57BL/6N mice subchronically treated with SR141716

To investigate whether our findings of Experiment 3 could be replicated by a pharmacological approach, we applied SR141716 in a subchronic manner (3 consecutive injections) in order to better mimic the CB1 receptor knockout phenotype. In general, FST exposure of C57BL/6N mice led to a significant rise in corticosterone secretion 30 min after FST stressor onset [*Time*: $F_{2,60}$ = 106.9, $p <$
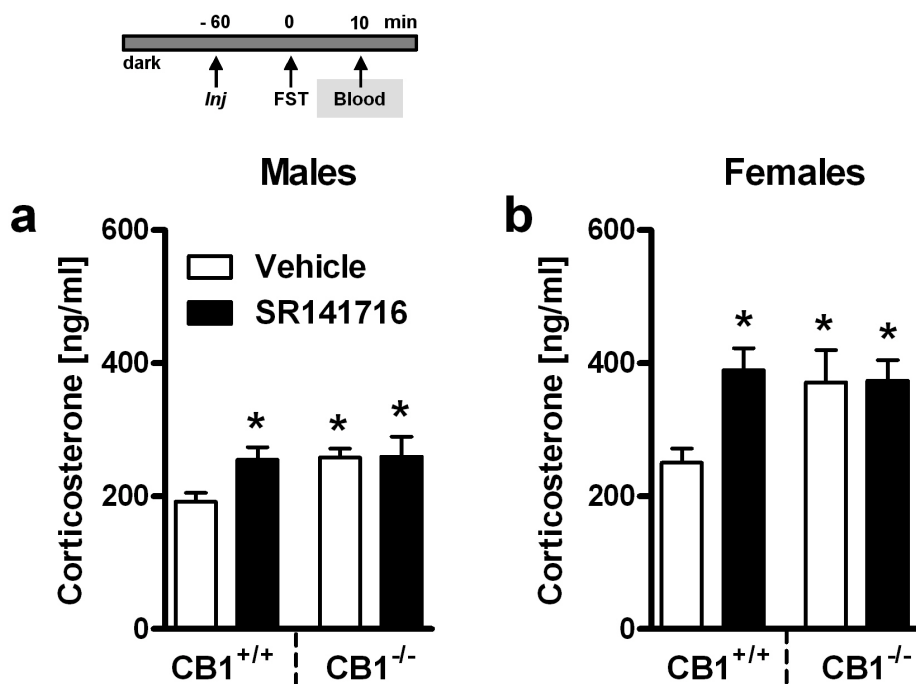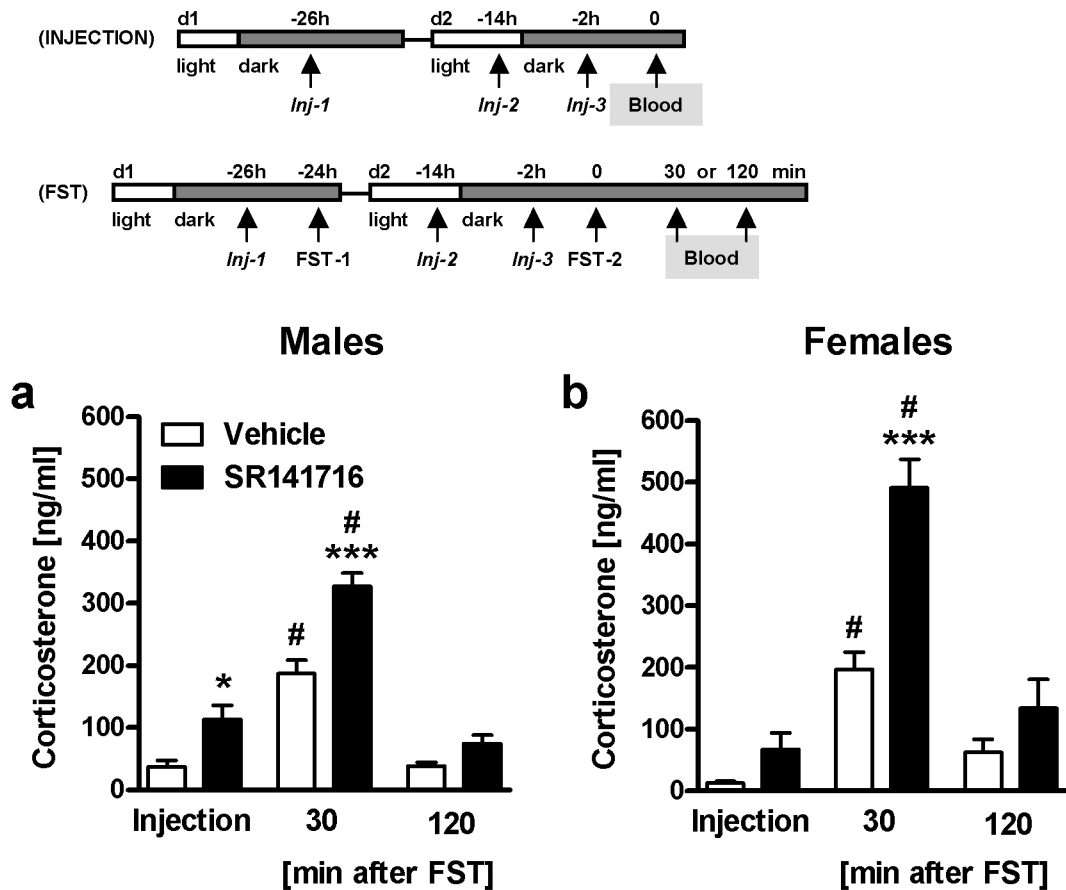
Figure 2.4.4 Subchronic pharmacological blockade of CB1 receptors enhances injection stress- and forced swim test (FST) stress-induced corticosterone secretion in a time-dependent manner. Experiment 4: Male (**a**) and female (**b**) C57BL/6N mice (n = 6 per group) were repeatedly treated (Injection = *Inj*; three times during two days) with vehicle or SR141716 (10 mg/kg i.p.) and either killed directly 2 h after the last injection (*Inj-3*) or exposed to the FST (FST-2; for details see Methods) 2 h after the last injection (*Inj-3*) and killed 30 min or 120 min after onset of the stressor for plasma corticosterone measurements. $p < 0.05$, $p < 0.001$ vs. respective vehicle group; $p < 0.05$ vs. respective injection stress control group (Injection).

0.001; 3-way ANOVA (*Treatment, Sex, Time*); Fig. 2.4.4], which was more pronounced in females than in males (*Sex x Time*: $F_{2,60} = 5.6$, $p = 0.006$). Corticosterone levels returned to injection stress-induced control levels 120 min after FST stressor onset. SR141716 treatment caused a general increase of corticosterone secretion both after injection stress and after FST stress (*Treatment*: $F_{1,60} = 55.5$, $p < 0.001$), which was most pronounced 30 min after FST stressor onset (*Treatment x Time*: $F_{2,60} = 12.2$, $p < 0.001$), similarly to what we had observed in CB1 receptor mutant mice. Females, independent of treatment, showed lower plasma levels of corticosterone than males in response to injection stress control conditions, but higher levels than males after FST stressor exposure (*Sex*: $F_{1,60} = 4.3$, $p = 0.043$; *Sex x Time*: $F_{2,60} = 5.6$, $p = 0.006$).

If analyzed separately for male and female mice, *post hoc* analyses following two-way ANOVA (*Treatment, Time*) revealed that male mice treated with SR141716 displayed elevated corticosterone levels as compared to their respective vehicle-treated controls under injection stress control conditions ($p < 0.05$) as well as 30 min after FST stressor onset ($p < 0.001$; Fig. 2.4.4a), whereas female mice treated with SR141716 only showed significantly elevated corticosterone levels as compared to their respective vehicle-treated controls 30 min after FST stressor onset ($p < 0.001$; Fig. 2.4.4b). 120 min after FST stressor onset corticosterone levels of both male and female mice treated with SR141716 or vehicle returned to levels seen in mice following injection stress only.

Experiment 5: Behavioral but not neuroendocrine effects of desipramine in response to the FST are compromised in CB1 receptor mutant mice

In order to investigate whether the corticosterone elevating effects of CB1 receptor impairment interfered with the behavioral and neuroendocrine actions of antidepressants, we subchronically treated male CB1 receptor mutant mice with desipramine before exposure to the FST.

Two-way ANOVA (*Genotype, Treatment*) of floating behavior during FST exposure on day 1 (FST-1) failed to show general *Genotype* ($F_{1,34} = 0.75$, $p = 0.39$) differences, but revealed an almost significant interaction between *Genotype* and *Treatment* ($F_{1,34} = 3.6$, $p = 0.068$) reflecting the fact that (i) vehicle-treated CB1$^{+/+}$ and CB1$^{-/-}$ mice showed similar floating behavior, and that (ii) subchronic desipramine treatment led to a significant decrease of floating in CB1$^{+/+}$ mice ($t_{20} = 2.2$, $p < 0.05$; planned pair-wise comparison using Student's t-test; Fig. 2.4.5a), but not in CB1$^{-/-}$ mice. No significant effect of desipramine treatment or geneotype was detected regarding floating behavior during FST on day 2 (FST-2), although treatment tended to decrease floating in both CB1$^{+/+}$ and CB1$^{-/-}$ mice to a similar extent (Fig. 2.4.5b; statistics not shown).

Two-way ANOVA (*Genotype, Treatment*) of struggling behavior during FST exposure on day 1 (FST-1; Fig. 2.4.5c) and day 2 (FST-2; Fig. 2.4.5d) revealed significant effects of *Treatment* on both days ($F_{1,34} > 9$, $p < 0.01$), independent of genotype (*Genotype x Treatment*: $F_{1,34} < 2.8$, $p > 0.1$), with no significant *Genotype* differences *per se* ($F_{1,34} < 3.4$, $p > 0.08$). *Post hoc* analyses revealed that

desipramine treatment led to a significant increase of struggling behavior in CB1$^{+/+}$ mice on both days ($p < 0.01$, day 1; $p < 0.05$, day 2), whereas the increase of struggling in CB1$^{-/-}$ mice was less pronounced and did not reach statistical significance on either day.
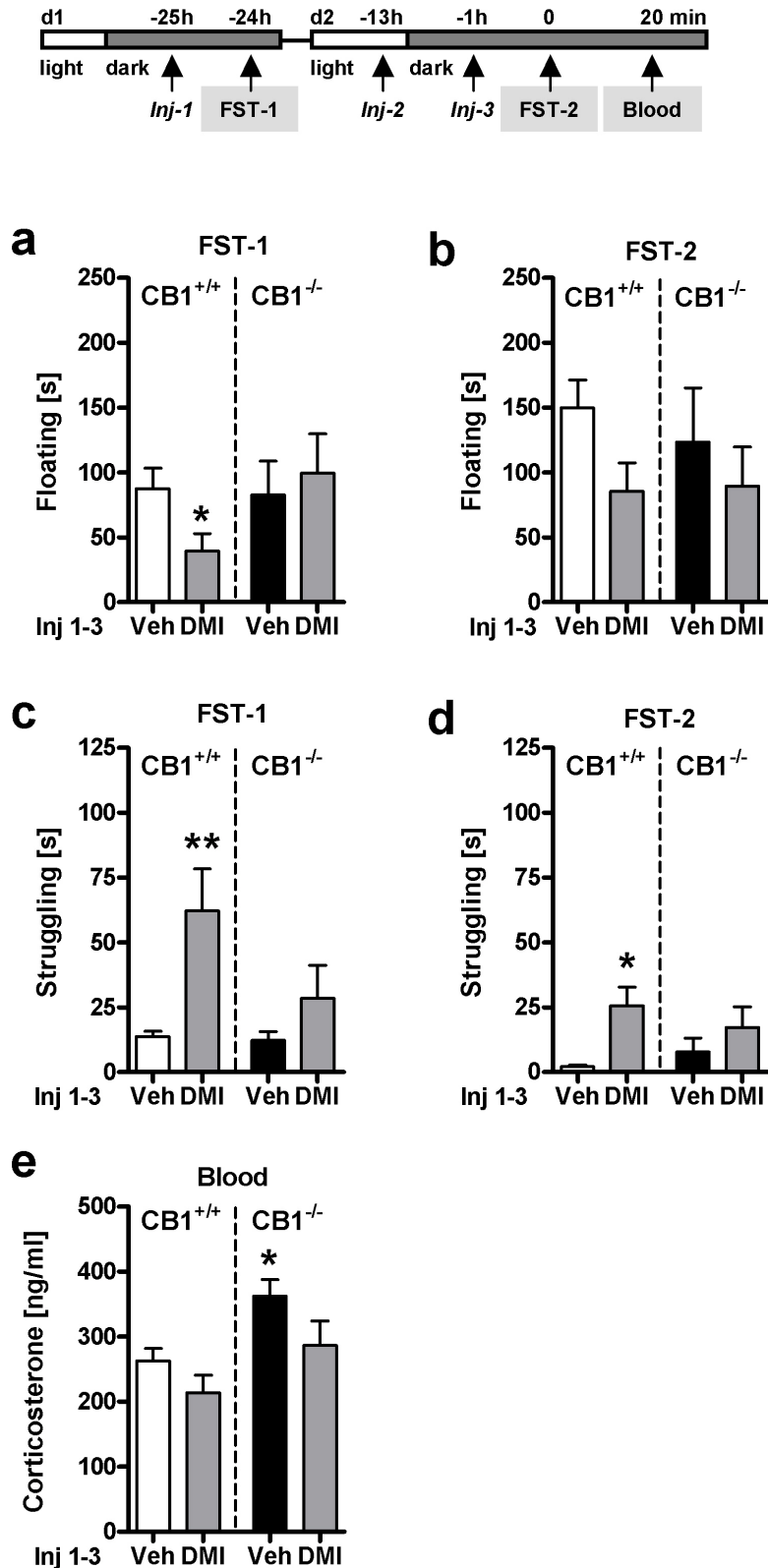
Figure 2.4.5 Behavioral and neuroendocrine responses to the forced swim test (FST) in CB1 receptor-deficient mice following treatment with desipramine. Experiment 5: Male CB1 receptor wild-type (CB1$^{+/+}$) and knockout (CB1$^{-/-}$) mice were exposed to the FST on two consecutive days (FST-1, d1; FST-2, d2) and treated (Injection = *Inj*) three times with either vehicle (Veh) or desipramine (DMI; 20 mg/kg i.p.) 1 h before the first (*Inj-1*) and the second FST (*Inj-3*) and once in between (*Inj-2*). Floating (**a**,**b**) and struggling (**c**,**d**) behavior during the entire FST exposure on day 1 (FST-1; **a**,**c**) and day 2 (FST-2; **b**,**d**). Corticosterone (**e**) levels 20 min after the onset of the second FST exposure (FST-2). Note that vehicle-treated CB1$^{-/-}$ mice showed a similar behavioral phenotype as vehicle-treated CB1$^{+/+}$ littermate controls. n = 8-12 per group; $^{*}p < 0.05$, $^{**}p < 0.01$ vs. respective vehicle-treated CB1$^{+/+}$ mice.

Two-way ANOVA (*Genotype, Treatment*) of corticosterone secretion 20 min after FST-2 onset (Fig. 2.4.5e) revealed a significant effect of *Treatment* ($F_{1,34} = 5.6$, $p < 0.05$), but no significant *Treatment x Genotype* interaction ($F_{1,34} = 0.003$, $p = 0.96$). This reflects the fact that desipramine reduced corticosterone secretion 20 min after FST in both CB1$^{+/+}$ and CB1$^{-/-}$ mice as compared to the respective vehicle-treated controls. A significant *Genotype* effect ($F_{1,34} = 4.7$, $p < 0.05$) confirmed our previous observation that CB1$^{-/-}$ mice showed generally higher corticosterone secretion than their CB1$^{+/+}$ littermates in response to FST stress. *Post hoc* analyses revealed that only vehicle-treated CB1$^{-/-}$ mice had significantly higher corticosterone levels than their wild-type littermates, whereas this difference failed to reach statistical significance between desipramine-treated CB1$^{-/-}$ and CB1$^{+/+}$ mice.

Experiment 6: Behavioral and neuroendocrine effects of desipramine in response to the FST remain unaffected by the pharmacological blockade of CB1 receptors

In order to assess, whether the slight impairment of antidepressant-like behavioral effects of desipramine seen in the previous experiment in CB1$^{-/-}$ mice represents a possible artifact of developmental changes in these mutant mice due to the life-long absence of the receptor, we repeated the experiment in C57BL/6N mice, but this time under the subchronic pharmacological blockade of CB1 receptors.
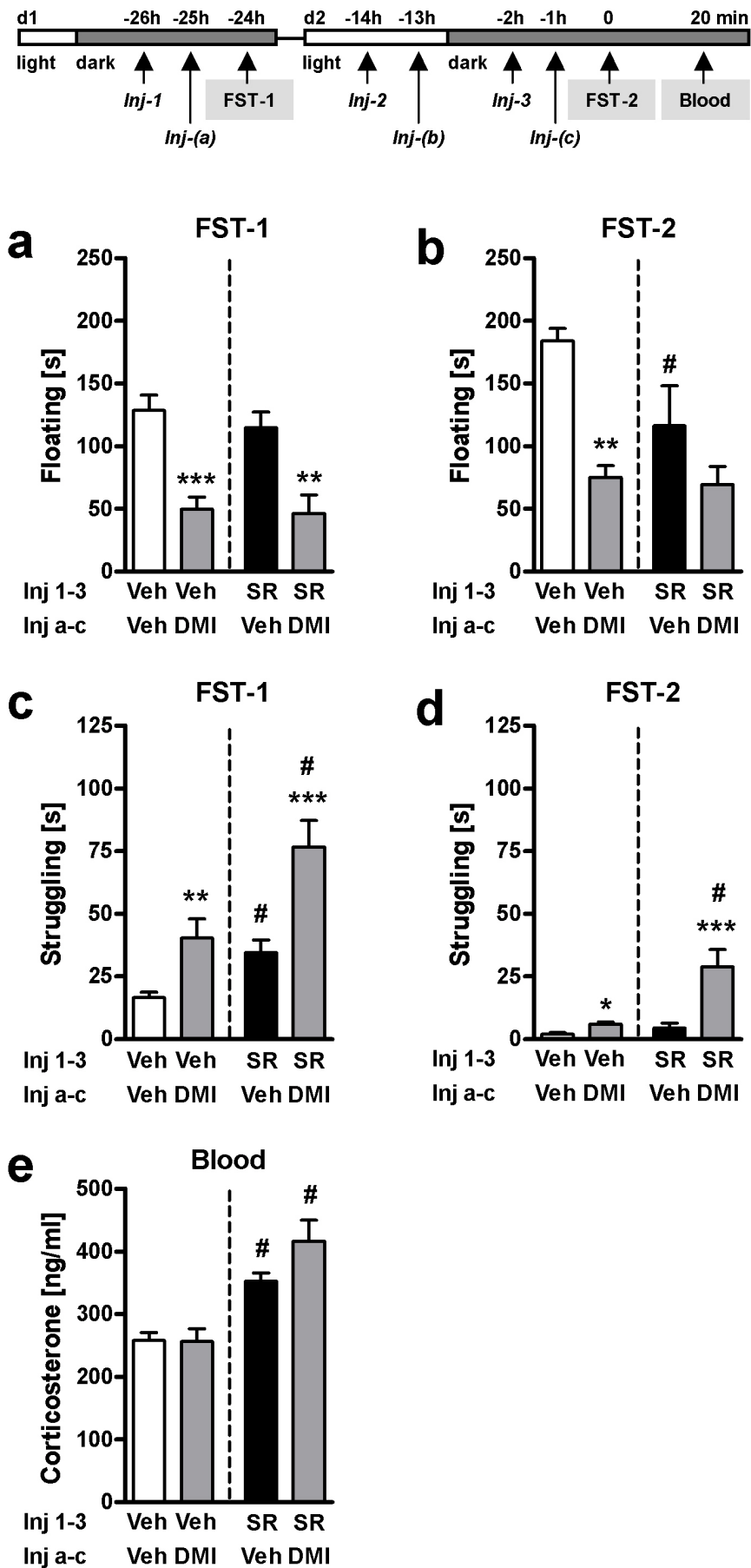
Figure 2.4.6 Lack of interaction between desipramine and SR141716 treatment in C57BL/6N mice. Experiment 6: Male C57BL/6N mice were exposed to the FST on two consecutive days (FST-1, d1; FST-2, d2) and treated three times (*Inj-a-c*) with either vehicle (Veh) or desipramine (DMI; 20 mg/kg i.p.), 1 h before the first and the second FST, and once in between. Mice were pre-treated with either vehicle (Veh) or SR141716 (SR; 10 mg/kg i.p.), 1 h before each desipramine treatment (*Inj-1-3*). Floating (**a,b**) and struggling (**c,d**) behavior during the entire FST exposure on day 1 (FST-1; **a,c**) and day 2 (FST-2; **b,d**). Corticosterone (**e**) levels 20 min after the onset of the second FST exposure (FST-2). n = 10-12 per group; $^{*}p < 0.05$, $^{**}p < 0.01$, $^{***}p < 0.001$ vs. respective vehicle-treated group (Veh-Veh or SR-Veh); $^{\#}p < 0.05$ vs. respective vehicle pre-treated group (Veh-Veh or Veh-DMI).

Two-way ANOVA (*Pre-treatment, Treatment*) of floating behavior during FST exposure on day 1 (FST-1) revealed a significant *Treatment* effect of desipramine ($F_{1,43} = 30.1$, $p < 0.001$; Fig. 2.4.6a). Contrarily to what we observed in the previous experiment with the genetic deletion of CB1 receptors, a non-significant *Pre-treatment x Treatment* interaction ($F_{1,43} = 0.1$, $p = 0.75$) reflecting that this time desipramine exerted its antidepressant-like effects (a reduction in floating) both in vehicle and in SR141716 pre-treated mice to a similar extent. The non-significant *Pre-treatment* effect ($F_{1,43} = 1.86$, $p = 0.18$) indicated that acute SR141716 treatment *per se* had no influence on floating behavior on day 1 (FST-1).

Two-way ANOVA (*Pre-treatment, Treatment*) of floating behavior during FST exposure on day 2 (FST-2) also revealed a significant *Treatment* effect of desipramine ($F_{1,42} = 13.3$, $p < 0.001$; Fig. 2.4.6b). A non-significant *Pre-treatment x Treatment* interaction ($F_{1,42} = 1.54$, $p = 0.22$) suggested that desipramine exerted its antidepressant-like effects (a reduction in floating) both in vehicle and in SR141716 pre-treated mice. However, a significant *Pre-treatment* effect ($F_{1,42} = 4.98$, $p = 0.031$) indicated that SR141716 pre-treatment *per se*, in contrast to day 1, reduced floating on day 2 (FST-2).

Two-way ANOVA (*Pre-treatment, Treatment*) of struggling behavior during FST exposure on day 1 (FST-1; Fig. 2.4.6c) and day 2 (FST-2; Fig. 2.4.6d), respectively, revealed significant effects of *Treatment* on both days ($F_{1,42} > 13.3$, $p < 0.001$) reflecting the fact that desipramine significantly increased struggling behavior. A non-significant *Pre-treatment x Treatment* interaction on day 1 ($F_{1,43} = 0.61$, $p = 0.44$) and a significant *Pre-treatment x Treatment* interaction on day 2 ($F_{1,42} = 4.07$, $p < 0.05$) suggested that desipramine exerted its effect on struggling in both vehicle and SR141716 pre-treated mice, and even induced a slightly stronger increase in struggling in the SR141716 pre-treated group on day 2 as compared to vehicle pre-treated mice (Fig. 2.4.6d). Significant *Pre-treatment*

effects on both days ($F_{1,42} > 16.1$, $p < 0.001$) revealed that SR141716 pre-treatment *per se* induced an increase of struggling behavior, which reached statistical significance in the *post hoc* test only on day 1.

Two-way ANOVA (*Pre-treatment, Treatment*) of corticosterone secretion 20 min after FST-2 (Fig. 6e) revealed no significant effect of *Treatment* ($F_{1,42} = 0.43$, $p = 0.52$) reflecting the fact that under the current experimental settings (two consecutive injections before FST), in contrast to previous results obtained in CB1$^{+/+}$ and CB1$^{-/-}$ mice (*Experiment 5*; Fig. 2.4.5e), desipramine did not influence FST stress-induced corticosterone secretion. A significant effect of *Pre-treatment* ($F_{1,42} = 31.2$, $p < 0.001$) confirmed that SR141716 pre-treatment increased FST stress-induced corticosterone secretion both in vehicle- and in desipramine-treated mice, independent of treatment (*Pre-treatment x Treatment*: $F_{1,42} = 1.7$, $p = 0.2$).

Experiment 7: Effects of chronic SR141716 pre-treatment on corticosterone secretion in response to an acute SR141716 challenge

Having consistently demonstrated corticosterone elevating effects of SR141716 in the aforementioned experiments, we conducted another experiment in order to assess the extent to which chronic SR141716 administration affects HPA axis activity.

Two-way ANOVA (*Pre-treatment, Challenge*) revealed significant effects of *Pre-treatment* ($F_{1,22} = 46.7$, $p < 0.001$; Fig. 2.4.7) with SR141716 for 9 days, of acute *Challenge* ($F_{1,22} = 49.7$, $p < 0.001$) with SR141716 on the tenth day, and a significant *Pre-treatment x Challenge* interaction ($F_{1,22} = 32.6$, $p < 0.001$). These results reflect that (i) chronic SR141716 pre-treatment for 9 days did not significantly influence vehicle injection stress-induced corticosterone secretion on day 10 (SR-Veh = Veh-Veh), suggesting that chronic SR141716 pre-treatment *per se* did not alter HPA axis reactivity in absence of an acute pharmacological challenge; (ii) acute SR141716 administration on day 10 in chronically vehicle pre-treated mice led to increased corticosterone levels (Veh-SR > Veh-Veh), similarly to previous findings after acute (Fig. 2.4.1, left panel) or subchronic administration of the antagonist (Fig. 2.4.4, injection stress levels); (iii) chronic SR141716 pre-treatment led to "tolerance" to its acute stimulatory effects on corticosterone secretion (SR-SR = SR-Veh < Veh-SR), assessed 2 h after injection.
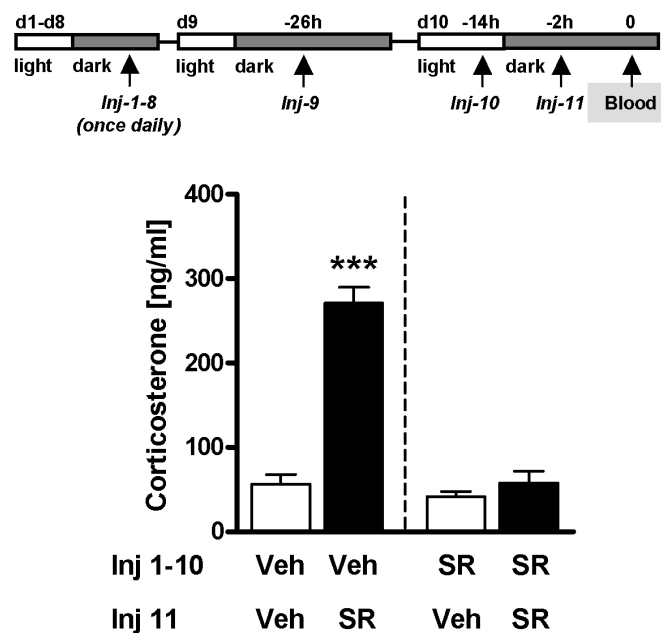
Figure 2.4.7 Chronic blockade of CB1 receptors by SR141716 leads to reduced responsiveness to corticosterone stimulating effects of an acute SR141716 challenge. Experiment 7: Male C57BL/6N mice were chronically pre-treated (Injection = *Inj*) with vehicle (Veh) or SR141716 (SR; 10 mg/kg i.p) for 10 days (d1-10; *Inj 1-10*). At day 10 (d10), half of the mice of each pre-treatment group (Veh = Vehicle; SR = SR141716) received as last injection (*Inj-11*) either vehicle or SR141716 (10 mg/kg) resulting in four different groups (Veh-Veh, Veh-SR, SR-Veh, SR-SR; n = 6-7 per group). Animals received one additional pre-treatment injection (*Inj-10*) 12 h before the last injection in order to comply with the treatment schedule that was previously applied for the subchronic experiments. Two hours after the last injection (*Inj-11*) animals were killed for corticosterone measurements. $^{***}p < 0.001$ vs. all other groups.

Experiment 8: Effects of chronic pharmacological blockade of CB1 receptors on behavioral and neuroendocrine responses to the FST

Having demonstrated that chronic SR141716 treatment leads to reduced responsiveness to its acute corticosterone stimulatory effects 2 h after intraperitoneal injection, we wondered whether chronic administration would also alter the behavioral and neuroendocrine response to the FST following an acute challenge with SR141716.

Chronic treatment with SR141716 for 8 days, followed by an acute challenge 2 h before FST-1 on day 9 and 2 h before FST-2 on day 10 resulted in a significant decrease of floating behavior [*Treatment*: $F_{1,28} = 6.8$, $p < 0.05$; two-way ANOVA (*Day, Treatment*); Fig. 2.4.8a] and, in parallel, in a significant increase of struggling behavior [*Treatment*: $F_{1,28} = 7.6$, $p < 0.05$; two-way ANOVA (*Day, Treatment*); Fig. 2.4.8b]. These behavioral effects of SR141716 were maintained
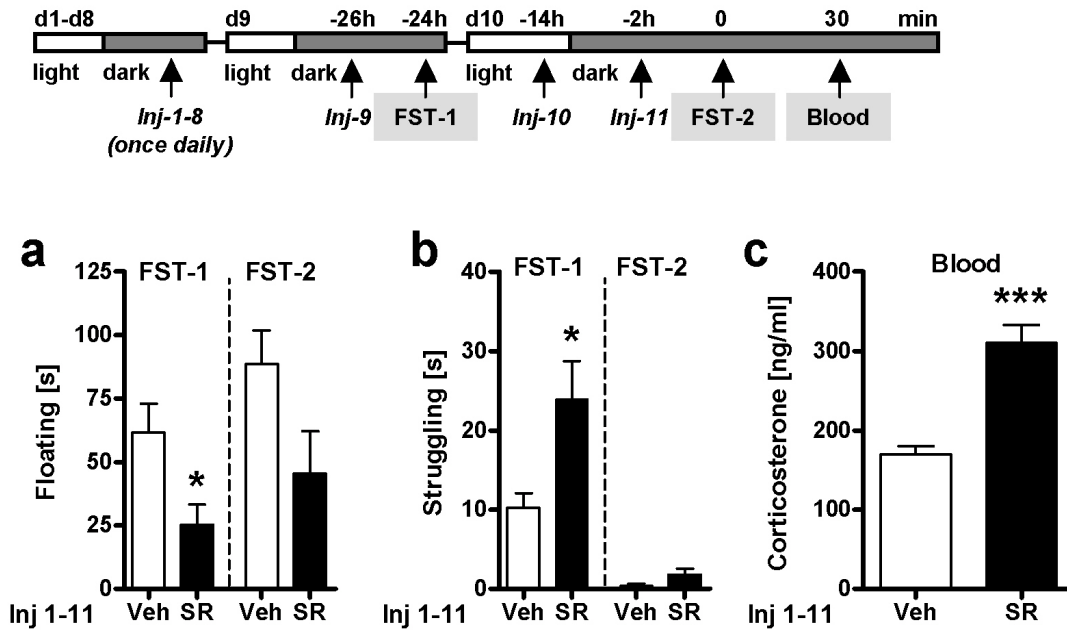
Figure 2.4.8. Chronic blockade of CB1 receptors by SR141716 alters behavioral and neuroendocrine responses to the forced swim test (FST). Experiment 8: Male C57BL/6N mice were exposed to the FST on two consecutive days, on day 9 (d9; FST-1) and day 10 (d10; FST-10) after chronic treatment (Injection = *Inj*) with vehicle (Veh) or SR141716 (SR; 10 mg/kg i.p) for 10 days (d1-10; *Inj 1-11*). The injection schedule during the last two days of chronic treatment (d9-10) was kept the same as that previously applied for the subchronic experiments. During days 9 and 10 animals were injected 2 h prior to FST-1 on day 9 (*Inj-9*), 12 h later (*Inj-10*), and last 2 h before FST-2 on day 10 (*Inj-11*). Floating (**a**) and struggling (**b**) behavior during the entire FST exposure on day 9 (FST-1**)** and day 10 (FST-2). Corticosterone (**c**) levels 30 min after the onset of the second FST exposure (FST-2) on day 10. $^*p < 0.05$, $^{***}p < 0.001$ vs. respective vehicle control.

throughout the first (FST-1) and second (FST-2) FST exposure (on day 9 and day 10 of chronic SR141716 treatment, respectively), although struggling behavior was almost absent during the second exposure (FST-2). Corticosterone secretion 30 min after the second FST exposure on day 2 (FST-2; day 10 of chronic treatment) was significantly elevated in SR1411716-treated animals as compared to vehicle-treated controls (t_{26} = 5.6, $p < 0.001$; Student's t-test; Fig. 2.4.8c) and was not different from FST-induced corticosterone levels of subchronically SR141716-treated mice (compare 30 min time point in Fig. 2.4.4a; statistics not shown).

2.4.5 Discussion

Preclinical and clinical research strongly suggests that disturbances of the HPA axis can play a major causal role in depression disorders (De Kloet et al., 2005), and recent findings in rodents imply that the endocannabinoid system is an important HPA axis modulator (Pagotto et al., 2006). Blockade of endocannabinoid signaling has been suggested as a novel antidepressant treatment by some authors (Witkin et al., 2005b; Griebel et al., 2005), whereas others regard CB1 receptor-deficient mice as an animal model of depression (Hill and Gorzalka, 2005a). The present study was designed to compare neuroendocrine and behavioral consequences of CB1 receptor impairment in response to FST exposure. We showed that (i) the genetic inactivation as well as the acute, subchronic and chronic pharmacological blockade of CB1 receptors lead to increased basal and peak levels of stress-induced corticosterone secretion; (ii) chronic SR141716 administration causes reduced responsiveness to its corticosterone stimulatory effects following an acute SR141716 challenge; (iii) the subchronic and chronic administration of SR141716 produces antidepressant-like behavioral effects in the FST similar to desipramine; (iv) desipramine-induced neuroendocrine and antidepressant-like behavioral effects are unaffected by pharmacological blockade of CB1 receptors. Together these results demonstrate that antidepressant-like behavioral effects of SR141716 coincide with exaggerated stress-induced corticosterone secretion.

Acute (Figs. 2.4.1-2), subchronic (Figs. 2.4.4 and 2.4.6) and chronic SR141716 treatment (Fig. 2.4.8), as well as genetic inactivation of CB1 receptors (Figs. 2.4.2 and 2.4.4-5), increased peak levels of corticosterone secretion 10, 20 and 30 min after FST stress, which is in accordance to previous findings from the literature (Patel et al., 2004; Barna et al., 2004). Moreover, our results confirm that HPA axis dysregulations in CB1 receptor-deficient mice are not due to developmental deficits, as they could be reliably mimicked by the pharmacological blockade of CB1 receptors. They also demonstrate that CB1 receptor inhibition confers similar stress-induced corticosterone elevating effects both in male and female mice. Therefore, our results help to establish CB1 receptor signaling as a universal mechanism for constraining stress-induced corticosterone secretion,

largely independent of sex, genetic background, type of stressor or type of CB1 receptor impairment (genetically or pharmacologically).

Some reports have raised doubts about the specificity of SR141716 for CB1 receptors as, for instance, the antagonist still exerted behavioral effects in CB1 receptor deficient mutants on a CD1 background (Haller et al., 2002). However, in our mutant line acute SR141716 administration had no effect on immediate FST stress-induced corticosterone secretion (Fig. 2.4.2), whereas it increased FST stress-induced corticosterone secretion in CB1$^{+/+}$ mice to the same levels that were seen in vehicle-treated CB1$^{-/-}$ mice. These results illustrate the similarities between the pharmacological and genetic impairment of CB1 receptors and suggest that SR141716-mediated effects on corticosterone are CB1 receptor-specific.

Untreated male CB1$^{-/-}$ mice had also elevated corticosterone levels as compared to their wild-type littermates under basal conditions (Fig. 2.4.3a). This underscores the notion of an HPA axis-modulating endocannabinoid tone, which is present under basal non-stress conditions (Chapter 2.2). The lack of genotype differences in basal corticosterone levels in female CB1 receptor mutant mice (Fig. 2.4.3b) is in contrast to our previous observations made at another time of the day (Chapter 2.2, Fig. 2.2.1), which might be explained by sex-specific differences in the circadian rhythm of endocannabinoid action. In fact, Valenti and co-workers recently demonstrated that the levels of the two major endocannabinoids 2-arachidonoyl-glycerol and anandamide undergo strong diurnal variations (Valenti et al., 2004), which might be differentially regulated between male and female mice. It has to be noted that with the pharmacological application of SR141716 it was impossible to investigate true basal corticosterone levels, as drug administration is invariably conferring mild stress to the animals. Nevertheless, apart from *Experiments 1* and *2*, where we first tested the drug, in the following experiments we injected SR141716 two hours prior to any additional stress exposure or blood sampling in order to minimize residual stress effects of the injection procedure.

Unexpectedly, chronic SR141716 administration led to a reduction of the corticosterone stimulating effects induced by an acute SR141716 challenge (Fig. 2.4.7), which is in contrast to results from another group (Wade et al., 2006). Noteworthy, corticosterone elevating effects of an acute SR141716 challenge after

subchronic treatment (compare the "Injection" bars of Fig. 2.4.4) were already lower than those after acute administration (Fig. 2.4.7), but still significantly higher than after chronic treatment (Fig. 2.4.7). This suggests that tolerance to the acute corticosterone stimulatory effects of SR141716 develops gradually over the time period of 10 days, which could explain why Wade and co-workers did not yet observe any "tolerance" effect after 5 days of treatment (Wade et al., 2006).

Despite these "tolerance" effects following intraperitoneal injection, chronic SR141716 administration did not lead to "tolerance" to its stimulatory effects on FST stress-induced corticosterone secretion (Fig. 2.4.8c), which were comparable to those observed after subchronic (Fig. 2.4.4) or acute SR141716 treatment (Fig. 2.4.1). One possible explanation is that "tolerance" might only develop towards a mild stressor (i.p. injection), which has been repeatedly applied over the 10 days period, and that this "tolerance" can be overridden by exposure to a novel, severe stressor such as FST. Another possibility is that "tolerance" only develops in those pathways and processes, which are involved in re-setting of the HPA axis (i.e., two hours after injection stress), but not in those responsible for the early corticosterone response (i.e., 30 min after FST stress). Such a scenario would provide another explanation for the different findings from Wade and co-workers, who measured plasma corticosterone one hour, but not two hours, after administration of SR141716.

We have chosen the FST as stressor in the present study, because this test is frequently applied to investigate antidepressant-like potentials of novel drugs (Cryan and Holmes, 2005). However, in this specific function, not the endocrine responses, but the behavioral performance during the test procedure is usually considered. Hence, we also investigated the behavioral stress coping of SR141716-treated mice. Acute, subchronic and chronic SR141716 administration (Figs. 2.4.6c,d and 2.4.8b) increased struggling behavior, whereas only subchronic and chronic (Figs. 2.4.6b and 2.4.8a), but not acute (Fig. 2.4.6a), SR141716 administration decreased floating in the FST. These results are in agreement with our previous findings, where we found no effect of acute SR141716 administration on total floating time at the first FST exposure on day 1, but a slight decrease following subchronic administration during repeated FST exposure on day 2 (Chapter 2.3., Fig. 2.3.2b). The lack of acute drug effects on floating behavior are at odds with other reports that demonstrated antidepressant-like effects of acute

treatment with the CB1 receptor antagonists AM251 and SR141716 in the FST (Shearman et al., 2003; Tzavara et al., 2003b; Griebel et al., 2005). Irrespective of the reasons for these discrepancies, our data imply that under our current experimental conditions (injection two hours prior to FST) the antidepressant-like effects of SR141716 with regard to floating behavior develop gradually, from no effect after acute SR141716 administration (Fig. 2.4.6a) via slight effects after subchronic (Fig. 2.4.6b) towards solid effects after chronic administration (Fig. 2.4.8a). Thus, in combination with our consistent findings on struggling, these results favor an antidepressant-like potential of chronic SR141716 administration at the behavioral level, in particular, as subchronic SR141716 (10 mg/kg) treatment was as effective as the classical antidepressant desipramine (20 mg/kg) in increasing struggling and decreasing floating behavior (Figs. 2.4.6b,d).

The fact that we did not observe any behavioral differences in the FST between vehicle-treated CB1$^{+/+}$ and CB1$^{-/-}$ mice (Figs. 2.4.5a-d) is in agreement with another study (Shearman et al., 2003) and suggests compensatory changes in CB1$^{-/-}$ mice due to the life-long absence of CB1 receptors. On the other hand, behavioral genotype differences might have been masked by preceding vehicle injection of the animals, since we have recently observed increased floating behavior of CB1$^{-/-}$ mice in comparison with CB1$^{+/+}$ mice without any prior treatment (Chapter 2.3, Fig. 2.3.1). Apparently, there is a discrepancy between the genetic inactivation and the pharmacological blockade of CB1 receptors with regard to the behavioral performance in the FST, whereas the FST stress-induced corticosterone secretion is almost identically affected by the pharmacological blockade and the genetic inactivation of CB1 receptors.

Recently, Gobshtis and co-workers demonstrated that SR141716 and desipramine mediate their effects on floating behavior in the FST independently from each other (Gobshtis et al., 2007). Hill and co-workers, however, proposed that CB1 receptor signaling is necessary for chronic desipramine treatment to exert its dampening effects on corticosterone secretion after FST exposure in rats (Hill et al., 2006). Although we failed to observe acute antidepressant-like behavioral effects of desipramine in CB1$^{-/-}$ mice (Figs. 2.4.5a,c), we demonstrated that the pharmacological blockade of CB1 receptors did not interfere with behavioral effects of desipramine in the FST (Figs. 2.4.6a,c). This is in line with the first study (Gobshtis et al., 2007) and suggests that the discrepant findings

obtained in CB1$^{-/-}$ mice are due to potential developmental changes. In this context, it has to be mentioned that Shearman and co-workers as well as our laboratory previously found intact antidepressant-like behavioral effects of desipramine in the FST in female CB1 receptor-deficient mice (Shearman et al., 2003) (Chapter 2.3, Fig. 2.3.4). This adds another layer of complexity to the role of CB1 receptors in the behavioral response to the FST, because it suggests that potential developmental changes in CB1 receptor-deficient mice that may lead to impaired desipramine responsiveness in the FST only occur in male mice and, thus, are sex-dependent.

Other than for the shared antidepressant-like behavioral effects, CB1 receptor impairment and desipramine treatment differed in their effects on FST stress-induced corticosterone secretion. Whereas desipramine either had no effects on corticosterone secretion following FST in vehicle pre-treated mice (Fig. 2.4.6e), or slightly decreased corticosterone secretion in CB1$^{+/+}$ mice (Fig. 2.4.5e), both the pharmacological blockade and the genetic knockout of CB1 receptors increased corticosterone secretion (Figs. 2.4.5e and 2.4.6e). We found no interaction between impaired CB1 receptor signaling and desipramine treatment, suggesting that CB1 receptors are not mediating the neuroendocrine effects of subchronic desipramine treatment in mice. The discrepant findings observed by us and Hill and co-workers (Hill et al., 2006) might be due to species-specific differences (mice vs. rats) or to different desipramine treatment schedules (subchronic vs. chronic).

In conclusion, we demonstrate that CB1 receptor signaling represents a general constraint mechanism for the secretion of corticosterone under basal conditions as well as in response to stress in male and female mice. Furthermore, we show that desipramine-induced behavioral and neuroendocrine effects are largely unaffected by the absence of CB1 receptor signaling. Considering that HPA-axis disturbances may be prognostically unfavorable for the treatment of depression (for review see De Kloet et al., 2005) and that antidepressant-like behavioral effects of subchronic and chronic SR141716 administration coincide with corticosterone elevating effects in the mouse FST, further evaluation of SR141716 is required, before its applicability for the treatment of depression can be proposed (Witkin et al., 2005b).

2.5 Endocannabinoid signaling influences forced swimming behavior in a monoamine-independent manner

In previous Chapters 2.2 and 2.4, we have demonstrated HPA axis hyperactivity following impaired CB1 receptor signaling under basal and stressful conditions. In the present Chapter, we evaluated whether these effects are influenced by impaired monoaminergic neurotransmission. In the previous Chapters 2.3 and 2.4, we could show that male $CB1^{-/-}$ mice show increased floating behavior in the FST in comparison with $CB1^{+/+}$ mice under naïve conditions, but not after vehicle injection. Furthermore, we found that the CB1 receptor antagonist SR141716, given acutely 2 h prior to the FST, had no effect on total floating time in C57BL/6N mice, but decreased floating after subchronic or chronic administration. To better compare our results with the current literature and to evaluate whether these discrepant behavioral effects of CB1 receptor impairment are truly injection-stress dependent, we systematically evaluated a number of endocannabinoid-modulating drugs in broad dose ranges in the FST, when applied acutely 1 h before testing, in the present study. Additionally, because of the apparent complexity of the role of endocannabinoid signaling for FST behavior, we decided to study FST stress-induced changes of endocannabinoid levels in various brain areas, and we evaluated whether the behavioral effects of the CB1 receptor antagonist SR141716 are monoamine-dependent.

The following experiments were performed in collaboration with Dr. G. Astarita from the research group of Prof. D. Piomelli, University of Irvine, CA, USA, who performed the endocannabinoid measurements (Fig. 2.5.5). I conducted the behavioral and pharmacological tests and evaluated the corticosterone plasma levels (Figs. 2.5.1-4).

2.5.1 Summary

The forced swim test (FST) is a behavioral assay in rodents that predicts the clinical efficacy of many types of antidepressants. The current study systematically evaluated the effects of endocannabinoid-modulating drugs in the

mouse FST. We show that acute treatment (0.5, 2, 10 mg/kg) with the cannabinoid type 1 (CB1) receptor antagonists SR141716 (rimonabant) and AM251 dose-dependently reduced immobility in the FST in male C57BL/6N mice without affecting locomotor activity. This antidepressant-like effect is specific for CB1 receptors as SR141716 had no effect in CB1 receptor-deficient mice. Several drugs that increase endocannabinoid levels, URB597 (0.05, 0.2, 1 mg/kg), AM404 (0.5, 3, 10 mg/kg) and UCM707 (0.5, 2, 10 mg/kg), had no effect on immobility in the FST. Depletion of serotonin or catecholamines via inhibition of tryptophan hydroxylase or tyrosine hydroxylase, respectively, did not attenuate the antidepressant-like behavioral effects of SR141716, nor did monoamine depletion influence SR141716's effect on glucocorticoid secretion. Finally, forced swim stress reduced levels of the endocannabinoid, anandamide, in the ventromedial prefrontal cortex, nucleus accumbens, basolateral amygdala, dorsal hippocampus and raphe nuclei, but not in the caudate putamen. Levels of the second major endocannabinoid, 2-arachidonoyl glycerol, were decreased in the dorsal hippocampus, but increased in the basolateral amygdala and caudate putamen. In conclusion, we illustrate the complexity of the endocannabinoid signaling response to forced swim stress and propose that the acute pharmacological blockade of CB1 receptors causes antidepressant-like effects in the mouse FST independent of monoaminergic neurotransmission.

2.5.2 Introduction

The endocannabinoid system is implicated in the modulation of emotions (Wotjak, 2005) and regulates anxiety- and depression-like behaviors in animals (Kathuria et al., 2003; Gobbi et al., 2005; Viveros et al., 2005; Hill and Gorzalka, 2005a). Endocannabinoids, including anandamide and 2-arachidonoyl glycerol (2-AG), function as retrograde modulators of synaptic activity, which, through activation of cannabinoid CB1 receptors, constrain neurotransmitter release from presynaptic terminals (Piomelli, 2003). As CB1 receptors are present on both GABAergic and glutamatergic terminals (Marsicano and Lutz, 2006; Monory et al., 2006), the endocannabinoid system is able to control the activation of both inhibitory and excitatory neurotransmission. Therefore, depending on its specific spatio-temporal activation within neuronal circuits, this system can act as a major "bi-directional" neuro-modulator (Marsicano and Lutz, 2006).

This "dual" role of endocannabinoid signaling has likely been the reason for a number of contradictory results in rodent anxiety and depression models (Kathuria et al., 2003; Gobbi et al., 2005; Hill and Gorzalka, 2005a; Viveros et al., 2005). Depending on a multitude of genetic, environmental and experimental factors, which determine the initial baseline stress level of the animal and, hence, the activity of the endocannabinoid system, opposite pharmacological interventions (e.g., CB1 receptor signaling blockade or enhancement) might result in the same behavioral effect (Wotjak, 2005; Viveros et al., 2005). An example of this complexity is the influence of endocannabinoid signaling on the behavioral performance of rodents in the forced swim test (FST), one of the most widely used behavioral paradigms to detect antidepressant-like activities of drugs (Lucki et al., 2001; Cryan and Mombereau, 2004). The test is based on the observation that rodents, when exposed to an inescapable situation (immersion in a beaker filled with water), will over several minutes cease to engage in escape-oriented movements and adopt an immobile passive "floating" posture. Acquired immobility is often interpreted as "behavioral despair" mimicking psychomotor impairments experienced by depressed patients (Cryan and Mombereau, 2004). However, this interpretation was later challenged in light of other explanations for immobility, such as a beneficial passive coping strategy to preserve energy or a learned

adaptation to swim stress (Cryan and Mombereau, 2004; West, 1990). Nevertheless, a reduction of immobility time in the FST is especially sensitive and specific to the actions of a broad range of antidepressants, which increase serotonergic and/or noradrenergic neurotransmission (West, 1990; Cryan and Mombereau, 2004).

The CB1 receptor antagonist, SR141716 (rimonabant), was shown to increase the efflux of serotonin and noradrenaline in the rat prefrontal cortex (Tzavara, et al., 2003b). CB1 receptors are expressed in mouse serotonergic raphe neurons (Haring et al., 2007) and in noradrenergic nerve terminals in the rat frontal cortex (Oropeza et al., 2007). In addition, CB1 receptor signaling influences the firing rate of serotonergic and noradrenergic neurons in the rat raphe nuclei and locus coeruleus, respectively (Gobbi et al., 2005; Muntoni et al., 2006). Together, this accumulating evidence supports the involvement of CB1 receptor signaling in the regulation of monoaminergic neurotransmission, which could, in turn, mediate endocannabinoid effects in the FST.

To date, both CB1 receptor antagonists, such as SR141716 or AM251, and endocannabinoid signaling enhancing drugs, such as URB597, an inhibitor of the anandamide degrading enzyme fatty acid amide hydrolase (FAAH), or AM404, an inhibitor of endocannabinoid re-uptake, were found to decrease total immobility in the FST (Gobbi et al., 2005; Tzavara et al., 2003b; Shearman et al., 2003; Hill and Gorzalka, 2005b; Hill et al., 2007; Griebel et al., 2005) (Chapter 2.4, Figs. 2.4.6 and 2.4.8). Furthermore, there have been reports that the acute pharmacological blockade or genetic inactivation of CB1 receptors did not influence FST behavior (Gobshtis et al., 2007; Gobbi et al., 2005; Hill et al., 2007; Hill and Gorzalka, 2005b; Shearman et al., 2003; Jardinaud et al., 2005), or even slightly increased immobility (Chapter 2.3, Figs. 2.3.1-2). Thus, it is yet far from understood which kind of endocannabinoid modulating drugs have antidepressant potential in this test. As Patel and Hillard have recently pointed out for the anxiety field (Patel and Hillard, 2006), systematic screening studies employing standardized conditions are needed to better understand the role of the endocannabinoid system in emotional processing. In addition, studies investigating the specific effect of forced swim stress on the activity of the endocannabinoid system are lacking.

Here, we studied the effects of several endocannabinoid-modulating drugs over broad dose ranges, work complemented by the examination of CB1 receptor

knockout mice. Furthermore, we examined the influence of impaired serotonergic and noradrenergic transmission on the behavioral and hormonal effects of SR141716. Finally, the effect of forced swim stress on endocannabinoid levels was assessed in several brain regions.

2.5.3 Materials and Methods

Animals

Mice were kept under standard conditions with food and water *ad libitum*. Male C57BL/6N mice were purchased from Charles River (USA). They were housed in groups of four in the animal facility of UT Southwestern in Dallas under a regular 12 h : 12 h light/dark schedule (lights on at 07:00 am). CB1 receptor knockout mice (CB1$^{-/-}$) and their wild-type littermates (CB1$^{+/+}$) were backcrossed to the C57BL/6N background (6 generations). They were generated and genotyped as described (Marsicano et al., 2002). CB1 receptor mutant mice were housed in the animal facility of The Max Planck Institute of Psychiatry under a 12 h : 12 h inverted light/dark schedule (lights on at 09:00 am). Male mutant mice were singly housed 1 week prior to experiments. Age of tested animals ranged between 8 and 12 weeks. Animal experiments were conducted in accordance with the *Guide for the Care and Use of Laboratory Animals* of the Government of Bavaria (Germany) or approved by UT Southwestern's Institutional Animal Care and Use Committee.

Drugs

All drugs were freshly prepared just prior to use and doses were calculated as the weight of the free base. Desipramine hydrochloride and paroxetine hydrochloride hemihydrate (Sigma-Aldrich, St. Louis, MO, USA) were dissolved in vehicle solution (2.5% dimethylsulfoxide in 0.9% saline). SR141716 (NIMH Chemical Synthesis and Drug Supply Program, USA), AM251 (Tocris Bioscience, Ellisville, MO, USA), AM404 (Tocris), UCM707 (Tocris) and URB597 (Cayman Chemical Company, Ann Arbor, MI, USA) were dissolved in vehicle solution (1 drop of Tween-80 in 1.5 ml of 2.5% dimethylsulfoxide in 0.9% saline). 4-Chloro-DL-phenylalanine methyl ester hydrochloride (PCPA) (Sigma-Aldrich) and alpha-methyl-DL-tyrosine methyl ester hydrochloride (AMPT) (ABCR, Karlsruhe, Germany) were dissolved in vehicle solution (0.9% saline). All drugs were injected i.p. in a volume of 10 ml/kg body weight.

Pharmacology

Desipramine, paroxetine, SR141716, AM251, AM404, UCM707 and URB597 were injected i.p. 1 h prior to the FST. Desipramine and paroxetine were used at a dose of 20 mg/kg, which was recently validated to produce antidepressant like effects in C57BL/6N mice (Chapter 2.3, Fig. 2.3.4; Chapter 2.4, Figs. 2.4.5-6). PCPA (250 mg/kg) was consecutively injected for three days (twice daily, every 12 h). The last injection was given 18 h prior to behavioral testing in the FST (17 h before injection with SR141716 or vehicle, respectively) (Cesana et al., 1993). This treatment schedule reduced the serotonin content of the brain by 70 - 85% without affecting catecholamine levels as shown previously (Mayorga et al., 2001; Chapter 3.2, Table 3.2.1). AMPT (200 mg/kg) was administered as a single dose 4 h before the FST (3 h before injection with SR141716 or vehicle, respectively) (Corrodi and Hanson, 1966). This treatment schedule reduced the

catecholamine content of the brain by 40 - 60% without affecting serotonin levels (Mayorga et al., 2001; Chapter 3.2, Table 3.2.2).

Forced swim test

Each mouse was placed into a 4-L glass beaker (height 25 cm; diameter 16 cm) containing water up to a height of 15 cm at 25 ± 1 °C for 6 min. The water was changed between animals. All mice were tested in a dark experimental room under red light conditions. Behavior during FST was videotaped using a camera, which was facing the glass beakers from the front. Immobility time (floating) was either scored manually by pressing preset keys on a computer keyboard, using customized freeware software (EVENTLOG; Robert Hendersen, 1986) or was analyzed via video-tracking using EthoVision software (Noldus, Asheville, North Carolina, USA). A mouse was judged floating when it stopped any movements except those that were necessary to keep its head above water. Animals' behavior was analyzed off-line by a trained observer who was blind to treatment and genotype.

All experiments with C57BL/6N mice were conducted during the second half of the light phase at UT Southwestern and were analyzed via EthoVison. The experiments involving CB1 receptor mutant mice were conducted during the second half of the dark phase under an inverted dark-light cycle at the Max Planck Institute of Psychiatry and were manually analyzed. Initial control experiments had revealed consistent antidepressant-like effects of SR141716 independent of the time of testing (data not shown).

Automated video analysis via EthoVision

Analysis of forced swim behavior via EthoVision was performed using the "Mobility" detection module. EthoVision settings were as follows: the subtraction method with a minimum pixel size of 15 for object detection and a sample rate of 6 video frames/second. The shape of the arena in which mice subjected to the FST were recognized as a target for video-tracking was designed in such a way that it enclosed the entire water filled beaker. Immobility time (floating) was defined as the amount of time that the percentage change in object area between consecutive video frames was below a defined threshold (immobility threshold). Mobility is measured by EthoVision as the change of the locations of the pixels belonging to the tracked mouse between the current and the previous sample frame. The amount of relocated pixels is calculated as a percentage of change in the object's area. In the first experiment, an animal's behavior in the FST in response to antidepressants was analyzed using a range of immobility thresholds from 1 up to 15% in steps of 1% in order to determine the most sensitive threshold to detect antidepressant-like effects. An immobility threshold of 10% proved to be most sensitive and was chosen for all further analysis. All further experiments were additionally also analyzed with an immobility threshold of 7%, which was most similar to manual scoring, but the revealed effects were virtually identical to the analysis with a 10% threshold and, therefore, are not shown.

Locomotor activity test

Locomotor activity was measured in an automated system (Med Associates Inc., St Albans, VT, USA). The locomotor activity chambers were plastic cages (16 x 27 x 21 cm) with 5 pairs of photocell beams at the y-axis and 3 pairs of photocell beams at the x-axis dividing the cage. Horizontal ambulatory activity was detected by way of beam interruptions. Data were recorded via a PC equipped with a customized software (Med Associates). Mice were introduced into the chambers and habituated for 30 min before they were randomly assigned to a treatment group. They were quickly removed from the chambers, injected with either vehicle or SR141716 (10 mg/kg) and re-introduced into the chambers, and their locomotor activity was recorded for another 2 h.

Stress experiments

After the FST, animals were placed back in their home cages and were left undisturbed until 30 min after the onset of the stressor, when they were killed by cervical dislocation. The 30 min time point after FST stress was chosen because it previously revealed the strongest effect of CB1 receptor blockade on the corticosterone response (Chapter 2.4, Figs. 2.4.3-4).

Treatment of blood samples and hormone analysis

After decapitation, trunk blood was collected in pre-chilled tubes containing EDTA. Blood samples were centrifuged for 15 min at 2500 g at 4 °C. Plasma samples were stored in aliquots at -80 °C until assay. Plasma corticosterone concentrations were measured in duplicate by a commercially available ELISA kit (Immunodiagnostic Systems, Fountain Hills, AZ, USA) according to manufacturer's instructions.

Tissue sampling and dissection for endocannabinoid measurements

C57BL/6N mice were either killed directly under basal conditions or exposed to the FST and killed 10 or 30 min after stressor onset. Brains were rapidly removed and quick-frozen in 2-methylbutane at –40°C (Sigma-Aldrich). Brains were stored at –80°C until further processing. Brain regions were punched from the frozen brains using a cryo-cut and cylindrical brain punchers (Fine Science tools, Foster City, CA, USA; internal diameter 2.0 mm for VPC, 1.0 mm for all other regions), as previously described (Cannich et al., 2004). The location and length of the punches were chosen based on the stereotaxic atlas of Paxinos and Franklin (2001) as described (Cannich et al., 2004) for the dorsal hippocampus (DH), ventromedial prefrontal cortex (VPC) and basolateral amygdala (BLA). Location of the 1.0 mm long punches for the other brain regions were as follows: nucleus accumbens (NAC; starting at 1.9 mm anterior to bregma; including the nucleus accumbens core and shell); caudate putamen (CPU; starting at 0.9 mm anterior to bregma); raphe nuclei (RN; starting at 4.2 mm posterior to bregma; just below the aqueduct, including mainly the caudal, dorsal, interfascicular, ventral and ventrolateral part of the dorsal raphe nucleus, the caudal linear

nucleus of the raphe and the raphe cap, but also minor parts of the ventrolateral periaqueductal gray, supraoculomotor cap and nucleus, supraoculomotor periaqeductal gray, medial longitudinal fasciculus and dorsal and laterodorsal tegmental nucleus).

Endocannabinoid measurements

Chemicals and chemical syntheses – Heptadecenoyl chloride and 2-heptadecanoylglycerol (2-HG) were purchased from Nu-Chek Prep (Elysian, MN, USA). Heptadecenoylethanolamide (HEA) was prepared by the reaction of the corresponding fatty-acid chloride with a 10-fold molar excess of ethanolamine (Sigma-Aldrich). The reaction was conducted in dichloromethane at 0-4˚C for 15 min, with stirring. The product was washed with water, dehydrated over sodium sulphate, filtered, and dried under N_2. It was characterized by liquid chromatography/mass spectrometry (LC/MS) and ^{1}H nuclear magnetic resonance spectroscopy. Purity was >98% by LC/MS.

Lipid extractions – Frozen punches were homogenized in 0.3 ml of methanol containing HEA and 2-HG as internal standards. Lipids were extracted with chloroform (2 vol) and washed with water (1 vol). Protein concentration was measured using the BCA protein assay (Pierce, Rockford, IL, USA). Organic phases were collected and dried under N_2. Endocannabinoids were fractionated by open-bed silica gel column chromatography, as described (Giuffrida et al., 2000). Briefly, the lipids were reconstituted in chloroform and loaded onto small glass columns packed with Silica Gel G (60-Å 230-400 Mesh ASTM; Whatman, Clifton, NJ). Endocannabinoids were eluted with 9:1 chloroform/methanol (vol/vol). Eluates were dried under N_2 and reconstituted in 0.1 ml of chloroform/methanol (1:4, vol/vol) for LC/MS analyses.

LC/MS analyses – We used an 1100-LC system coupled to a 1946D-MS detector (Agilent Technologies, Inc., Palo Alto, CA) equipped with an electrospray ionization interface. Endocannabinoids were separated using a XDB Eclipse C18 column (50x4.6 mm i.d., 1.8 μm, Zorbax), eluted with a gradient of methanol in water (from 75% to 85% in 2.5 min and then to 90% in 7.5 min) at a flow rate of 1.0 ml/min. Column temperature was kept at 40˚C. MS detection was in the positive ionization mode, capillary voltage was set at 3 kV and fragmentor voltage was varied from 120V. N_2 was used as drying gas at a flow rate of 13 liters/min and a temperature of 350˚C. Nebulizer pressure was set at 60 PSI. Quantifications were performed in positive mode by monitoring the sodium adducts of the molecular ions (AEA, *m/z* 370.3; 2-AG, *m/z* 401.3; HEA, *m/z* 334.3; 2-HG, *m/z* 367.3).

Statistical analysis

Data were analyzed for multiple comparisons using one or two way analysis of variance (ANOVA) followed by *post-hoc* Newman-Keuls Multiple Comparisons Test. For two-group comparisons unpaired Student's *t*-test was used. For correlation analysis Pearson calculations were applied. Differences were considered statistically significant if $p < 0.05$. Data are presented as mean ± SEM.

2.5.4 Results

Evaluation of forced swim behavior in mice using the mobility parameter of EthoVision

The mobility parameter of EthoVision's video-tracking system was previously shown to reliably assess immobility times and its reduction by the antidepressant desipramine in the rat FST (Berndsen and Broersen, 2007). Furthermore, the same mobility detection module of EthoVision has recently been demonstrated to reliably detect immobility in the mouse tail suspension test (TST) (Juszczak et al., 2006). To evaluate whether the same analysis method could be applied to the mouse FST, we analyzed the effects of the noradrenaline reuptake inhibitor desipramine (20 mg/kg) and the selective serotonin reuptake inhibitor (SSRI) paroxetine (20 mg/kg) in C57BL/6N mice. To find the most sensitive immobility threshold for the detection of antidepressant-like effects, we analyzed FST behavior over a wide range of different immobility thresholds ranging from 1 to 15% (Fig. 2.5.1a). Separate one way ANOVAs for a general drug effect between the three groups (vehicle, paroxetine and desipramine) were separately performed for each different immobility threshold. Significant *Drug* effects were revealed for all immobility thresholds between 5 and 15% ($F_{2,21} > 3.64$, $p < 0.044$). *Post hoc* analyses revealed significant effects of both paroxetine and desipramine for all immobility thresholds between 7 and 15% ($p < 0.05$). Comparing the ANOVA *p*-values between different immobility thresholds revealed the lowest *p*-value for an immobility threshold of 10% ($p = 0.015$). Thus, this immobility threshold was regarded the most sensitive to detect antidepressant-like effects in the FST and was applied to all further analysis.

In addition to EthoVision, video-taped behavior of the aforementioned experiment was also scored manually. As depicted in Figs. 2.5.1b,c, an applied EthoVision immobility threshold of 7% was most similar to manual scoring. However, one way ANOVA revealed no significant *Drug* effect for the manual score ($F_{2,21} = 2.07$, $p = 0.152$), whereas EthoVision detected a significant main *Drug* effect ($F_{2,21} = 4.54$, $p = 0.023$). Separate analysis for paroxetine and desipramine effects revealed the following: A decrease of immobility as induced by desipramine could be detected by manual scoring ($t_{14} = 2.45$, $p = 0.028$; Student's t-test) as well

a

b

c
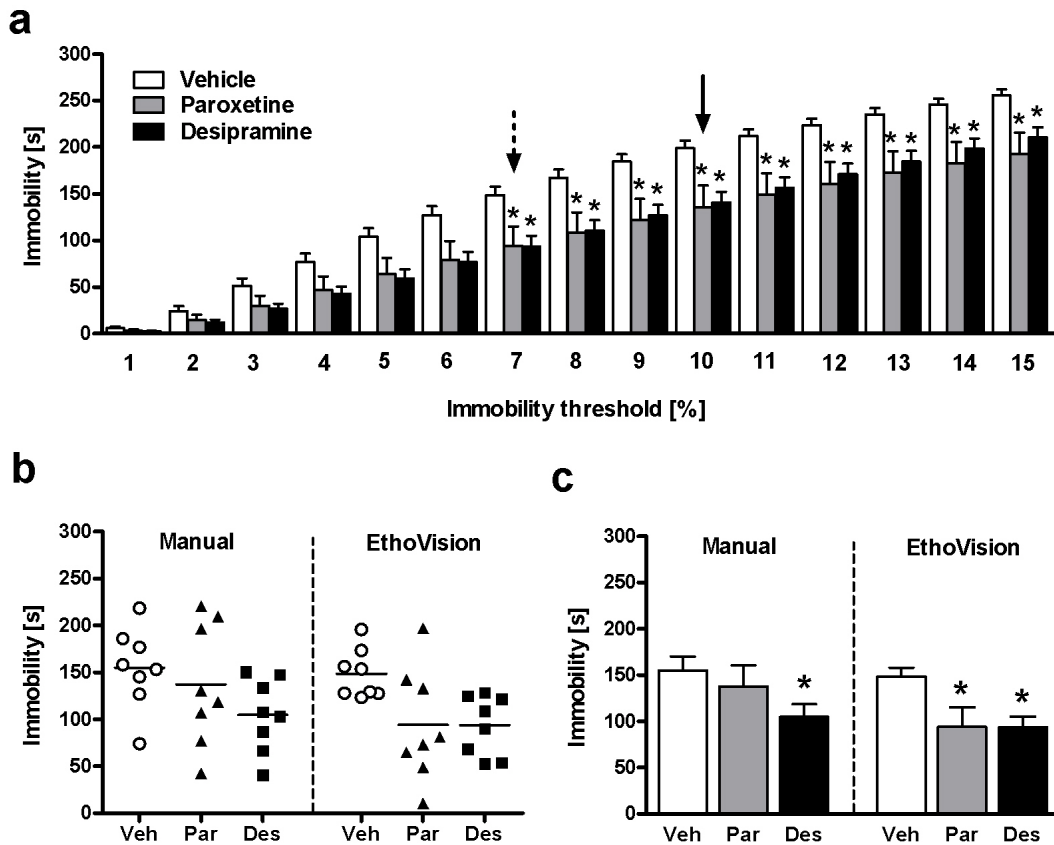
Figure 2.5.1 Validation of EthoVision video-tracking for the detection of immobility behavior in the mouse FST. (**a**) Detection of antidepressant-like effects (decreased immobility) in paroxetine (20 mg/kg) and desipramine (20 mg/kg) treated C57BL/6N mice in the FST via EthoVision within a wide range of pre-set immobility thresholds (1-15%). The dashed arrow refers to an immobility threshold of 7%, which was most similar to values obtained by manual scoring. The solid arrow refers to an immobility threshold of 10%, which was most sensitive to detect antidepressant-like effects, and which was used for further analysis. (**b,c**) Comparison of antidepressant-like effects between manual scoring and EthoVision (immobility threshold 7%) for vehicle (Veh), paroxetine (Par) and desipramine (Des) treatment. The total immobility time per 6 min FST exposure is depicted. n = 8 per group. $^*p < 0.05$ vs. respective vehicle treated controls.

as by automated scoring using EthoVision (t_{14} = 3.76, p = 0.002). The effect of paroxetine, however, could only be detected by EthoVision (t_{14} = 2.37; p = 0.033), and not via manual scoring (t_{14} = 0.62, p = 0.54). Accordingly, including all 24 animals derived from the three treatment groups (vehicle, paroxetine, desipramine) for correlation analysis between EthoVision (7% immobility score) and manual scoring revealed no significant correlation (r^2 = 0.09, p = 0.17). However, excluding the paroxetine treatment group and including only vehicle and desipramine treated mice in the correlation analysis (n = 16) revealed a significant correlation between automated and manual scoring (r^2 = 0.37, p = 0.012). This correlation was even stronger when an immobility score of 10%, which was ultimately used for all automated analysis in the present study (see above), was applied for the

EthoVision data ($r^2 = 0.44$, $p = 0.005$).

Whereas the antidepressant-like effects of tricyclic antidepressants such as desipramine or imipramine can be reliably detected in the mouse FST, the detection of antidepressant-like effects of SSRIs such as paroxetine or fluoxetine in the mouse FST has turned out to be much more difficult, and is often seen only in a very limited number of mouse strains (Lucki et al., 2001). In C57BL/6N mice, paroxetine seems to influence locomotor coordination during swimming, which renders certain mice unable to stay afloat over the entire 6 minutes of the test, but allows their bodies to sink below the water surface with just their nostrils sticking out in order to breathe. Thus, they acquire a vertical rather than horizontal swimming or immobility posture. As the manual scorer relies on some objective measures for the judgment of immobility, such as no movement of the paws, some of these paroxetine treated mice are judged immobile even if their bodies actually still move. Thus, the objective evaluation of body movement via the detection of total pixel change with EthoVision proved to be superior to the manual evaluation with regard to antidepressant-like effects of SSRIs (compare the scatter plot in Fig. 2.5.1b for paroxetine treated mice).

In conclusion, as we were able to detect both noradrenergic as well as serotonergic antidepressant-like effects via video-tracking with EthoVision, we applied this automated detection system to the screen of endocannabinoid modulating drugs.

Pharmacological blockade of CB1 receptors induces antidepressant-like effects in the mouse FST

The pharmacological blockade of CB1 receptors with the CB1 receptor antagonist SR141716 (0, 0.05, 2, 10 mg/kg) led to a dose-dependent decrease of immobility in the FST [*Drug*: $F_{3,40} = 7.07$, $p < 0.001$; one-way ANOVA (*Drug*); Fig. 2.5.2a]. *Post hoc* analysis revealed that SR141716, at the doses of 2 and 10 mg/kg, significantly reduced immobility as compared to vehicle. The pharmacological blockade of CB1 receptors with a different CB1 receptor antagonist, AM251 (0, 0.05, 2, 10 mg/kg), also led to a dose-dependent decrease of immobility in the FST [*Drug*: $F_{3,28} = 6.37$, $p = 0.002$; one-way ANOVA (*Drug*); Fig. 2.5.2b]. *Post hoc* analysis revealed that AM251, at the doses of 2 and 10 mg/kg,
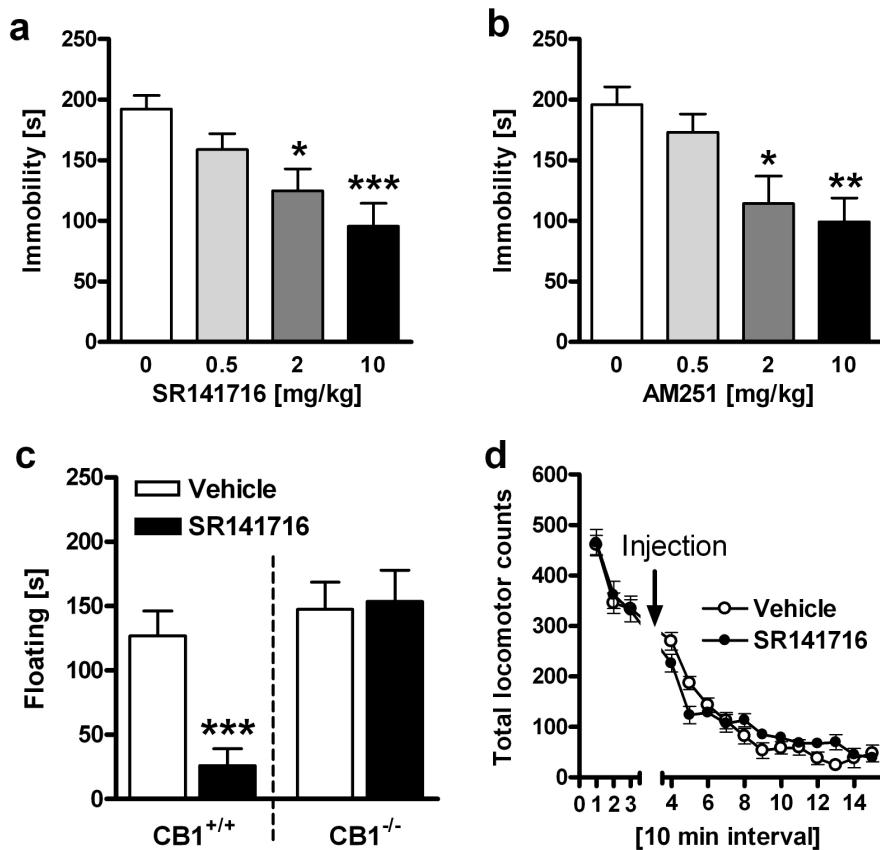
Figure 2.5.2 The pharmacological blockade of CB1 receptor signaling induces antidepressant-like effects in the mouse FST. C57BL/6N mice were acutely treated with vehicle (0 mg/kg) or the CB1 receptor antagonists SR141716 (0.5, 2, 10 mg/kg) (**a**) or AM251 (0.5, 2, 10 mg/kg) (**b**), respectively, and exposed to the FST. The total duration of immobility per 6 min exposure is depicted. (**c**) CB1 receptor knockout (CB1$^{-/-}$) mice or their wild-type littermate controls (CB1$^{+/+}$) were either treated with vehicle (0 mg/kg) or SR141716 (10 mg/kg) and exposed to the FST. The total immobility time per 6 min FST is shown. (**d**) Total locomotor activity of male C57BL/6N mice over 2.5 h is displayed in 10 min bins. Animals were introduced into the locomotor boxes and, after a habituation period of 30 min, were injected with vehicle (0 mg/kg) or SR141716 (10 mg/kg). n = 8-12 per group. $^{*}p < 0.05$, $^{**}p < 0.01$, $^{***}p < 0.001$ vs. respective vehicle treated group (0 mg/kg).

significantly reduced immobility as compared to vehicle. The reduction in immobility observed with SR141716 or AM251 was comparable to that seen after desipramine or paroxetine administration.

To assess the specificity of the antidepressant-like effect of SR141716 (10 mg/kg), we administered the antagonist to CB1 receptor knockout and wild-type littermate mice (Fig. 2.5.2c). Two-way ANOVA (*Genotype, Drug)* revealed a significant effect of *Genotype* ($F_{1,37} = 12.3$, $p = 0.001$), of *Drug* ($F_{1,37} = 5.04$, $p = 0.031$), and a significant *Genotype x Drug* interaction ($F_{1,37} = 6.4$, $p = 0.016$). *Post hoc* analysis revealed that SR141716 significantly reduced immobility in wild-type mice, but not in CB1 receptor knockout mice. The mutant mice did not exhibit any difference in immobility under vehicle-treated conditions.

To ensure that the antidepressant-like effect of SR141716 was not confounded by locomotor activation, we assessed the effects of the drug on locomotor function in C57BL/6N mice (Fig. 2.5.2d). Two-way ANOVA (*Drug, Time)* for repeated measures (*Time*) revealed a significant effect of *Time* ($F_{11,231} = 46.3$, *p* < 0.001) illustrating locomotor habituation. No significant *Drug* effect ($F_{1,21} = 0.1$, *p* = 0.75), but a significant *Drug x Time* interaction ($F_{11,231} = 3.27$, *p* < 0.001), was revealed. This suggested no general effect of SR141716 on locomotor activity, but possibly a very slight reduction during the first half hour after injection and a very slight increase during the next one and a half hours as compared to vehicle treated controls. *Post hoc* analysis revealed no significant differences between SR141716 and vehicle treated animals at any given time point. Furthermore, as the experiment was conducted during the light, inactive phase of the animals, the very slight locomotor increase that was detected with SR141716 towards the end of the experiment (after significant habituation to the novel environment had occurred) could reflect increased wakefulness, which is induced by SR141716 (Santucci, et al., 1996), rather than true locomotor activation.

Enhancement of endocannabinoid signaling does not influence forced swimming behavior

The pharmacological enhancement of endocannabinoid signaling, via administration of the fatty acid amide hydrolase (FAAH) inhibitor URB597 (Fig. 2.5.3a) or via the administration of the endocannabinoid re-uptake inhibitors AM404 (Fig. 2.5.3b) or UCM707 (Fig. 2.5.3c), failed to affect immobility behavior of C57BL/6N mice in the FST over a wide dose range of the drugs [*Drug*: $F_{3,28} < 1.02$, *p* > 0.4; one-way ANOVA (*Drug*)].

SR141716 exerts its antidepressant-like effects in the FST independently of monoaminergic signaling

In order to assess whether SR141716 exerts its antidepressant-like effects in the FST via activation of serotonergic or catecholaminergic neurotransmission, we pre-treated animals with the tryptophan hydroxylase inhibitor PCPA or the tyrosine hydroxylase inhibitor AMPT to specifically reduce serotonin or

a

b

c
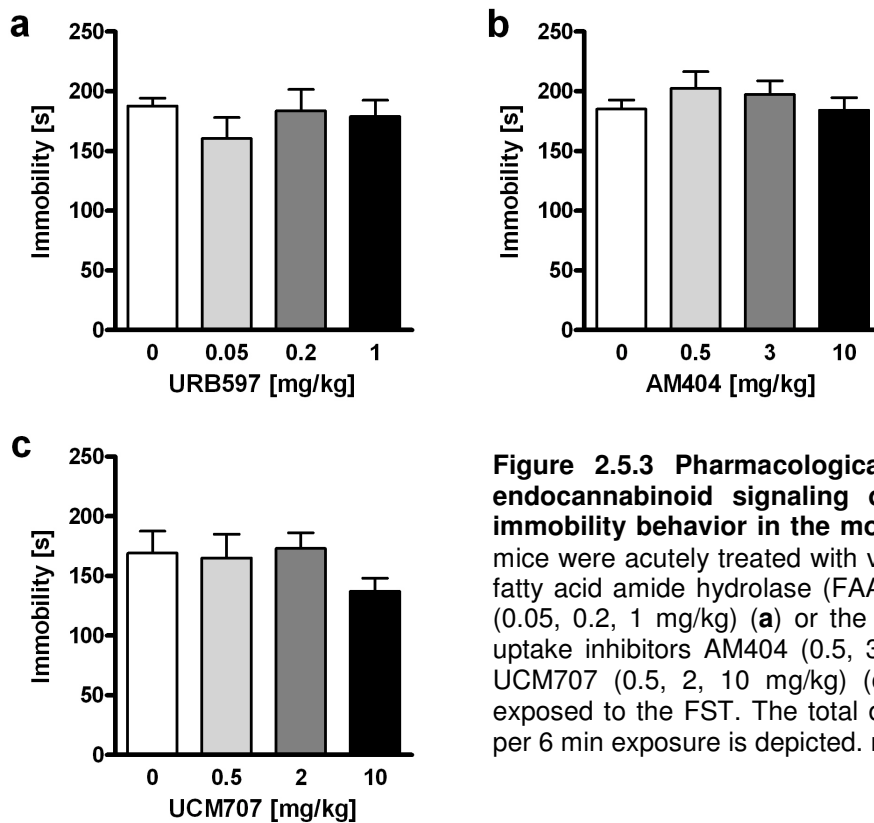
Figure 2.5.3 Pharmacological enhancement of endocannabinoid signaling does not influence immobility behavior in the mouse FST. C57BL/6N mice were acutely treated with vehicle (0 mg/kg), the fatty acid amide hydrolase (FAAH) inhibitor URB597 (0.05, 0.2, 1 mg/kg) (**a**) or the endocannabinoid re-uptake inhibitors AM404 (0.5, 3, 10 mg/kg) (**b**) and UCM707 (0.5, 2, 10 mg/kg) (**c**), respectively, and exposed to the FST. The total duration of immobility per 6 min exposure is depicted. n = 8-10 per group.

catecholamine concentrations, respectively, in the brain before treatment with SR141716 (10 mg/kg). Neither pre-treatment with PCPA [*Drug x Pre-treatment*: $F_{1,42}$ = 0.02, *p* = 0.89; two-way ANOVA (*Drug, Pre-treatment*); Fig. 2.5.4a], nor pre-treatment with AMPT [*Drug x Pre-treatment*: $F_{1,44}$ = 1.01, *p* = 0.32; two-way ANOVA (*Drug, Pre-treatment*); Fig. 2.5.4b] influenced the antidepressant-like effects of SR141716 (*Drug*: $F_{1,42}$ = 11.78, *p* = 0.0014, for the PCPA pre-treatment; *Drug*: $F_{1,44}$ = 20, *p* < 0.001, for the AMPT pre-treatment). PCPA and AMPT administration, in the absence of SR141716, failed to alter immobility in the FST (*Pre-treatment*: $F_{1,42}$ = 2.02, *p* = 0.16, for the PCPA pre-treatment; *Pre-treatment*: $F_{1,44}$ = 0.91, *p* = 0.35, for the AMPT pre-treatment).

In addition, we analyzed the influence of PCPA and AMPT pre-treatment on the hormonal stress response to forced swimming in vehicle- and SR141716-treated animals as a control for the pharmacological activity of the applied drugs. Two-way ANOVA of forced swim stress-induced corticosterone secretion revealed a significant *Pre-treatment* effect of PCPA ($F_{1,35}$ = 16.3, *p* < 0.001) indicating that PCPA pre-treatment potentiated stress-induced corticosterone secretion (Fig. 2.5.4c). Two-way ANOVA also revealed a significant *Drug* effect ($F_{1,35}$ = 13.4, *p* < 0.001) indicating that SR141716 treatment increased forced swim stress-induced
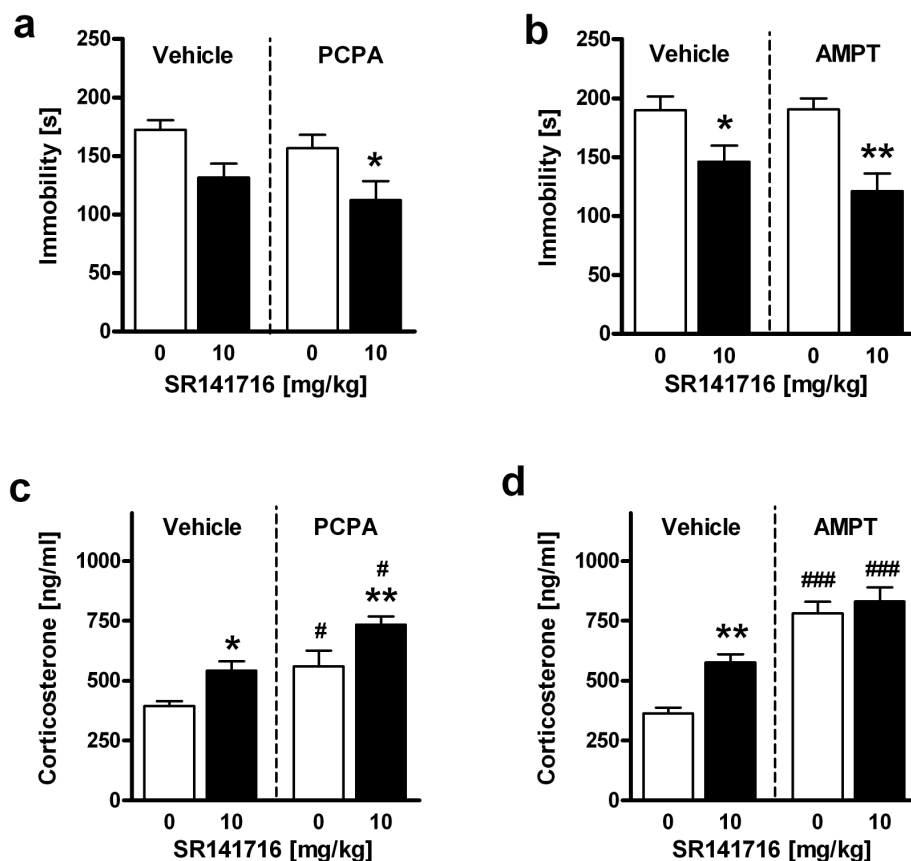
Figure 2.5.4 Effects of PCPA or AMPT pre-treatment on SR141716-induced behavioral and hormonal responses to forced swim stress. C57BL/6N mice were either pre-treated with vehicle or the tryptophan hydroxylase inhibitor PCPA (250 mg/kg twice daily for three days) (**a,c**) or with vehicle or the tyrosine hydroxylase inhibitor AMPT (200 mg/kg, once, 4 h before FST exposure) (**b,d**). One hour before the FST, PCPA and AMPT pre-treated mice were injected with vehicle (0 mg/kg i.p.) or SR141716 (10 mg/kg i.p.). Total immobility times per 6 min FST exposure are depicted for the PCPA pre-treatment group in (**a**) and for the AMPT pre-treatment group in (**b**). 30 min after the onset of the forced swim stress, corticosterone levels were determined. Plasma corticosterone concentrations for the PCPA pre-treatment group are depicted in (**c**) and for the AMPT pre-treatment group in (**d**). n = 9-12 per group. $^*p < 0.05$, $^{**}p < 0.01$, vs. respective vehicle treated group (0 mg/kg); $^#p < 0.05$, $^{###}p < 0.001$ vs. respective vehicle pre-treated group.

corticosterone secretion. A non-significant *Pre-treatment x Drug* interaction ($F_{1,35} = 0.1$, $p = 0.75$) indicated that SR141716 exerted its corticosterone elevating effect independent of vehicle or PCPA pre-treatment.

Two-way ANOVA of forced swim stress-induced corticosterone secretion in the AMPT pre-treated group revealed a significant *Pre-treatment* effect of AMPT ($F_{1,35} = 61.3$, $p < 0.001$) indicating that AMPT pre-treatment strongly elevated stress-induced corticosterone secretion (Fig. 2.5.4d). Two-way ANOVA also revealed a significant *Drug* effect ($F_{1,35} = 9.35$, $p < 0.01$) indicating that SR141716 treatment increased stress-induced corticosterone secretion in mice pre-treated with vehicle, as found in the previous experiment as well. An almost significant *Pre-treatment x Drug* interaction ($F_{1,35} = 3.57$, $p = 0.067$) indicated that SR141716

exerted its corticosterone elevating effect only in mice pre-treated with vehicle, but was not able to further potentiate the already elevated corticosterone levels in the AMPT pre-treated group.

Forced swim stress alters endocannabinoid concentrations in a brain region-specific and time-dependent manner

To assess the impact of forced swimming on the endocannabinoid system, we measured by LC/MS the levels of both anandamide and 2-AG in several brain regions at 10 and 30 min after swimming onset. Forced swimming was accompanied by an almost brain-wide downregulation of anandamide levels. One-way ANOVA followed by *post-hoc* analysis revealed swim stress-induced reductions in the levels of anandamide at both time points after swimming onset in the VPC ($F_{2,20}$ = 3.79, p = 0.04; Fig. 2.5.5a), in the NAC ($F_{2,21}$ = 11.8, p < 0.001; Fig. 2.5.5b), in the BLA ($F_{2,21}$ = 6.9, p = 0.005; Fig. 2.5.5g), in the DH at 10 min ($F_{2,21}$ = 6.02, p = 0.009; Fig. 2.5.5h) and in the RN ($F_{2,17}$ = 15.1, p < 0.001; Fig. 5i). No change in anandamide levels was observed in the caudate putamen (CPU) ($F_{2,21}$ = 0.35, p = 0.71; Fig. 2.5.5c). 2-AG levels were transiently increased 10 min after swimming onset in the CPU ($F_{2,21}$ = 4.23, p = 0.029; Fig. 2.5.5f) and BLA ($F_{2,21}$ = 4.47, p = 0.024; Fig. 2.5.5j), but returned to baseline by 30 min. In contrast, 2-AG levels were reduced at 10 and 30 min after swimming onset in the DH ($F_{2,21}$ = 5.08, p = 0.016; Fig. 2.5.5k), and showed a statistically non-significant trends towards a reduction at 30 min in the VPC ($F_{2,21}$ = 2.64, p = 0.095; Fig. 2.5.5d) and NAC ($F_{2,20}$ = 2.93, p = 0.077; Fig. 2.5.5e). No changes in 2-AG levels were observed in the RN ($F_{2,17}$ = 2.48, p = 0.11; Fig. 2.5.5i).
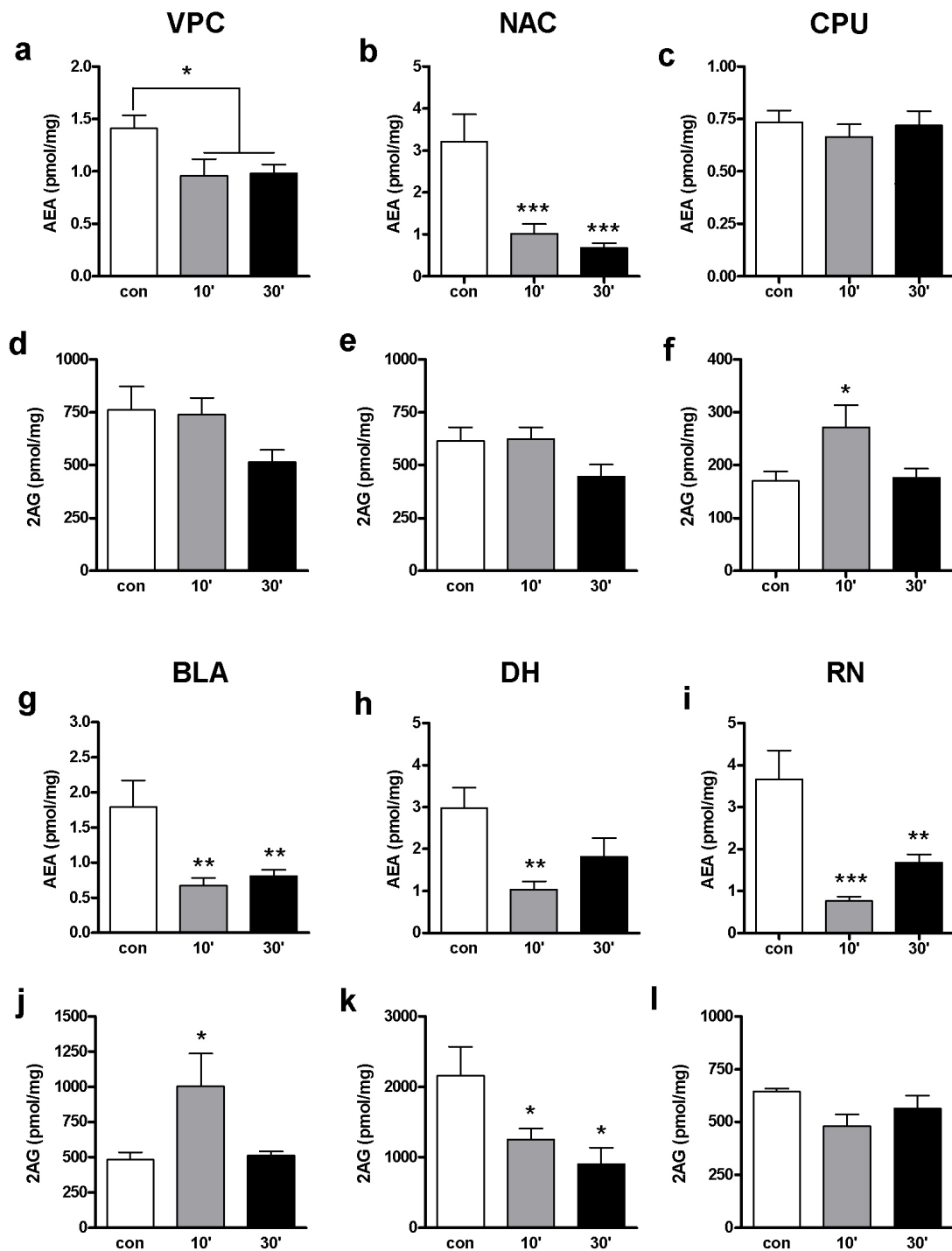
Figure 2.5.5 Forced swim stress-induced alterations in brain endocannabinoid levels. Male C57BL/6N mice were either killed under basal control conditions (con) or exposed to a 6 min FST and killed 10 (10') or 30 min (30') after onset of swimming. Brain regions were dissected and levels of 2-arachidonoyl glycerol (2-AG) and anandamide (AEA), normalized to total protein content, were determined. AEA and 2-AG levels in the ventromedial prefrontal cortex (VPC; **a,d**), nucleus accumbens (NAC; **b,e**), caudate putamen (CPU; **c,f**), basolateral amygdala (BLA; **g,j**), dorsal hippocampus (DH; **h,k**) and the raphe nuclei (RN; **i,l**). n = 6-8 per group. $^{*}p < 0.05$, $^{**}p < 0.01$, $^{***}p < 0.001$ vs. respective unstressed control group. Data for this Figure were kindly provided by Dr. G. Astarita.

2.5.5 Discussion

The goal of the present study was to systematically characterize the role of endocannabinoid signaling for stress coping behavior (immobility = floating) in the mouse FST. We demonstrated that pharmacological blockade of CB1 receptors, via the closely related antagonists SR141716 and AM251, decreased immobility in the FST in C57BL/6N mice in a dose-dependent manner (Figs. 2.5.2a,b). Our results are in accordance with other publications, which also demonstrated antidepressant-like effects of SR141716 or AM251 in the FST in NIH Swiss mice (3 mg/kg) (Tzavara et al., 2003b), in Wistar rats (3 and 10 mg/kg p.o.) (Griebel et al., 2005) and in C57BL/6 mice (1 and 10 mg/kg) (Shearman et al., 2003). Even though our results fit well with the current literature, they were unexpected, because, when injected 2 h prior to the FST, we recently demonstrated that SR141716 (10 mg/kg) slightly, but statistically non-significantly, increased total immobility time in male and female C57BL/6N mice after acute administration at day 1 (Chapter 2.3, Figs. 2.3.2b,e).

Nevertheless, it was difficult to compare present with previous results as they were conducted in different laboratories under slightly different conditions (UT Southwestern, USA vs. Max Planck Institute of Psychiatry, Germany). Therefore, we ran an additional experiment with SR141716 administration 1 h prior to testing with CB1 receptor knockout mice and their wild-type littermates under our previously established conditions in Munich (Fig. 2.5.2c). Indeed, SR141716 injection 1 h prior to testing reduced immobility in wild-type animals, consistent with the present results obtained with C57BL/6N animals (Fig. 2.5.2a). Therefore, these results argue for a significant influence of the injection schedule (1 h vs. 2 h prior to testing) on SR141716 mediated behavioral effects in the FST. SR141716 exerted no effects in CB1 receptor knockout mice, confirming its specificity for the CB1 receptor (Chapter 2.3, Fig. 2.3.3). No genotype effect was observed between vehicle-injected CB1 receptor knockout and wild-type animals with regard to floating, in agreement with previous findings (Chapter 2.4, Fig. 2.4.5). These discrepancies between the effects of acute pharmacological blockade and the genetic inactivation of CB1 receptors on FST behavior suggest that CB1 receptor knockout mice develop secondary changes due to a lifelong absence of the

receptor, which might compensate for the impairment of endocannabinoid signaling in the FST. Similar results were obtained with the CB1 receptor antagonist AM251 and another CB1 receptor knockout strain (Zimmer et al., 1999), where AM251 exerted its antidepressant-like effects only in wild-type mice (Shearman et al., 2003).

Previously, we demonstrated that naïve CB1 receptor knockout mice showed a slight increase of total immobility time when compared to wild-type mice (Chapter 2.3, Fig. 2.3.1b,e). This phenotype seems to depend on basal levels of stress and arousal, as vehicle injection 1 h prior to testing apparently masked potential genotype differences (Chapter 2.4, Fig. 2.4.5 and Fig. 2.5.2c present study). Two different CB1 receptor knockout lines that were generated (Zimmer et al., 1999; Ledent et al., 1999) have not yet been tested under naïve conditions, but failed to show any genotype differences in floating behavior following vehicle injection, too (Jardinaud et al., 2005; Shearman et al., 2003).

Interactions between stress and the endocannabinoid system have recently gained much attention (Viveros et al., 2005; Hill et al., 2005; Patel et al., 2005; Hohmann et al., 2005). One conclusion from this work is that the stress level of the animals before or during a behavioral test dramatically affects the actions of endocannabinoid-modulating drugs (Viveros et al., 2005; Wotjak, 2005). For instance, we recently demonstrated anxiolytic-like effects of URB597 (Moreira et al., in press) only in wild-type mice, which had been tail-clipped and ear-marked and, thus, had been subjected to increased stress exposure. The aversiveness of the test context was also shown to play an important role (Haller et al., 2004b; Naidu et al., 2007). Furthermore, although we have recently shown a slight increase in immobility in the FST with SR141716, when administered i.p. 2 h prior to testing, the same injection procedure resulted in decreased immobility upon repeated SR141716 administration for two or ten days before testing (Chapter 2.4, Figs. 2.4.6 and 2.4.8). Therefore, it is conceivable that, when mice are tested under conditions of greater stress (injected 1 h instead of 2 h before testing; injected repeatedly instead of once; or, in case of the CB1 receptor mutant mice, injected instead of being naïve), the acute application of a CB1 receptor antagonist such as SR141716 leads to antidepressant-like activities in the FST. Consistent with this hypothesis, SR141716 administration was also shown to reduce chronic mild stress-evoked increases of immobility in the mouse FST (Griebel et al., 2005).

We found no significant ambulatory locomotor-stimulating effect of SR141716 (10 mg/kg; Fig. 2.5.2d) in agreement with the literature (Patel and Hillard, 2006; Tzavara et al., 2003b). This suggests that general locomotor activation was not a confounding factor for the antidepressant-like effects in the FST. However, the possibility remains that the transient increase of 2-AG in the CPU (Fig. 2.5.5f) enhanced fine locomotor coordination during swimming and floating. This effect might have been blocked by SR141716 administration, thus decreasing the ability of mice to maintain a stable floating position.

As the pharmacological blockade of CB1 receptors reduced immobility in the FST, we hypothesized that drugs that enhance endocannabinoid signaling might lead to an increase of immobility. However, neither the FAAH inhibitor URB597, nor the endocannabinoid reuptake inhibitors AM404 and UCM707, significantly influenced immobility behavior in the FST (Figs. 2.5.3b,c,d), corroborating findings from FAAH knockout mice, which also showed no deficit in FST behavior (Naidu et al., 2007). These findings in mice disagree with the results of recent studies in rats, where endocannabinoid-elevating drugs such as URB597 and AM404 were shown to exert antidepressant-like effects in the FST (Gobbi et al., 2005; Hill and Gorzalka, 2005b; Hill et al., 2007). We are unaware of another laboratory which has tested these substances in the mouse FST. It therefore seems preliminary to hypothesize a species-dependent differential effect of endocannabinoid signaling on FST behavior, as has been recently suggested for anxiety behavior (Haller et al., 2007). However, additional systematic screening studies of endocannabinoid-modulating drugs in the rat FST could help clarify this issue (Hill and Gorzalka, 2005b).

As mentioned in the Introduction, accumulating evidence suggests an interaction between endocannabinoid and monoaminergic signaling (Gobbi et al., 2005; Oropeza et al., 2007; Haring et al., 2007), and SR141716 administration in rats was shown to increase monoamine efflux in the prefrontal cortex (Tzavara et al., 2003b). Thus, we hypothesized that SR141716 might produce its antidepressant-like effects in the FST via activating monoaminergic neurotransmission, similarly to classical antidepressants. However, neither decreasing serotonin synthesis by PCPA pre-administration, nor decreasing catecholamine synthesis by AMPT pre-administration, was able to attenuate the antidepressant-like effects exerted by SR141716 in the FST (Figs. 2.5.4a,b),

suggesting mediation of this effect via other neurotransmitter systems. Whether the direct regulation of GABAergic or glutamatergic neurotransmission is involved requires further exploration. The depletion of serotonin by PCPA or of catecholamines by AMPT *per se* did not alter baseline activity in the FST, similar to previous results (Chapter 3.2, Figs. 3.2.9a,b) (Mayorga et al., 2001). These observations suggest that monoamines may be more critically involved in mediating antidepressant-like effects of classical antidepressants rather than in determining baseline responses in the FST.

As shown previously (Chapter 2.4, Figs. 2.4.3-4), SR141716 administration increased forced swim stress-induced corticosterone secretion in vehicle pre-treated mice (Figs. 2.5.4c,d), which corroborates the HPA axis-stimulating effects of SR141716 (Wade et al., 2006). Whereas AMPT pre-treatment already maximally stimulated corticosterone secretion after swim stress, which could, as a result, not be further elevated by SR141716 (Fig. 2.5.4d), moderate stimulation of corticosterone secretion by PCPA pre-treatment could be further increased by SR141716 (Fig. 2.5.4c). This suggests that the ability of endocannabinoids to dampen corticosterone secretion is not mediated via influencing serotonergic neurotransmission. The results further imply a general independence of the behavioral effects of CB1 receptor antagonists from stress-induced corticosterone secretion.

Further work is needed to understand the physiological consequences of forced swim stress-induced changes in endocannabinoid levels. One possibility, based on the antidepressant-like effects of CB1 receptor antagonists, is that the broad downregulation of anandamide represents a coping response to stress exposure. Another possibility is that the enhanced levels of 2-AG in certain brain regions may mediate some of the deleterious effects of stress. Nevertheless, these hypotheses remain purely speculative, as our current understanding of the differential role of 2-AG and anandamide in the regulation of neurotransmission is insufficient (Piomelli, 2003). Although both endocannabinoids were shown to be temporally and spatially differentially regulated by stress (Hohmann et al., 2005), their specific influence on GABAergic and glutamatergic neurotransmission is not well characterized. Future experiments dealing with brain-region specific injections of endocannabinoid modulating drugs may help to further decipher the exact role of endocannabinoid signaling in FST behavior.

In conclusion, we show that the neurochemical response to forced swim stress in mice involves endocannabinoid signaling in a very complex, brain region-specific and temporally-regulated manner. Furthermore, we demonstrate that the pharmacological blockade of CB1 receptors reduces immobility in the FST independently of monoaminergic signaling, but possibly via inhibiting 2-AG-mediated CB1 receptor signaling in CPU or BLA.

2.6 Outlook and preliminary results from ongoing research on the role of the endocannabinoid system in depression-like behaviors

2.6.1 Defining the site of action for and the neuronal subpopulation involved in endocannabinoid-mediated HPA axis regulation

As mentioned in the Introduction (Chapter 2.1), CB1 receptors are present in many different brain areas and also in endocrine glands outside of the brain, which are involved in HPA axis regulation. However, it has not yet been understood how endocannabinoid signaling at these different sites is orchestrated to fine tune stress hormone release. In preliminary experiments, we could verify that a functional endocannabinoid system exists in the pituitary and the adrenal glands of mice. By quantitative real-time PCR (qRT-PCR), we could verify that CB1 receptors and the endocannabinoid degrading enzymes FAAH and MAGL are expressed in the mouse pituitary and adrenal glands (data not shown), whereas the exact location of CB1 receptors within the subregions of these organs is currently being investigated by ISH and immunohistochemistry. Additionally, we could show that in response to stress both endocannabinoids, 2-AG and anandamide, are not only regulated in limbic brain regions known to be involved in stress perception (such as the amygdala and the hippocampus, see Fig. 2.5.5), but also in the hypothalamus, the pituitary gland and the adrenal glands (data not shown). Further experiments employing acute challenge tests with CRH and ACTH in CB1 receptor-deficient mice suggested that, in contrast to our *in vitro* findings (see Fig. 2.2.2), CB1 receptors in the intact organism are not involved in the integration of the CRH signal into ACTH release at the level of the pituitary, but are involved in the integration of the ACTH signal into corticosterone release at the level of the adrenal gland (data not shown). Furthermore, we could replicate our findings of insufficient dexamethasone-mediated corticosterone suppression in female CB1 receptor-deficient mice in males, corroborating the fact that CB1 receptors are involved in corticosterone feedback (data not shown). Because dexamethasone is believed to act primarily at GR-mediated feedback at the level of the pituitary, we are now planning to challenge CB1 receptor-deficient mice with

corticosterone (which crosses the blood brain barrier) to see whether glucocorticoid feedback under these conditions is also hampered in CB1 receptor-deficient mice. Finally, after Di and co-workers have shown a glucocorticoid-mediated fast-feedback mechanism involving endocannabinoids at the level of the hypothalamus in rat brain slices using electrophysiology (Di et al., 2003), we aim at finding *in vivo* evidence for this hypothesis, by measuring endocannabinoid tissues levels after acute corticosterone challenge in the hypothalamus, the hippocampus, the pituitary and the adrenals. Furthermore, as Di and co-workers have suggested that predominantly CB1 receptors on PVN innervating glutamatergic neurons are responsible for the above mentioned feedback mechanism (Di et al., 2003), we have been employing a number of conditional CB1 receptor mutant mice that lack the receptor only in specific subpopulations and regions of the brain (Monory et al., 2006; Marsciano et al., 2003) in order to investigate the *in vivo* situation. Indeed, preliminary results point towards a predominant contribution of CB1 receptor signaling on subcortical glutamatergic synapses for HPA axis regulation (data not shown). Taken together, it becomes apparent that, in addition to CB1 receptor signaling on glutamatergic hypothalamic neurons, also CB1 receptor signaling within the adrenal glands may might aid in regulating HPA axis function.

2.6.2 Investigating the role of endocannabinoid signaling for social stress processing in mice

Having demonstrated that the endocannabinoid system is involved in acute behavioral and neuroendocrine stress processing in response to the FST (compare previous Chapters), we have been investigating whether the endocannabinoid system also modulates acute and chronic social stress processing in mice. This research project was carried out in collaboration with the laboratories of Prof. E.J. Nestler at UT Southwestern, Dallas, TX, USA and of Prof. D. Piomelli, University of Irvine, CA, USA. As mentioned in the Introduction (Chapter 1.3.1.5) the laboratory of E.J. Nestler has recently established an animal model of depression based on chronic social defeat in mice. This model was employed to answer the above hypothesis. Similar to what we have done for the FST (compare Fig. 2.5.5), we have also measured tissue levels of both major

endocannabinoids, 2-AG and anandamide, in a variety of different brain regions and in the adrenals and pituitary after acute and chronic (10 days) social defeat. We could demonstrate that endocannabinoid signaling is actively involved not only in acute, but also in chronic social stress processing, and in fact, in a time-specific and locally restricted manner (data not shown). Currently, we are investigating, whether chronic social stress exposure does also alter the mRNA and protein expression levels of the CB1 receptor, the endocannabinoid degrading enzymes FAAH and monoacyl glycerol lipase (MAGL), and the endocannabinoid synthesizing enzymes N-arachidonyl phosphatidylethanolamine phospholipase D (NAPE-PLD) and 1,2-diacyl-glycerol lipase (DAGL) (Piomelli, 2003). Depending on the result, we might furthermore also study in brain tissue membrane preparations whether the enzymatic activity of the degrading or synthesizing enzymes are influenced, which might explain the observed different endocannabinoid levels after stress. Complementing the biochemical analysis, we also employed pharmacological means in order to study the role of endocannabinoid signaling during social defeat stress for long-term consequences of the stressor. However, neither enhancing endocannabinoid signaling during chronic social defeat by daily injections of endocannabinoid signaling enhancing drugs URB597 or AM404, nor blocking CB1 receptor signaling via SR141716 did significantly influence social defeat-induced long-lasting social avoidance towards other neutral, unfamiliar, non-aggressive mice (data not shown). Testing chronically socially defeated animals that had been concomitantly treated with SR141716 in a variety of other depression- and anxiety-related behavioral tests 2-4 weeks after termination of the defeat stress revealed that SR141716 treated and defeated mice reacted with increased anxiety measures in comparison to vehicle treated defeated mice (data not shown). Furthermore, similar to what we have shown for the FST (compare Chapter 2.4), SR141716 treatment augmented corticosterone secretion in response to acute and chronic defeat, but did not induce long-lasting disturbances of HPA axis function (data not shown). Taken together these data imply that endocannabinoid signaling is involved in acute and chronic social stress processing in mice, but not in the development of long-term social avoidance in response to chronic defeat. Moreover, endocannabinoid signaling seems to have a stress-protective role as chronic pharmacological blockade of CB1 receptors

during chronic social defeat induces long-lasting anxiogenic behavioral responses in mice.

2.7 Generation of bacterial artificial chromosome-based transgenic mice conditionally overexpressing a CB1 receptor – Venus fusion protein

In the previous Chapters 2.2.2-6, we have studied the role of CB1 receptor signaling for neuroendocrine and behavioral stress processing. To facilitate the investigation of the underlying precise mechanisms on the cellular level, concomitantly with the above research, we followed a transgenic strategy to visualize CB1 receptor expression and trafficking in the future. Employing such an approach might, for instance, help to find the reason for the encountered "tolerance" effect to the corticosterone-elevating actions of an acute SR141716 challenge in response to long-term chronic treatment with the antagonist (compare Fig. 2.4.8).

The present work was accomplished in collaboration with Prof. Dusan Bartsch of the Central Institute of Mental Health, Mannheim, Germany. Prof. D. Bartsch was responsible for the purification and oocyte injection of the CB1-Venus-BAC (compare Fig. 2.7.12). All other experiments were performed by me (Figs. 2.7.1-11).

2.7.1 Summary

The CB1 receptor belongs to the class of G-protein coupled receptors (GPCRs) and, as such, is prone to endocytosis, trafficking and degradation upon agonist exposure. Thus, the receptor is capable of desensitization and resensitization, and is able to mediate tolerance to cannabinoids. It was the aim of the current study to generate a transgenic mouse model based on the fusion of the CB1 receptor to the fluorescent Venus protein, in order to investigate the dynamics of CB1 receptor trafficking. A CB1-EGFP (enhanced green fluorescent protein) fusion was generated and its molecular properties were evaluated in cultured HEK293 and CHO cells. Similar to the native receptor, the fusion protein was membrane-bound and was prone to agonist-stimulated endocytosis and inverse agonist-stimulated translocation from intracellular stores to the plasma membrane. Furthermore, CB1-EGFP was able to mediate CB1 receptor agonist-stimulated cAMP response element (CRE)-dependent luciferase expression and

extracellularly regulated kinase-1/2 (ERK 1/2) phosphorylation in a manner similar to the native receptor. Hence, based on this CB1-EGFP fusion, two homologous recombination cassettes, where EGFP was exchanged for the much enhanced fluorescent Venus protein, were designed: CB1-Venus-Easy and CB1-Venus-Soph. Both cassettes were later exposed to homologous recombination in *E.coli* with the endogenous CB1 locus, which was present on a CB1-containing bacterial artificial chromosome (CB1-BAC), via Red/ET cloning to yield CB1-Venus-Easy- and CB1-Venus-Soph-BAC. The latter construct was injected into pro-nucleus stage mouse embryos, giving rise to four potential founder animals that had integrated the CB1-Venus-Soph-BAC into their genome. The CB1-Venus-Soph-BAC had been equipped with a *lox2272* flanked transcriptional STOP cassette that renders the expression of the CB1-Venus protein in transgenic mice conditional on the co-expression of Cre recombinase. Altogether, we generated a transgenic mutant mouse line, which allows the conditional overexpression of a CB1-Venus fusion protein and, thus, will greatly facilitate CB1 receptor trafficking research in order to elucidate its relevance for endogenous as well as exogenous cannabinoid action.

2.7.2 Introduction

The CB1 receptor is one of the most abundant GPCRs in the brain (Piomelli, 2003). The receptor couples predominantly to pertussis toxin (PTX) sensitive trimeric inhibitory $G_{i/o}$ proteins, although its coupling to stimulatory G_s proteins under certain circumstances was also described (Demuth and Molleman, 2006). Whereas many GPCR ligands bind to the extracellular N-terminal domain of the respective receptors, cannabinoid agonists, due to their lipophilic nature, have been suggested to bind to CB1 receptors directly within their 7-transmembrane helical clusters (Demuth and Molleman, 2006). Upon ligand binding, CB1 receptors undergo conformational changes, which initiate, via G-protein subunit release and activation, several intracellular signaling cascades such as the opening of inward-rectifying K_{ir}^+-channels, the closing of N- and P/Q-type Ca^{2+}-channels, the inhibition of adenylyl cyclase, and, hence, the downregulation of cyclic adenosine monophosphate (cAMP) (Diaz-Laviada and Ruiz-Llorente, 2005). In addition, CB1 receptor signaling is able to activate the mitogen-activated protein (MAP) kinase cascade. However, mechanisms that may link CB1 receptor activation with the MAPK cascade, such as β-arrestin interactions, "receptor transactivation" or $G_{\beta\gamma}$-subunit-mediated phosphatidyl inositol-3 kinase (PI3K) activation, have only begun to be explored (Diaz-Laviada and Ruiz-Llorente, 2005; Demuth and Molleman, 2006).

Upon acute and/or prolonged activation, GPCRs usually undergo receptor desensitization (attenuation of receptor responsiveness) to prevent hyper-stimulation, which involves, among other processes, receptor endocytosis (Ferguson, 2001; Kallal and Benovic, 2000). Upon stimulus termination, GPCRs are frequently recycled back from endocytotic compartments to the plasma membrane, often referred to as "resensitization". However, if the stimulus is long-lasting, GPCRs are known to undergo degradation instead of resensitization, which is associated with sorting of the receptors from endocytotic to lysosomal compartments. This receptor downregulation can contribute (in addition to receptor endocytosis and/or inactivation, for instance, through phosphorylation) to a phenomenon, which is encountered after continuous drug administration, and which is commonly referred to as tolerance (fading response of receptors to drugs after prolonged stimulation) (Ferguson, 2001).

120

Comparable to other GPCRs, CB1 receptors are also known to undergo endocytosis and receptor trafficking, and tolerance to cannabinoids is a well known phenomenon. However, studies investigating these molecular processes are still sparse and confined to the last ten years of research. Many of the earlier studies were conducted in immortalized cell lines with transfected receptor constructs, but recent studies in primary neuronal cell cultures were unable to confirm many of these early findings. For instance, whereas CB1 receptor internalization upon agonist exposure occurs very fast (within 15 min up to 3 h) in immortalized cell lines (Jin et al., 1999; Hsieh et al., 1999; Leterrier et al., 2004), this process takes much longer in neurons (up to 16 h) (Coutts et al., 2001). Whereas CB1 receptors are endocytosed via both clathrin-coated vesicles and via caveolae in immortalized cell lines (Keren and Sarne, 2003), endocytosis in neurons seems to occur almost exclusively via clathrin-coated pits (Leterrier et al., 2006). Thus, due to these discrepancies, conclusions derived from studies in immortalized cell lines clearly demand confirmation in primary neuronal cultures or *in vivo*. A recent study has followed this approach (Tappe-Theodor et al., 2007). The authors first demonstrated the interaction of G-protein associated sorting protein (GASP1) with CB1 receptors *in vitro*. Then they found that this interaction is necessary for the agonist-induced sorting of CB1 receptors to the lysosomal compartment and, thus, for its final degradation in cell lines. Afterwards, they confirmed these conclusions *in vivo*, demonstrating that analgesic tolerance to cannabinoids is dependent on agonist-induced CB1 receptor degradation following a functional CB1-GASP1 interaction.

Two other studies from different laboratories have recently tried to establish the role of CB1 receptor endocytosis for the predominantly axonal presynaptic location of CB1 receptors by using hippocampal primary cultures (McDonald et al., 2007; Leterrier et al., 2006). Both studies found CB1 receptor immunoreactivity not only in the axonal but also in the somatodendritic compartment of the neuron. However, somatodendritic CB1 receptors underwent constant cycles of endocytosis and recycling, whereas CB1 receptors in the axon remained relatively stably inserted in the plasma membrane. Thus, both research studies put forward a theory of axonal CB1 receptor targeting through constitutive somatodendritic endocytosis. Newly synthesized receptors are initially delivered to both axonal and somatodendritic compartments, but subsequently, they are constantly eliminated

from the somatodendritic membrane because of constitutive endocytosis. Axonal compartments did possess a much lower endocytotic capacity than the somatodendritic compartment, thus providing retention of the receptor. This finding is supported by a commonly proposed membrane "diffusion barrier" at the axonal initial segment, which divides axonal and somatodendritic membrane compartments of neurons and hinders membrane proteins of the axonal compartment from diffusing into the somato-dendritic membrane compartment (Nakada et al., 2003).

Despite these similarities, both studies differ in the proposed driving force for this axonal targeting of the CB1 receptor: Whereas Leterrier and co-workers consider the pharmacologically active state of the receptor responsible for this process and believe in constitutive activation-driven endocytosis, McDonald and co-workers rather believe in receptor motifs or conformational states that are different from those used by agonist-induced internalization and that may also involve different endocytotic proteins between axonal and somatodendritic compartments. These contrasting conclusions are probably due to different neuronal primary culture conditions, to different neuron transfection protocols or to the use of differentially tagged proteins.

The aforementioned problems that are encountered with the interpretation of results derived from current *in vitro* technology illustrate the need for an *in vivo* tool to facilitate the investigation of CB1 receptor trafficking properties, which might delineate its relevance for the dynamics of endocannabinoid signaling as well as for exogenous drug efficacy involving cannabinoid tolerance.

Fluorescent proteins including green fluorescent protein (GFP) from the jellyfish *Aequorea Victoria* have been successfully applied for a long time in order to study and visualize receptor trafficking processes in the living cell (Kallal and Benovic, 2000). A wide variety of GPCRs has been fused to fluorescent proteins in the past, and most of these fusion receptor proteins were found not to be hampered in its function by the attached fluorescent protein (Arun et al., 2005).

This has prompted researchers to use such receptor fusions as basis for the generation of transgenic mice. However, to my knowledge, until to date, only two studies have used GPCR-GFP fusions in order to elucidate the function of these receptors within the brain. Both studies represent transgenic knock-in strategies of

GPCR-GFP fusions (rhodopsin-GFP or δ-opioid receptor-GFP, respectively) into the original gene locus (Scherrer et al., 2006; Chan et al., 2004).

In addition to the knock-in approach, another technique to generate transgenic mice, which is based on bacterial artificial chromosome (BAC) technology, has gained increasing attention (Gong et al., 2003; Sparwasser et al., 2004). Using this methodology, the gene of interest is located ideally in the middle of a large BAC (150-300 kb length). Hence, also all gene regulatory elements are present on the BAC, up- and downstream of the gene of interest. These BACs are maintained in a low copy number in *E. coli*, and, thus, the homologous recombination process can be performed in bacteria, omitting the laborious and expensive use of embryonic stem cells. Homologous recombination between a circular BAC and a linearized recombination cassette flanked by short terminal homology arms can be achieved by so called Red/ET cloning via the expression of either the Rac prophage-derived recombination proteins RecE/RecT or their Redα/Redβ λ phage-derived counterparts from a pRed/ET expression plasmid, which has been transformed into the *E.coli* strain harboring the BAC of interest (Zhang et al., 1998; Muyrers et al., 1999). Once the gene locus of interest of the respective BAC has been altered via homologous recombination according to required needs, the vector backbone of the BAC is excised via restriction enzymes and the linearized BAC is purified and injected into the pro-nucleus of 0.5 day old mouse embryos in order to generate transgenic offspring. The BAC will integrate randomly into the genome, due to its large size usually only as a single copy or in a very low copy number, and the transgenic mouse will possess the gene of interest (e.g., the fused receptor protein encoded from the BAC) as a third or multiple copy in addition to the two alleles of the original gene.

In the present study, we used BAC technology in combination with Red/ET cloning to generate a transgenic mouse model comprised of the CB1 receptor fused to the fluorescent Venus protein (a very bright, yellow variant of GFP) (Nagai et al., 2002). In a first step, the CB1 receptor protein was C-terminally fused to an enhanced variant of GFP (EGFP) and its expression, trafficking, and signaling properties were compared to the non-fused native receptor to ensure its proper functioning. In the second step, based on this CB1-EGFP fusion protein, a homologous recombination cassette was cloned consisting of CB1-Venus preceded by a *lox2272* flanked transcriptional STOP cassette and a *FRT* flanked

neomycin resistance cassette. This allowed the eventual excision of the respective cassettes via Cre or Flp recombinase expression. In the third step, this recombination cassette was exposed to homologous recombination with a BAC that contained the original CB1 receptor gene locus yielding a modified BAC consisting of the CB1-Venus fusion protein and its preceding *lox2272* flanked STOP cassette. In the fourth step this modified BAC was injected into the pro-nucleus of 0.5 day old embryos in order to generate CB1-Venus-containing transgenic mice.

2.7.3 Materials and Methods

Cell culture and transfection

Cells were cultured in Dulbecco's modified Eagle's medium DMEM (Invitrogen, Karlsruhe, Germany) supplemented with 10% heat-inactivated fetal calf serum (FCS; Invitrogen), 2 mM glutamine (Invitrogen) and 1% antibiotic-antimicotic mixture (penicillin-streptomycin-amphotericin) (Invitrogen) at 37 ºC in a humidified 5% CO_2 incubator. Cells were plated at a density of 2 x 10^5 cells/well (HEK293) or 1 x 10^5 cells/well (CHO) in 24-well plates with 0.5 ml medium/well. Cells were grown until they reached a confluency of about 80 – 90% and were then transfected with Lipofectamine 2000 (Invitrogen) according to the manufacturer's protocol. All transfections were performed in triplicate. The total amount of transfected plasmid DNA per well was equalized by adjusting with empty pBluescript II KS+ vector (pBS; Stratagene, Zuidoost, Netherlands).

Luciferase reporter assays

Firefly luciferase activities were measured using a luciferase assay kit from Promega (Mannheim, Germany) according to manufacturer's instructions. CHO and HEK293 cells were seeded in 24-well plates and transfected 24 h later with 625 ng DNA/well (500 ng of pEGFP-N1, pMS1, pcDNA3, or pcDNA3-CB1, respectively, in combination with 125 ng of pCRE-Luc each). After 24 h cells were washed and stimulated for 4 h with vehicle (0.2% dimethylsulfoxide in serum free medium), 5 µM forskolin (FSK; Sigma), 1 µM CP-55,940 (Tocris), or 10 µM SR141716 (NIMH drug supply program) in combination with 1 µM CP-55,940 (Tocris), respectively. Stimulation was terminated by washing with phosphate buffered saline (PBS) followed by lysis in 100 µl/well of 1 x passive lysis buffer (PLB; Promega). Lysis was allowed to proceed for 15 min at room temperature under constant shaking of the culture plates. Lysates were stored at -80ºC until further processing. Measurement of luciferase activity was performed in a 96-well format. 20 µl of cell lysate from each well were combined with 50 µl of luciferase assay reagent II (LAR II; Promega), and luciferase activities were determined in an automated luminometer (Luminat 1420 LB 96; Wallac GmbH, Freiburg, Germany). Light emission was measured for 5 s. The respective remaining volumes of cell lysates were used for protein content measurements via Bradford reagent (Bio-Rad, Munich, Germany).

Western blots

For Western blot analysis 1 x 10^7 HEK293 or 5 x 10^6 CHO cells, respectively, were seeded in each well of a 6-well plate using 2 ml of medium/well. Cells were transfected 24 h later with 4 µg DNA/well. 6 h later the medium was changed to DMEM without serum. 18 h later cells were stimulated with 1 µM of the CB1 receptor agonist CP-55,940 (Tocris) in DMEM without serum. 5 min or 15 min later, respectively, stimulation was terminated by washing in ice cold PBS. Using a cell scraper, cells were collected in 100 µl/well ice cold RIPA lysis buffer (0.1% SDS, 1% Triton X-

100, 1% sodium deoxycholate in Tris buffered saline (TBS); all chemicals from Sigma, Munich, Germany) containing protease inhibitor solution (complete Mini EDTA-free protease inhibitor cocktail; Roche Diagnostics, Mannheim, Germany) and phosphatase inhibitors (phosphatase inhibitor cocktails I and II, Sigma), and lysis was allowed to proceed for 20 min on ice. Lysates were cleared by centrifugation (15 min, 16 000 x g, 4°C) and the protein content of the supernatant was quantified using the *DC* protein assay (Bio-Rad). Supernatants were stored at -80°C until further processing.

Equal amounts of protein (30 µg each) from the different lysates were mixed with Roti-load sample buffer (Roth, Karlsruhe, Germany), boiled for 5 min, electrophoresed on a 10% SDS–polyacrylamide gel and then blotted electrophoretically to a polyvinylidene difluoride (PVDF) membrane (Immobilon-P; Millipore, Schwalbach, Germany). Blots were blocked in TBST (20 mM Tris/HCl, 150 mM NaCl, 0.1% Tween-20, at pH 7.6) containing 5% fat-free milk powder for 1 h at room temperature. Blots were incubated with rabbit polyclonal anti-phospho-ERK1/2 (Thr202/Tyr204; 1:1000; #9101; Cell Signaling, Danvers, MA, USA) diluted in 5% fat-free milk powder in TBST overnight at 4°C. After washing, the blots were incubated for 1 h with an anti-rabbit secondary antibody conjugated to horseradish peroxidase (1:2000 in TBST containing 5% fat-free milk powder; DAKO, Glostrup, Denmark). After washing, blots were developed using the enhanced chemoluminescence method (ECL+plus; Amersham, Buckinghamshire, UK) and exposure to BioMax films (Sigma) for 1 to 30 min. After stripping (in 2% SDS, 50 mM DTT, 50 mM Tris/HCl at pH 7.0 for 30 min at 70°C), the blots previously probed with anti-phospho-ERKs were now incubated with a polyclonal anti-ERK1/2 antibody (total ERKs, 1:1000; #9102; Cell Signaling).

Receptor expression and trafficking analysis

HEK293 cells were seeded on poly-D-lysine (Sigma)-coated glass cover slips in a 24 well format (1 x 10^5 cells/well). After 24 h, they were transfected with 400 ng DNA/well (300 ng of pEGFP-N1, pMS1, pcDNA3, pcDNA3-CB1, or pEGFP-CRH-R1, respectively, in combination with 100 ng of DsRed2-C1 each). 24 h later, cells were washed and stimulated for 30 min or 2 h with 100 nM WIN 55,212-2 (Tocris) or 1 µM SR141716 (NIMH). Thereafter cells were washed and fixed with 200 µl/well of 4% paraformaldehyde in PBS for 10 min. Cells were washed in PBS, and cell nuclei counterstained with 4',6-diamidin-2'-phenylindol-dihydrochorid (DAPI; Roche; 200 µl/well of 1 µg DAPI/ml PBS for 10 min). Cells were washed in PBS, and cover slips were embedded in ProTaqs Mount Fluor (Biocyc, Luckenwalde, Germany). Cover slips were allowed to dry at room temperature in the dark and were stored at 4°C. Cells on cover slips were visualized under a fluorescence microscope (Axioplan 2 imaging; Zeiss, Jena, Germany) with a 40 x magnification objective.

DNA constructs and cloning procedures

All molecular cloning procedures including transformations in DH5α, XL1-Blue or DH10B bacteria were performed according to standard protocols (Sambrook and Russell, 2001). DNA

sequencing was performed by SeqLab (Göttingen, Germany). Primers and oligonucleotides were synthesized by MWG Biotech (Ebersberg, Germany). Restriction enzymes and modification enzymes were purchased from New England BioLabs (NEB, Frankfurt, Germany). PCR reactions for cloning purposes were performed with high-fidelity *Pfu* polymerase or *Herculase* (both from Stratagene), or, for screening purposes, with *Taq* polymerase ("home-made"). PCR, oligonucleotide annealing and ligation reactions were carried out under appropriate conditions in a Robocycler (Stratagene). Supplementary Table 6.1.2 shows the nucleotide sequences of the used primers and oligonucleotides. Supplementary Table 6.1.1 shows the used and generated plasmids with its specific features. Plasmid Mini-, Midi-, Maxi-preparations, and PCR product- , nucleotide- and gel-extraction-purifications were carried out with commercially available kits (Qiagen, Hilden, Germany) according to manufacturer's instructions. BAC DNA was prepared with the Large-Construct-Kit from Qiagen and analyzed via pulsfield-gel-electrophoresis (PFGE) with a Chef-Mapper XA (Bio-Rad). All newly generated plasmids were verified by sequencing.

Generation of CB1-EGFP fusion plasmids pMS1, pMS4 and pMS5 (Fig. 2.7.1)

All three CB1-EGFP fusion plasmids (pMS1,4,5) were generated by insertion of PCR amplified CB1 into the multiple cloning site (MCS) of the pEGFP-N1 vector (Clontech, Mountain View, CA, USA) thereby creating C-terminal CB1-EGFP fusion constructs. The CB1 restriction cassettes were PCR amplified from the CB1 coding sequence (cds) of the pcDNA3-CB1 vector with artificially designed overhang primers (CB1-N1-Fp, CB1-N1-52-Fp, CB1-N1-26-Fp, CB1-N1-Rv). The reverse primer (Rv) was the same for all three constructs and was designed in such a way that the original CB1 stop codon was deleted (in order to allow the C-terminal fusion with EGFP), that a triple glycin linker was introduced between the CB1 and EGFP coding frames in order to allow higher flexibility of the fused EGFP, and that a *Kpn*I restriction site was introduced. The three different forward primers (Fw) were designed in such a way that the start codon of the CB1 coding region was preceded by the consensus Kozak sequence in order to allow efficient translation, and that a *Sac*I restriction site was introduced. Furthermore Fw-primers were designed in such a way that in the CB1-N1-52-Fp (resulting in pMS4) and the CB1-N1-26-Fp (resulting in pMS5) constructs the part of the N-terminus of the CB1 cds, which encodes the extracellular N-tail of the receptor (Andersson et al., 2003), was reduced from 116 codons (encoding 116 amino acids) to 52 or 26 codons, respectively. Furthermore, all primers were designed in such a way that the CB1 restriction cassettes could be integrated in frame with EGFP into pEGFP-N1. All PCR amplified CB1 restriction cassettes were cloned via *Sac*I / *Kpn*I restriction digest into the pEGFP-N1 vector creating plasmids pMS1,4,5.

For all cellular assays (Western blots, luciferase assays), the properties of the CB1-EGFP fusion of the pEGFP-N1 based pMS1 plasmid were compared to those of the native CB1 receptor encoded on the pcDNA3 vector. Although the properties of both cloning vectors pcDNA3 and pEGFP-N1, are comparable, the "empty" vectors sometimes produced different background values in cellular systems. Thus, it would be advantageous to compare the CB1-EGFP fusion of pEGFP-N1 with the native CB1 receptor encoded on the same pEGFP-N1 vector backbone. This could, for

instance, be achieved by insertion of a stop codon within pMS1 immediately 3' of the CB1 cds, thus allowing for the expression of only the CB1 receptor without its EGFP attachment. Therefore, such a vector was designed for more detailed future *in vitro* analysis of the CB1-EGFP properties in comparison with the native CB1, after the above mentioned "background vector problem" was encountered. pMS1 was cut with *Sac*II / *Age*I deleting a 115 bp segment covering the last 80 bp of the 3'-part of the CB1 cds, the triple glycin linker and the MCS 5' in front of the fused EGFP cds. Artificially designed and annealed oligos (pMS1-oligo-STOP-Fw and –Rv) containing the excised 80 bp fragment of the 3'-part of CB1 followed by a novel, additional CB1 stop codon and followed by a novel, introduced *EcoR*I site for screening purposes, were ligated into the pMS1 vector in place of the above cut segment. The pMS9 (CB1-STOP-*EcoR*I-EGFP) vector was generated.

Generation of the CB1-Venus recombination cassettes CB1-Venus-Easy and CB1-Venus-Soph

Both recombination cassettes were designed in order to recombine with the endogenous CB1 locus of BAC clone RP24-407G18.1, which was purchased from CHORI [BACPAC Resource Center (BPRC) at Children's Hospital Oakland Research Institute (CHORI), Oakland, CA, USA]. The RPCI-24 BAC CHORI library had been derived from a single male C57BL/6J mouse. Brain and spleen genomic DNA samples had been isolated and partially digested with *Mbo*I. *Mbo*I fragments had been cloned into the pTARBAC1 vector between the *BamH*I sites. Ligation products had been transformed into DH10B electrocompetent cells. The cds of CB1 (1,422 bp) was located between bp 121,449-122,879 of the RP24-407G18.1 BAC clone (CB1-BAC; 179,450 bp).

In order to identify potential low frequency cutting restriction enzymes, which cut in the CB1-BAC clone, it was digested with a variety of putative restriction enzymes, which had been primarily assessed via computer software. However, after digestion of the CB1-BAC clone and analysis via PFGE, only restriction enzymes *Asc*I (three restriction sites, two of them only 189 bp apart), *Pme*I (two restriction sites) and *Mlu*I (one restriction site) were suitable and revealed clear cut restriction bands (data not shown). These restriction sites were used for the subsequent generation of the CB1-Venus recombination cassettes. They were integrated in the cassettes during the cloning procedure to facilitate later restriction screening of successful recombination candidates with the CB1-BAC.

The CB1-Venus-Easy cassette was designed to contain the neomycin/kanamycin antibiotics resistance gene derived from transposon-5 (Tn5-neo) flanked by two Flp recombinase target sites (*FRT*) within the 3'-UTR of the CB1-Venus fusion gene (Fig. 2.7.7). Downstream of *FRT*-Tn5-neo-*FRT*, the right homology arm (RH) was integrated. The cloning cassette was assembled within the original pCB1-EGFP-N1 (pMS1) plasmid backbone. EGFP was first replaced by enhanced yellow fluorescent protein (EYFP) and later by a further engineered form of EYFP, which has even more enhanced fluorescence, Venus, as compared to EGFP (Nagai et al., 2002).

The CB1-Venus-Soph cassette was generated similarly as the CB1-Venus-Easy construct and made use of the *FRT*-Tn5-neo-*FRT* cassette from the CB1-Venus-Easy plasmid. CB1-Venus-Soph was designed to hold a *lox2272* flanked transcriptional STOP cassette together with the integrated *FRT*-Tn5-neo-*FRT* cassette of CB1-Venus-Easy within the intron of the CB1 gene a few

hundred basepairs upstream of the CB1 cds of the second exon (Fig. 2.7.8). This *lox2272* flanked STOP cassette was followed by a short intronic sequence of the CB1 gene, its CB1 cds fused to Venus and a short right homology arm.

Generation of CB1-Venus-Easy (Fig. 2.7.7)

In the first step, EYFP was amplified and fused with a *FRT* site at its 3'-end by PCR from pEYFP-N1 via overhang PCR primers. The EYFP-Fw primer was designed to bind upstream of the EYFP cds and its preceding MCS on pEYFP-N1. The EYFP-*FRT*-Rv overhang primer was designed to bind to a few bp at the 3'-end of the EYFP cds in pEYFP-N1 and to further integrate in its overhang a *Xho*I site directly following the EYFP stop codon and adjacent the *FRT* site, followed by a *Pvu*I and *Not*I restriction site. The resulting PCR fragment was cloned via *Age*I / *Not*I restriction digest into the pMS1 vector, thus replacing EGFP of the CB1-EGFP fusion with EYFP-*FRT*, thereby creating the pCB1-EYFP-*FRT* (pMS14) vector.

In the second step, an artificially designed and annealed oligo (Tn5-neo-*FRT*-RH-Fw and –Rv), containing a *Hind*III and *Pme*I restriction site followed by a *FRT* site, a *Mlu*I restriction site, a right homology arm (consisting of the first 49 bp of the 3'-UTR of the CB1 gene), an *Avr*II and an *Acc65*I restriction site, was inserted at the 3'-end of the Tn5-neo resistance gene of the pJ.182 vector via *Hind*III / *Acc65*I restriction digest. A Tn5-neo-*FRT*-RH DNA fusion fragment within pJ.182 was generated creating plasmid pJ.182-Tn5-neo-*FRT*-RH (pMS12).

In the third step, the Tn5-neo-*FRT*-RH cassette was amplified from pMS12 via PCR with a regular Rv-primer (Tn5-neo-*FRT*-RH-*Pvu*I-Rv) and an overhang Fw-primer (Tn5-neo-*FRT*-RH-*Pvu*I-Fw) introducing a *Pvu*I site at the 5'-end. The amplified cassette was cut with *Pvu*I / *Avr*II and inserted at the 3' end of the CB1-EYFP-*FRT* cassette into the fully *Pvu*I / *Avr*II digested pMS14 vector. Vector pMS17 was generated containing a CB1-EYFP-*FRT*-Tn5-neo-*FRT*-RH cassette.

In the final step, the EYFP cds of pMS17 was exchanged against the Venus cds. The Venus cds was amplified from plasmid pCS2-Venus via an overhang Fw-primer (Venus-Fw) introducing an *Age*I restriction site upstream of the Venus cds and via the overhang EYFP-*FRT*-Rv primer (the same primer that had been used above in the first step). The amplified PCR product was cloned via *Age*I / *Pvu*I restriction digest into pMS17 creating the final pMS17V plasmid containing the CB1-Venus-Easy recombination cassette consisting of CB1-Venus-*FRT*-Tn5-neo-*FRT*-RH (Fig. 2.7.7).

Generation of CB1-Venus-Soph (Fig. 2.7.8)

In the first step, EYFP was amplified and fused with a right homology arm (RH; consisting of the first 48 bp of the 3'-UTR of the CB1 gene) at its 3'-end by PCR from pEYFP-N1 via overhang PCR primers. The EYFP-Fw primer was designed to bind upstream of the EYFP cds and its preceding MCS on pEYFP-N1. The EYFP-RH-Rv primer was designed as an overhang primer binding to a couple of bp at the 3'-end of the EYFP cds in pEYFP-N1 and integrating in its overhang an *Asc*I site directly following the EYFP stop codon, adjacent the right homology arm,

followed by a *Sac*I and *Not*I restriction site. The resulting PCR fragment was cloned via *Age*I / *Not*I restriction digest into pMS1, thus replacing EGFP of the CB1-EGFP fusion with EYFP-RH and creating the pCB1-EYFP-RH (pMS11) vector.

In the second step, a 371 bp intron/5'-UTR CB1 fragment (consisting of the 62 bp of the 5'-UTR of the CB1 exon 2 and of 309 bp of the CB1 intron 5' further upstream up to the *Avr*II site; compare Fig. 2.7.6) preceded 5' by a *lox2272* site, was introduced upstream of the CB1 cds of pMS11. This was done via PCR amplification of the intron/5'-UTR sequence from the CB1-BAC clone RP24-407G18.1 via an overhang Fw-primer (*lox2272*-Intron-CB1-Fw) binding to the 5'-end of the intronic sequence and integrating a preceding *loxP2272* site and a *Mlu*I and *Xho*I restriction site within its overhang, and via a regular Rv-primer (*lox2272*-Intron-CB1-Rv) binding within the CB1 cds +103-132 bp downstream of the start codon immediately behind the *EcoR*V restriction site (compare Fig. 2.7.6). The amplified PCR product was cloned via *Xho*I / *EcoR*V restriction digest into pMS11 creating the p-*lox2272*-Intron-CB1-EYFP-RH (pMS18) vector.

In the third step, an artificially designed and annealed oligo (LH-*lox2272*-STOP-Fw and –Rv) containing a *Sac*I and *Nhe*I restriction site followed by a left homology arm (LH; 50 bp from the intronic CB1 gene sequence immediately 5' upstream of the intronic *Avr*II site), a *lox2272* site and a *Spe*I and *Xba*I restriction site, was cut with *Sac*I / *Xba*I and inserted at the 5'-end of the transcriptional STOP cassette [containing multiple SV40 and bovine growth hormone (bGH) polyadenylation signals] of the *Sac*I / *Xba*I cut pBS-3p(A) M.305 vector. A LH-*lox2272*-STOP fusion cassette within the pBS-3p(A) M.305 vector was generated, leading to plasmid pMS15.

In the fourth step, the *Nhe*I / *Xho*I cut LH-*lox2272*-STOP cassette from pMS15 and the *Xho*I / *Mlu*I cut *FRT*-Tn5-neo-*FRT* cassette from pMS17 were combined via a triple ligation with the *Nhe*I / *Mlu*I cut vector backbone of pMS18 to generate the pLH-*lox2272*-STOP-*FRT*-Tn5-neo-*FRT*-*lox2272*-Intron-CB1-EYFP-RH (pMS19) vector.

In the final step, the EYFP cds of pMS19 was exchanged against the Venus cds. The Venus cds was amplified from plasmid pCS2-Venus via an overhang Fw-primer (Venus-Fw) introducing an *Age*I restriction site upstream of the Venus cds and via an overhang Venus-Rv primer introducing an *Asc*I restriction site downstream of the Venus cds. The amplified PCR product was cloned via *Age*I / *Asc*I restriction digest into pMS19 creating the final pMS19V plasmid containing the CB1-Venus-Soph recombination cassette consisting of LH-*lox2272*-STOP-*FRT*-Tn5-neo-*FRT*-*lox2272*-Intron-CB1-Venus-RH (Fig. 2.7.8).

Verification of the functionality of lox2272 sites of pMS19V (Fig. 2.7.9)

Competent DH5α bacteria were electroporated with p705-Cre [expressing Cre recombinase; carrying chloramphenicol (Chl) resistance] and pMS19V [carrying kanamycin (Kan) resistance] using standard protocols. p705 is based on the pSC101 temperature-sensitive origin, which maintains a low copy number and replicates at 30ºC but not at 40ºC. Furthermore, Cre recombinase is expressed from the lambdaPR promoter weakly at 30ºC, but strongly at 37ºC. Thus, after transformation, bacteria were grown for 2 days at 30ºC on LB agar plates (Chl$^{25\mu g/ml}$, Kan$^{50\mu g/ml}$). Resistent colonies were picked and incubated overnight at 30ºC in 1.4 ml LB medium

2.7 Generation of BAC CB1-Venus mice

(Chl[25], Kan[50]) shaking at 1100 rpm, followed by 4 hours incubation at 37ºC. Bacteria were harvested, plasmids isolated, digested with *Nhe*I / *Kpn*I, and restriction fragments were analyzed via agarose gel electrophoresis.

Red/ET cloning of CB1-Venus-Easy and -Soph into CB1-BAC RP24-407G18.1 creating CB1-Venus-Easy- and CB1-Venus-Soph-BAC

Red/ET cloning was performed with the Quick & Easy BAC Modification Kit from Genebridges (Heidelberg, Germany) according to manufacturer's instructions. The pSC101-BAD-pbaA (pRed/ET) plasmid was transformed via electroporation into the CB1-BAC RP24-407G18.1 containing *E. coli* DH10B strain and selected via Chl[15µg/ml], Tetracyclin[3µg/ml] (Tet). Surviving colonies were further screened by assessing *Hind*III digestions of plasmid preparations. Transformed bacteria containing both the CB1-BAC and the pRed/ET plasmid were made competent after induction of Red/ET recombination protein expression from pRed/ET via addition of 10% L-arabinose to the culture medium. Afterwards, they were either electroporated with the linearized CB1-Venus-Soph recombination cassette (which was isolated as a 4,549 bp fragment from the *Sac*I / *Nhe*I / *ApaL*I digested pMS19V plasmid) or with the linearized CB1-Venus-Easy recombination cassette (which was isolated as a 2,405 bp fragment from the *Nsi*I / *Avr*II digested pMS17V plasmid). Cultures were streaked on Kan[15], Chl[15] agar plates and were grown at 37ºC overnight without Tet in order to loose the pRed/ET expression plasmid. Growing colonies should have undergone recombination, thereby integrating the Tn5-neo resistance cassette from the CB1-Venus-Easy or -Soph cassettes into the chloramphenicol-resistant CB1-BAC allowing bacteria to grow on Kan + Chl medium. Surviving colonies were picked and analyzed via colony PCR for the correct integration of the recombination cassettes. PCR primers were designed to span the left (pMS19V-L-Fw, -Rv) or right (pMS19V-R-Fw, -Rv) side of CB1-Venus-Soph, or the left (pMS17V-L-Fw, -Rv) or right (pMS17V-R-Fw, pMS19-R-Rv) side of CB1-Venus-Easy, cassette integration, respectively, or to bind in the CB1 (pMS17V-L-Fw, CB1-Rv), Venus (Venus-Fw, -Rv) or neo cds (Tn5-Neo-Fw, -Rv). Positive recombined CB1-Venus-Soph-BAC clones were further identified via *Asc*I and *Mlu*I digestion and PFGE analysis. *Not*I digestion of the recombined BAC ensured that the BAC vector backbone could be eliminated successfully from the clone. Final identification of the correct insertion was determined via sequencing of the right and left CB1-Venus-Soph-BAC integration sites.

Generation of CB1-Venus-Soph-BAC transgenic mice

The purification and oocyte injection of the CB1-Venus-BAC was performed in collaboration with Prof. Dusan Bartsch of the Central Institute of Mental Health (Mannheim, Germany). The successfully recombined CB1-Venus-Soph-BAC was linearized via *Not*I digestion. Insert was purified from the *Not*I excised pTARBAC1 vector backbone (compare Fig. 2.7.11). About half of the micro-injections were performed with the purified fragment (533 embryos), while 418 embryos were injected with BACs that were only NotI digested but not purified. The microinjected oocytes were

transplanted into pseudo-pregnant female mice resulting in a total offspring of 25 mice (10 mice resulted from the linearized and purified fragment, and 15 mice resulted from the fragment that was only linearized, but not purified). Genomic DNA was isolated from mouse tails and probed for genomic insertion of the Tn5-neo cassette of the CB1-Venus-Soph-Bac via PCR using Founder-Neo-Fw and –Rv primers.

2.7.4 Results

The CB1-EGFP fusion protein has similar properties as the native CB1 receptor

For the study and visualization of the *in vivo* trafficking properties of the CB1 receptor, we generated a CB1-EGFP fusion protein (Fig. 2.7.1). EGFP was fused to the C-terminus of the CB1 receptor via a triple glycin linker to allow for a higher flexibility of the fused EGFP tail. A Kozak consensus sequence was introduced immediately upstream of the CB1 coding sequence (cds) to allow an efficient translation. The CB1-EGFP fusion was generated using the pEGFP-N1 vector, resulting in plasmid pMS1. Additionally to pMS1, two other CB1-EGFP fusion constructs were generated, which contained shorter N-terminal extra-membrane receptor tails: pMS4 [encoding only 52 amino acids (AAs) of the 116 AAs long N-terminal tail, thereby missing one putative extracellular glycosylation site] and pMS5 (encoding only 26 AAs of the N-terminal tail, thereby missing all three putative extracellular glycosylation sites). However, in our hands, these shortened constructs were indistinguishable from the full length construct (pMS1) in terms of expression and signal transduction (data not shown).

Figure 2.7.1 Overview of the CB1-EGFP fusion construct of plasmid pMS1. The CB1-EGFP fusion was designed in such a way that the CB1 receptor coding sequence (without stop codon) was fused 5' to the EGFP coding sequence (cds), separated by a triple glycin coding linker (5'-GGCGGCGGC-3'; Triple-Gly-linker). Furthermore, 5' upstream of the CB1 cds a consensus Kozak sequence (5'-GCCGCCACCATG-3') was introduced to ensure efficient translation. The translated CB1-EGFP construct resulted in a NH_2-CB1-Gly-Gly-Gly-EGFP-COOH fusion protein. The CB1-EGFP fusion was expressed from the pMS1 plasmid (pCB1-EGFP-N1).
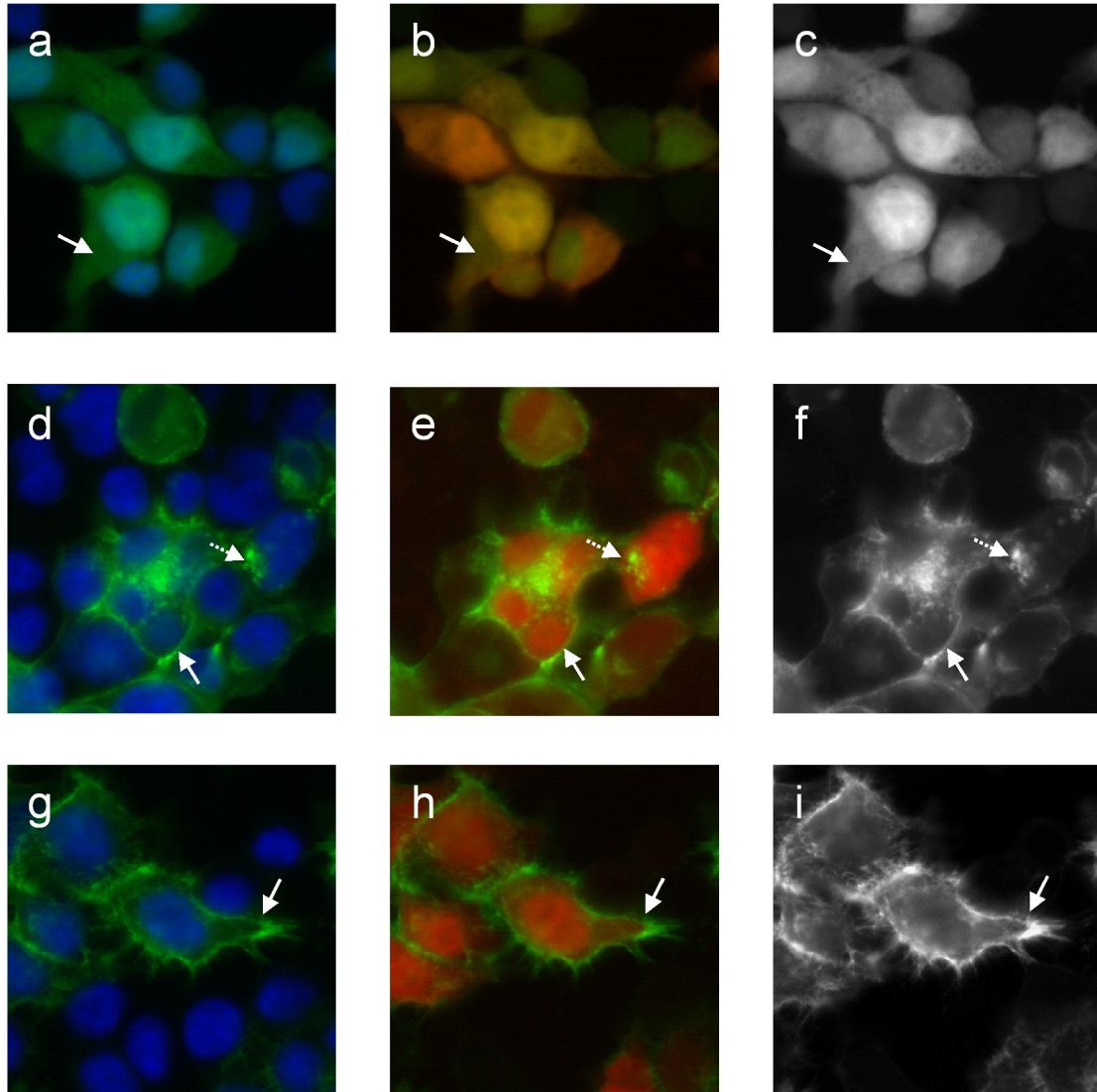
Figure 2.7.2 Expression of the CB1-EGFP fusion protein in HEK293 cells. HEK293 cells were transiently co-transfected with pDsRed2-C1 and either pEGFP-N1 (**a**,**b**,**c**), pMS1 (**d**,**e**,**f**) or pEGFP-CRH-R1 (**g**,**h**,**i**) and observed via fluorescent microscopy 48h later. Cell nuclei were counterstained with DAPI. Expression of the proteins EGFP, CB1-EGFP and EGFP-CRH-R1 (all in green color) from the respective plasmids is either displayed together with DAPI stained nuclei in blue (**a**,**d**,**g**), with DsRed2, which is localized in the cytoplasm, in red (**b**,**e**,**h**), or alone (**c**,**f**,**i**; in grayscale). Arrows in (**a**,**b**,**c**) clearly demonstrate the expression of EGFP in the entire cell soma. Note the co-expression with DsRed2, which is also expressed in the cell soma, in yellow/orange (**b**). Solid arrows in (**d**,**e**,**f**) demonstrate the membrane expression of CB1-EGFP. Note the CB1-EGFP membrane expression in comparison to the cytosolic expression of DsRed2 (**e**). CB1-EGFP expression is also partly observed in speckles within the cell (broken arrows; **d**,**e**,**f**), suggesting intracellular localization of part of the receptors in the endoplasmatic reticulum and/or endosomal compartments. Arrows in (**g**,**h**,**i**) demonstrate the membrane expression of EGFP-CRH-R1 as a positive control for the membrane expression of CB1-EGFP. Note the membrane localization of EGFP-CRH-R1 in comparison to the cytosolic expression of DsRed2 (**h**). The EGFP-CRH-R1 seems, in contrast to CB1-EGFP, to be almost exclusively expressed at the cell surface and even in fine cellular membrane protrusions (compare **f**,**i**).
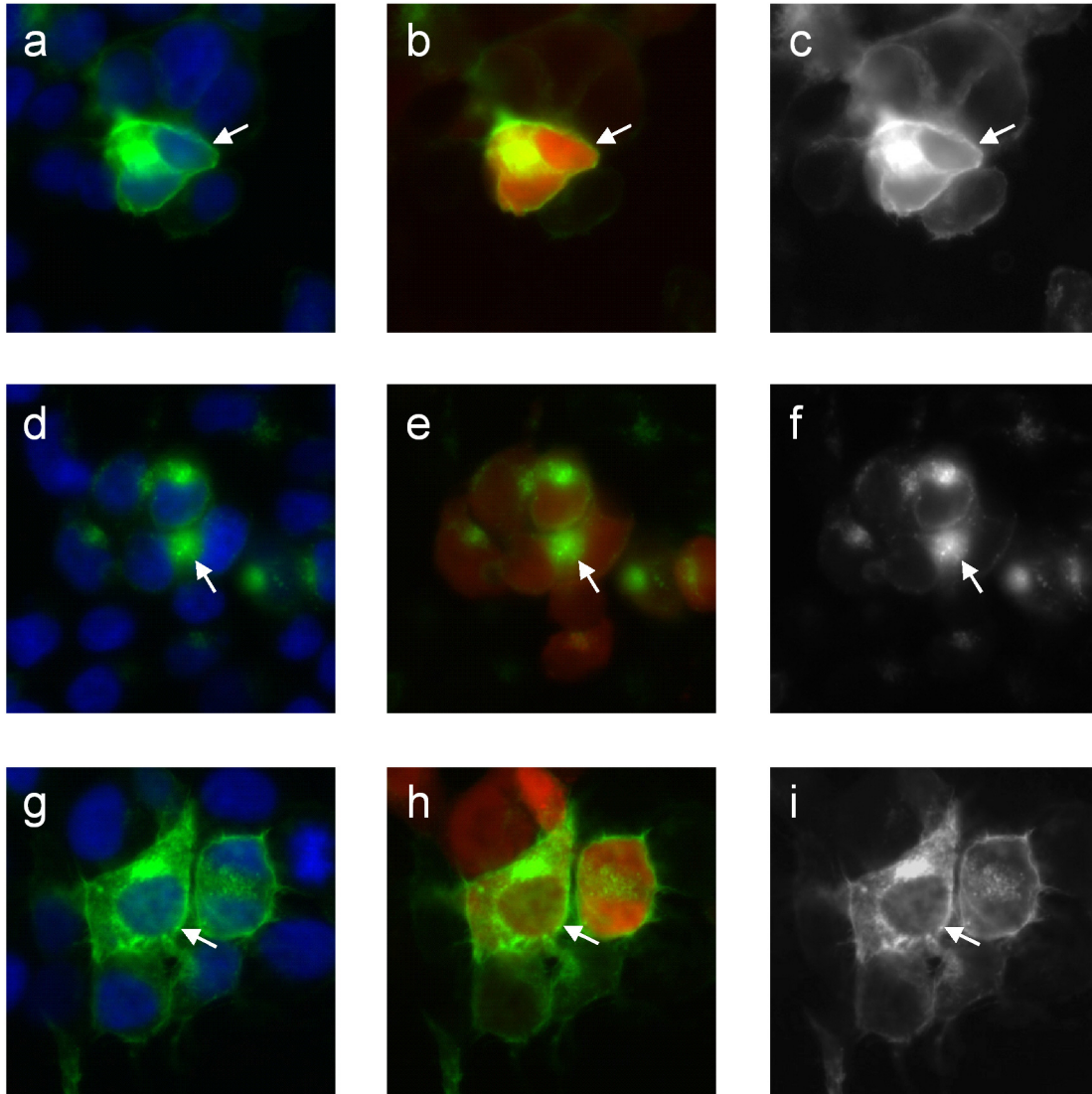
Figure 2.7.3 CB1-EGFP receptor trafficking in response to agonist/antagonist stimulation.
HEK293 cells were transiently co-transfected with pDsRed2-C1 and pMS1, 48h later stimulated for 2 h with either vehicle (**a**,**b**,**c**), the CB1 agonist WIN 55,212-2 (100 nM; **d**,**e**,**f**) or the CB1 antagonist SR141716 (1 µM; **g**,**h**,**i**) and observed via fluorescent microscopy. Cell nuclei were counterstained with DAPI. Expression of the CB1-EGFP protein (green color) from pMS1 is either displayed together with DAPI stained nuclei in blue (**a**,**d**,**g**), with DsRed2, which is localized in the cytoplasm, in red (**b**,**e**,**h**), or alone (**c**,**f**,**i**; in grayscale). Arrows in (**a**,**b**,**c**) demonstrate the membrane expression of CB1-EGFP under unstimulated conditions (vehicle). Arrows in (**d**,**e**,**f**) demonstrate the intracellular location of the CB1-EGFP receptor after CB1 agonist stimulated endocytosis. Arrows in (**g**,**h**,**i**) demonstrate increased CB1 antagonist-stimulated membrane localization of CB1-EGFP due to the inverse agonist properties of SR141716, which provoke trapping of CB1-EGFP within the membrane. Note the CB1-EGFP expression even in fine cell membrane protrusions (**h**,**i**).

The subcellular localization of CB1-EGFP receptor expression was investigated by transient transfection in HEK293 cells (Fig. 2.7.2). Co-expression experiments with the DsRed protein, which is localized in the cell soma, clearly demonstrated the membrane localization of the receptor fusion (Fig. 2.7.2e). This became further evident in comparison with non-receptor fused EGFP, which is

expressed in the entire soma (Fig. 2.7.2b). As a positive control, we further investigated a CRH-R1 construct, where EGFP was fused to the N-terminus of the receptor, and also found clear membrane localization of EGFP-CRH-R1 (Fig. 2.7.2h), comparable to CB1-EGFP. However, whereas EGFP-CRH-R1 was almost exclusively located at the cell membrane, CB1-EGFP was, in addition to the cell membrane, also visible in some intracellular clusters (Figs. 2.7.2e.f).

CB1-EGFP trafficking was investigated in HEK293 cells by CB1 agonist and antagonist treatment (Fig. 2.7.3). Whereas CB1-EGFP was mostly located at the cell membrane in vehicle treated HEK293 cells (Figs. 2.7.3a,b,c), upon stimulation with the CB1 agonist WIN 55,212-2 for 30 min (data not shown) or 2 h, the fused receptor was almost exclusively visible in intracellular clusters (presumably endosomal compartments) (Figs. 2.7.3d,e,f). Upon stimulation with the CB1 antagonist SR141716 for 2 h, the cell membrane localization of the receptor fusion
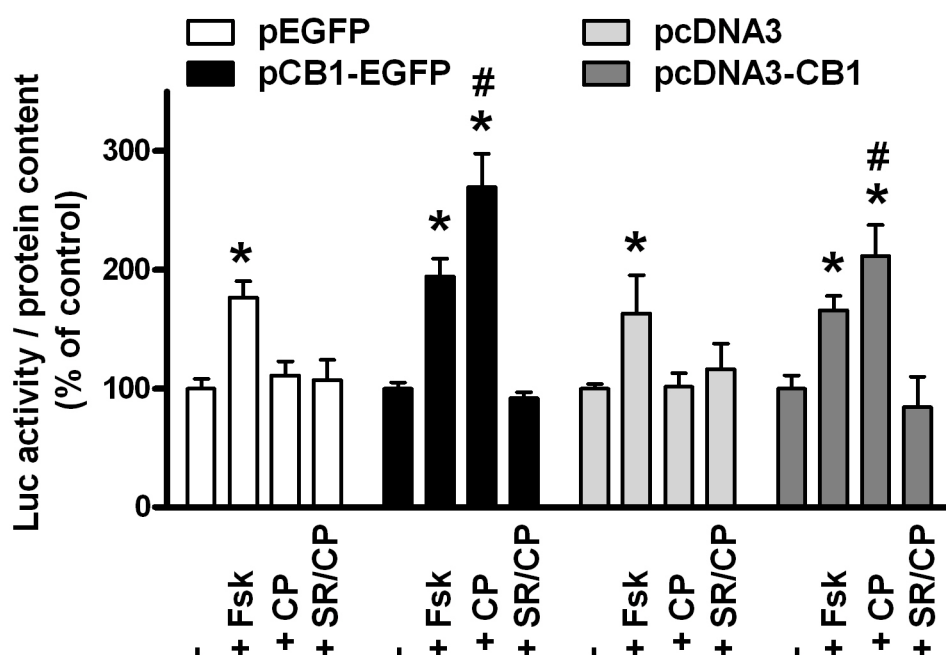
Figure 2.7.4 Agonist-stimulated CB1-EGFP-mediated CRE-luciferase reporter gene expression. HEK293 cells were transiently co-transfected with pCRE-Luc (containing the luciferase reporter gene under the control of a CRE-containing promoter) and either pEGFP (pEGFP-N1), pCB1-EGFP (pMS1), pcDNA3 or pcDNA3-CB1. 24h later, cells were stimulated for 4 h with either vehicle (-), forskolin (5 µM; Fsk), the CB1 agonist CP-55,940 (1 µM; CP) or a combination of CP-55,940 (1 µM) and the CB1 antagonist SR141716 (10 µM; SR/CP). Luciferase activities were measured luminometrically, were normalized to protein content and were expressed as percentage activity of the respective vehicle control group. Note that Fsk was able to stimulate luciferase acitivity with all four different plasmids (as it is a direct activator of adenylyl cyclase), whereas CP was only able to stimulate luciferase activity with the pCB1-EGFP and pcDNA3-CB1 plasmids. (n = 3 per group), $^*p < 0.05$ vs. respective vehicle (-) group, $^#p < 0.05$ vs. respective Fsk group.

even increased as compared to vehicle treated cells, and CB1-EGFP became also visible on fine cell membrane protrusions (Figs. 2.7.3g,h,i).

G-protein coupled signal transduction properties of CB1-EGFP, in comparison with the native receptor, were investigated via luciferase reporter gene assays, where luciferase expression was dependent upon binding of phospho-CREB to cAMP response elements (CRE) within its promoter. Respective empty vectors (without the CB1 cds) served as negative controls. CB1 agonist CP-55,940 stimulation of HEK293 cells, which were transiently transfected with CB1-EGFP (pMS1) and pCRE-Luc, for 4 h significantly increased luciferase activity [$F_{3,8}$ = 80.2, $p < 0.001$; One-way ANOVA (*Treatment*); Fig. 2.7.4], which was blocked by co-administration of the CB1 antagonist SR141716. Treatment with forskolin, which is a direct activator of adenylyl cyclase, induced a similar activation of luciferase activity as CP-55,940, although not as strong ($p < 0.05$; as no careful dose-response relationship for CP-55,940 and forskolin was established, no direct conclusion can be drawn from their different potencies under present conditions). Evaluation of the native CB1 receptor (pcDNA3-CB1) gave almost identical results ($F_{3,8}$ = 25.7, $p < 0.001$). Both empty vectors (pEGFP-N1 and pcDNA3) did not
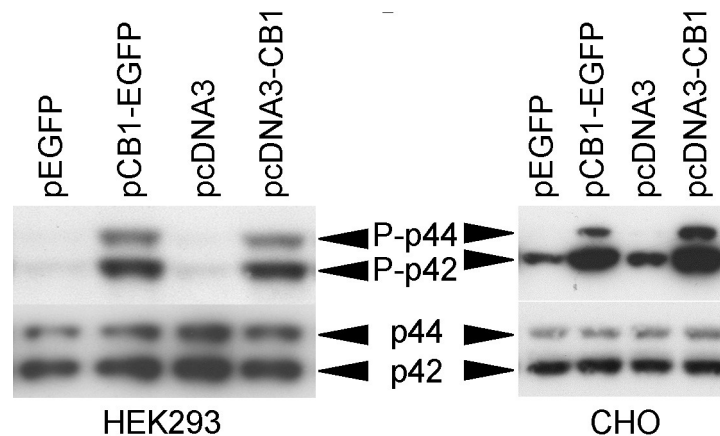
Figure 2.7.5 Agonist-stimulated CB1-EGFP-mediated MAPK phosphorylation. HEK293 and CHO cells were transiently co-transfected with either pEGFP (pEGFP-N1), pCB1-EGFP (pMS1), pcDNA3 or pcDNA3-CB1. 24 h later, cells were stimulated for 15 min with the CB1 agonist CP-55,940 (1 μM). Phosphorylated extracellular signal-regulated MAP kinase (pERK-1/2; P-p44/P-p42) expression and total ERK expression (ERK-1/2; p44/p42) was analyzed via Western blot. Note the CB1 agonist-stimulated ERK-1/2 phosphorylation only with the pCB1-EGFP and pcDNA3-CB1 plasmids.

show any luciferase activation upon CB1 agonist stimulation as expected, because HEK293 cells do not natively express CB1 receptors. However, forskolin produced similar luciferase activation of pCRE-Luc with all four tested (empty and CB1 expressing) vectors (statistics not shown). Evaluation of CB1-mediated pCRE-Luc reporter gene activation within CHO cells revealed similar results as the ones obtained with HEK293 cells (data not shown).

MAP kinase signal transduction properties were evaluated via Western blot. CB1 agonist CP-55,940 stimulation of HEK293 or CHO cells, which were transiently transfected with CB1-EGFP (pMS1), for 15 min significantly increased ERK-1/2 phosphorylation (Fig. 2.7.5), almost identically to the native CB1 receptor (pcDNA3-CB1). Both empty vectors (pEGFP-N1 and pcDNA3) did not show any stimulation of ERK-1/2 phosphorylation upon CB1 agonist exposure as expected, because HEK293 and CHO cells do not natively express CB1 receptors.

Generation of the CB1-Venus-Easy and –Soph recombination cassettes

Based on the evaluated CB1-EGFP fusion, two different DNA cassettes for homologous recombination with the original CB1 locus (Fig. 2.7.6) were cloned: CB1-Venus-Easy (Fig. 2.7.7) and CB1-Venus-Soph ("sophisticated"; Fig. 2.7.8). They were cloned in such a way that the *FRT*-Tn5-neo-*FRT* kanamycin resistance cassette from CB1-Venus-Easy could directly be used for integration into CB1-Venus-Soph. During the cloning process, EGFP was exchanged for Venus. CB1-Venus-Easy consisted of the CB1-Venus fusion followed by a 3' downstream Flp recombinase recognition site (*FRT*)-flanked Tn5-neo kanamycin resistance cassette, which was followed 3' further downstream by a right homology arm (RH) consisting of 49 bp of the 3'-UTR of the CB1 gene directly adjacent to the CB1 stop codon (Fig. 2.7.7). As left homology arm (LH) of CB1-Venus-Easy served a part of the CB1 cds (-539 bp upstream of the last CB1 codon until the *Nsi*I restriction site). The right homology arm was designed to be flanked by unique *Mlu*I and *Avr*II restriction sites to allow for replacement of the sequence in case of insufficient recombination frequency (because of many bp repeats within the RH 3'-UTR sequence, shaping of secondary and tertiary structures was expected that could potentially interfere with homologous recombination).
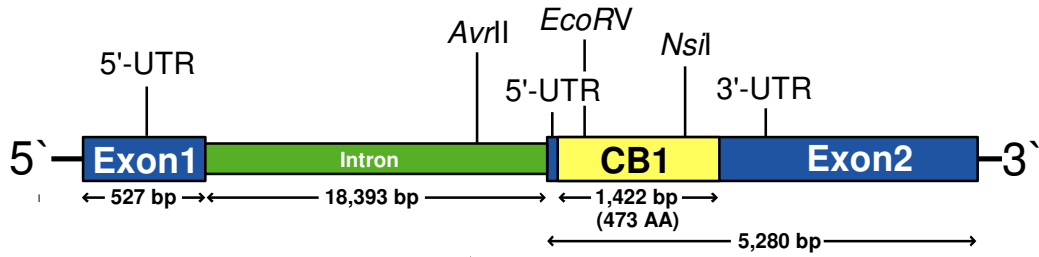
Figure 2.7.6 Overview of the genomic organization of the CB1 receptor gene. The CB1 gene contains two exons (Exon1, 527 bp; Exon 2, 5,280 bp) and one intron (18,393 bp). The coding sequence (cds) of CB1 (1,422 bp encoding 473 amino acids) is entirely located on Exon 2. Important restriction sites that were used for the cloning or linearization of the CB1-Venus-Easy and –Soph constructs are depicted. The *Avr*II site is located -309 bp 5' upstream of Exon 2 and -371 bp 5' upstream of the CB1 cds. This is the location, where the *lox2272* flanked STOP-*FRT*-Tn-5-neo-*FRT* cassette of CB1-Venus-Soph was integrated (compare Fig. 2.7.8).
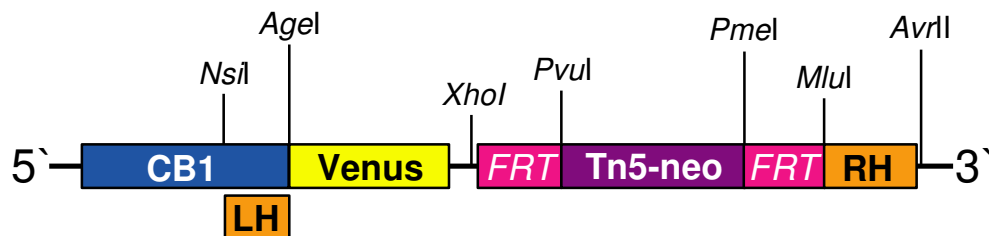
Figure 2.7.7 Overview of the CB1-Venus-Easy recombination cassette. A *FRT* (Flp recognition target site)-flanked Tn5-neo kanamycin resistance cassette was integrated immediately 3' downstream of the CB1-Venus fusion of pMS1. The right homology arm (RH) for later recombination consisted of 49 bp of the CB1 3'-UTR immediately 3' downstream of the CB1 stop codon and was introduced immediately 3' adjacent to the *FRT*-Tn5-neo-*FRT* cassette. As left homology arm (LH) for later recombination served the last 539 bp of the CB1 coding sequence (*Nsi*I restriction site until last CB1 codon). The CB1-Venus-Easy recombination cassette was cloned within the pEGFP-N1 vector backbone resulting in the plasmid pMS17V. The recombination cassette was linearized from pMS17V via restriction digestion with *Nsi*I and *Avr*II. Further unique important restriction sites are depicted.

CB1-Venus-Soph consisted of the CB1-Venus fusion followed 3' by a right homology arm, which was composed of 49 bp of the 3'-UTR of the CB1 gene directly adjacent to the CB1 stop codon (Fig. 2.7.8). Furthermore, CB1-Venus-Soph contained a transcriptional STOP cassette followed 3' by the *FRT*-Tn5-neo-*FRT* cassette from CB1-Venus-Easy, which was, as a whole (STOP + Tn5-neo), flanked by *lox2272* sites, that was integrated into the *Avr*II restriction site of the CB1 intron -371 bp 5' upstream of the CB1 start codon. This *lox2272* flanked STOP-*FRT*-Tn5-neo-*FRT* cassette was preceded 5' by a left homology arm, which was composed of 50 bp of the CB1 intronic sequence 5' upstream of the *Avr*II site. The RH was designed to be flanked by unique *Asc*I and *Sac*I restriction sites to
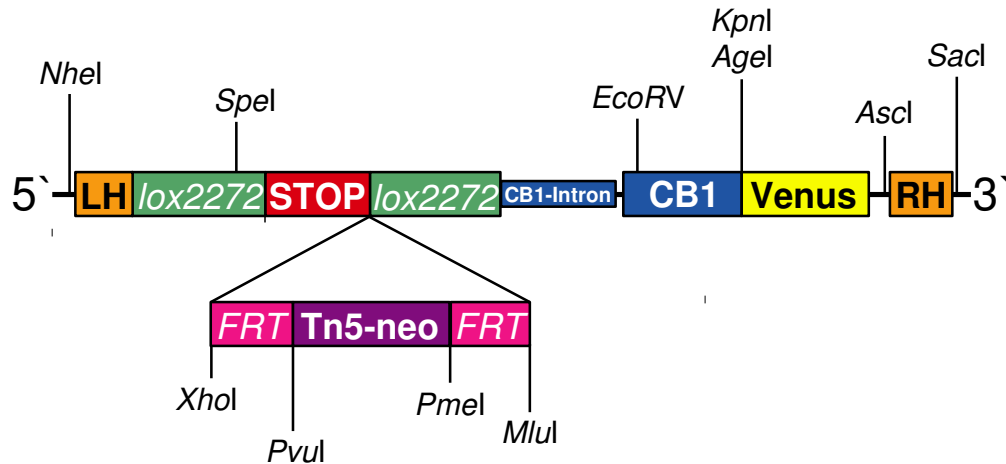
Figure 2.7.8 Overview of the CB1-Venus-Soph recombination cassette. A *lox2272* (Cre recombinase recognition target site)-flanked transcriptional STOP cassette was integrated within the *Avr*II restriction site of the CB1 intron -371 bp upstream of the CB1 coding sequence (cds). Within this cassette, immediately 5' upstream of the right *lox2272* site, the *FRT*-Tn5-neo-*FRT* cassette from CB1-Venus-Easy was introduced. As left homology arm (LH) for later recombination served 50 bp of the CB1 intronic sequence immediately 5' upstream of the *Avr*II restriction site. The LH was introduced 5' upstream of the left *lox2272* site. As right homology arm (RH) for later recombination served 48 bp of the CB1 3'-UTR immediately 3' downstream of the CB1 stop codon. The RH was introduced 3' adjacent to the CB1-Venus cds. The CB1-Venus-Soph recombination cassette was cloned within the pEGFP-N1 vector backbone resulting in the plasmid pMS19V. The recombination cassette was linearized from pMS19V via restriction digestion with *Nhe*I and *Sac*I. Further unique important restriction sites are depicted.

allow for replacement of the sequence in case of insufficient recombination frequency.

lox2272 sites of CB1-Venus-Soph (pMS19V) are functional in *E.coli*

For the construction of CB1-Venus-Soph mutated *loxP* sites, *lox2272*, were used. These *lox2272* sites had been previously shown to function properly (Lee and Saito, 1998) in eukaryotic cells, but not to recombine with the original *loxP* sites. To test whether Cre/*loxP* recombination worked in our system with the mutated *lox2272* sites, we co-transformed *E.coli* with pMS19V and the p705-Cre expression plasmid and investigated the recombination event. Restriction analysis of the recombined pMS19V plasmid revealed the correct restriction fragments in all 8 assessed clones suggesting that recombination had occurred without error (Fig. 2.7.9).
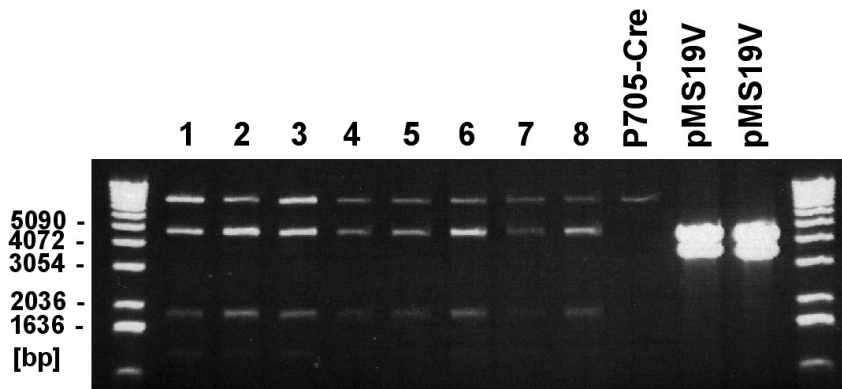
Figure 2.7.9 Screening of *lox2272*/Cre-mediated recombination of CB1-Venus-Soph. pMS19V (containing the CB1-Venus-Soph cassette) was co-transformed with p705-Cre (expressing Cre recombinase) into *E. coli*. Plasmid DNA was isolated after induction of Cre expression and digested with *Nhe*I / *Kpn*I. *Nhe*I cuts directly 5' upstream of the left homology arm of CB1-Venus-Soph and *Kpn*I cuts in between the CB1-Venus fusion (compare Fig. 2.7.8). Thus, restriction of non-recombined pMS19 as control resulted in a 4,736 bp (vector backbone) and a 3,740 bp fragment (containing the *lox2272* flanked STOP cassette). *Nhe*I / *Kpn*I digestion of recombined pMS19V plasmid (clones 1-8) revealed the same 4,736 bp (vector backbone) fragment, but instead of the 3,740 bp fragment a recombined 1,848 bp fragment supposedly belonging to the LH-*lox2272*-CB1Intron-CB1cds fragment (after Cre mediated excision of STOP-*FRT*-Tn5-neo-*FRT*-*lox2272*; compare Fig. 2.7.8). *Nhe*I / *Kpn*I digestion of p705-Cre results only in the linearization of the plasmid, which appears as a third 9,769 bp band in lanes 1-8 and as a single band with p705-Cre alone (control). Some of the 1,848 bp bands are barely visible due to insufficient UV-exposure time of the DNA gel.

Homologous recombination of CB1-Venus-Easy and -Soph with the CB1-BAC

CB1-Venus-Soph was the preferred cassette for homologous recombination, because it would render CB1-Venus expression in a conditional manner (dependent on Cre-mediated excision of the *lox2272* flanked region). However, although homologous recombination with the Red/ET system functions preferably between end homology regions (homology arms) a large stretch of internal homology in the recombination cassette (such as the CB1-intron-CB1cds part of CB1-Venus-Soph) can lead to unwanted recombination between one homology arm and the internal homology instead of between both terminal homology arms. Thus, CB1-Venus-Easy was also designed, which has as an advantage no internal homology, but as a disadvantage lacks the transcriptional STOP cassette, leading to permanent expression of CB1-Venus.
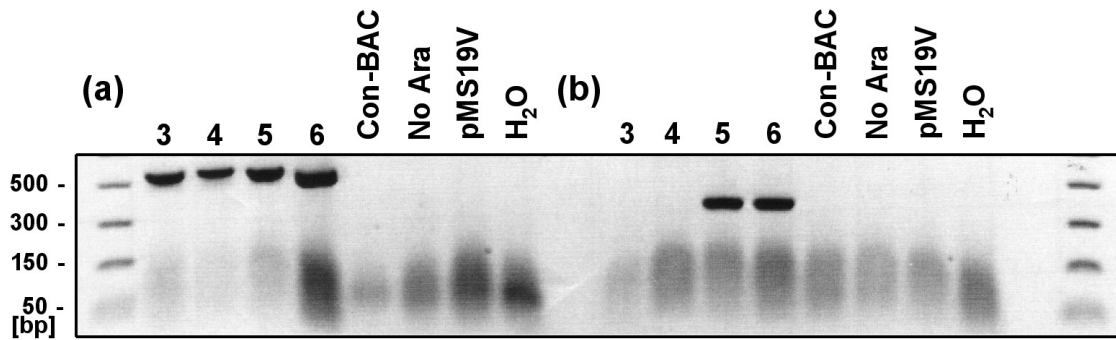
Figure 2.7.10 PCR-Screening of putative CB1-Venus-Soph-BACs after homologous recombination. Kanamycin resistant *E. coli* clones after homologous recombination (Red/ET cloning) of CB1-BAC with the CB1-Venus-Soph resistant cassette were screened via PCR. One PCR product (540 bp) spanned the 5' (left) integration site (**a**) and another PCR product (400 bp) spanned the 3' (right) integration site (**b**). As independent controls served H_2O (no template), plasmid pMS19V (containing the CB1-Venus-Soph cassette), a control BAC without the *CB1* locus (Con-BAC), and a positive clone from the CB1-BAC + CB1-Venus-Soph recombination, where the expression of recombination mediating proteins from the pRed/ET plasmid had not been induced via arabinose (No Ara). Note that whereas clones 5 and 6 show positive bands at the left and right integration sites, clones 3 and 4 only show positive bands at the left integration site, suggesting recombination between the left homology arm and the internal homologous sequence part of the CB1-Venus-Soph cassette instead of the right homology arm.

Both cassettes were recombined via Red/ET cloning in *E.coli* with the endogenous CB1 locus of CB1-BAC, and kanamycin resistant clones were screened for the correct insertion of the cassettes via PCR, covering the left and right insertion sites. PCR screening of the recombined CB1-Venus-Soph-BAC colonies revealed two positive clones (number 5 and 6), where the cassette had been homologously recombined between the left and right homology arms of the CB1-Venus-Soph cassette (Figs. 2.7.10a,b). These clones were further evaluated via PCR for CB1, Tn5-neo and Venus, ensuring that the entire cassette had integrated (data not shown). It has to be noted that in two of the analyzed CB1-Venus-Soph-BAC clones (number 3 and 4) the CB1-Venus-Soph cassette had integrated via homologous recombination between the left homology arm and the internal CB1-intron-CB1-cds sequence of the cassette under loss of Venus and the right homology arm (Figs. 2.7.10a,b).

Two positive clones were also identified for the successful homologous recombination of the CB1-Venus-Easy cassette (data not shown), but they were not further processed because of the successful recombination of the preferred CB1-Venus-Soph cassette. The correct integration site of CB1-Venus-Soph into the CB1-BAC within positive clones 5 and 6 (see above) was further verified via
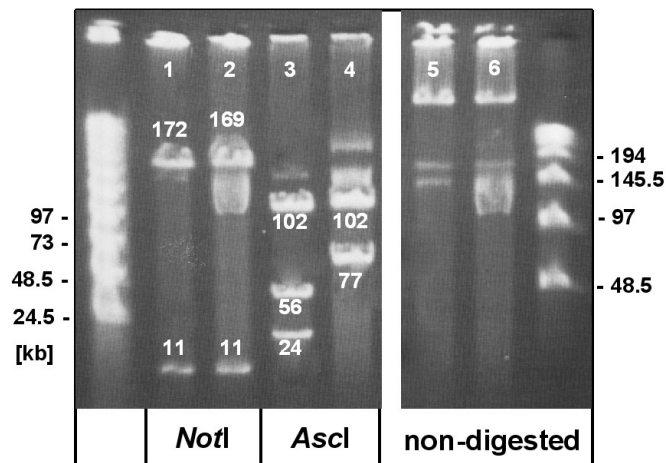
Figure 2.7.11 Restriction digest of CB1-Venus-Soph-BAC. *Not*I digestion of the successfully recombined CB1-Venus-Soph-BAC clone 5 (compare Fig. 2.7.10) was able to excise the pTARBAC1 vector backbone (10,585 bp) from the recombined CB1-Venus-Soph-BAC (lane 1) as well as from the non-recombined CB1-BAC control (lane 2). *Asc*I digestion of the recombined CB1-Venus-Soph-BAC (lane 3) resulted in 4 restriction fragments (102,042 bp; 56,225 bp; 23,616 bp; 189 bp) due to an artificially inserted AscI site between the CB1-Venus coding sequence and the right homology arm of the CB1-Venus-Soph recombination cassette (compare Fig. 2.7.8). *Asc*I digestion of non-recombined CB1-BAC control (lane 4) resulted only in three restriction fragments (102,042 bp; 77,219 bp; 189 bp). Additional high-molecular weight bands are supposedly due to incompletely digested BAC DNA [compare undigested bands of CB1-Venus-Soph-BAC (lane 5) and CB1-BAC (lane 6)]. DNA marker bands had apparently migrated a little bit slower than digested BAC lanes, probably due to overloading.

*Asc*I (Fig. 2.7.9) and *Mlu*I (data not shown) digestion and restriction fragment analysis of CB1-Venus-BAC via PFGE. To ensure that the CB1 backbone could be successfully excised from the CB1-Venus-Soph-BAC, it was *Not*I digested and separated via PFGE. Restriction fragments revealed the correct size of about 11 kb for the backbone and 172 kb for the linearized BAC (Fig. 2.7.11). Finally, the positive CB1-Venus-Soph-BAC clones were additionally analyzed via sequencing, which revealed the correct insertion site (data not shown).

Generation of CB1-Venus-Soph-BAC transgenic mice

Purification and pronucleus injection of the CB1-Venus-Soph-BAC was performed in collaboration with Prof. Dusan Bartsch (see Methods). The first four putative founder mice, which had integrated the neomycin cassette of CB1-Venus-Soph into their genome, could be identified via PCR genotyping of isolated mouse tail DNA (Fig. 2.7.12).). All four putative founder mice resulted from injection of the

linearized, but not purified, CB1-Venus-Soph-BAC, whereas injection of the linearized and purified fragment did not give rise to any potential founders.
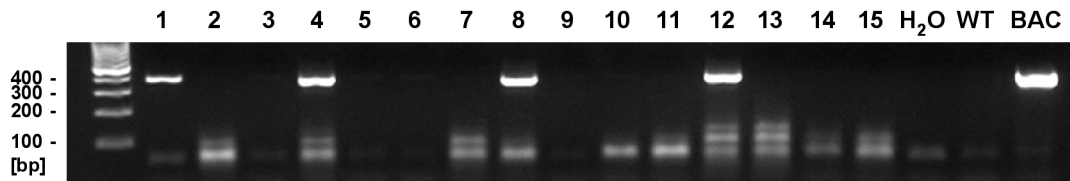
Figure 2.7.12 Genomic DNA screening of putative CB1-Venus-Soph-BAC transgenic mice via PCR. Putative CB1-Venus-Soph-BAC transgenic mice resulting from pronuclear oocyte injections of the CB1-Venus-Soph-BAC were screened for insertion of the CB1-Venus-Soph-BAC via PCR analysis of the Tn5-neo coding sequence using genomic DNA purified from tail biopsies. Out of 25 mice four putative founder animals were identified (lanes 1,4,8,12; PCR analyses of only 15 animals, which resulted from the injection of the linearized but not purified fragment, are depicted). The length of the PCR product was 380 bp. Purified CB1-Venus-Soph-BAC (BAC) served as positive control, wild-type (WT) mouse tail DNA and H_2O as negative controls. This Figure was kindly provide by Dr. D. Bartsch.

2.7.5 Discussion

In the present study, we demonstrate the cloning of a CB1-EGFP receptor fusion protein, which has similar properties as the endogenous CB1 receptor. Furthermore, based on this CB1-EGFP fusion, we present the generation of a conditional CB1-Venus-BAC transgenic mouse mutant.

The CB1-EGFP receptor was generated as a fusion of EGFP to the C-terminus of CB1, because in almost all GPCR-EGFP fusions that had so far been generated as such, EGFP did not influence endogenous GPCR properties (Arun et al., 2005; Kallal and Benovic, 2000). However, in order to render a disturbance of GPCR C-terminal signaling proteins by the attached EGFP even more unlikely, we introduced a triple-glycin linker in between the CB1 and EGFP cds in order to allow free spatial movement of the fused EGFP protein. It has to be noted that recently an EGFP-CB1 fusion was generated by another group, where EGFP, preceded by a human growth hormone derived signal sequence, was fused to the N-terminus of the receptor (McDonald et al., 2007). This fusion was shown to have similar properties to the endogenous CB1 receptor in terms of cAMP signaling and agonist-induced endocytosis. As ligands of CB1 are likely to bind within its 7-transmembrane spanning pore (Demuth and Molleman, 2006), and not to its extracellular N-terminus, it is conceivable that also N-terminal EGFP-CB1 fusions function normally.

The native CB1 receptor with its proposed 116 amino acids long N-terminal extracellular tail is devoid of an endoplasmatic reticulum (ER) N-terminal cleavable signal sequence (Andersson et al., 2003). Instead, its first trans-membrane domain is thought to function as the ER sorting signal (reverse signal anchor sequence). As this renders CB1 translocation into the ER inefficient, a relatively high percentage of CB1 receptors becomes misfolded and again degraded before they reach the cell surface. Andersson and co-workers demonstrated that by shortening the N-terminal tail CB1 receptor expression can be dramatically improved in cell culture, and even though putative extracellular glycosylation sites are deleted by this procedure, they do not seem to be of any crucial role for receptor function (Andersson et al., 2003).

As we were concerned that our CB1-EGFP receptor construct (plasmid pMS1) might not have sufficient surface expression, we also generated two other

constructs with shortened N-terminal tails, pMS4 and pMS5. Nevertheless, in our hands these constructs did not show any different properties from pMS1 in terms of expression or signal transduction properties (data not shown). It is possible that these differences were of rather subtle nature and would have become apparent only by careful agonist dose-response relationship evaluations. However, as it was not our intention to study, the role of the N-terminal tail in detail, but only to generate a functional CB1-EGFP fusion with sufficient expression, we did not pursue this issue further.

Using immunohistochemistry, the native CB1 receptor was shown to be expressed not only at the surface of HEK293 cells, AtT20 cells and hippocampal neurons, but also in a significant proportion in intracellular vesicular compartments (Hsieh et al., 1999; Jin et al., 1999; Coutts et al., 2001). If the major part of these intracellularly located CB1 receptors is present in organelles associated with protein sorting such as Golgi or ER, or rather to endocytotic vesicles associated with receptor trafficking is not yet clear (Leterrier et al., 2004; Andersson et al., 2003). Nevertheless, our CB1-EGFP fusion exhibited a similar expression pattern as that reported for the native CB1 receptor as the fusion was clearly located at the membrane, but also within intracellular vesicles (Figs. 2.7.2 d,e,f). Hence, the plasma and intracellular membrane sorting ability of the CB1-EGFP receptor was conserved. In addition, our CB1-EGFP fusion had also a similar endocytosis profile in HEK293 cells (being in a significant proportion endocytosed after 30 min of agonist stimulation, data not shown, and completely endocytosed after 2 h; Figs. 2.7.3 d,e,f) as the native receptor (Hsieh et al., 1999; Leterrier et al., 2004).

In cultured cells, the endocannabinoid system exists under certain circumstances in a tonically active state, which likely do not only arise from the endogenous release of endocannabinoids and subsequent binding to CB1 receptors under baseline conditions, but also from the presence of unstimulated CB1 receptor that are in a constitutively active state (Pertwee, 2005). In such cases, when applied in high concentrations, the CB1 antagonist SR141716 was found to exert inverse agonism activity, likely via an additional allosteric binding site, that shifts CB1 receptors from an "active" (coupled to intracellular signal proteins) to an "inactive" (uncoupled) state. These inverse agonism properties of SR141716 on CB1 receptors is regarded as the reason for SR141716-induced translocation of intracellular CB1 receptors to the plasma membrane, probably due

to membrane stabilization of the inactive form of the receptor that does not internalize (Leterrier et al., 2004; Rinaldi-Carmona et al., 1998). In the present study, we could observe a similar scenario upon SR141716 administration with CB1-EGFP (Figs. 2.7.3 g,h,i) as it was reported for the native receptor.

However, whether this phenomenon also exists in neurons is currently unclear, as two studies using hippocampal primary cultures have either reported the existence (Leterrier et al., 2006) or the non-existence (McDonald et al., 2007) of inverse agonist-induced CB1 externalization. Thus, a CB1-EGFP transgenic mouse model could help solving this issue by allowing the *in vivo* observation and circumventing problems due to different culture or transfection conditions.

To evaluate whether the signal transduction properties of CB1 are preserved in the CB1-EGFP fusion we used a CRE-driven luciferase reporter gene assay. As CB1 is generally coupled to $G_{i,o}$ inhibitory G-proteins, we hypothesized that agonist stimulation of CB1 would lead to an inhibition of adenylyl cyclase, which in turn, would reduce protein kinase A (PKA) activation, hence reducing CREB phosphorylation and therewith its binding to CRE promoter elements. However, we observed exactly the opposite phenomenon, because CB1, and similarly CB1-EGFP, activation did not inhibit, but stimulated CRE mediated luciferase expression (Fig. 2.7.4). A similar effect was observed in response to direct adenylyl cyclase stimulation via forskolin. Thus, it is possible that in our cell culture system CB1 did not couple to inhibitory but rather to stimulatory G_s proteins, which has as well sometimes been described in the literature (Demuth and Molleman, 2006). Indeed, one study exists, which used a similar CRE luciferase reporter assay as we did and demonstrated coupling of CB1 to G_s proteins (Calandra et al., 1999). However, as we did not directly measure cAMP levels, the possibility can not be excluded that CB1 activation induced CREB phosphorylation via signal transduction pathways different from PKA (Johannessen et al., 2004). Nevertheless, CB1-EGFP was equally effective as the native CB1 receptor in activating luciferase reporter expression (Fig. 2.7.4), even though the exact mechanism remains to be elucidated.

Although regulation of MAP kinases is usually associated with tyrosine receptor kinase activation, accumulating evidence exists that GPCRs can also stimulate MAP kinases. Accordingly, CB1 receptor activation has recently been shown to activate ERKs within the brain (Derkinderen et al., 2003; Cannich et al.,

2004). Thus, we studied the ability of CB1-EGFP to activate ERKs in cell culture and found that CB1 agonist stimulation induced a fast and strong activation of ERK-1/2 phosphorylaton within 5 min (data not shown) reaching the strongest effect within 15 min (Fig. 2.7.5). Also with regard to ERK phosphorylation CB1-EGFP acted similarly to native CB1.

In conclusion, our CB1-EGFP fusion behaves similarly to the wild-type CB1 receptor with regard to membrane expression, trafficking, and signal transduction. It remains to be stated that in the meantime two other CB1-EGFP fusion constructs have been developed by different groups, one N-terminal, one C-terminal, which were also proven not to be compromised in their CB1-like function. Thus, in all likelihood the CB1-Venus fusion of our transgenic CB1-Venus-Soph-BAC mouse should function normally, at least with regard to the most important CB1 receptor properties.

The invention of Red/ET cloning as a possibility for homologous recombination in *E.coli* (Zhang et al., 1998) prompted us to use this technology to generate a transgenic mouse based on our CB1-EGFP fusion construct. Although Red/ET cloning is favored between left and right terminal homology arms, a high percentage of internal homology can hinder this recombination event. Red/ET cloning of CB1-Venus-Soph (Fig. 2.7.8) resulted in about 50% of homologous recombination between the left homology arm and the internal homology sequence and in about 50% of recombination between the left and right terminal homology arms (compare Fig. 2.7.10). Thus, we were able to obtain homologous integration of the entire CB1-Venus-Soph recombination cassette into CB1-BAC and did not have to switch to CB1-Venus-Easy (which has no internal homology; compare Fig. 2.7.7).

The CB1-Venus-Soph cassette was designed in such a way that a *lox2272* flanked transcriptional STOP cassette was inserted into the *Avr*II restriction site (Fig. 2.7.6) of the CB1 intron. This site was chosen, because after Cre recombinase mediated excision one *lox2272* site will remain within the genome, which could potentially interfere with gene function. However, in the previously established floxed CB1$^{f/f}$ mouse line, which was generated in our laboratory (Marsicano et al., 2002) the 5' upstream *loxP* site was integrated exactly at the same position within the CB1 intron, and CB1$^{f/f}$ mice were indistinguishable from

wild-type mice suggesting that a remaining *loxP* site at this intronic position does no impair CB1 gene function.

We did not use conventional *loxP* sites but Cre recombinase recognition sites with two base substitutions within the 8 bp spacer region, named *lox2272* (Lee and Saito, 1998). These sites were recently selected in mammalian cell culture screens as to exhibit almost exclusive and efficient recombination with its identical *lox2272* site, but very low recombination efficiency with original *loxP* sites (Lee and Saito, 1998; Kim et al., 2007). Although *loxP* based Cre recombination is highly favored between *loxP* elements that are located close to each other within a small distance on the same chromosome, *loxP* mediated rearrangements of up to three quarters of one single chromosome (Zheng et al., 2000) and even between different chromosomes has been reported (Van Deursen et al., 1995).

Thus, we reasoned that the use of *lox2272* would enable us to cross CB1-Venus-Soph-BAC transgenic mice with *loxP* containing CB1$^{f/f}$ mice, with complete CB1 knockout mice (which would after complete Cre recombination mediated excision of the floxed CB1 gene still harbor one remaining *loxP* site), or even with conditional CaMK-CB1$^{-/-}$, Glu-CB1$^{-/-}$ or GABA-CB1$^{-/-}$ mice (Monory et al., 2006) with an extremely low risk of unwanted chromosome re-arrangements between *lox2272* and *loxP* sites.

We could demonstrate that *lox2272* sites within our CB1-Venus-Soph recombination cassette work properly in terms of Cre mediated excision of their enclosed DNA fragment in *E. coli* (Fig. 2.7.9). Accordingly, as *lox2272* were recently shown to work effectively within a mammalian chromosome in cell culture (Kondo et al., 2003) and even in transgenic mice (Araki et al., 2002), they can be expected to effectively mediate Cre recombination in our CB1-Venus-Soph-BAC transgene.

FRT flanking of our Tn5-neo antibiotics resistance cassette used for the selection of positive recombined BAC clones was applied in order to be able to excise this cassette later from the genome of CB1-Venus-Soph-BAC transgenic mice via crossing with Flp deleter mice (Rodriguez et al., 2000). Although neo resistance cassettes are often not excised from the genome after the generation of transgenic mice, it is generally useful to do so in order to prevent any unwanted influence of the integrated DNA fragment on endogenous gene function (Schmidt-Supprian et al., 2007).

We chose to exchange the initially used EGFP within the CB1-EGFP fusion later for EYFP, and finally for Venus, a mutated version of EYFP with enhanced properties. Venus had been generated by the mutation of 5 different amino acids within EYFP, which resulted in enhanced maturation and folding, and increased tolerance to acidosis or Cl⁻ exposure (Nagai et al., 2002). Therefore, the in vivo application of Venus is expected to offer increased fluorescent stability in comparison with EGFP. Recently, the generation of the first transgenic mouse incorporating Venus has been reported, further encouraging functionality of Venus within our CB1-Venus-Soph-BAC transgene (Oberto et al., 2007).

Finally, in collaboration with Prof. D. Bartsch, we were able to generate the first four potential CB1-Venus-Soph-BAC founder mice (Fig. 2.7.12). They are currently being simultaneously bred with wild-type mice to confirm stable germ-line transmission of the transgene to the F1 generation, and with Cre deleter mice to achieve global excision of the *lox2272* flanked transcriptional STOP cassette, which should result in whole body-wide expression of CB1-Venus. In the next step, offspring of the different founder lines with Cre deleter mice will be evaluated for the correct expression pattern of CB1-Venus in comparison with native CB1.

In summary, we have generated a CB1-Venus-Soph-BAC transgenic mouse, which allows the conditional overexpression of the CB1-Venus fusion. This transgenic mouse is a highly versatile tool to approach many yet unexplained questions of endocannabinoid signaling. Potential applications are exemplified below:

Certainly, one of the first steps in future research directions must be the selection, by multiple breeding steps of CB1-Soph-BAC transgenic mice to CB1 knockout animals, of a strain, which only expresses the CB1-Venus fusion but not the native receptor. Evaluation of those mice should reveal whether CB1 knockout specific phenotypes can be rescued by CB1-Venus, and hence, should establish *in vivo* functionality of CB1-Venus.

In addition, by crossing the CB1-Venus-Soph-BAC mouse to various neuron population specific Cre recombinase expressing lines, a detailed mapping of CB1 receptors within other neuronal circuits could be enabled. Ultra-microscopic technology, which was recently modified in the Max Planck Institute of Psychiatry, ought to be extremely helpful as it allows for the three-dimensional visualization of neuronal networks within the entire mouse brain (Dodt et al., 2007). As CB1

receptor expression in neurons does not seem to be restricted to the axon, but due to constitutive endocytosis also occurs to a high percentage in the somatodendritic region (Leterrier et al., 2006; McDonald et al., 2007), it can be expected that in addition to nerve fibers, cell bodies will also be visible via fluorescent imaging. This could greatly facilitate the electrophysiological patching of CB1 positive neurons (or even of specific CB1 positive neuron populations, after crossing with Cre lines).

It will certainly be possible to investigate dynamics of CB1-Venus trafficking in neurons via primary cell culture or organotypic slice culture preparations, but due to emerging advanced microscopy technology, such as two-photon excitation laser scanning microscopy (Svoboda and Yasuda, 2006), even *in vivo* investigations within the living brain can be envisioned. Not only the dynamics of CB1 endocytosis, recycling and degradation by itself, but also the relevance of these events, for instance, for potential CB1 receptor signaling on the endocytotic pathway (McPherson et al., 2001), for CB1 desensitization (Kouznetsova et al., 2002) and cannabinoid tolerance (Tappe-Theodor et al., 2007; Scherrer et al., 2006) or for differential responses of CB1 activation to different classes of agonists and antagonists could be studied (Bonhaus et al., 1998; Pertwee, 2005).

It remains to be noted that the use of the yellow fluorescent protein Venus would render fluorescence-resonance energy transfer (FRET) studies of CB1-Venus (FRET-Acceptor) protein-protein interactions with potential enhanced cyan fluorescent protein (ECFP; FRET Donor)-coupled interaction partners feasible (Chen et al., 2003). This could be achieved via transfection of CB1-Venus-Soph-BAC neurons with ECFP-tagged proteins or via crossing of CB1-Venus-Soph-BAC mice with ECFP-tagged protein positive transgenic mice (which would also allow co-localization studies).

In addition, the advantages that quantum dots provide for cellular imaging, such as high photostability, brightness and a broad excitation spectrum, could be taken advantage of by coupling of a quantum dot (with a different emission wavelength than CB1) with a CB1 agonist (a collaboration with the group of ML López-Rodríguez in Madrid, Spain, on the synthesis of such a compound has already been established). Quantum dots bearing a natural CB1 ligand as effector molecule might provide the means for long-term real-time visualization of CB1 trafficking dynamics upon ligand binding as has successfully been demonstrated in a similar manner for epidermal growth factor receptors (Lidke et al., 2004).

Finally, the number of potential applications for the CB1-Venus-Soph-BAC is vast, but beforehand, the potential founder animals still await thorough investigation to ensure that *lox2272* mediated Cre recombination is efficient, that CB1-Venus expression follows the native receptor, and that CB1-Venus is indeed functional in a way as to rescue CB1 knockout phenotypes.

CHAPTER 3

THE CORTICOTROPIN-RELEASING HORMONE SYSTEM AND DEPRESSION

3.1 Introduction to the corticotropin-releasing hormone system and depression

As mentioned in Chapter 1.4.3 of the Introduction, one major theory for the development of major depression represents disturbances of the HPA axis, which can be caused by CRH overexpression. However, it becomes apparent that, in addition to the paraventricular nucleus (PVN), also hyperactivation of other central CRH neuropeptidergic circuits, which act on behaviorally relevant extra-pituitary brain areas, can occur in depressed patients. For instance, downregulation of CRH binding sites in the prefrontal cortex of depressed suicide victims has been causally related to central CRH hypersecretion (Nemeroff, 1996). Furthermore, it is speculated that elevated CRH concentrations in the cerebrospinal fluid reflect hypersecretion of CRH from extrahypothalamic neurons (Arborelius et al., 1999). Accordingly, CRH-like immunoreactivity has, in addition to the PVN, been observed in the cortex, the central nucleus of the amygdala (CeA) (Van Bockstaele et al., 1998), the bed nucleus of the stria terminalis (BNST), the hippocampus, the nucleus accumbens, substantia nigra, raphe nuclei, and locus coeruleus (LC) (Swanson et al., 1983).

To address the putative role of the CRH system for the pathophysiology of depression in animal models a number of mouse mutants have been created that target different players of the intricate CRH brain system, such as CRH-R1, CRH receptor type 2 (CRH-R2), CRH, CRH binding protein or urocortin I (for review see Keck et al., 2005). However, interpretation of these mouse models has been complicated by the complete knockout or the ubiquitous overexpression of the individual proteins, which, due to these life-long disturbances, can lead to compensatory mechanisms from other members of the CRH system. Only one conditional transgenic moue line has so far been created eliminating the CRH-R1

only from the forebrain (Muller et al., 2003). This *CRH-R1$^{lox/lox}$camk2a-cre* mouse, for instance, clearly demonstrated that anxiogenic effects of CRH are mediated via limbic CRH-R1 activation independent of HPA axis influence.

Although the anxiogenic role of CRH in rodent models of anxiety is well established, its role in depression-related tests is much less understood. In the following study we used conditional CRH overexpressing mutants in an attempt to decipher CRH-sensitive pathways within the brain that can modulate depression-like behavior.

3.2 Conditionally overexpressing mouse mutants highlight paradoxical antidepressant-like effects of corticotropin-releasing hormone

In the previous chapters 2.2.2-6, we investigated the role of the endocannabinoid system for stress processing in mice. We found that CB1 receptor-deficient mice showed, in addition to other deficits, increased HPA axis responsiveness, which was partly due to increased CRH overexpression in the paraventricular nucleus (PVN) of the hypothalamus (Chapter 2.2, Fig. 2.2.3). However, we did not find any additional CRH dysregulation at extra-hypothalamic sites in these mice (Chapter 2.2). In the present Chapter, we explored conditional transgenic mice that overexpress CRH in various brain regions in order to further investigate the role of chronic CRH hyperactivation for depression-like behavior.

The work described in this chapter was accomplished in close shared collaboration with Dr. A. Lu from the Molecular Neurogenetics group of Dr. J. Deussing of the Max Planck Institute of Psychiatry in Munich. Dr. A. Lu and co-workers generated (Fig. 3.1) and characterized conditional CRH overexpressing mutant mice neurochemically (Figs. 3.2.2, 3.2.3, 3.2.8a,c,e, 3.2.9c-f) and neuroendocrinologically (Fig. 3.2.4). I analyzed mutant mice behaviorally and pharmacologically (Figs. 3.2.5, 3.2.6, 3.2.7, 3.2.8b,d, 3.2.9a,b) and performed the microdialysis experiments (Fig. 3.2.10; Table 3.3.3). Neurochemical analysis of PCPA and AMPT treated mutant mice (Tables 3.2.1-2) was performed in collaboration with N. Whittle from the group of Dr. N. Singewald (University of Innsbruck, Department of Pharmacology and Toxicology, Austria).

3.2.1 Summary

CRH hyperactivity has been implicated in the human pathophysiology of affective disorders. Paradoxically, however, CRH receptor type 1 (CRH-R1) antagonists proved widely ineffective in classical antidepressant-screening paradigms in rodents, and centrally administered CRH or CRH-R1 agonists were even shown to exert antidepressant-like effects. To elucidate these controversial

findings we created multiple mouse lines overexpressing CRH in a spatially restricted fashion. Only overexpression of CRH in the entire central nervous system (CNS), but not forebrain-restricted overexpression, resulted in stress induced HPA axis hyperactivity and in antidepressant-like behavior in antidepressant screening paradigms. These effects were related to acute activity of exogenously overexpressed CRH on the animals' stress response and recapitulated the effect of stress-induced activation of the endogenous CRH system. Moreover, we present evidence for a CRH-dependent modulation of catecholaminergic neurotransmission, likely due to enhanced noradrenergic activity in the locus coeruleus, as molecular mechanism underlying the antidepressant-like effect of CRH.

3.2.2 Introduction

CRH plays a prominent role in coordinating the neuroendocrine, autonomic, behavioral and immunological responses to various stressful stimuli (Steckler and Holsboer, 1999; Holsboer, 1999). Besides its function as the major physiological regulator of the HPA axis, CRH is capable of modulating a wide range of behaviors including anxiety, arousal, sensory information processing, learning and memory as well as locomotor activity (Steckler and Holsboer, 1999; Dunn and Berridge, 1990). Most behavioral effects of CRH are attributed to extrahypothalamic neuronal circuits including neocortical, limbic and brainstem structures where CRH functions as a neuromodulator (Smagin et al., 2001). Dysregulation of the CRH system and accompanying chronically elevated levels of CRH are implicated in human stress-related and affective disorders, including anxiety disorders and major depression (Nemeroff et al., 1988; Nemeroff et al., 1984; Holsboer, 1999; De Kloet et al., 2005). For example, in patients suffering from depression clinical studies have demonstrated elevated levels of CRH in the cerebrospinal fluid (Nemeroff et al., 1984), increased numbers of CRH and CRH/arginine vasopressin expressing neurons in the paraventricular nucleus of the hypothalamus (PVN) (Raadsheer et al., 1994a), elevated CRH mRNA levels in the PVN (Raadsheer et al., 1995), and decreased CRH binding sites in the frontal cortex (Nemeroff et al., 1988). Additionally, animal studies involving central application of CRH revealed phenotypic alterations reminiscent of symptoms observed in affected subjects (Dunn and Berridge, 1990). Moreover, CRH receptor antagonists are capable of attenuating the behavioral consequences of stress, underscoring the role of endogenous CRH in mediating many stress-induced behaviors (Heinrichs et al., 1995). Finally, a first clinical trial has demonstrated the efficacy of a selective CRH-R1 antagonist in treating depressed patients (Zobel et al., 2000).

However, CRH-R1 antagonists in rodents have demonstrated no or only weak efficacy in classical antidepressant screening paradigms such as the forced swim test and the tail suspension test (Nielsen, 2006), when the animals were tested under basal conditions. These findings are in accordance with the observation that anxiolytic-like activities of CRH-R1 antagonists such as DMP696 and R121919 are best observed in animals, which are hyperresponsive or more

susceptible to stress and, thus, exhibit already increased levels of CRH (Menzaghi et al., 1994; Zorrilla et al., 2002).

To study the effects of central CRH hyperactivity in a suitable animal model, CRH transgenic mouse lines have previously been established expressing CRH either under the control of the broadly active metallothionein (CRH-Tg) or the CNS-restricted Thy-1.2 (CRH-OE$_{2122}$) promoter (Stenzel-Poore et al., 1992; Groenink et al., 2002). In both cases, unrestricted and exceeding CRH overexpression resulted in generally elevated ACTH and corticosterone levels accompanied by symptoms of Cushing-like syndrome, rendering the interpretation of behavioral results difficult. To circumvent these problems, we developed a mouse model which permits the overexpression of CRH in a conditional fashion without producing marked neuroendocrine disturbances under basal conditions. Combining the knock-in of a single copy of the murine *Crh* cDNA into the *ROSA26* (*R26*) locus (Zambrowicz et al., 1997) with the Cre/loxP system enabled us to overexpress CRH in a spatio-temporally regulated fashion at different dosages. Using *nestin-cre* (Tronche et al., 1999), *camk2a-cre* (Minichiello et al., 1999), and *dlx-cre* (Monory et al., 2006) mice to restrict CRH overexpression to the CNS, and to specific types of neurons within the forebrain respectively, validated this mouse line as an ideal tool to study the behavioral and neuroendocrine effects of spatially confined CRH overexpression in mice.

3.2.3 Materials and Methods

Targeting vector

The targeting vector was based on pROSA26-1 bearing 5.5-kb homology to the murine *ROSA26* locus (*R26*) and a diphtheria toxin (DTA) expression cassette (Soriano, 1999c). It was constructed by introducing the following components into the unique *Xba*I site of pROSA26-1: adenovirus splice acceptor (SA), *loxP, PGK-Neo* - including PGK polyadenylation sequence (pA) and two copies of the SV40 pA (*PGK-Neo*-3×pA), *loxP*, *IRES-LacZ* and bovine growth hormone (bGH) pA (from 5´ to 3´). The SA and bGH pA were subcloned from pSAβgeo (Friedrich and Soriano, 1991). The *IRES-LacZ* was isolated and modified from ETLpA-/LTNL (Mombaerts et al., 1996). The loxP flanked *PGK-Neo*-3×pA cassette was amplified by PCR from genomic tail DNA of *R26* reporter mice (Soriano, 1999). The DTA cassette was inverted and concomitantly a *Swa*I site was introduced for linearization. The murine *Crh* cDNA was inserted in a unique *Pac*I site between the second *loxP* site and the *IRES-LacZ* cassette. External probes used for identification of homologous recombination events were amplified by PCR from genomic DNA and cloned using the TOPO TA cloning kit (Invitrogen, Karlsruhe, Germany). 5´-probe: forward 5´-GCG-AGA-CTC-GAG-TTA-GGC-3´ and reverse 5´-GCG-GCC-GCC-GCC-CGC-CTG-CG-3´ (150-bp); 3´-probe: forward 5´-GTT-GAG-CCA-CTG-AGA-ATG-G-3´ and reverse 5´-GAA-ACT-ACA-ACC-ATT-GTT-CAT-3´ (662-bp).

Generation of conditional CRH overexpressing mice

The linearized targeting vector was electroporated into TBV2 embryonic stem (ES) cells (129S2). Mutant ES cell clones were identified by Southern blot analysis of genomic ES cell DNA digested with *Eco*RV or *Apa*I using the external 5'- or 3'-probe respectively. Mutant ES cells were used to generate chimeric mice by blastocyst injection. Germ-line transmission of the modified *R26* allele (*R26^{flopCrh}*, <u>fl</u>oxed st<u>op</u>) was confirmed in offspring from male chimeras bred to wild-type C57BL/6J mice. For the conditional, CNS restricted overexpression of CRH (CRH-COE-Nes), obtained *R26^{+/flopCrh}* mice were crossed to transgenic *nestin-cre* mice (Tronche et al., 1999). Resulting heterozygous *R26^{+/flopCrh}* and *R26^{+/flopCrh}* *nestin-cre* F_1 animals were intercrossed in order to obtain in the F_2 generation animals of the desired genotypes: *R26^{+/+}* (CRH-COE^{wt}-Nes), *R26^{flopCrh/flopCrh}* (CRH-COE^{con}-Nes), *R26^{+/flopCrh}* *nestin-cre* (CRH-COE^{het}-Nes), and *R26^{flopCrh/flopCrh}* *nestin-cre* (CRH-COE^{hom}-Nes). For the forebrain restricted overexpression of CRH in principal neurons (CRH-COE-Cam), *R26^{+/flopCrh}* mice were crossed to transgenic *camk2a-cre* mice (Minichiello et al., 1999). As above, *R26^{+/+}* (CRH-COE^{wt}-Cam), *R26^{flopCrh/flopCrh}* (CRH-COE^{con}-Cam), *R26^{+/flopCrh}* *camk2a-cre* (CRH-COE^{het}-Cam), and *R26^{flopCrh/flopCrh}* *camk2a-cre* (CRH-COE^{hom}-Cam) animals were obtained in the F_2 generation. CRH-COE-Dlx mice overexpressing CRH in GABAergic neurons of the forebrain were generated accordingly using *dlx-cre* mice (Monory et al., 2006).

Genotyping was performed by PCR using primers: ROSA-1, 5´-AAA-GTC-GCT-CTG-AGT-TGT-TAT-3´; ROSA-2, 5´-GCG-AAG-AGT-TTG-TCC-TCA-ACC-3´ and ROSA-4, 5´-GGA-GCG-GGA-GAA-ATG-GAT-ATG-3´. Standard PCR conditions resulted in a 398-bp wild-type and a 320-bp mutant PCR product. The presence of *nestin*-, *camk2a*- and *dlx-cre* was evaluated using primers CRE-F, 5´-GAT-CGC-TGC-CAG-GAT-ATA-CG-3´ and CRE-R 5´-AAT-CGC-CAT-CTT-CCA-GCA-G-3´ resulting in a PCR product of 574-bp. Genotypes were confirmed by Southern blot analysis of *Eco*RV-digested tail DNA using the 5´-probe and a Cre recombinase specific probe (Muller et al., 2003). The efficiency of *nestin-cre* mediated excision of the transcriptional terminator sequence was demonstrated by Southern blot analysis of *Eco*RV-digested genomic DNA prepared from cortex, hippocampus, thalamus, cerebellum, tail and liver using the external 5´-probe. Mice used for this study were kept on a mixed 129S2/Sv × C57BL/6J background.

X-Gal staining

2-3-months-old animals (n = 4-5 per genotype) were sacrificed by an overdose of isoflurane and transcardially perfused with 4% paraformaldehyde, 2 mM $MgSO_4$ and 5 mM EGTA. Subsequent X-Gal staining was performed on free floating 50 or 100 µm-thick vibratome sections or on intact organs as previously described (Mombaerts et al., 1996).

In situ hybridization

10-week-old mice were sacrificed in the morning (10:00 am) by an overdose of isoflurane. For quantification of immediate early genes c-fos and zif268 animals were either sacrificed under basal conditions or subjected to 10 min of forced swimming 30 min prior to sacrifice. Brains were carefully removed and immediately shock frozen on dry ice. Frozen brains were cut on a cryostat in 20 µm-thick sections. For quantitative in situ hybridization cryostat sections of CRH-COE[con] and CRH-COE[hom] brains were mounted side by side on SuperFrost Plus slides (Menzel GmbH, Braunschweig, Germany). This procedure allowed for parallel *in situ* hybridization of sections under identical conditions assuring meaningful quantification and comparison of hybridization signals. All sections were processed for in situ hybridization according to a modified version of the procedure described by Dagerlind et al. (1992). The following riboprobes were used: CRH, nucleotides 1306-1661 of GenBank accession no. AY128673; c-fos, nucleotides 608-978 of GenBank accession no. NM_010234; zif268, nucleotides 245-786 of GenBank accession no. NM_007913; LacZ, nucleotides 192-569 of GenBank accession no. U46489. Specific riboprobes were generated by PCR applying T7 and T3 or SP6 primers using plasmids containing above mentioned cDNAs as templates. Antisense and sense cRNA probes were transcribed from 200 ng of respective PCR product and directly used as a template for the synthesis of radiolabeled transcripts by *in vitro* transcription with ^{35}S-UTP (Amersham Biosciences, Piscataway, NJ, USA) using T7 and T3 RNA polymerase (Roche, Penzberg, Germany) respectively. After 20 min of DNase I (Roche) treatment, the probes were purified by the RNeasy Clean up protocol (Qiagen, Hilden, Germany) and measured in a scintillation counter. For hybridization, sections were pretreated, and prehybridized

as described previously (Dagerlind et al., 1992). Subsequently, they were hybridized overnight with a probe concentration of 7×10^6 cpm/ml at 57 °C and washed at 64 °C in 0.1× SSC and 0.1 mM DTT. The hybridized slides were dipped in autoradiographic emulsion (type NTB2; Eastman Kodak, Rochester, NY, USA), developed after 3–6 weeks, and counterstained with cresyl violet.

For quantification, autoradiographs were digitized and relative levels of mRNA were determined by computer-assisted optical densitometry (ImageJ, http://rsb.info.nih.gov/ij/). For in situ hybridizations routinely three different exposure times were applied in order to assure that the signals to be quantified were in the linear range.

CRH radioimmunoassay

2-3-months-old mice were sacrificed by cervical dislocation at 10:00 am. Brains were carefully removed and used in total or further dissected for selective preparation of cortex, hippocampus, thalamus and cerebellum. The CRH-specific radioimmunoassay (RIA) on tissue homogenates was performed after prior extraction as previously described (Stalla et al., 1986).

Endocrine analyses

Two weeks before the experiments, 3-5 months old animals were separated and singly housed with a 12 h : 12 h light/dark schedule (lights off at 07:00 pm). All experiments and data analyses were performed separately for male and female animals. To determine the basal hormone plasma levels, mice were left undisturbed throughout the night before the experiment. Blood sampling was performed in the early morning (07:30–09:30 am) and afternoon (04:30–05:30 pm) by collecting trunk blood from animals rapidly decapitated under light isoflurane anesthesia or by incision of the tail with the time from first handling of the animal to completion of bleeding not exceeding 45 s. For evaluation of the endocrine response to stress, we collected blood samples immediately after and 30 min after 10 min restraint stress for which animals were placed in a 50 ml conical tube with the bottom removed. Stress experiments were performed in the morning (07:30–10:00 am). Plasma corticosterone and ACTH concentrations were measured in duplicate by commercially available RIA kits (ICN Biomedicals, Irvine, CA, USA).

Subjects for behavioral testing

Mice were singly housed two weeks prior to experiments under standard laboratory conditions (22 ± 1 °C, 55±5% humidity) with food and water ad libitum under a 12 h : 12 h inverted light/dark schedule (lights off at 09:00 am). Age of tested animals ranged between 3 and 6 months. Animal experiments were conducted in accordance with the *Guide for the Care and Use of Laboratory Animals* of the Government of Bavaria, Germany. Experiments were performed during the dark, active phase of the animals between 01:00 pm and 06:00 pm under red-light conditions where not otherwise stated. Animals' behavior in the tail suspension and forced swim test was analyzed on-line by trained observers who were blind to treatment and genotype. If not stated

otherwise, male mice were used for the experiments. Experiments to assess the behavioral consequences of stress-regulated activation of endogenous CRH were performed on previously described CRH-R1 knockout mice (Timpl et al., 1998). Experiments to assess the behavioral consequences of altered CRH-R2 signaling were performed on previously described CRH-R2 knockout mice (Coste et al., 2000) and on CNS specific urocortin II overexpressing mice (UCNII-COE-Nes), which were generated accordingly to the here described CRH-COE-Nes mice by Dr. J. Rhode from the group of Dr. J. Deussing (MPI of Pychiatry, Munich, Germany).

Open field

Animals were tested under red light in an open field (26 x 26 x 38 cm high) made of white floor and clear plastic walls, and equipped with infrared photocell sensors. Testing lasted for 30 min. Distance travelled and rearings were measured using the Tru Scan Software Vers 1.1 A (Coulbourn Instruments, Allentown, PA, USA) (sampling frequency, 4 Hz).

Light-dark exploration

Animals were tested in a box divided into two equally sized compartments (26 x 13 x 38 cm high). One compartment was made of clear plastic walls, had a white floor, and was illuminated by bright light (700 lux). The other compartment was made of black plastic, not illuminated and covered by a black roof. An opening, 7.5 x 7.5 cm wide, connected the two parts of the box. Two infrared sensor rings (sensor spacing 1.52 cm) allowed for measurement of vertical and horizontal activity (sampling frequency, 4 Hz), and were connected to a computer equipped with the Tru Scan Software Vers 1.1 A (Coulbourn Instruments). The box was surrounded by an additional uniform white plastic box (47 x 47 x 38 cm). The session started by placing the animal in the centre of the dark compartment and lasted for 5 min. From raw data the distance travelled, time spent, moving and resting, and vertical movements of the animal (rearings) were calculated for each compartment. Further, the latency to enter the illuminated compartment for the first time was recorded.

Forced swim test

The FST was carried out on two consecutive days as previously described (Materials and Methods section of Chapter 2.3). For the analysis of the influence of restraint stress experience on FST behavior, animals were subjected to 1 h of restraint stress in a 50 ml conical tube 4 h before exposure to forced swimming according to a previously established protocol for stress-induced activation of CRH-R1 (Radulovic et al., 1999).

3.2 Transgenic CRH overexpression induces antidepressant-like behavior

Tail suspension test

Animals were suspended by the end of their tail with adhesive tape to a steel bar that was 35 cm above the floor. Each session lasted 6 min and was videotaped. The duration of immobility was scored using EVENTLOG software. Mice were considered immobile only when they hung passively without moving the limbs or the head.

Pharmacology

All drugs were freshly prepared in a volume of 10 ml/kg. DMP696 (Bristol-Myers Squibb, Munich, Germany) was suspended in a 0.9 % saline solution containing 5 % dimethyl sulfoxide, 5 % polyethylene glycol 400 and 10 µl of Tween® 80 per 1.5 ml (all chemicals from Sigma-Aldrich, Steinheim, Germany), and injected i.p. 1 h prior to the forced swim test on day 1 and day 2. For the analysis of DMP696 influences on stress induced ACTH levels, mice were decapitated immediately after the FST on day 2.

Para-chlorophenylalanine methyl ester (PCPA) and α-methyl-*para*-tyrosine methyl ester (AMPT) (all drugs from Sigma-Aldrich) were suspended in a 0.9 % saline solution containing 1 % dimethylsulfoxide and administered i.p.. PCPA (250 mg/kg) was administered twice daily (every 12 h) for 3 days with the last dose given 18 h before the FST (Mayorga et al., 2001). AMPT (200 mg/kg) was administered as a single dose 4 h before the FST (Mayorga et al., 2001).

Neurochemical analysis of AMPT- and PCPA-induced monoamine changes

Mice pre-treated with AMPT and PCPA were killed directly after the FST. Brains were freshly dissected on ice and hippocampi removed, weighed and stored at -80°C until analysis. Hippocampal tissue samples were diluted 20 fold w/v with HCl (0.1M) in an ice bath and homogenised by sonication (40 sec, 75% duty cycle, 3.5 micro tip limit; Branson sonifier 250, Sonic Power Company, Danbury, CT, USA). Homogenized tissue was then ultracentrifuged (35,000 r.p.m., 20 min, 4°C; Beckman L-60 Ultracentrifuge, Munich, Germany) and the resulting aqueous layer filtered (0.22µm ×13 mm, PVDF, Millex Filters; Millipore, Bedford, USA). Filtrate was aliquoted in 20 µl samples into separate Eppendorf tubes and stored at -80°C until further analysis.

Determination of serotonin (5-HT), 5-hydroxyindoleacetic acid (5-HIAA), 3,4-dihydrophenylacetic acid (DOPAC), and 4-hydroxy-3-methoxyphenylacetic acid (HVA) was performed by reverse-phase high performance liquid chromatography (HPLC) with electrochemical detection as previously described (Singewald et al., 1997). Hippocampal filtrates (20 µl stock solutions) were diluted and 50 µl was automatically injected by a CMA 200 refrigerated autosampler (CMA Microdialysis AB, Stockholm, Sweden). The mobile phase consisted of 93 % phosphate buffer (0.1 M NaH_2PO_4, 1 mM sodium octanesulphonic acid, 10 mM NaCl, and 0.5 mM Na_2-EDTA) and 7% acetonitrile, and the pH was adjusted to 4.0 with *o*-phosphoric acid (all chemicals: Merck, Darmstadt, Germany). For noradrenaline (NA) and dopamine (DA) tissue quantification, hippocampal filtrates (20 µl stock solutions) were diluted and concentration was

determined by a radioenzymatic assay as previously described (Singewald and Philippu, 1993). This assay involves COMT-catalyzed O-methylation using [³H]S-adenosylmethionine as methyl donor and separation of the resulting [³H]normetanephrine by thin layer chromatography.

Microdialysis

Surgical procedures - Mice were implanted with sterile, re-usable stainless steel guide cannulas (MAB 4.15.G; Microbiotech, Stockholm, Sweden), just entering the dorsal part of the hippocampus. Coordinates with the toothbar set at 0 mm, were: lateral 2.8 mm, posterior 3 mm and ventral 2 mm, with bregma as an overall zero. To connect a liquid swivel system during the microdialysis experiment, a small peg was adhered to the skull. After the surgery, mice were housed individually in special plexiglass cages (25 x 25 x 35 cm) and were allowed to recover for 10 - 14 days.

Microdialysis procedure - A microdialysis probe with a length of 3 mm (MAB 4.15.3.Cu; cuprophane membrane; outer diameter 0.18 mm; Microbiotech) was inserted into the hippocampus under a light and short-lasting isoflurane anesthesia (= day -1). Mice were connected to a dual-channel swivel (Microbiotech) and a counter balancing system (SMCLA counter balanced lever arm; Instech Laboratories, Plymouth Meeting, PA, USA) via a steel wire head block tether (MINF head block tether; Instech), which was connected to the peg on their head. Microdialysis probes were perfused with sterile Ringer solution (Delta Pharma, Pfullingen, Germany) at a flow rate of 0.1 μl/min using a micro-infusion pump. Mice were allowed to adapt to the tether-microdialysis tubing connection for one day (day 0) before the experiment started. At experiment days 1 and 2 the flow rate was adjusted to 2 μl/min 1 h prior to the start of baseline sampling. Fluorethylenepolymer tubing with a dead volume of 1.2 μl/10 cm length (Microbiotech) was used for all connections. Experiments were performed on four animals simultaneously. Microdialysis samples were collected in a small vial, which was placed in a small ice-filled bucket on the top of the microdialysis cage. Samples were used for the determination of hippocampal extracellular levels of monoamines and their metabolites and were stored at -80ºC until measurement. Every 20 min one sample was drawn, which was equally split before storage for later HPLC determination of serotonin/dopamine + metabolites, and for noradrenaline + metabolites from the same sample.

Assessment of home cage behavior - Behavior displayed by the animals during the microdialysis experiments on day 1 and day 2 was scored by visual observation. Every 20 min interval the main behavior performed by an animal during that time period was written down in a protocol. Observed behaviors were categorized as follows: (a) resting behavior (i.e., sleeping sitting or lying); (b) active behavior (i.e., grooming, eating and drinking, exploring).

Experimental protocol - 24 h after insertion of the microdialysis probe 20 min samples were collected from 8 to 12 am on day 1 (mice were kept in a normal light-dark rhythm with lights on at 7 am). After the collection of 6 baseline samples (after 2 h), mice were exposed to 6 min FST at 10 am. Afterwards mice were placed back in their home cages and sampling was continued for another 2 h. The forced swim test took place during the first six minutes (10:00 – 10:06 am) of the collection of sample number 7 (10:00-10:20 am). The same procedure was repeated 24 h later at

day 2 to evaluate monoamine changes after repeated forced swimming. During the experiment behavioral activity was monitored as described above.

Analysis of monoamines and metabolites

Samples were assayed for 5-HT, 5-HIAA, DA, DOPAC, NA and MHPG without prior purification using HPLC with electrochemical detection. The HPLC system consisted of a Sunflow 100 isocratic pump (Sunchrom, Friedrichsdorf, Germany), a Mistral column thermostat (Spark Holland Instruments, Emmen, Netherlands), a Rheodyne injection valve (Rheodyne 7125; Rheodyne, Rhonert Park, CA, USA) and an Antec electrochemical detector (Antec; Leyden, Zoeterwoude, Netherlands). Ten µl of microdialysates were injected into the column using a 100-Wl loop (partial loop filling). 5-HT, 5-HIAA, DA, DOPAC and NA, MHPG were analyzed under different conditions on the same YMC Hydrosphere C18 column, 150 x 3.0 mm ID (YMC Europe GmbH, Schermbeck, Germany). Diluted monoamine and metabolite internal standards (in appropriate concentration ranges) were freshly prepared from stock solutions and used to calculate concentrations in the microdialysis samples. All chromatograms were analyzed using a Gynkotek chromatography data analysis system (Dionex, Idstein, Germany).

Analysis of 5-HT, 5-HIAA, DA and DOPAC - The mobile phase consisted of 20 % methanol, 13.4 mM citric acid, 40 mM Na-acetate, 0.1 mM EDTA and 0.15 mM sodium octyl sulphate (pH 4.95; all chemicals from Sigma). Flow rate was 500 µl/min, the column thermostat was set at 32ºC, and the potential of the electrochemical detector set at 550 mV against an Ag/AgCl reference electrode. The detection limit at a signal-to-noise ratio of 3 was 0.5 fmol per HPLC injection.

Analysis of NA and MHPG - The mobile phase consisted of 6 % methanol, 3.8 mM citric acid, 15 mM Na-acetate, 0.1 mM EDTA and 0.22 mM sodium octyl sulphate (pH 5.03). Flow rate was 400 µl/min, the column thermostat was set at 32ºC, and the potential of the electrochemical detector was set at 650 mV against an Ag/AgCl reference electrode. The detection limits for NA and MHPG at a signal-to-noise ratio of 3 were 2 and 6 fmol per HPLC injection, respectively.

Histology - At the end of the experiment, animals were killed, brains removed and stored at -80ºC. 50 µm thick horizontal brain slices were cut on a cryostat, were stained with cresyl violet and were histologically examined for correct microdialysis probe insertion. Only data from mice, where microdialysis probes had been properly placed in the hippocampus were used for further analyses.

Statistical analysis

Data were analyzed for multiple comparisons using one-, two- or three-way analyses of variance (ANOVA), for repeated measures where appropriate, followed by *post-hoc* Newman-Keuls Multiple Comparison Test. For two-group comparisons unpaired Student's *t*-test was used. Differences were considered statistically significant when *p* < 0.05. Data are presented as mean ± SEM.

3.2.4 Results

Generation of mutant mice conditionally overexpressing CRH in the CNS (CRH-COE-Nes)

We used homologous recombination in embryonic stem cells to target the ubiquitously expressed *ROSA26 (R26)* locus with a single copy of the murine *Crh* cDNA preceded by a *loxP* flanked (floxed) transcriptional "Stop" sequence (Figs. 3.2.1a-c). As previously reported (Soriano, 1999), mice homozygous for the modified *R26* allele (*R26^flopCrh/flopCrh*, <u>fl</u>oxed St<u>op</u>), which is Cre recombinase sensitive, were indistinguishable from wild-type littermates, behaviorally (data not shown), as well as with respect to endogenous CRH mRNA (Figs. 3.2.2e, f) and protein levels (Fig. 3.2.3a). Homozygous *R26^flopCrh/flopCrh* mice were crossed to transgenic *nestin-cre* mice (Tronche et al., 1999) allowing for a CNS-restricted overexpression of CRH in double transgenic animals (CRH-COE-Nes). In the F_2 generation we obtained *R26^{+/+}*, *R26^flopCrh/flopCrh*, *R26^{+/flopCrh}* *nestin-cre* and *R26^flopCrh/flopCrh* *nestin-cre* mice (Fig. 3.2.1d), which we will refer to as CRH-COE^wt-Nes, CRH-COE^con-Nes, CRH-COE^het-Nes and CRH-COE^hom-Nes respectively. On the genomic level, Cre-mediated deletion of the transcriptional terminator sequence was observed only in the CNS but not in peripheral organs of CRH-COE^hom-Nes mice (Fig. 3.2.1e).

Verification of the CNS-restricted overexpression of CRH in CRH-COE-Nes mice

To assess the spatial distribution of exogenous CRH expression in detail, we made use of the introduced *IRES-LacZ* reporter gene which is co-activated upon Cre-mediated excision of the transcriptional terminator sequence (Fig. 3.2.1a). X-Gal staining of intact organs revealed the absence of any specific staining in CRH-COE^con-Nes mice (Fig. 3.2.2a). CRH-COE^het-Nes and CRH-COE^hom-Nes mice exhibited an intense staining in the brain and spinal cord while peripheral organs were devoid of *LacZ*-dependent staining. Increased staining intensities in the intact brain and spinal cord as well as on coronal brain sections of

166
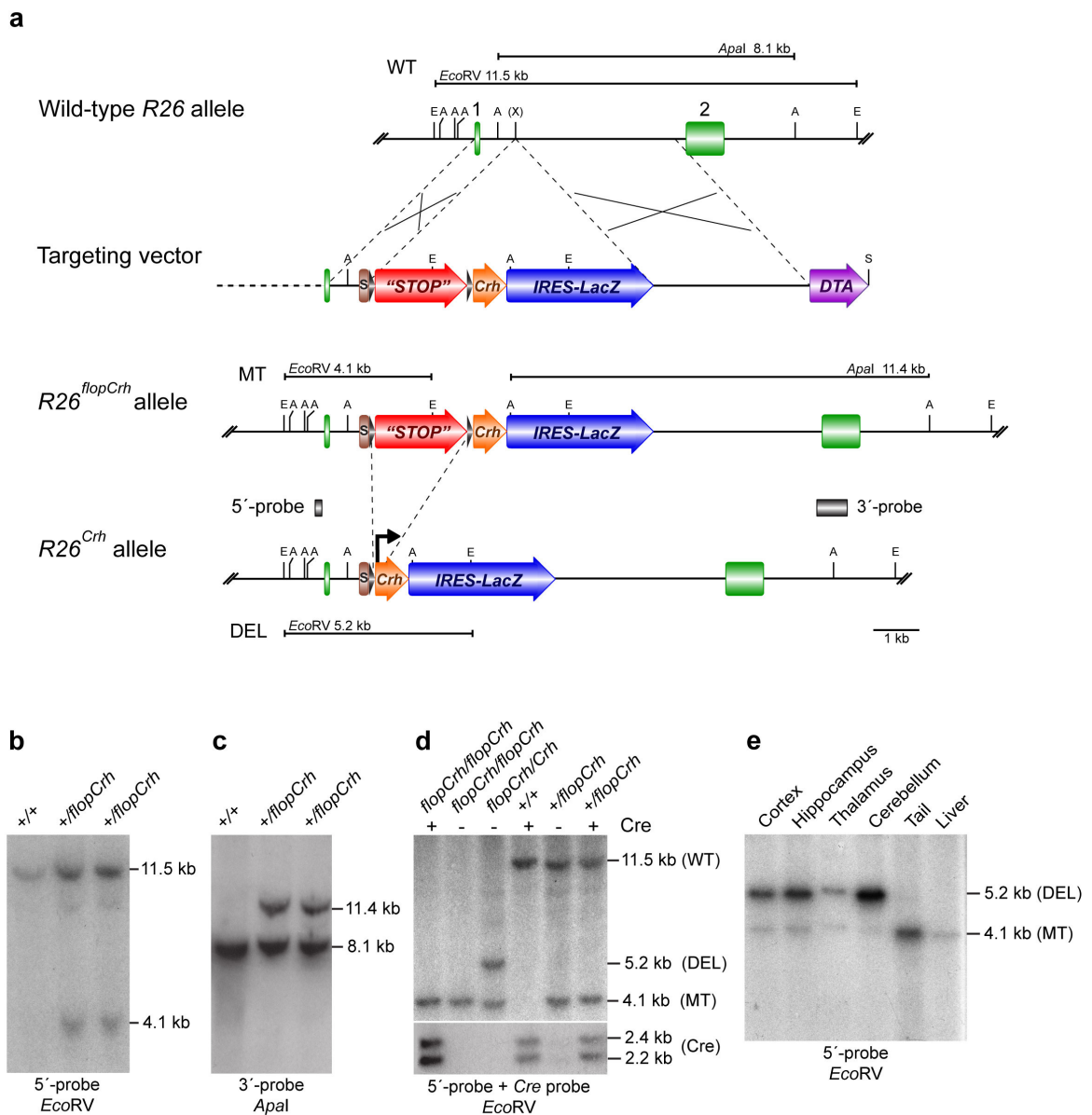
Figure 3.2.1 Generation of CNS-restricted CRH overexpressing mice. (**a**) Strategy for conditional, Cre-mediated expression of CRH from the *R26* locus. Partial restriction maps of wild-type *R26* locus, targeting vector, recombined *R26^flopCrh* allele and activated *R26^Crh* allele (WT: wild-type fragment; MT: mutant fragment following homologous recombination; DEL: deletion fragment resulting from Cre-mediated excision of the "Stop" cassette; A: *Apa*I; E: *Eco*RV; S: *Swa*I; X: *Xba*I; S: splice acceptor; loxP sites are indicated as black arrowheads). (**b**) Southern blot analysis of wild-type and targeted ES cell clones. The *R26* 5'-probe was hybridized to *Eco*RV-digested genomic ES cell DNA. The targeted allele was indicated by the presence of an additional mutant 4.1-kb fragment. (**c**) The *R26* 3'-probe was hybridized to *Apa*I-digested DNA from the same ES cell clones confirming homologous recombination by detection of an additional mutant fragment at 11.4-kb. (**d**) Southern blot analysis of *Eco*RV-digested tail DNA of CRH-COE-Nes mice simultaneously hybridized with the 5'-probe and a Cre-recombinase-specific probe. The hybridizing fragments obtained correspond to the indicated genotypes. (**e**) Southern blot analysis of *Eco*RV-digested genomic DNA from various tissues of a CRH-COE^hom-Nes animal hybridized with the 5'-probe, showing the extent of Cre-mediated deletion of the transcriptional terminator sequence as indicated by the presence of an additional 5.2-kb fragment. This Figure was kindly provided by Dr. A. Lu.
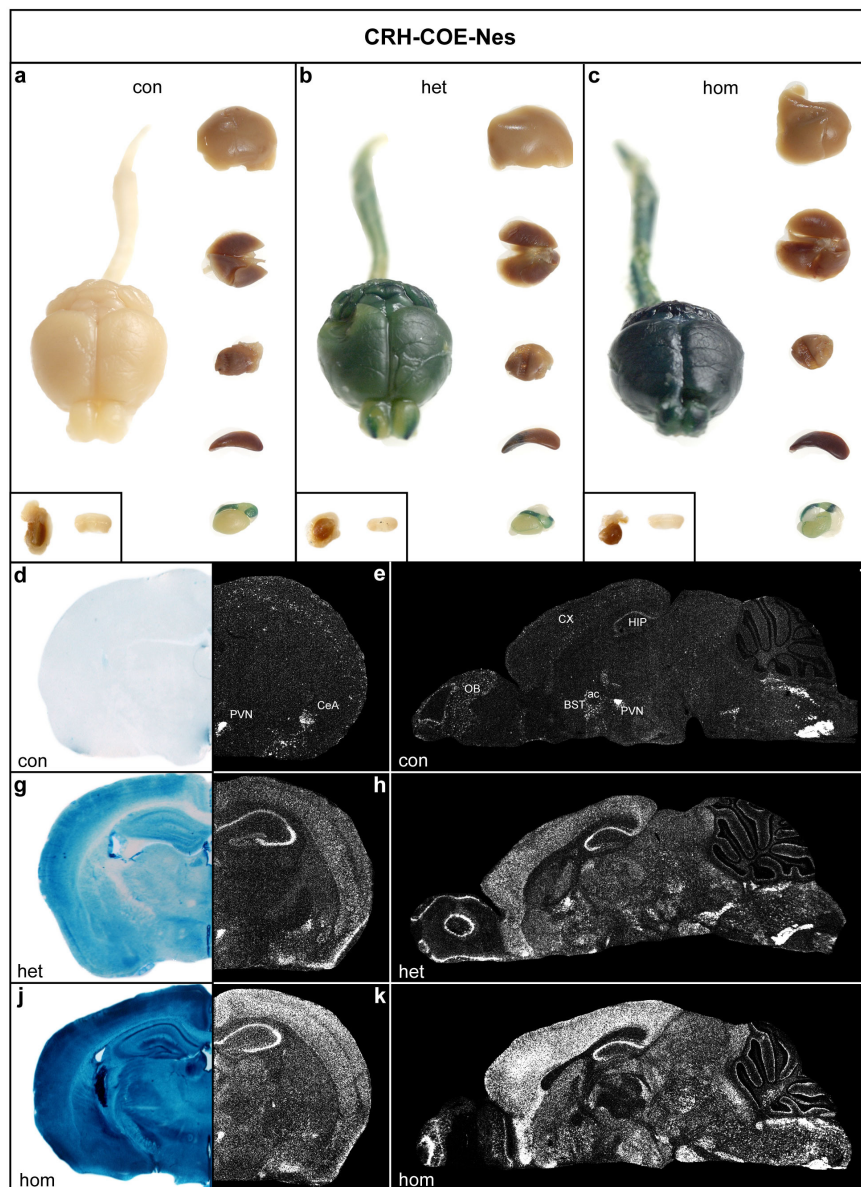
Figure 3.2.2 Verification of the CNS-restricted overexpression of CRH in CRH-COE-Nes mice. Intact organs of (**a**) control, (**b**) heterozygous and (**c**) homozygous CRH-COE-Nes mice were stained overnight with X-Gal. (left: brain with spinal cord; right, from top: liver, lung, heart, spleen, testis with epididymis; inlay: adrenal gland (left) and pituitary (right). Note background staining of the epididymis. Intense blue staining in the brain and spinal cord of CRH-COE^{het}- and CRH-COE^{hom}-Nes mice reflects the brain specific overexpression of the *IRES-LacZ* reporter gene. No staining was observed in peripheral organs of CRH-COE-Nes mice. Determination of *IRES-LacZ* reporter gene expression by X-Gal staining on coronal sections of (**d**) CRH-COE^{con}-, (**g**) CRH-COE^{het}- and (**j**) CRH-COE^{hom}-Nes mice.
Crh overexpression was demonstrated by *in situ* hybridization using a specific radiolabeled riboprobe detecting both, endogenous and exogenous CRH expression. Representative dark field photomicrographs of coronal and sagittal brain sections of CRH-COE-Nes mice are depicted. (**e**,**f**) CRH-COE^{con}-Nes mice display the characteristic, heterogeneous *Crh* expression throughout the entire CNS with strong expression in the paraventricular nucleus (PVN) of the hypothalamus, central nucleus of the amygdala (CeA), bed nucleus of stria terminalis (BST), olfactory bulb (OB) and nuclei of the brainstem. Additionally, CRH expressing neurons are found scattered within the cortex (CX) and hippocampus (HIP). In (**h**,**i**) CRH-COE^{het}- and (**k**,**l**) CRH-COE^{hom}-Nes mice exogenous CRH is expressed throughout the brain corresponding to the pattern of *IRES-LacZ* reporter gene expression. The level of exogenous *Crh* mRNA expression is gene dosage dependent as demonstrated by the stronger *in situ* hybridization signals detected in CRH-COE^{hom}- versus CRH-COE^{het}-Nes animals (ac, anterior commissure). This Figure was kindly provided by Dr. A. Lu.
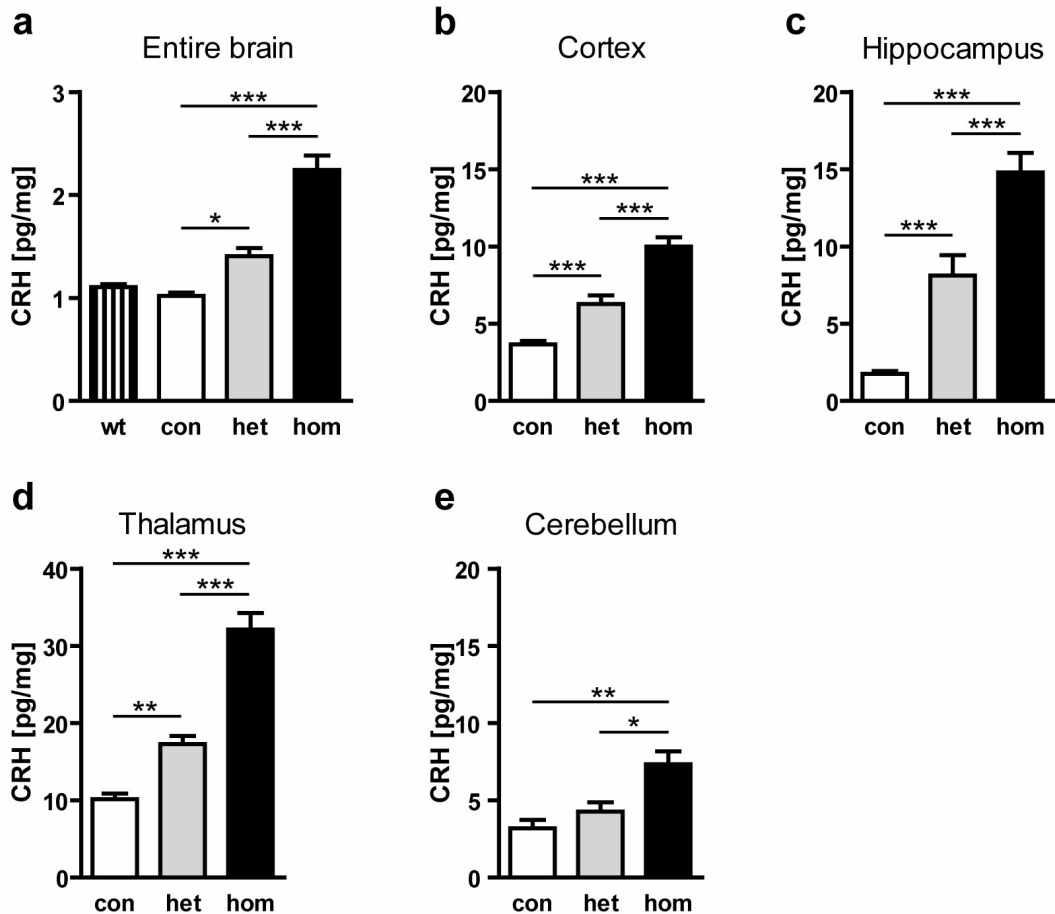
Figure 3.2.3 CRH overexpression from the *R26* locus results in a gene dosage dependent increase of CRH protein content in the brain. CRH protein content in the (**a**) entire brain, (**b**) cortex, (**c**) hippocampus, (**d**) thalamus and (**e**) cerebellum of CRH-COE[het]-Nes (het) and CRH-COE[hom]-Nes (hom) mice in comparison to CRH-COE[con]-Nes (con) mice (n = 5-12 per group). The CRH content in the brain of CRH-COE[con]-Nes mice is indistinguishable from wild-type CRH-COE[wt]-Nes (wt) mice (**a**). CRH content is depicted in pg/mg tissue wet weight. $^*p < 0.05$, $^{**}p < 0.01$, $^{***}p < 0.001$. This Figure was kindly provided by Dr. A. Lu.

CRH-COE[hom]- compared to CRH-COE[het]-Nes animals reflected the assumed gene dosage effect (Figs. 3.2.2b,c,g,j). The conditional overexpression of CRH was verified by *in situ* hybridization using a CRH-specific riboprobe. In CRH-COE[con]-Nes mice, endogenous CRH expression was detected heterogeneously throughout the entire CNS as previously described (Cummings et al., 1983) (Figs. 3.2.2e,f). In CRH-COE[het]- and CRH-COE[hom]-Nes mice, the pattern of CRH induction paralleled the activation of the *IRES-LacZ* reporter gene as demonstrated by X-Gal staining. Expression of exogenous CRH was detected at varying levels throughout the brain and attributed to the CNS-wide expression of *nestin-cre* and to the ubiquitous activity of the *R26* locus. CRH mRNA was detected at highest levels in the olfactory bulb, cortex and hippocampus, again in a

gene dosage-dependent manner (Figs. 3.2.2h,i,k,l). Moreover, we confirmed the increased CRH peptide content in the entire brain and various brain areas of CRH-COE^{het}-Nes and CRH-COE^{hom}-Nes mice using a CRH-specific radioimmunoassay (statistics not shown; Supplementary Figs. 3.2.1a-e). No difference in CRH peptide content was observed between CRH-COE^{wt}- and CRH-COE^{con}-Nes mice (Fig. 3.2.3a). These results confirmed the $R26^{flopCrh}$ allele as a tightly regulated gain-of-function system, which allows overexpression of CRH at different dosages in a spatially and temporally controlled fashion.

The HPA axis of male but not female CRH-COE-Nes mice is hypersensitive to stress

Basal plasma ACTH and corticosterone levels did not differ significantly between male CRH-COE^{con}-, CRH-COE^{het}- and CRH-COE^{hom}-Nes mice over the circadian cycle, neither at the diurnal through, nor at the diurnal peak (Figs. 3.2.4a,c). To examine the response of the HPA axis to stress, animals were subjected to 10 min of restraint stress in the morning (am) and killed either directly or 30 min after the end of the stressor (Figs. 3.2.4b,d). Restraint stress resulted in significantly elevated ACTH [$F_{2,32}$ = 7.5, p < 0.01; one-way ANOVA (*Genotype*)] and corticosterone ($F_{2,32}$ = 4.10, p < 0.05) levels in CRH-COE^{het}- and CRH-COE^{hom}-Nes mice compared to CRH-COE^{con}-Nes littermates. In CRH-COE^{hom}-Nes mice, corticosterone levels remained significantly elevated 30 min after the stress compared to CRH-COE^{con}-Nes and CRH-COE^{het}-Nes mice ($F_{2,27}$ = 4.10, p < 0.05).

Similar to males, female CRH-COE^{hom}-Nes animals showed no difference in basal ACTH and corticosterone levels compared to CRH-COE^{con}-Nes mice (Figs. 3.2.4e,f). However, in contrast to males, female CRH-COE^{hom}-Nes mice did not show elevated ACTH and corticosterone secretion in response to restraint stress in comparison with CRH-COE^{con}-Nes mice (Figs. 3.2.4e,f).
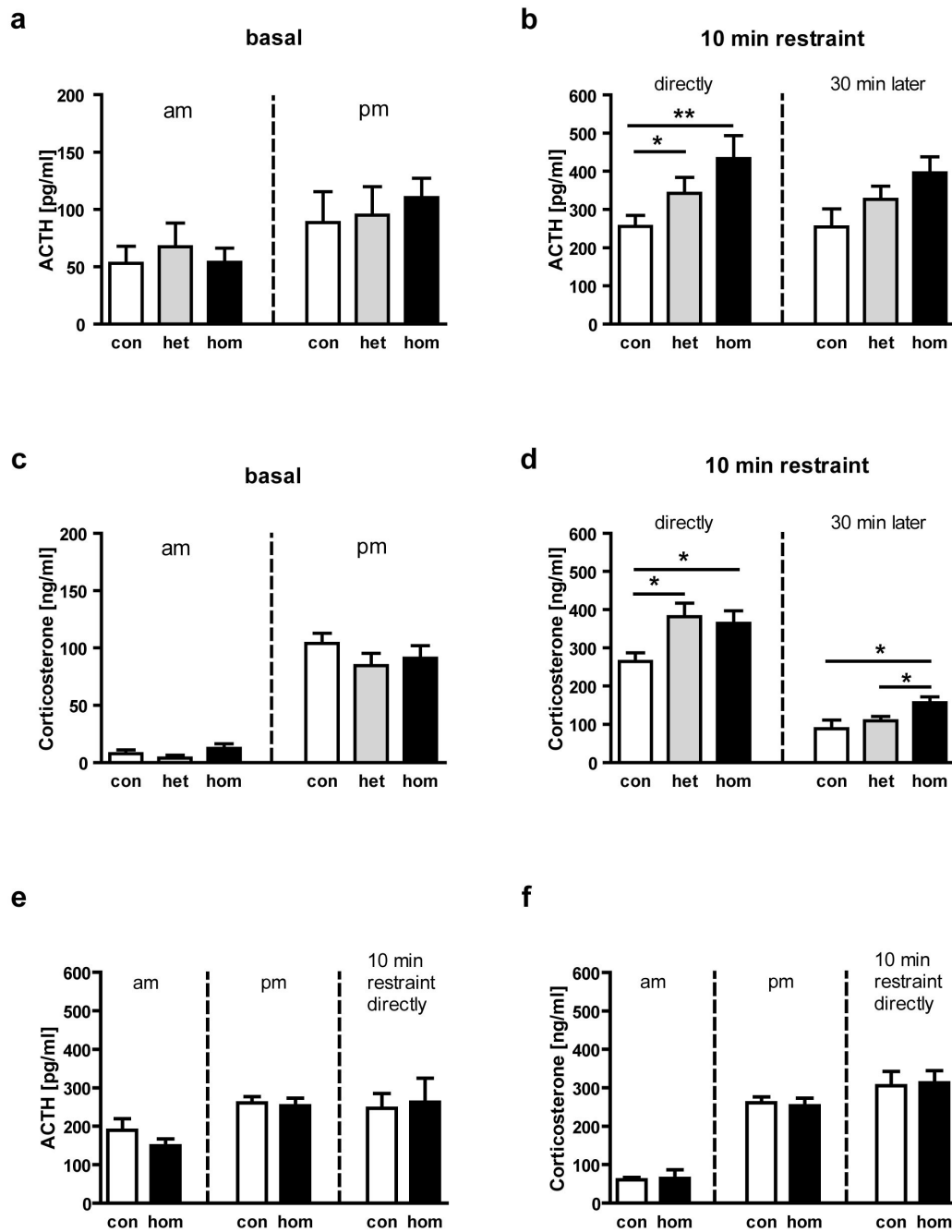
Figure 3.2.4 Stress induced HPA axis hyperactivity in CRH-COE-Nes mice is sex dependent.
(**a**) Male CRH-COE[con]- (con), CRH-COE[het]- (het) and CRH-COE[hom]-Nes (hom) mice showed no differences in basal plasma ACTH levels in the morning (am) or evening (pm) (n = 4-8 per group). (**b**) Following 10 min of restraint stress in the morning (am), ACTH levels were significantly elevated in male het and hom mice compared to con littermates directly after the stressor. 30 min after the stressor ACTH levels were still elevated, without reaching statistical significance (n = 9-14 per group). (**c**) Male con, het and hom mice showed no differences in basal plasma corticosterone levels in the morning (am) or evening (pm) (n = 10-13 per group). (**d**) Restraint stress resulted in significantly elevated corticosterone levels in male het and hom mice compared to con littermates directly after the stressor. In hom mice, corticosterone levels remained significantly elevated 30 min after the stress compared to con and het mice (n = 6-15 per group). (**e**) Female con and hom mice showed no differences in basal plasma ACTH levels in the morning (am), evening (pm), or directly after 10 min restraint stress in the morning (n = 6-10 per group). (**f**) Female con and hom mice showed no differences in basal plasma corticosterone levels in the morning (am), evening (pm), or directly after 10-min restraint stress in the morning (n = 6-15 per group). $^{*}p < 0.05$, $^{**}p < 0.01$. This Figure was kindly provided by Dr. A. Lu.

171

CNS-restricted overexpression of CRH leads to increased exploratory behavior

To assess the influence of CRH overexpression on emotionality, CRH-COE-Nes mice were tested in the open field and light-dark box. During a 30 min habituation period to an open field, CRH-COE^{hom}-Nes (hom) mice showed no difference in total distance moved compared to CRH-COE^{con}-Nes (con) littermates and habituated equally well [*Genotype*: $F_{1,18} = 0.8$, $p = 0.38$; *3 min Interval*: $F_{9,162} = 26.2$, $p < 0.001$; *3 min Interval* x *Genotype*: $F_{9,162} = 0.4$, $p = 0.91$; two-way ANOVA (*3 min Interval, Genotype*) for repeated measures (*3 min Interval*); Fig. 3.2.5a]. However, CRH-COE^{hom}-Nes mice showed increased vertical movements (rearings) (*Genotype*: $F_{1,18} = 4.6$, $p < 0.05$) compared to CRH-COE^{con}-Nes mice indicating elevated explorative behavior.

In the light-dark box, CRH-COE^{hom}-Nes mice and CRH-COE^{con}-Nes littermates did not differ in total distance moved or percentage of time spent in the lit compartment (Fig. 3.2.5b). CRH-COE^{hom}-Nes mice showed a shorter latency to
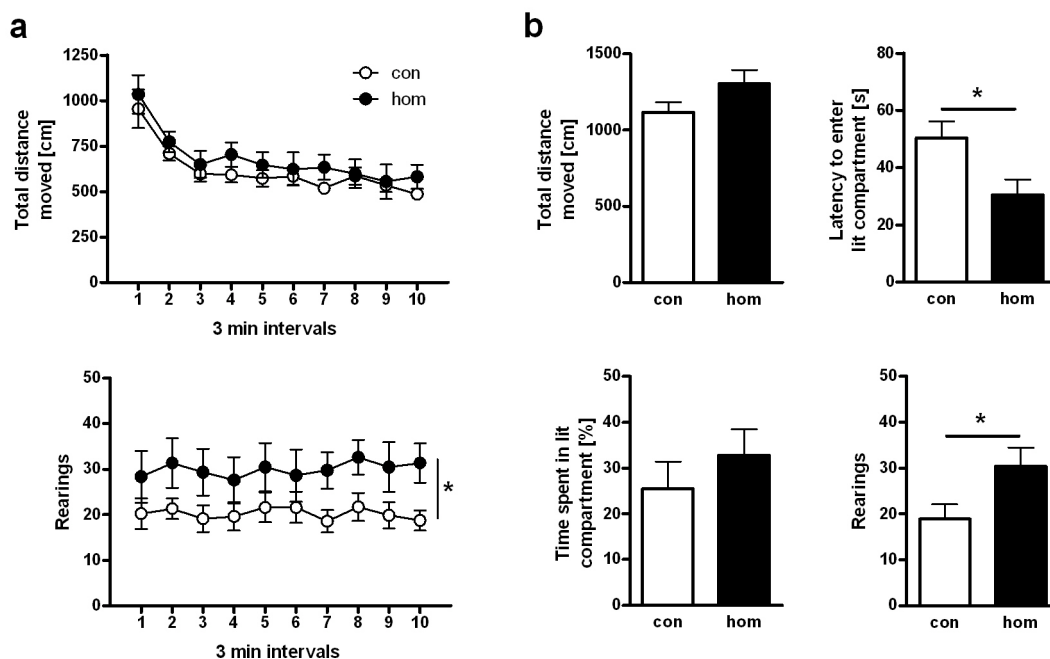
Figure 3.2.5 CRH overexpression leads to increased explorative behavior. (**a**) Total distance moved and number of vertical movements (rearings) of CRH-COE^{hom}-Nes (hom) and CRH-COE^{con}-Nes (con) mice during a 30 min habituation period to an open field (n = 8-12 per group). (**b**) Total distance moved, latency to enter the lit compartment, percentage of time spent in the lit compartment and number of rearings of hom and con mice during 5 min exposure to the light-dark box (n = 8-12 per group). *$p < 0.05$.

enter the lit compartment for the first time (t_{18} = 2.4, p < 0.05; unpaired t-test), and an increased number of vertical movements (rearings) (t_{18} = 2.2, p < 0.05), suggesting increased explorative behavior.

CNS-restricted overexpression of CRH results in decreased immobility in the forced swim and the tail suspension tests

To examine stress coping behaviors, CRH-COE-Nes mice were exposed to the forced swim test (FST). In males, CRH overexpression resulted in a dose-dependent increase in struggling both on day 1 [$F_{2,30}$ = 3.4, p < 0.05; one-way ANOVA (*Genotype*)] and on day 2 ($F_{2,30}$ = 4.3, p < 0.05) with CRH-COE^{hom}-Nes mice struggling generally more than CRH-COE^{con}-Nes or CRH-COE^{het}-Nes littermates (Fig. 3.2.6a). Furthermore, both CRH-COE^{hom}-Nes and CRH-COE^{het}-Nes mice floated significantly less than CRH-COE^{con}-Nes littermates both on day 1 ($F_{2,30}$ = 20.0, p < 0.001) and on day 2 ($F_{2,30}$ = 15.0, p < 0.001; Fig. 3.2.6c). Female CRH-COE^{hom}-Nes mice showed essentially the same phenotype in the FST as males: they floated significantly less than their CRH-COE^{con}-Nes littermates both at day 1 (t_{21} = 2.7, p < 0.05; unpaired t-test) and at day 2 (t_{21} = 3.4, p < 0.01; Fig. 3.2.7a).

Exposure to cold water (25ºC) in the FST leads to fast body cooling in mice (Arai et al., 2000). In order to exclude that the phenotype of CRH-COE^{het}- and CRH-COE^{hom}-Nes mice in the FST did not solely derive from a faster reduction of body temperature compared to CRH-COE^{con}-Nes littermates, we repeated the FST at 32ºC water temperature. Also at 32°C, CRH-COE^{hom}-Nes mice floated significantly less than their CRH-COE^{con}-Nes littermates both at day 1 (t_{18} = 2.4, p < 0.05) and at day 2 (t_{18} = 2.2, p < 0.05; Fig. 3.2.7b).

To further corroborate the finding that CRH promotes increased active stress coping (i.e., a reduction of immobility), we subjected male animals to the tail suspension test (TST) (Steru et al., 1985). Again, CRH-COE^{hom}-Nes mice were significantly less immobile than their CRH-COE^{con}-Nes and CRH-COE^{het}-Nes littermates ($F_{2,83}$ = 8.9, p < 0.001), while in this test no difference was observed between CRH-COE^{het}-Nes and CRH-COE^{con}-Nes animals (Fig. 3.2.6b).
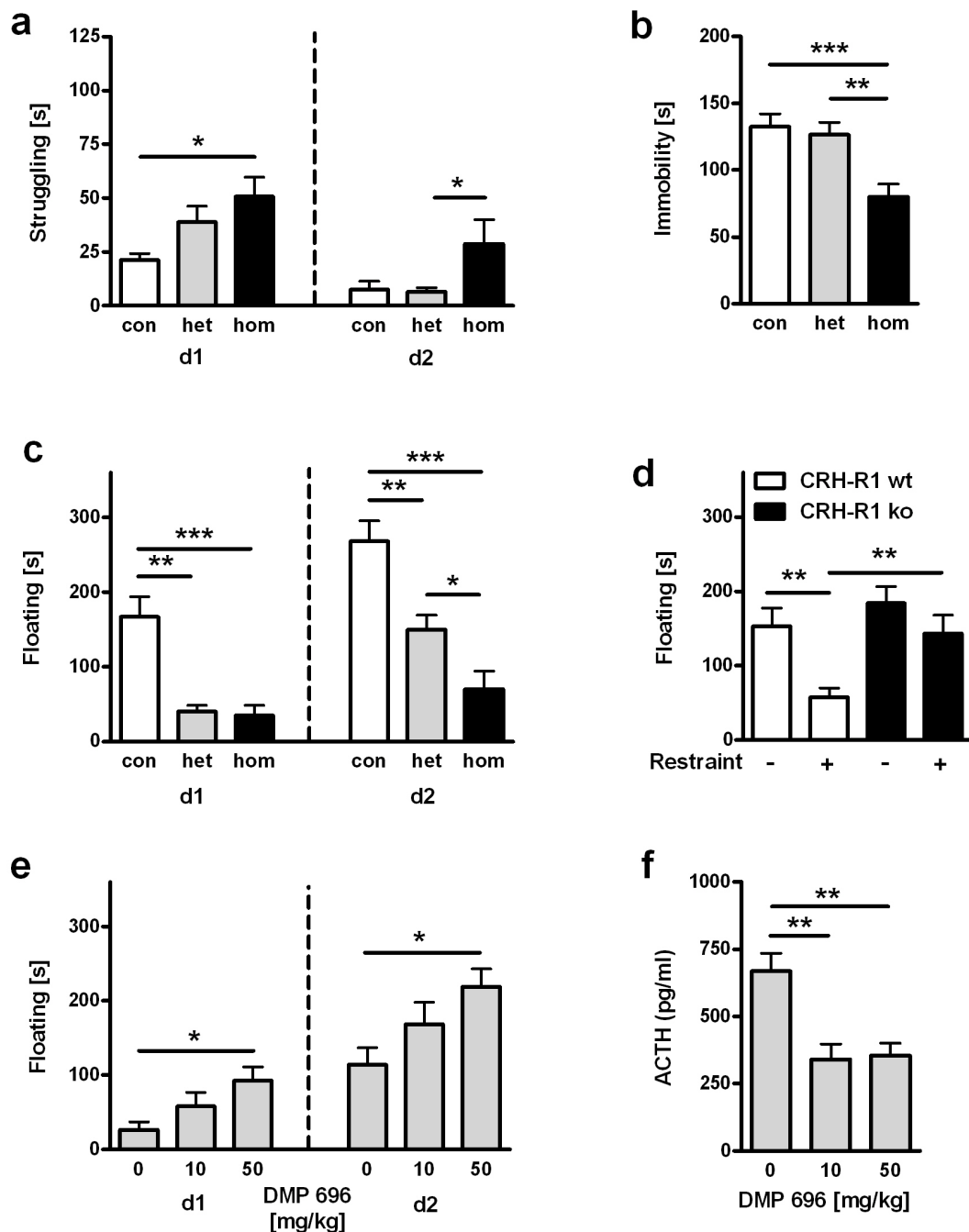
Figure 3.2.6 CRH overexpression leads to increased active stress coping behavior in antidepressant screening paradigms. Total struggling (**a**) and floating time (**c**) of male CRH-COE^{con}- (con), CRH-COE^{het}- (het) and CRH-COE^{hom}-Nes (hom) mice during 6 min exposure to the forced swim test (FST) on day 1 (d1) and on day 2 (d2) (n = 9-15). (**b**) Total immobility time of con, het and hom mice during 6 min exposure to the tail suspension test. Data were collapsed from two independent experiments, which revealed essentially the same results, resulting in n = 27-30 mice per genotype. (**d**) CRH-R1 wild-type (wt) and CRH-R1 knockout (ko) mice were restrained for 1 h and were subsequently exposed to the forced swim test 3 h later (4 h after restraint onset). Total floating time during 6 min FST are depicted (n = 13-16 per group). (**e**) Het mice were treated with the CRH-R1 antagonist DMP696 (applied at 10 and 50 mg/kg i.p. 1h prior to testing on day 1 and on day 2) and were exposed to a 6 min FST on day 1 and day 2. Total floating time is depicted (n = 12-13 per group). (**f**) DMP696-treated het mice from Fig. **e** were killed after the FST on day 2 and plasma ACTH levels were determined (n = 5-6 per group). $^*p < 0.05$, $^{**}p < 0.01$, $^{***}p < 0.001$.

174

The effects of CRH overexpression on FST behavior can be reversed by the selective CRH-R1 antagonist DMP696

To ascertain that the behavioral as well as the neuroendocrine consequences of CRH overexpression relate to acute effects of CRH rather than to long-term changes in brain physiology caused by the life-long overexpression of CRH, we treated male CRH-COE^{het}-Nes mice with the selective CRH-R1 antagonist DMP696 (He et al., 2000). Antagonist treatment dose-dependently reversed the FST phenotype by increasing the floating time both on day 1 [$F_{2,35}$ = 4.4, p < 0.05; one-way ANOVA (*Drug*); Fig. 3.2.6e] and on day 2 ($F_{2,35}$ = 4.4, p < 0.05). Furthermore, DMP696 attenuated the swim stress-induced hyperactivation of the HPA axis ($F_{2,14}$ = 10.6, p < 0.01; Fig. 3.2.6f). These results demonstrate that overexpressed CRH mediates its behavioral and neuroendocrine effects acutely via CRH-R1.

Conditional CRH overexpression mimics the behavioral consequences of stress-induced activation of the endogenous CRH system

To assess to what extent overexpression of exogenous CRH mimics the behavioral consequences of stress-regulated activation of endogenous CRH, we analyzed FST behavior of CRH-R1 knockout mice (Timpl et al., 1998) and wild-type littermates without or with preceding 1-h restraint stress (Fig. 3.2.6d). In accordance with our previous findings (Liebsch et al., 1995; Sillaber et al., 2002), ablation of CRH-R1 failed to affect floating behavior in naive animals, thus arguing against a general involvement of endogenous CRH in FST behavior under baseline conditions. However, preceding restraint stress resulted in a decrease in floating in CRH-R1 wild-type mice compared to non-stressed CRH-R1 wild-type controls (t_{27} = 3.7, p < 0.01; unpaired *t*-test) that was similar to the behavior of CRH-COE^{het}-Nes and CRH-COE^{hom}-Nes mice (compare Fig. 3.2.6c). The floating response was also significantly less pronounced than that of restraint stressed CRH-R1 knockout mice (t_{29} = 3.1, p < 0.01), which remained unaffected by the stressor (t_{27} = 1.2, p = 0.24). These results imply that the CRH system must be activated by prior stressor exposure before endogenous CRH may modulate behavior in the FST via CRH-R1.

CRH-R2 activation does not influence forced swim behavior

To elucidate the potential role of the CRH-R2 system for forced swim behavior in mice, we exposed CRH-R2 knockout and wild-type mice to the FST. However, no genotype difference in floating behavior could be detected, neither on day 1 (t_{17} = 0.3, p = 0.77; unpaired t-test) nor on day 2 (t_{17} = 0.6, p = 0.55; Fig. 3.2.7c). Additionally, we also tested CNS-specific urocortin II overexpressing UCNII-COE-Nes mice in the FST. Also in these mice no genotype difference in floating behavior between UCNII-COE^{hom}-Nes and UCNII-COE^{con}-Nes mice could be detected, neither on day 1 (t_{31} = 1.3, p = 0.2) nor on day 2 (t_{31} = 1.7, p = 0.1; Fig. 3.2.7d).
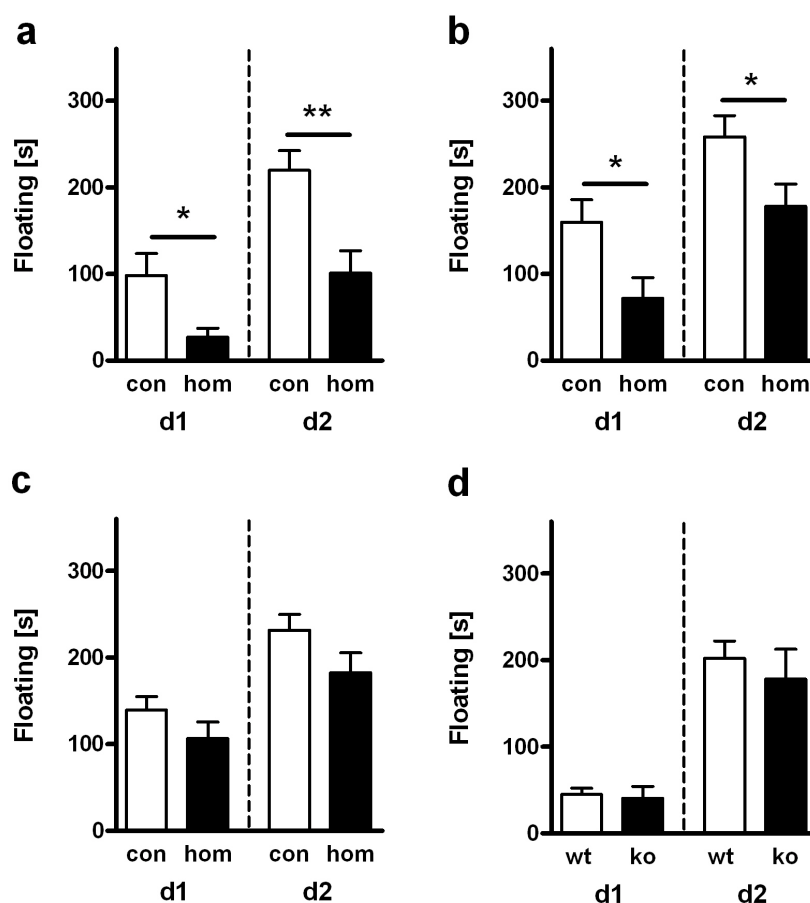
Figure 3.2.7 Reduced floating in the FST is not mediated via the CRH-R2 system. (**a**) Total floating time of female CRH-COE^{con}- (con) and CRH-COE^{hom}-Nes (hom) mice during 6 min exposure to the forced swim test on day 1 (d1) and on day 2 (d2) (n = 11-12 per genotype). (**b**) Total floating time of male CRH-COE^{con}- (con) and CRH-COE^{hom}-Nes (hom) mice during the FST on day 1 and on day 2 at 32ºC water temperature (n = 8-12 per genotype). (**c**) Total floating time of male UCNII-COE^{con}- (con) and UCNII-COE^{hom}-Nes (hom) mice during the FST on day 1 and on day 2 (n = 15-18 per genotype). (**d**) Total floating time of CRH-R2 wild-type (wt) and CRH-R2 knockout (ko) mice during the FST on day 1 and on day 2 (n = 9-10 per genotype). $^*p < 0.05$.

Forebrain-restricted overexpression of CRH in principal neurons or GABAergic interneurons does not affect FST stress coping behavior

In order to specify the brain regions and neurochemical substrates involved in the immobility reducing effect of exogenous CRH, we exploited the properties of the conditional $R26^{flopCrh}$ allele. Breeding CRH-COE^{con} mice to *camk2a-cre* (Minichiello et al., 1999) and *dlx-cre* (Monory et al., 2006) mice restricted the CRH overexpression to principal neurons, respectively GABAergic interneurons, of the anterior forebrain including limbic brain structures. Analogous to CRH-COE-Nes
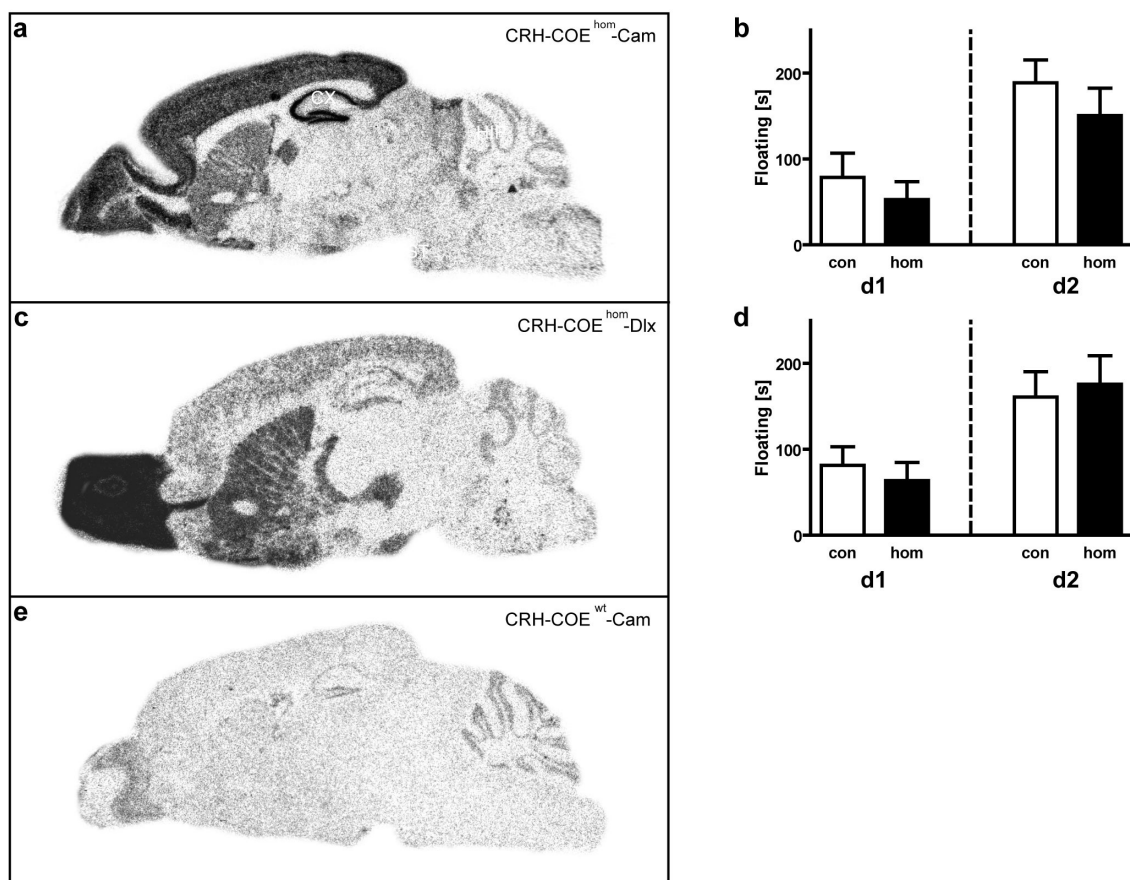
Figure 3.2.8 Forebrain restricted overexpression of CRH does not affect antidepressant-like behavior in the forced swim test. In situ hybridization using a LacZ-specific riboprobe, which detects the CRH-LacZ fusion transcript, confirmed exogenous CRH expression in the forebrain of CRH-COE^{hom}-Cam and CRH-COE^{hom}-Dlx mice. (**a**) Sagittal section of a CRH-COE^{hom}-Cam mouse brain shows strong overexpression of CRH in the olfactory bulb, all cortical layers, hippocampus and striatum. (**b**) Total floating time of CRH-COE^{con}-Cam (con) and CRH-COE^{hom}-Cam (hom) mice in a 6 min forced swim test on day 1 (d1) and on day 2 (d2) (n = 10-13 per genotype). (**c**) Sagittal section of a CRH-COE^{hom}-Dlx mouse brain shows strong overexpression of CRH in the olfactory bulb, striatum, reticular nucleus, cortical layers and hippocampus. (**d**) Total floating time CRH-COE^{con}-Dlx (con) and CRH-COE^{hom}-Dlx (hom) mice in a 6 min forced swim test on day1 (d1) and day 2 (d2) (n = 11 per genotype). (**e**) Sagittal section of a CRH-COE^{wt}-Cam mouse brain demonstrating background in situ hybridization signals of the LacZ-specific riboprobe. Sections of CRH-COE^{wt}-Dlx mice exhibited identical background hybridization signals (data not shown). ISH pictures a,c,e were kindly provided by Dr. A. Lu.

mice we obtained in the F_2 generation desired control (CRH-COE^{con}-Cam/-Dlx), heterozygous (CRH-COE^{het}-Cam/-Dlx) and homozygous (CRH-COE^{hom}-Cam/-Dlx) CRH-COE-Cam/-Dlx mice, respectively. In situ hybridization confirmed the forebrain restricted expression of exogenous CRH in both overexpressing mouse lines (Figs. 3.2.8a,c,e). The function of the HPA axis of homozygous CRH-COE-Cam/-Dlx mice was not significantly altered compared to control mice neither under basal nor under stress conditions (data not shown).

To examine whether forebrain restricted expression of CRH is sufficient to recapitulate the immobility reducing effect of exogenous CRH expressed throughout the CNS in CRH-COE^{hom}-Nes mice, male CRH-COE-Cam and CRH-COE-Dlx mice were exposed to the FST. Forebrain restricted CRH overexpression failed to significantly affect floating or struggling behavior (data not shown) in homozygous CRH-COE^{hom}-Cam (Figs. 3.2.8b) or CRH-COE^{hom}-Dlx (Fig. 3.2.8d) mice compared to control littermates, both at day 1 and at day 2 (statistics not shown). These results clearly exclude principal neurons as well as GABAergic interneurons and projection neurons within limbic forebrain structures such as BNST, amygdala, hippocampus or prefrontal cortex as being responsible for the altered stress coping behavior observed in CRH-COE-Nes mice in the FST and TST.

Active stress coping behavior of CRH overexpressing mice depends on catecholaminergic transmission

CRH-COE-Cam as well as CRH-COE-Dlx mice suggest an involvement of more caudal brain nuclei within the mid/hind brain of CRH-COE^{hom}-Nes mice including monoaminergic cell populations overexpressing CRH, which promote reduced immobility in the FST and TST. In an attempt to understand the neurochemical mechanisms underlying the behavior of CRH-COE^{hom}-Nes mice in the FST, animals were pre-treated either with the tryptophan hydroxylase inhibitor PCPA or with the tyrosine hydroxylase inhibitor AMPT before testing in the FST. PCPA pre-treatment reduced hippocampal serotonin levels by 85 % in CRH-COE^{con}-Nes mice and by 71 % in CRH-COE^{hom}-Nes mice (Table 3.2.1). Catecholamine levels were not affected. Blockade of tryptophan hydroxylase failed to significantly affect floating behavior of CRH-COE^{con}-Nes (t_{17} = 1.8, p = 0.09;

unpaired *t*-test) and CRH-COE^{hom}-Nes mice ($t_{15} = 1.1$, $p = 0.3$) in the FST (Fig. 3.2.9a). In accordance to our previous findings in naïve animals (compare Fig. 3.2.6c), vehicle treated CRH-COE^{hom}-Nes mice floated less than vehicle treated CRH-COE^{con}-Nes littermates ($t_{17} = 3.7$, $p < 0.01$).

Table 3.2.1 Monoamine and metabolite concentrations in hippocampal tissue of vehicle and PCPA pre-treated male CRH-COE-Nes animals.

	con				hom			
	n	Veh	n	PCPA	n	Veh	n	PCPA
NA	9	0.76 ± 0.04	9	0.81 ± 0.11	9	0.80 ± 0.15	8	0.83 ± 0.09
DA	10	0.23 ± 0.03	9	0.27 ± 0.03	9	0.25 ± 0.03	8	0.23 ± 0.03
DOPAC	8	7.52 ± 0.28	9	7.20 ± 0.33	8	7.68 ± 0.39	7	7.28 ± 0.44
HVA	10	5.69 ± 0.78	8	4.00 ± 0.48	9	6.56 ± 0.72	7	6.74 ± 0.93
5-HT [a]	10	145.0 ± 21.67	8	46.9 ± 4.62	9	124.6 ± 14.42	7	35.6 ± 4.15
5-HIAA [a]	10	39.3 ± 5.36	8	2.64 ± 0.34	9	39.3 ± 5.49	7	3.55 ± 0.83

Mean ± SEM [pmol/mg tissue]. Two-way ANOVA results (*Genotype, Treatment*): [a]*Treatment*: $p < 0.001$. (NA) noradrenaline, (DA) dopamine, (DOPAC) 3,4-dihydroxyphenylacetic acid, (HVA) homovanillic acid, (5-HT) serotonin, (5-HIAA) 5-hydroxyindoleacetic acid, (Veh) vehicle, (PCPA) *para*-chlorophenylalanine methyl ester. Data for this Table were kindly provided by N. Whittle.

AMPT pre-treatment reduced hippocampal noradrenaline levels by 35 % in CRH-COE^{con}-Nes mice and by 43 % in CRH-COE^{hom}-Nes mice (Table 3.2.2). Dopamine levels were reduced by 38 % in CRH-COE^{con}-Nes mice and by 47 % in CRH-COE^{hom}-Nes mice. Serotonin levels were not affected. Blockade of tyrosine hydroxylase failed to affect floating behavior of CRH-COE^{con}-Nes mice ($t_{12} = 0.5$, $p = 0.64$), but induced a significant increase of floating in CRH-COE^{hom}-Nes mice ($t_{13} = 2.5$, $p < 0.05$; Fig. 3.2.9b) suggesting that decreased floating in CRH-COE^{hom}-Nes mice is at least partly mediated by increased catecholaminergic neurotransmission in these animals. Similar as above, vehicle treated CRH-COE^{hom}-Nes mice floated less than vehicle treated CRH-COE^{con}-Nes littermates ($t_{13} = 4.7$, $p < 0.001$).

Table 3.2.2 Monoamine and metabolite concentrations in hippocampal tissue of vehicle and AMPT pre-treated male CRH-COE-Nes animals.

		con					hom		
	n	Veh	n	AMPT	n	Veh	n	AMPT
NA [a]	7	0.72 ± 0.11	6	0.47 ± 0.06	8	0.84 ± 0.11	8	0.48 ± 0.08
DA [a]	7	0.16 ± 0.02	6	0.10 ± 0.01	8	0.17 ± 0.03	8	0.09 ± 0.02
DOPAC [a]	7	2.42 ± 0.48	5	0.84 ± 0.11	8	2.35 ± 0.44	6	0.91 ± 0.16
HVA [a]	7	5.61 ± 0.76	6	2.51 ± 0.76	8	5.85 ± 0.83	7	2.19 ± 0.48
5-HT	7	187.7 ± 33.24	7	170.0 ± 39.24	8	146.3 ± 30.42	8	177.1 ± 31.66
5-HIAA	7	68.39 ± 11.25	7	61.33 ± 12.05	8	56.44 ± 10.16	8	63.33 ± 8.90

Mean (SEM [pmol/mg tissue]. Two-way ANOVA results (*Genotype, Treatment*): [a]*Treatment*: $p < 0.01$. (NA) noradrenaline, (DA) dopamine, (DOPAC) 3,4-dihydroxyphenylacetic acid, (HVA) homovanillic acid, (5-HT) serotonin, (5-HIAA) 5-hydroxyindoleacetic acid, (Veh) vehicle, (AMPT) α-mehtyl-para-tyrosinge methyl ester. Data for this Table were kindly provided by N. Whittle.

CRH overexpression enhances FST-mediated activation of the locus coeruleus

To determine to which extent CRH overexpression activates catecholaminergic neurons, we analyzed by in situ hybridization the transcript levels of immediate early genes (IEGs) c-fos and zif268 with focus on the locus coeruleus (LC), nucleus of the solitary tract (NST), ventral tegmental area (VTA), substantia nigra (SN) and dorsal raphe nucleus (DRN). As previously demonstrated in the rat, expression of c-fos and zif268 in these nuclei was undetectable under basal conditions (data not shown) (Cullinan et al., 1995). However, 30 min post forced swim stress, a marked increase of c-fos and zif268 expression was detected in the LC (Figs. 3.2.9c,e) but not in the VTA and SN or DRN (data not shown). Quantification of the signals revealed in CRH-COE[hom]-Nes mice a statistically significant stronger increase of c-fos (1.35-fold; $t_6 = 4.24$, $p < 0.01$) and zif268 (1.55-fold; $t_6 = 6.15$, $p < 0.001$) transcript levels compared to CRH-COE[con]-Nes mice (Figs. 3.2.9d,f) suggesting an enhanced stress-dependent activation of the LC due to CRH overexpression.
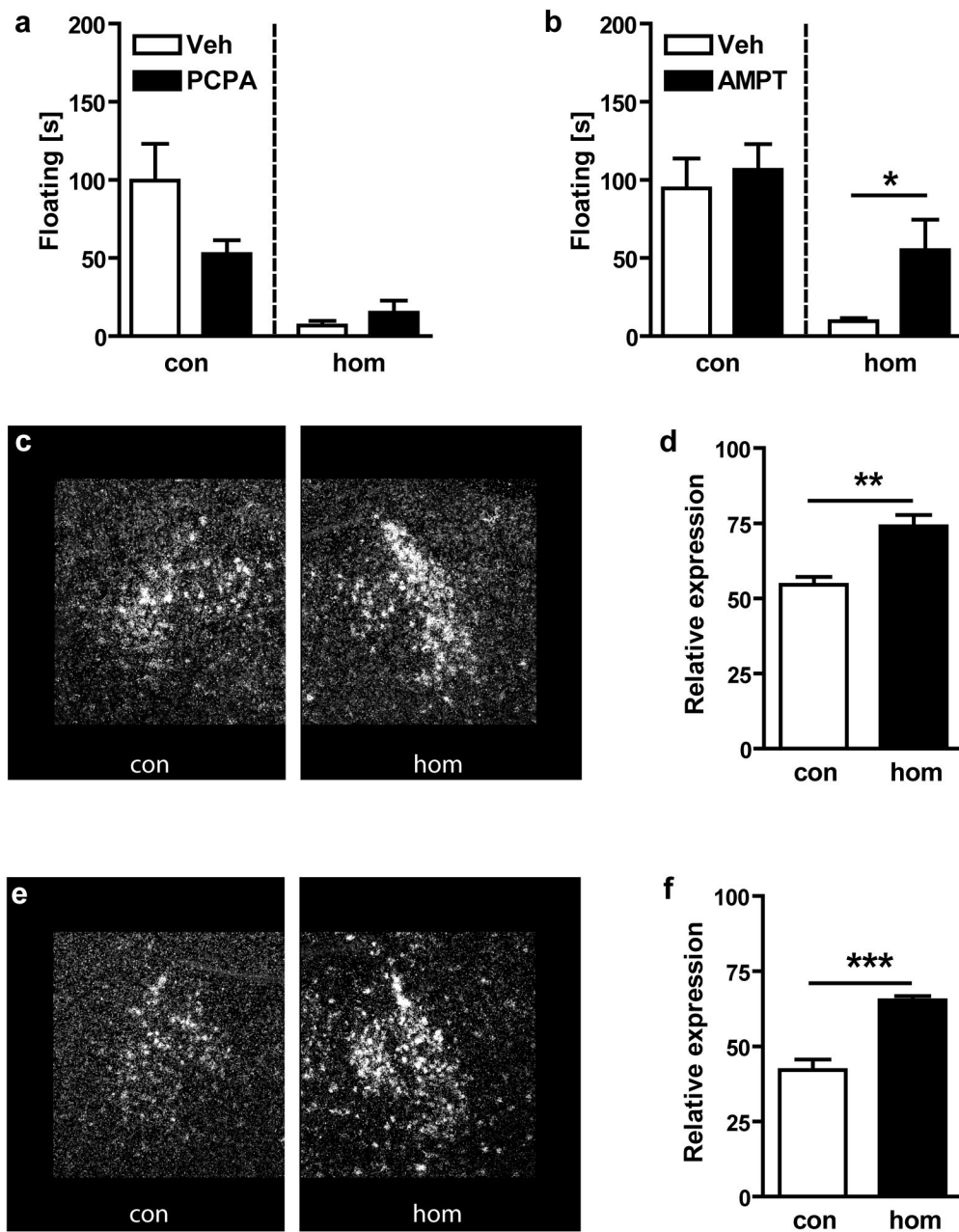
Figure 3.2.9 Antidepressant-like behavior of CRH-COE[hom]-Nes mice is partly mediated by increased catecholaminergic neurotransmission, which originates from CRH-mediated hyperactivation of the locus coeruleus. (**a**) Total floating time of PCPA pre-treated CRH-COE[con]-(con) or CRH-COE[hom]-Nes (hom) mice during a 6 min forced swim test (n = 8-10 per group). (**b**) Total floating time of AMPT pre-treated con or hom mice during a 6 min forced swim test (n = 7-8 per group). (**c,d**) Forced swim stress induced expression of c-fos mRNA in the locus coeruleus of con and hom mice (n = 5 per group). (**e,f**) Forced swim stress induced expression of zif268 mRNA in the locus coeruleus of con and hom mice (n = 5 per group). Representative dark field photomicrographs of in situ hybridizations of coronal brain sections are depicted in (**c,e**) and the corresponding relative quantification in (**d,f**). $^{*}p < 0.05$, $^{**}p < 0.01$, $^{***}p < 0.001$. Sub-Figures c-f were kindly provided by Dr. A. Lu.

CRH overexpression does not alter FST-induced monoaminergic neurotransmission in the hippocampus

Via *in vivo* microdialysis we investigated whether CNS-restricted CRH overexpression leads to altered hippocampal monoaminergic neurotransmission. Mice were repeatedly subjected to 6 min forced swimming on day 1 and on day 2. Before FST exposure, baseline monoamine efflux was measured for 2 h, and after onset of FST exposure, stress-induced monoamine efflux was measured for another 2 h each day. Experiments were performed during the light, inactive phase of the animals. Mice spent about 25 % of the 2 h before the FST with active behaviors (grooming, eating, exploring; data not shown) and the other 75 % with inactive behaviors (sleeping, resting). After FST exposure mice engaged in strong activity (100 %), mainly grooming, for 1 h, before they started to become inactive and to sleep, settling down again to about 25 % of activity. CRH-COE^{hom}-Nes and CRH-COE^{con}-Nes mice showed no difference in activity-related behavior during baseline or after FST stress on both days (statistics not shown).

Average baseline monoamine and metabolite efflux in the hippocampus of CRH-COE-Nes did not change from day 1 to day 2 for 5-HIAA, DOPAC and HVA (Table 3.2.3). NA and 5-HT baseline levels increased marginally from day day 1 to day 2 and DA levels decreased from day 1 to day 2. MHPG baseline levels decreased from day 1 to day 2 in CRH-COE^{con}-Nes mice, but increased from day 1 to day 2 in CRH-COE^{hom}-Nes mice. 5-HIAA baseline levels were generally lower in CRH-COE^{con}-Nes mice than in CRH-COE^{hom}-Nes mice on both days.

FST exposure induced a strong (50 – 150 %) increase of NA, DA and 5-HT efflux in the hippocampus as compared to baseline values (Figs. 3.2.10c,e,g; statistics not shown), which reached its peak 20 – 40 min later and returned to baseline 60 – 80 min later. The peak was sharp and short-lasting for NA in comparison to more blunt and longer-lasting peaks for DA and 5-HT. Metabolite efflux of the respective monoamines, MHGP for NA, DOPAC for DA and 5-HIAA for 5-HT generally followed the efflux curves of their monoamines in a delayed manner (Figs. 3.2.10d,f,h). FST induced metabolite increases were lower than that of their corresponding monoamines (30 – 80 % of baseline) and longer lasting (up to 2 h). Analysis of FST induced monoamine or metabolite efflux revealed neither significant genotype differences between CRH-COE^{hom}-Nes and CRH-COE^{con}-Nes

mice, nor significant habituation from day 1 to day 2 (statistics not shown). In general, the inter-animal variation of monoamine efflux during baseline and FST exposure was smallest for NA, medium for DA and largest for 5-HT.

Table 3.2.3 Monoamine and metabolite concentrations in hippocampal baseline dialysates of CRH-COE-Nes animals (averaged over 2 h of baseline sampling).

	con			hom		
	n	day 1	day 2	n	day 1	day 2
NA[a]	6	6.4 ± 0.7	6.8 ± 1.0	7	7.0 ± 0.5	8.2 ± 0.9
MHPG[c]	6	150.3 ± 11.3	137.5 ± 9.4	7	176.0 ± 13.6	179.2 ± 16.6
5-HT[a]	6	5.4 ± 1.8	7.7 ± 2.2	7	3.3 ± 0.5	5.6 ± 0.7
5-HIAA[b]	6	1360 ± 96.2	1270 ± 70.9	7	1625 ± 107.7	1671 ± 97.5
DA[a]	6	2.1 ± 0.3	1.2 ± 0.3	7	1.4 ± 0.2	1.0 ± 0.2
DOPAC	5	87.8 ± 17.2	74.6 ± 15.2	7	73.7 ± 7.7	71.7 ± 8.1
HVA	6	169.0 ± 15.9	148.3 ± 15.4	7	175.1 ± 16.3	162.4 ± 14.9

Mean $\pm$ SEM [fmol/10 µl dialysate].Two-way ANOVA results (*Day, Genotype*): [a]*Day*: $F > 6.2$, $P < 0.05$, [b]*Genotype*: $F_{1,11} = 6.8$, $P < 0.05$, [c]*Day x Genotype*: $F_{1,11} = 7.0$, $P < 0.05$. (NA) noradrenaline, (MHPG) 3-methoxy-4-hydroxyphenylglycol, (5-HT) serotonin, (5-HIAA) 5-hydroxyindoleacetic acid, (DA) dopamine, (DOPAC) 3,4-dihydroxyphenylacetic acid, (HVA) homovanillic acid, (con) CRH-COE[con]-Nes, (hom) CRH-COE[hom]-Nes.
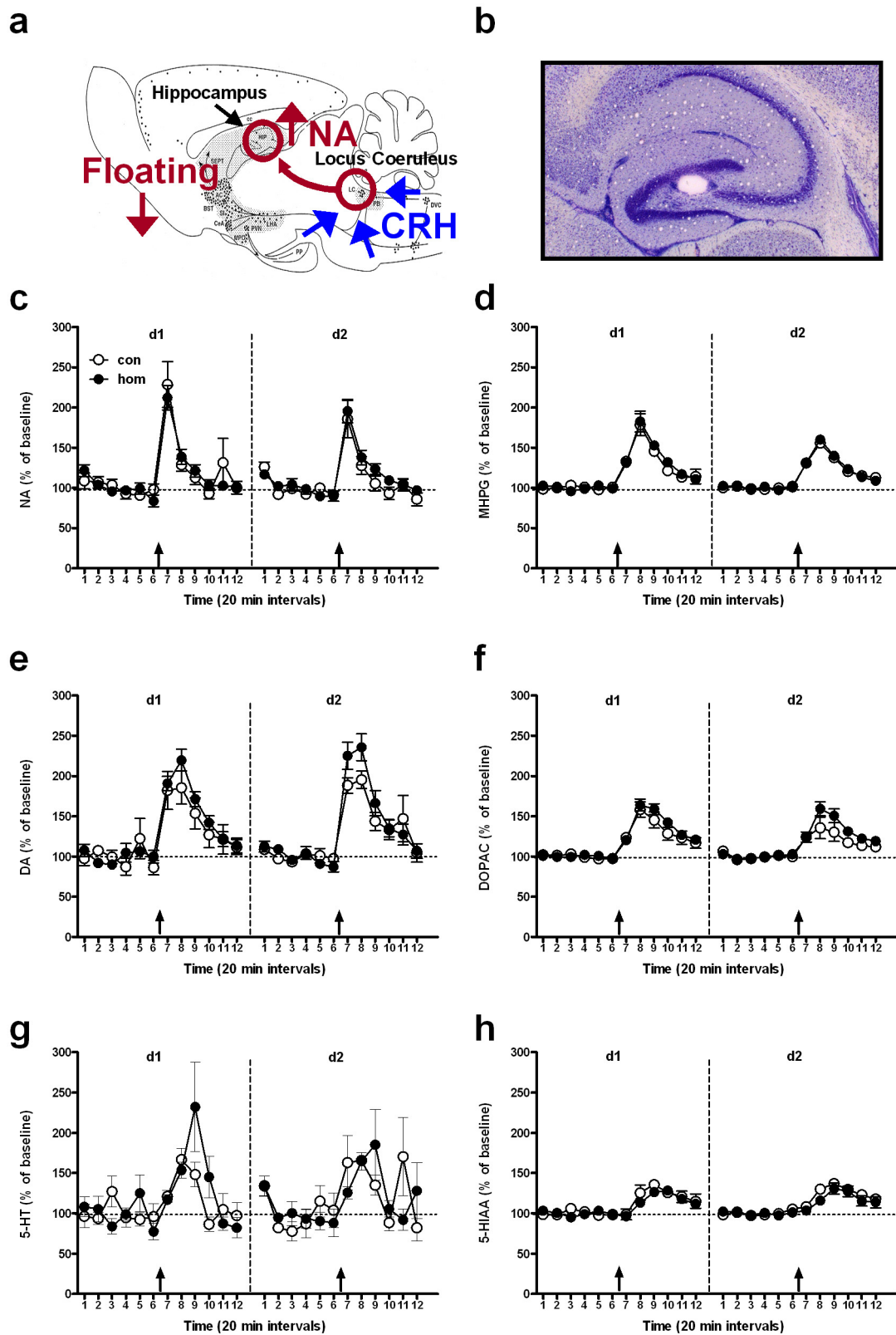
Figure 3.2.10 Transgenic CRH overexpression does not influence hippocampal monoamine efflux during forced swimming. (**a**) Graphics chart depicting the theoretical activation of noradrenergic locus coeruleus neurons by transgenic CRH overexpression, which, through potentially increased hippocampal noradrenergic neurotransmission, leads to reduced floating in the forced swim test. (**b**) Exemplary horizontal brain slice showing the placement of a microdialysis probe within the hippocampus. (**c**-**h**) Hippocampal monoamine and metabolite efflux of CRH-COE^{con}- (con) and CRH-COE^{hom}-Nes (hom) mice normalized to the respective mean con values during baseline. Mice were microdialysed for 2 h under baseline conditions, subsequently exposed to 6 min of forced swimming (indicated by the arrows), placed back in their home cages and microdialysed for additional 2 h. The identical procedure was carried out on two consecutive days, day 1 (d1) and day 2 (d2) (n = 6 per group). (**c**) Noradrenaline (NA), (**d**) 3-methoxy-4-hydroxyphenylglycol (MHPG), (**e**) dopamine (DA), (**f**) 3,4-dihydroxyphenylacetic acid (DOPAC), (**g**) serotonin (5-HT), (**h**) 5-hydroxyindoleacetic acid (5-HIAA).

3.2.5 Discussion

We used a knock-in approach to generate a mouse model, which allowed the overexpression of CRH at different levels in a spatially restricted manner. Superior to standard transgenesis this conditional mouse model provides the opportunity to generate and compare different CRH overexpressing mouse lines - as demonstrated by breeding to *nestin*-, *camk2a*- and *dlx-cre* mice - avoiding common uncertainties of transgene production such as copy number or site of transgene insertion. While the pattern of CRH overexpression exclusively depends on the spatial and/or temporal properties of the introduced Cre recombinase, the transcriptional control via *R26* guarantees for identical expression levels.

Our conditional approach enabled us to specifically investigate the CNS effects of different dosages of CRH in CRH-COE-Nes mice (Fig. 3.2.3) without affecting the peripheral CRH system (Fig. 3.2.2) or the circadian HPA axis regulation under basal conditions (Fig. 3.2.4). Nevertheless, chronic overexpression of exogenous CRH activates compensatory mechanisms affecting the expression levels of endogenous CRH and CRH-R1 in a brain region-specific manner as demonstrated in CRH-COE-Nes mice (data not shown). Alterations of endogenous CRH and CRH-R1 levels will mutually interfere with existing regulatory circuits and, in concert with effects of exogenous CRH expression, add another layer of complexity. For instance, expression of CRH in the PVN of CRH-COE[hom]-Nes is significantly decreased under basal conditions (data not shown) and thereby probably sensitizes or up-regulates CRH-R1 in pituitary corticotrophs. As a consequence, basal ACTH and corticosterone plasma levels of male CRH-COE[het]- and CRH-COE[hom]-Nes mice are indistinguishable from those of control littermates, whereas the HPA axis of these animals is hyperreactive in response to stress (Fig. 3.2.4). Interestingly, female CRH-COE[hom]-Nes mice displayed no such stress-dependent HPA axis hyperreactivity (Fig. 3.2.4), supporting previous observations of gender differences in biological functions of the endogenous CRH system (Bale and Vale, 2003). In CRH-COE[hom]-Nes mice we observed increased expression of CRH in the CeA as well as of CRH-R1 in the BLA and Hippocampus (data not shown). In contrast, Thy-1-driven overexpression in projection neurons of CRH-OE[2122] mice results in a rather uniform down-regulation of CRH-R1 in several brain nuclei (Korosi et al., 2006). However, it is of notice that chronically increased

corticosterone levels (Groenink et al., 2002) might here dominate the effects on CRH-R1 expression compared to transgene CRH expression.

Male CRH-COE-Nes mice exhibited a marked gene-dosage dependent antidepressant-like behavior in the FST (Figs. 3.2.6a,c), which was independently confirmed in the TST (Fig. 3.2.6b). It is unlikely that the antidepressant-like effects of CRH in the FST are mediated by excessive stress hormone secretion, as female CRH-COE-Nes mice, which displayed normal HPA-axis reactivity, showed similar behavioral alterations in the FST (Fig. 3.2.7a). Accordingly, neither CRH-R1 deletion (Sillaber et al., 2002) nor adrenalectomy resulted in altered forced swimming behavior (Nishikawa et al., 2004b). In line with our observations, intracerebroventricular injection of CRH or cortagine, a potent CRH-R1 agonist, as well as site-directed injection of CRH into the locus coeruleus, reduces immobility in the FST in rats and mice, indicating antidepressant-like activity (Butler et al., 1990; Garcia-Lecumberri and Ambrosio, 2000; Tezval et al., 2004). Furthermore, also CRH-Tg mice showed reduced immobility in the FST compared to wild-type littermates (Van Gaalen et al., 2002). These findings seem contradictory to the widely accepted pro-depressive role of CRH. However, behavior in the Porsolt FST certainly also involves a strong component of arousal, alertness and stress coping, which has to be considered besides the original interpretation of immobility as "behavioral despair" (Porsolt et al., 1977). Decreased immobility in CRH-COE[hom]-Nes mice, therefore, might rather reflect enhanced responsiveness and arousal to a stressful situation than antidepressant-like behavior. This hypothesis is corroborated by our findings of increased exploratory behavior in CRH-COE[hom]-Nes mice in the open field and light-dark box (Fig. 3.2.5), which might be due to increased arousal of the animals. Additionally, CRH-COE[hom]-Nes mice showed normal locomotor activity excluding locomotor confounds as a reason for increased active stress coping behavior in the FST and TST.

Although we did not observe any anxiogenic effect of CRH overexpression in CRH-COE[hom]-Nes mice in the light-dark paradigm, these observations are too preliminary to conclude lacking effects of CRH overexpression on anxiety behavior in these animals. The light-dark paradigm is very sensitive to alterations in light intensity, as well as to the construction of the boxes (for instance, whether the light box is connected to the dark box only by an opening in the dividing wall or by a small tunnel). Thus, further in depths experiments exploring anxiety-like behavior

of CRH-COE-Nes under different conditions and in various tests have to be considered.

CRH influences neuronal connectivity as it has been demonstrated in the developing hippocampus (Chen et al., 2004). Hence, CRH overexpression from early embryogenesis on might have caused adaptive changes of neuronal physiology to compensate for this chronic state of CRH excess, resulting in the observed antidepressant-like behavior and HPA axis hyperreactivity. However, the attenuation of antidepressant-like behavior as well as of HPA axis hyperreactivity by pretreatment of CRH-COE[het]-Nes mice with the CRH-R1 selective antagonist DMP696 (He et al., 2000) suggests that these phenotypes are an acute consequence of CRH overexpression (Figs. 3.2.6e,f). Considering the observation that CRH-R1 antagonists exhibit highest efficacy in animal models, which are hyperresponsive to stress and exhibit increased levels of CRH (Griebel et al., 2002; Zorrilla et al., 2002; Nishikawa et al., 2004), CRH-COE-Nes mice may constitute a mouse model with strong and predictable responsiveness to CRH-R1 antagonists.

To assure that the antidepressant-like behavioral phenotype of CRH-COE-Nes mice is not of artificial nature, arising from excessive ectopic expression of CRH in the brain, we elucidated the role of the endogenous CRH system in FST behavior. Under basal, non-activated conditions the endogenous CRH system does not influence FST behavior as neither the genetic disruption nor the pharmacological blockade of CRH-R1 affected FST behavior (Sillaber et al., 2002a; Liebsch et al., 1995; Nielsen et al., 2004). However, we could demonstrate that stress mediated activation of the endogenous CRH system prior to the FST elicited antidepressant-like behavior in wild-type mice but not in CRH-R1 knockout mice (Fig. 3.2.6d). These findings suggest that ectopic overexpression of CRH in CRH-COE-Nes mice mimics the behavioral consequences of stress-mediated activation of the endogenous CRH system, and that the antidepressant-like behavior is mediated via CRH-R1 dependent signaling pathways.

CRH binds preferably to CRH-R1, but is, in high local concentrations, also able to activate CRH-R2 (Keck et al., 2005). To investigate whether also CRH-R2 signaling influences forced swimming behavior, we tested CRH-R2 wild-type and knockout mice as well as CNS specific urocortin II overexpressing mice (urocortin II is a CRH related peptide that almost exclusively binds to CRH-R2) in the FST

(Figs. 3.2.7c,d). However, the CRH-R2 system was unable to mediate alterations in forced swim behavior further corroborating increased CRH-R1 signaling as being responsible for the FST phenotype of CRH-COE^{hom}-Nes mice.

The forebrain restricted disruption of CRH-R1 in *CRH-R1$^{lox/lox}$camk2a-cre* mice decreases anxiety-related behavior (Muller et al., 2003) suggesting the involvement of CRH/CRH-R1-dependent pathways in structures of the anterior forebrain including those of the limbic system, in emotionality control. In order to investigate whether these structures are also causally related to the observed antidepressant-like effect of CRH, we spatially restricted CRH overexpression using *camk2a-cre* mice. Similar to CRH-OE$_{2122}$ mice (Groenink et al., 2002), CRH overexpression in the forebrain (Figs. 3.2.8a,b) did not recapitulate the antidepressant-like behavior observed in CRH-COE-Nes (this study) and CRH-Tg mice (Stenzel-Poore et al., 1992), presumably owing to the overexpression in principal neurons only.

To date the cellular and subcellular localization of CRH and its receptors including receptor-mediated effects at synapses are not well understood. In the hippocampus, endogenous CRH expression has been assigned to somata, axons and boutons of GABAergic interneurons from where CRH is released in the cause of acute physiological stress (Chen et al., 2004). CRH release excites pyramidal cells, which express CRH-R1 postsynaptically on their dendritic spines. However, using *dlx-cre* mice to direct CRH overexpression to GABAergic interneurons, in order to model more closely endogenous expression sites in the forebrain, failed to affect FST behavior (Figs. 3.2.8c,d). The absence of the FST phenotype in forebrain specific CRH overexpressing mouse lines argues against volume transmission throughout the brain as mediating CRH effects, but clearly favors a mechanism involving synaptic release. Furthermore, our results suggest that CRH overexpression in more caudal brain nuclei of the mid/hind brain could promote the antidepressant-like effects of CRH.

In the brain stem of mice and rats CRH-R1 is expressed in serotonergic neurons of the median and dorsal raphe (DR) (Staub et al., 2006) and in dopaminergic neurons of the substantia nigra (SN) and ventral tegmental area (VTA) (Van Pett et al., 2000). CRH is highly expressed in noradrenergic neurons of the locus coeruleus (LC), (Bittencourt and Sawchenko, 2000) and i.c.v. injection of CRH has been demonstrated to induce a strong Fos immunoreactivity in the LC

indicating the activation of CRH-R-dependent signaling pathways (Bittencourt and Sawchenko, 2000). Accordingly, CRH is capable to potentiate noradrenergic (Butler et al., 1990; Valentino et al., 1983), dopaminergic (Summers et al., 2003) and serotonergic (Linthorst et al., 2002) neurotransmission. Here we could demonstrate that the pharmacological blockade of catecholamine synthesis by AMPT, but not of serotonin synthesis by PCPA, could partially reverse the phenotype of CRH-COE[hom]-Nes mice in the FST (Figs. 3.2.9a,b). Therefore, it is likely that CRH overexpression activates the endogenous catecholaminergic system similarly to antidepressants, which would explain the paradox of CRH as a "false positive" in the FST and TST.

Quantification of c-fos and zif268 expression in response to forced swim stress further identifies the hyperactivation of noradrenergic neurons of the LC in CRH-COE[hom]-Nes mice (Figs. 3.2.9c-f). Intracoerulear microinfusion of CRH in rats has demonstrated that CRH can serve as an excitatory neurotransmitter in the LC (Curtis et al., 1997) resulting in enhanced noradrenaline release in LC projection areas (Smagin et al., 1995). CRH-noradrenaline interactions not only occur in the LC, where CRH activates the LC, but also at the projections of the forebrain noradrenergic system, where noradrenaline stimulates CRH release (Koob, 1999). For instance, stress induces noradrenaline release in the PVN and thereby stimulates secretion of CRH (Alonso et al., 1986). This feed-forward mechanism could be a causal factor to the hyperreactivity of the HPA axis upon stress.

However, even though the aforementioned results clearly point to a noradrenergic activation in CRH-COE[hom]-Nes animals as being responsible for reduced floating in the FST, analyzing intra-hippocampal monoamine and their corresponding metabolite efflux during FST via *in vivo* microdialysis did not reveal any genotype differences between CRH-COE[con]- and CRH-COE[hom]-Nes mice (Fig. 3.2.10). This is unlikely a methodological problem as strong increases (about 100 %) of NA, 5-HT and DA (and their metabolites) effluxes were observed in response to FST both on day 1 and on day 2.

Thus, one possible explanation is that increased locus coeruleus activity in CRH-COE-Nes mice affects noradrenergic neurotransmission in brain regions different from the hippocampus. Other prominent CRH-noradrenaline interaction areas, which are involved in stress responses, represent for instance the BNST and the CeA (Koob, 1999). However, such small brain areas are almost impossible

to target via *in vivo* microdialysis in mice as an insertion of a microdialysis probe would inescapably destroy most of these small structures.

Another possible explanation is that the stress invariably associated with surgery during microdialysis and with later connection of the head of the mouse to the microdialysis tubing and wire tether system induced strong activation of the endogenous CRH system in CRH-COE^{con}-Nes mice that would mimic ectopic CRH overexpresssion of CRH-COE^{hom}-Nes mice. Thus, any real genotype effect might have been obscured, similar to what has been observed with CRH-R1 wild-type mice that were pre-exposed to restraint stress and then also showed CRH-mediated reduction in floating. Furthermore, the observation that microdialysed CRH-COE-Nes mice that were connected to the tether-swivel-system were unable to swim freely without hindrance during FST and, in addition, did not show considerable immobility, supports the above notion.

In conclusion, we have created a novel, highly flexible transgenic mouse model, which can aid in dissecting the contribution of CRH-sensitive pathways involved in the transition from physiological to pathological stress responses that are thought to underlie the etiology of affective and anxiety disorders (Holsboer, 1999a). Furthermore, we have unequivocally identified CRH as a "false positive" in the FST, likely due to CRH-mediated activation of noradrenergic neurons, questioning the ubiquitous usability of the FST as a test for antidepressant actions and/or depression-related behavior in transgenic mice. Clearly, future testing of conditional CRH-COE mice in other depression-related behavioral paradigms is warranted to clarify the contribution of chronically elevated central CRH circuitries to depression symptoms. Moreover, crossing $R26^{flopCrh/flopCrh}$ mice to noradrenergic-neuron-specific Cre transgenic mice ought to be envisioned to further explore CRH-noradrenaline interactions.

CHAPTER 4

FINAL DISCUSSION

In the present Ph.D. thesis, we used transgenic and pharmacological tools to investigate the roles of the endocannabinoid and CRH systems in depression-like endo-phenotypes in the mouse. We could demonstrate that (i) the activity state of the endocannabinoid system is regulated in a brain region-specific and temporally controlled manner in response to stress; (ii) CB1 receptor signaling serves as a major constraint mechanism for basal and stress-induced corticosterone secretion; (iii) endocannabinoid signaling bi-directionally modulates behavioral stress coping in the FST in a monoamine-independent manner; (iv) CB1 receptor-deficient mice may serve as an animal model for depression as they display deficits in behavioral stress coping, HPA axis function and neurotrophin expression; (v) CB1 receptor-Venus overexpressing transgenic mice may help to understand the role of CB1 receptor trafficking for endocannabinoid signaling and to decipher the exact location of CB1 receptor protein within neuronal circuits; (vi) transgenic CRH overexpressing mice display antidepressant-like behaviors due to increased arousal, which is likely induced by CRH-mediated activation of noradrenergic neurons.

(i) Although almost all endocannabinoid actions in the brain are transmitted through only one receptor, the CB1 receptor, its presence on both excitatory and inhibitory presynaptic terminals renders the effects of CB1 receptor signaling extremely complex. Studying major endocannabinoid, 2-AG and anandamide, tissue levels in various brain regions in response to the FST (Chapter 2.5, Fig. 2.5.5) and in response to acute and chronic social defeat stress (Chapter 2.6.2, data not shown) has demonstrated this complexity and has provided evidence for the temporally and spatially restricted differential regulation of both endocannabinoids. Interpretation of the results is, at our current understanding of the role of 2-AG and anandamide for the regulation of neurotransmission, very difficult, but our data imply that 2-AG and anandamide could, in fact, have different functions. These may include, for instance, the action at CB1 receptors of different

synapses, or the induction of different intracellular signaling pathways. Nevertheless, our data clearly show that both endocannabinoids are implicated in the immediate brain region-specific response to different kinds of stressors.

(ii) Recent reports have suggested that CB1 receptor signaling modulates HPA axis activity (Pagotto et al., 2006). We could show that pharmacological and genetic CB1 receptor inactivation does not only induce basal, but also injection stress-, FST stress- and social defeat stress-induced hypersecretion of corticosterone. In addition, our data indicated that CB1 receptor signaling at different levels of the HPA axis, such as the hippocampus, PVN, pituitary and adrenal glands is orchestrated to serve the fine tuning of HPA axis responsiveness. Our results underscore the notion of an HPA axis-modulating endocannabinoid tone, which is already present under basal non-stress conditions. However, particularly in response to stress endocannabinoids seem to be synthesized and recruited "on demand" in order to prevent hyperactivation of the HPA axis. Taken together, our data establish CB1 receptor signaling as a major restraint mechanism for corticosterone secretion in mice, largely independent of sex, genotype, kind of stressor and type of intervention (pharmacological vs. genetic).

(iii) We found that endocannabinoid signaling is involved in shaping the behavioral stress response of mice in the FST. However, the direction of this involvement seems to be intrinsically tied to the initial stress level of the animal and the experimental and environmental conditions. Furthermore, there were considerable discrepancies between the genetic and the pharmacological inhibition of CB1 receptor signaling pointing to developmental deficits of CB1$^{-/-}$ mice. Accordingly, although antidepressant-like effects of the CB1 antagonist SR141716 in the FST were monoamine-independent, behavioral reactions of CB1$^{-/-}$ mice in response to antidepressants were slightly altered compared to CB1$^{+/+}$ mice, likely because of developmental deficits. These findings demonstrate one common problem of total gene knockout animals: the possible development of secondary changes due to the life-long absence of the respective gene product (here the CB1 receptor). Therefore, results from knockout mice should always be handled with care and ought to be compared with results obtained from

pharmacologic interventions (in case the respective drugs are available). Considering that a number of discrepant findings have been obtained with regard to the role of endocannabinoids for behavioral stress coping in the FST (Viveros et al., 2005), we also failed to demonstrate a clear-cut antidepressant-like or depression-like effect of impaired CB1 receptor signaling in this test. Thus, despite the fact that endocannabinoid signaling modulates emotional stress processing, the direction of its intervention seems to vary significantly, likely depending on the neuronal circuits active at the time of testing. Certainly, future evaluation of the role of CB1 receptor signaling for depression-related phenotypes in mice requires a systematic investigation on the activation of the endocannabinoid system in dependence of the aversiveness of the test conditions and the stress level of the animal.

(iv) CB1 receptor-deficient mice have been suggested to represent an animal model for depression, as they display a number of different depression-related symptoms (Hill and Gorzalka, 2005a). Our results further strengthen this notion, because CB1$^{-/-}$ mice showed decreased glucocorticoid feedback, illustrated by impaired dexamethasone suppression and decreased GR receptor mRNA expression in the hippocampus, increased basal and stress-induced corticosterone secretion, increased CRH mRNA expression in the PVN, decreased BDNF mRNA expression in the hippocampus and increased "behavioral despair" in the FST, when tested under naïve conditions. All these symptoms, which could also be described as endo-phenotypes of depression, are found in depressed patients (Gottesman and Gould, 2003; Holsboer, 2000; De Kloet et al., 2005; Chen et al., 2001; Nemeroff, 1996) and, therefore, further qualify CB1 receptor-deficient mice as an animal model for depression.

(v) As mentioned in detail in the Discussion of Chapter 2.7, conditional CB1-Venus-BAC transgenic mice offer plenty opportunities for future research on CB1 receptor dynamics and expression at the cellular level. By crossing with respective Cre recombinase expressing mouse lines or by the *in situ* application of Cre expressing viruses, this mouse model will prove very useful for the identification of specific CB1 receptor-regulated neuronal circuits and/or subpopulations, which are responsible for depression-related behavior and neurochemical alterations. In

addition, the mouse model will allow the future investigation of "tolerance" effects, such as those that were observed with regard to the loss of acute stimulatory corticosterone elevating effects of the CB1 antagonist SR141716 following chronic administration of the drug (Chapter 2.4, Fig. 2.4.7).

(vi) By using mice with brain area-specific overexpression of CRH, we have demonstrated that transgenic CRH overexpression in mid-hindbrain regions is likely responsible for the antidepressant-like behavior of these animals in the FST and TST. Two things are interesting to note:

First, whereas the antidepressant-like behavioral effects of CRH are likely induced by the CRH-mediated activation of noradrenergic neurons in the LC, antidepressant-like behavioral effects of the CB1 antagonist SR141716 were monoamine-independent. These findings illustrate that, even though antidepressant-like effects of drugs in the FST are generally very specific for monoaminergic actions, there are apparent exceptions to this general rule. Future research has to demonstrate, whether the antidepressant-like effects of SR141716 are due to direct alterations of GABA- or glutamatergic transmission, or due to the influence on other neurotransmitter systems different from monoamines, such as, for instance, acetylcholine.

Second, due to this CRH-mediated increase in noradrenergic activity, CRH produces antidepressant-like effects in the FST, although CRH overproduction in humans has clear pro-depressive effects. Thus, CRH represents, so to speak, a "false positive" in the FST and questions the reliability of this test in detecting antidepressant-like drugs. Certainly, this example illustrates the need to carefully evaluate new drugs in a variety of depression-related behavioral paradigms to assess their antidepressant potential, before drawing premature conclusions from the performance in a single test.

In conclusion, we have demonstrated the usefulness of a combined genetic and pharmacological approach in defining molecular correlates of depression in mice. Our findings regarding the pro-depressive role of impaired CB1 receptor function suggest that mutations in the CB1 receptor gene might predispose humans to insufficient neuroendocrine and behavioral stress coping and, hence, to

psychiatric disorders. Accordingly, the CB1 receptor might provide an interesting target for future association studies in depressed patients.

5. LIST OF REFERENCES

Aguado T., Monory K., Palazuelos J., Stella N., Cravatt B., Lutz B., Marsicano G., Kokaia Z., Guzman M., and Galve-Roperh I. (2005) The endocannabinoid system drives neural progenitor proliferation. *Faseb J.* 19, 1704-1706

Alonso G., Szafarczyk A., Balmefrezol M., and Assenmacher I. (1986) Immunocytochemical evidence for stimulatory control by the ventral noradrenergic bundle of parvocellular neurons of the paraventricular nucleus secreting corticotropin releasing hormone and vasopressin in rats. *Brain Res.* 397, 297-307.

Andersson H., D'Antona A.M., Kendall D.A., von H.G., and Chin C.N. (2003) Membrane assembly of the cannabinoid receptor 1: impact of a long N-terminal tail. *Mol. Pharmacol.* 64, 570-577.

Anisman H. and Matheson K. (2005) Stress, depression, and anhedonia: caveats concerning animal models. *Neurosci. Biobehav. Rev.* 29, 525-546.

Antonijevic I.A. (2006) Depressive disorders - is it time to endorse different pathophysiologies? *Psychoneuroendocrinology* 31, 1-15.

Arai I., Tsuyuki Y., Shiomoto H., Satoh M., and Otomo S. (2000) Decreased body temperature dependent appearance of behavioral despair in the forced swimming test in mice. *Pharmacol. Res.* 42, 171-176.

Araki K., Araki M., and Yamamura K. (2002) Site-directed integration of the cre gene mediated by Cre recombinase using a combination of mutant lox sites. *Nucleic Acids Res.* 30, e103.

Arborelius L., Owens M.J., Plotsky P.M., and Nemeroff C.B. (1999) The role of corticotropin-releasing factor in depression and anxiety disorders. *J. Endocrinol.* 160, 1-12.

Arun K.H., Kaul C.L., and Ramarao P. (2005) Green fluorescent proteins in receptor research: an emerging tool for drug discovery. *J. Pharmacol. Toxicol. Methods* 51, 1-23.

Ayuso-Gutierrez J.L. (2005) Depressive subtypes and efficacy of antidepressive pharmacotherapy. *World J. Biol. Psychiatry* 6 Suppl 2, 31-37.

Bale T.L. and Vale W.W. (2003) Increased depression-like behaviors in corticotropin-releasing factor receptor-2-deficient mice: sexually dichotomous responses. *J. Neurosci.* 23, 5295-5301.

Ban T.A. (2001) Pharmacotherapy of depression: a historical analysis. *J. Neural Transm.* 108, 707-716.

Barna I., Zelena D., Arszovszki A.C., and Ledent C. (2004) The role of endogenous cannabinoids in the hypothalamo-pituitary-adrenal axis regulation: in vivo and in vitro studies in CB1 receptor knockout mice. *Life Sci.* 75, 2959-2970.

Berndsen S. and Broersen L. (2007) Evaluation of Porsolt Swim Test activity: Using the Mobility Parameter of EthoVision. Case study. http://www.noldus.com/site/content/files/ case_studies/pu_neuro_pst.pdf

Berton O. and Nestler E.J. (2006) New approaches to antidepressant drug discovery: beyond monoamines. *Nat. Rev. Neurosci.* 7, 137-151.

Berton O., McClung C.A., DiLeone R.J., Krishnan V., Renthal W., Russo S.J., Graham D., Tsankova N.M., Bolanos C.A., Rios M., Monteggia L.M., Self D.W., and Nestler E.J. (2006) Essential role of BDNF in the mesolimbic dopamine pathway in social defeat stress. *Science* 311, 864-868.

Bilkei-Gorzo A., Racz I., Valverde O., Otto M., Michel K., Sarstre M., and Zimmer A. (2005) Early age-related cognitive impairment in mice lacking cannabinoid CB1 receptors. *Proc. Natl. Acad. Sci. U. S. A.* 102, 15670-15675.

Binder E.B., Salyakina D., Lichtner P., Wochnik G.M., Ising M., Putz B., Papiol S., Seaman S., Lucae S., Kohli M.A., Nickel T., Kunzel H.E., Fuchs B., Majer M., Pfennig A., Kern N., Brunner J., Modell S., Baghai T., Deiml T., Zill P., Bondy B., Rupprecht R., Messer T., Kohnlein O., Dabitz H., Bruckl T., Muller N., Pfister H., Lieb R., Mueller J.C., Lohmussaar E., Strom T.M., Bettecken T., Meitinger T., Uhr M., Rein T., Holsboer F., and Muller-Myhsok B. (2004) Polymorphisms in FKBP5 are associated with increased recurrence of depressive episodes and rapid response to antidepressant treatment. *Nat. Genet.* 36, 1319-1325.

Bisogno T., Berrendero F., Ambrosino G., Cebeira M., Ramos J.A., Fernandez-Ruiz J.J., and Di M., V (1999) Brain regional distribution of endocannabinoids: implications for their biosynthesis and biological function. *Biochem. Biophys. Res. Commun.* 256, 377-380.

Bittencourt J.C. and Sawchenko P.E. (2000) Do centrally administered neuropeptides access cognate receptors?: an analysis in the central corticotropin-releasing factor system. *J. Neurosci.* 20, 1142-1156.

Bjorkqvist K. (2001) Social defeat as a stressor in humans. *Physiol. Behav.* 73, 435-442.

Blendy J.A. (2006) The role of CREB in depression and antidepressant treatment. *Biol. Psychiatry* 59, 1144-1150.

Bonhaus D.W., Chang L.K., Kwan J., and Martin G.R. (1998) Dual activation and inhibition of adenylyl cyclase by cannabinoid receptor agonists: evidence for agonist-specific trafficking of intracellular responses. *J. Pharmacol. Exp. Ther.* 287, 884-888.

Borsini F. and Meli A. (1988) Is the Forced Swimming Test A Suitable Model for Revealing Antidepressant Activity. *Psychopharmacology* 94, 147-160.

Borsini F., Volterra G., and Meli A. (1986) Does the behavioral "despair" test measure "despair"? *Physiol. Behav.* 38, 385-386.

Brinster R.L., Chen H.Y., Warren R., Sarthy A., and Palmiter R.D. (1982) Regulation of metallothionein thymidine kinase fusion plasmids injected into mouse eggs. *Nature* 296, 39-42.

Buckley N.E., Hansson S., Harta G., and Mezey E. (1998) Expression of the CB1 and CB2 receptor messenger RNAs during embryonic development in the rat. *Neuroscience* 82, 1131-1149.

Butler P.D., Weiss J.M., Stout J.C., and Nemeroff C.B. (1990) Corticotropin-releasing factor produces fear-enhancing and behavioral activating effects following infusion into the locus coeruleus. *J. Neurosci.* 10, 176-183.

Buwalda B., Kole M.H.P., Veenema A.H., Huininga M., de Boer S.F., Korte S.M., and Koolhaas J.A. (2005) Long-term effects of social stress on brain and behavior: a focus on hippocampal functioning. *Neurosci. Biobehav. Rev.* 29, 83-97.

Calandra B., Portier M., Kerneis A., Delpech M., Carillon C., Le F.G., Ferrara P., and Shire D. (1999) Dual intracellular signaling pathways mediated by the human cannabinoid CB1 receptor. *Eur. J. Pharmacol.* 374, 445-455.

Cannich A., Wotjak C.T., Kamprath K., Hermann H., Lutz B., and Marsicano G. (2004) CBI cannabinoid receptors modulate kinase and phosphatase activity during extinction of conditioned fear in mice. *Learning & Memory* 11, 625-632.

Caspi A. and Moffitt T.E. (2006) Gene-environment interactions in psychiatry: joining forces with neuroscience. *Nat. Rev. Neurosci.* 7, 583-590.

Caspi A., Sugden K., Moffitt T.E., Taylor A., Craig I.W., Harrington H., McClay J., Mill J., Martin J., Braithwaite A., and Poulton R. (2003) Influence of life stress on depression: moderation by a polymorphism in the 5-HTT gene. *Science* 301, 386-389.

Cesana R., Ceci A., Ciprandi C., and Borsini F. (1993) Mesulergine antagonism towards the fluoxetine anti-immobility effect in the forced swimming test in mice. *J. Pharm. Pharmacol.* 45, 473-475.

Chalmers D.T., Lovenberg T.W., Grigoriadis D.E., Behan D.P., and De Souza E.B. (1996) Corticotrophin-releasing factor receptors: from molecular biology to drug design. *Trends Pharmacol. Sci.* 17, 166-172.

Chan F., Bradley A., Wensel T.G., and Wilson J.H. (2004) Knock-in human rhodopsin-GFP fusions as mouse models for human disease and targets for gene therapy. *Proc. Natl. Acad. Sci. U. S. A.* 101, 9109-9114.

Chen B., Dowlatshahi D., MacQueen G.M., Wang J.F., and Young L.T. (2001) Increased hippocampal BDNF immunoreactivity in subjects treated with antidepressant medication. *Biol. Psychiatry* 50, 260-265.

Chen Y., Brunson K.L., Adelmann G., Bender R.A., Frotscher M., and Baram T.Z. (2004) Hippocampal corticotropin releasing hormone: pre- and postsynaptic location and release by stress. *Neuroscience* 126, 533-540.

Chen Y., Mills J.D., and Periasamy A. (2003) Protein localization in living cells and tissues using FRET and FLIM. *Differentiation* 71, 528-541.

Chevaleyre V., Takahashi K.A., and Castillo P.E. (2006) Endocannabinoid-mediated synaptic plasticity in the CNS. *Ann. Rev. Neurosci.* 29, 37-76.

Chrousos G.P. and Gold P.W. (1992) The concepts of stress and stress system disorders. Overview of physical and behavioral homeostasis. *JAMA* 267, 1244-1252.

Conti A.C., Cryan J.F., Dalvi A., Lucki I., and Blendy J.A. (2002) cAMP response element-binding protein is essential for the upregulation of brain-derived neurotrophic factor transcription, but not the behavioral or endocrine responses to antidepressant drugs. *J. Neurosci.* 22, 3262-3268.

Corchero J., Fuentes J.A., and Manzanares J. (1999) Chronic treatment with CP-55,940 regulates corticotropin releasing factor and proopiomelanocortin gene expression in the hypothalamus and pituitary gland of the rat. *Life Sci.* 64, 905-911.

Corrodi H. and Hanson L.C. (1966) Central effects of an inhibitor of tyrosine hydroxylation. *Psychopharmacologia.* 10, 116-125.

Coste S.C., Kesterson R.A., Heldwein K.A., Stevens S.L., Heard A.D., Hollis J.H., Murray S.E., Hill J.K., Pantely G.A., Hohimer A.R., Hatton D.C., Phillips T.J., Finn D.A., Low M.J., Rittenberg M.B., Stenzel P., and Stenzel-Poore M.P. (2000) Abnormal adaptations to stress and impaired cardiovascular function in mice lacking corticotropin-releasing hormone receptor-2. *Nat. Genet.* 24, 403-409.

Cota D., Marsicano G., Tschop M., Grubler Y., Flachskamm C., Schubert M., Auer D., Yassouridis A., Thone-Reineke C., Ortmann S., Tomassoni F., Cervino C., Nisoli E., Linthorst A.C., Pasquali R., Lutz B., Stalla G.K., and Pagotto U. (2003) The endogenous cannabinoid system affects energy balance via central orexigenic drive and peripheral lipogenesis. *J. Clin. Invest* 112, 423-431.

Coutts A.A., navi-Goffer S., Ross R.A., MacEwan D.J., Mackie K., Pertwee R.G., and Irving A.J. (2001) Agonist-induced internalization and trafficking of cannabinoid CB1 receptors in hippocampal neurons. *J. Neurosci.* 21, 2425-2433.

Crown W.H., Finkelstein S., Berndt E.R., Ling D., Poret A.W., Rush A.J., and Russell J.M. (2002) The impact of treatment-resistant depression on health care utilization and costs. *J. Clin. Psychiatry* 63, 963-971.

Cryan J.F. and Holmes A. (2005) The ascent of mouse: Advances in modelling human depression and anxiety. *Nat. Rev. Drug Discov.* 4, 775-790.

Cryan J.F. and Mombereau C. (2004) In search of a depressed mouse: utility of models for studying depression-related behavior in genetically modified mice. *Mol. Psychiatry* 9, 326-357.

Cryan J.F., Mombereau C., and Vassout A. (2005) The tail suspension test as a model for assessing antidepressant activity: Review of pharmacological and genetic studies in mice. *Neurosci. Behav. Rev.* 29, 571-625.

Cullinan W.E., Herman J.P., Battaglia D.F., Akil H., and Watson S.J. (1995) Pattern and time course of immediate early gene expression in rat brain following acute stress. *Neuroscience* 64, 477-505.

Cummings S., Elde R., Ells J., and Lindall A. (1983) Corticotropin-releasing factor immunoreactivity is widely distributed within the central nervous system of the rat: an immunohistochemical study. *J. Neurosci.* 3, 1355-1368.

Curtis A.L., Lechner S.M., Pavcovich L.A., and Valentino R.J. (1997) Activation of the locus coeruleus noradrenergic system by intracoerulear microinfusion of corticotropin-releasing factor: effects on discharge rate, cortical norepinephrine levels and cortical electroencephalographic activity. *J. Pharmacol. Exp. Ther.* 281, 163-172.

Dagerlind A., Friberg K., Bean A.J., and Hokfelt T. (1992) Sensitive mRNA detection using unfixed tissue: combined radioactive and non-radioactive in situ hybridization histochemistry. *Histochemistry* 98, 39-49.

Dallman M.F. (2003) Fast glucocorticoid feedback favors 'the munchies'. *Trends Endocrinol. Metab.* 14, 394-396.

Dallman M.F., Pecoraro N., Akana S.F., La Fleur S.E., Gomez F., Houshyar H., Bell M.E., Bhatnagar S., Laugero K.D., and Manalo S. (2003) Chronic stress and obesity: a new view of "comfort food". *Proc. Natl. Acad. Sci. U. S. A.* 100, 11696-11701.

Davey R.A. and MacLean H.E. (2006) Current and future approaches using genetically modified mice in endocrine research. *Am. J. Physiol. Endocrinol. Metab.* 291, E429-E438.

De Kloet E.R. (1995) Steroids, stability and stress. *Front. Neuroendocrinol.* 16, 416-425.

De Kloet E.R., Joels M., and Holsboer F. (2005) Stress and the brain: from adaptation to disease. *Nat. Rev. Neurosci.* 6, 463-475.

De Kloet E.R., Vreugdenhil E., Oitzl M.S., and Joels M. (1998) Brain corticosteroid receptor balance in health and disease. *Endocr. Rev.* 19, 269-301.

Demuth D.G. and Molleman A. (2006) Cannabinoid signalling. *Life Sci.* 78, 549-563.

Derkinderen P., Valjent E., Toutant M., Corvol J.C., Enslen H., Ledent C., Trzaskos J., Caboche J., and Girault J.A. (2003) Regulation of extracellular signal-regulated kinase by cannabinoids in hippocampus. *J. Neurosci.* 23, 2371-2382.

Despres J.P., Golay A., and Sjostrom L. (2005) Effects of rimonabant on metabolic risk factors in overweight patients with dyslipidemia. *N. Engl. J. Med.* 353, 2121-2134.

Di Marzo, V., Melck D., Bisogno T., and De P.L. (1998) Endocannabinoids: endogenous cannabinoid receptor ligands with neuromodulatory action. *Trends Neurosci.* 21, 521-528.

Di S., Malcher-Lopes R., Halmos K.C., and Tasker J.G. (2003) Nongenomic glucocorticoid inhibition via endocannabinoid release in the hypothalamus: A fast feedback mechanism. *J. Neurosci.* 23, 4850-4857.

Diaz-Laviada I. and Ruiz-Llorente L. (2005) Signal transduction activated by cannabinoid receptors. *Mini Rev. Med. Chem.* 5, 619-630.

Dodt H.U., Leischner U., Schierloh A., Jahrling N., Mauch C.P., Deininger K., Deussing J.M., Eder M., Zieglgansberger W., and Becker K. (2007) Ultramicroscopy: three-dimensional visualization of neuronal networks in the whole mouse brain. *Nat. Methods* 4, 331-336.

Dowlatshahi D., MacQueen G.M., Wang J.F., and Young L.T. (1998) Increased temporal cortex CREB concentrations and antidepressant treatment in major depression. *Lancet* 352, 1754-1755.

Duman R.S. and Monteggia L.M. (2006) A neurotrophic model for stress-related mood disorders. *Biol. Psychiatry* 59, 1116-1127.

Duman R.S., Heninger G.R., and Nestler E.J. (1997) A molecular and cellular theory of depression. *Arch. Gen. Psychiatry* 54, 597-606.

Dunn A.J. and Berridge C.W. (1990) Is corticotropin-releasing factor a mediator of stress responses? *Ann. N. Y. Acad. Sci.* 579, 183-191.

Entsuah A.R., Huang H., and Thase M.E. (2001) Response and remission rates in different subpopulations with major depressive disorder administered venlafaxine, selective serotonin reuptake inhibitors, or placebo. *J. Clin. Psychiatry* 62, 869-877.

Fagiolini A. and Kupfer D.J. (2003) Is treatment-resistant depression a unique subtype of depression? *Biol. Psychiatry* 53, 640-648.

Ferguson S.S. (2001) Evolving concepts in G protein-coupled receptor endocytosis: the role in receptor desensitization and signaling. *Pharmacol. Rev.* 53, 1-24.

Fride E., Suris R., Weidenfeld J., and Mechoulam R. (2005) Differential response to acute and repeated stress in cannabinoid CB1 receptor knockout newborn and adult mice. *Behav. Pharmacol.* 16, 431-440.

Friedrich G. and Soriano P. (1991) Promoter traps in embryonic stem cells: a genetic screen to identify and mutate developmental genes in mice. *Genes Dev.* 5, 1513-1523.

Fuchs E. and Flugge G. (2002) Social stress in tree shrews: effects on physiology, brain function, and behavior of subordinate individuals. *Pharmacol. Biochem. Behav.* 73, 247-258.

Gaetani S., Cuomo V., and Piomelli D. (2003) Anandamide hydrolysis: a new target for anti-anxiety drugs? *Trends Mol. Med.* 9, 474-478.

Galiegue S., Mary S., Marchand J., Dussossoy D., Carriere D., Carayon P., Bouaboula M., Shire D., Lefur G., and Casellas P. (1995) Expression of Central and Peripheral Cannabinoid Receptors in Human Immune Tissues and Leukocyte Subpopulations. *Eur. J. Biochem.* 232, 54-61.

Garcia-Lecumberri C. and Ambrosio E. (2000) Differential effect of low doses of intracerebroventricular corticotropin-releasing factor in forced swimming test. *Pharmacol. Biochem. Behav.* 67, 519-525.

Gaveriaux-Ruff C. and Kieffer B.L. (2007) Conditional gene targeting in the mouse nervous system: Insights into brain function and diseases. *Pharmacol. Ther.* 113, 619-634.

Giuffrida A., Rodriguez de F.F., and Piomelli D. (2000) Quantification of bioactive acylethanolamides in rat plasma by electrospray mass spectrometry. *Anal. Biochem.* 280, 87-93.

Gobbi G., Bambico F.R., Mangieri R., Bortolato M., Campolongo P., Solinas M., Cassano T., Morgese M.G., Debonnel G., Duranti A., Tontini A., Tarzia G., Mor M., Trezza V., Goldberg S.R., Cuomo V., and Piomelli D. (2005) Antidepressant-like activity and modulation of brain monoaminergic transmission by blockade of anandamide hydrolysis. *Proc. Natl. Acad. Sci. U. S. A.* 102, 18620-18625.

Gobshtis N., Ben Shabat S., and Fride E. (2007) Antidepressant-induced undesirable weight gain: Prevention with rimonabant without interference with behavioral effectiveness. *Eur. J. Pharmacol.* 554, 155-163.

Gold P.W., Drevets W.C., and Charney D.S. (2002) New insights into the role of cortisol and the glucocorticoid receptor in severe depression. *Biol. Psychiatry* 52, 381-385.

Gong S., Zheng C., Doughty M.L., Losos K., Didkovsky N., Schambra U.B., Nowak N.J., Joyner A., Leblanc G., Hatten M.E., and Heintz N. (2003) A gene expression atlas of the central nervous system based on bacterial artificial chromosomes. *Nature* 425, 917-925.

Gonzalez S., Manzanares J., Berrendero F., Wenger T., Corchero J., Bisogno T., Romero J., Fuentes J.A., Di Marzo V., Ramos J.A., and Fernandez-Ruiz J. (1999) Identification of endocannabinoids and cannabinoid CB1 receptor mRNA in the pituitary gland. *Neuroendocrinology* 70, 137-145.

Gottesman I.I. and Gould T.D. (2003) The endophenotype concept in psychiatry: etymology and strategic intentions. *Am. J. Psychiatry* 160, 636-645.

Griebel G., Simiand J., Steinberg R., Jung M., Gully D., Roger P., Geslin M., Scatton B., Maffrand J.P., and Soubrie P. (2002) 4-(2-Chloro-4-methoxy-5-methylphenyl)-N-[(1S)-2-cyclopropyl-1-(3-fluoro-4- methylphenyl)ethyl]5-methyl-N-(2-propynyl)-1, 3-thiazol-2-amine hydrochloride (SSR125543A), a potent and selective corticotrophin-releasing factor(1) receptor antagonist. II. Characterization in rodent models of stress-related disorders. *J. Pharmacol. Exp. Ther.* 301, 333-345.

Griebel G., Stemmelin J., and Scatton B. (2005) Effects of the cannabinoid CB1 receptor antagonist rimonabant in models of emotional reactivity in rodents. *Biol. Psychiatry* 57, 261-267.

Groenink L., Dirks A., Verdouw P.M., Schipholt M., Veening J.G., van der G.J., and Olivier B. (2002) HPA axis dysregulation in mice overexpressing corticotropin releasing hormone. *Biol. Psychiatry* 51, 875-881.

Haller J., Bakos N., Szirmay M., Ledent C., and Freund T.F. (2002) The effects of genetic and pharmacological blockade of the CB1 cannabinoid receptor on anxiety. *Eur. J. Neurosci.* 16, 1395-1398.

Haller J., Matyas F., Soproni K., Varga B., Barsy B., Nemeth B., Mikics E., Freund T.F., and Hajos N. (2007) Correlated species differences in the effects of cannabinoid ligands on anxiety and on GABAergic and glutamatergic synaptic transmission. *Eur. J. Neurosci.* 25, 2445-2456.

Haller J., Varga B., Ledent C., and Freund T.F. (2004) CB1 cannabinoid receptors mediate anxiolytic effects: convergent genetic and pharmacological evidence with CB1-specific agents. *Behav. Pharmacol.* 15, 299-304.

Haller J., Varga B., Ledent C., Barna I., and Freund T.F. (2004) Context-dependent effects of CB1 cannabinoid gene disruption on anxiety-like and social behaviour in mice. *Eur. J. Neurosci.* 19, 1906-1912.

Haring M., Marsicano G., Lutz B., and Monory K. (2007) Identification of the cannabinoid receptor type 1 in serotonergic cells of raphe nuclei in mice. *Neuroscience*.

He L., Gilligan P.J., Zaczek R., Fitzgerald L.W., McElroy J., Shen H.S., Saye J.A., Kalin N.H., Shelton S., Christ D., Trainor G., and Hartig P. (2000) 4-(1,3-Dimethoxyprop-2-ylamino)-2,7-dimethyl-8-(2,   4-dichlorophenyl)pyrazolo[1,5-a]-1,3,5-triazine: a potent, orally bioavailable CRF(1) receptor antagonist. *J. Med. Chem.* 43, 449-456.

Heine V.M., Zareno J., Maslam S., Joels M., and Lucassen P.J. (2005) Chronic stress in the adult dentate gyrus reduces cell proliferation near the vasculature and VEGF and Flk-1 protein expression. *Eur. J. Neurosci.* 21, 1304-1314.

Heinrichs S.C., Menzaghi F., Merlo P.E., Britton K.T., and Koob G.F. (1995) The role of CRF in behavioral aspects of stress. *Ann. N. Y. Acad. Sci.* 771, 92-104.

Herkenham M., Lynn A.B., Johnson M.R., Melvin L.S., Decosta B.R., and Rice K.C. (1991) Characterization and localization of cannabinoid receptors in rat-brain - A quantitative in vitro autoradiographic study. *J. Neurosci.* 11, 563-583.

Herman J.P., Figueiredo H., Mueller N.K., Ulrich-Lai Y., Ostrander M.M., Choi D.C., and Cullinan W.E. (2003) Central mechanisms of stress integration: hierarchical circuitry controlling hypothalamo-pituitary-adrenocortical responsiveness. *Front. Neuroendocrinol.* 24, 151-180.

Hermann H., Marsicano G., and Lutz B. (2002) Coexpression of the cannabinoid receptor type 1 with dopamine and serotonin receptors in distinct neuronal subpopulations of the adult mouse forebrain. *Neuroscience* 109, 451-460.

Hill M.N. and Gorzalka B.B. (2005a) Is there a role for the endocannabinoid system in the etiology and treatment of melancholic depression? *Behav. Pharmacol.* 16, 333-352.

Hill M.N. and Gorzalka B.B. (2005b) Pharmacological enhancement of cannabinoid CB1 receptor activity elicits an antidepressant-like response in the rat forced swim test. *Eur. Neuropsychopharmacol.* 15, 593-599.

Hill M.N., Ho W.S., Sinopoli K.J., Viau V., Hillard C.J., and Gorzalka B.B. (2006) Involvement of the endocannabinoid system in the ability of long-term tricyclic antidepressant treatment to suppress stress-induced activation of the hypothalamic-pituitary-adrenal axis. *Neuropsychopharmacology* 31, 2591-2599.

Hill M.N., Karacabeyli E.S., and Gorzalka B.B. (2007) Estrogen recruits the endocannabinoid system to modulate emotionality. *Psychoneuroendocrinology* 32, 350-357.

Hill M.N., Patel S., Carrier E.J., Rademacher D.J., Ormerod B.K., Hillard C.J., and Gorzalka B.B. (2005) Downregulation of endocannabinoid signaling in the hippocampus following chronic unpredictable stress. *Neuropsychopharmacology* 30, 508-515.

Hohmann A.G., Suplita R.L., Bolton N.M., Neely M.H., Fegley D., Mangieri R., Krey J.F., Walker J.M., Holmes P.V., Crystal J.D., Duranti A., Tontini A., Mor M., Tarzia G., and Piomelli D. (2005) An endocannabinoid mechanism for stress-induced analgesia. *Nature* 435, 1108-1112.

Holsboer F. (1999) The rationale for corticotropin-releasing hormone receptor (CRH-R) antagonists to treat depression and anxiety. *J. Psychiatr. Res.* 33, 181-214.

Holsboer F. (2000) The corticosteroid receptor hypothesis of depression. *Neuropsychopharmacology* 23, 477-501.

Holsboer F. (2001) Stress, hypercortisolism and corticosteroid receptors in depression: implicatons for therapy. *J. Affect. Disord.* 62, 77-91.

Howlett A.C., Barth F., Bonner T.I., Cabral G., Casellas P., Devane W.A., Felder C.C., Herkenham M., Mackie K., Martin B.R., Mechoulam R., and Pertwee R.G. (2002) International Union of Pharmacology. XXVII. Classification of cannabinoid receptors. *Pharmacol. Rev.* 54, 161-202.

Hsieh C., Brown S., Derleth C., and Mackie K. (1999) Internalization and recycling of the CB1 cannabinoid receptor. *J. Neurochem.* 73, 493-501.

Hungund B.L., Szakall I., Adam A., Basavarajappa B.S., and Vadasz C. (2003) Cannabinoid CB1 receptor knockout mice exhibit markedly reduced voluntary alcohol consumption and lack alcohol-induced dopamine release in the nucleus accumbens. *J. Neurochem.* 84, 698-704.

Hungund B.L., Vinod K.Y., Kassir S.A., Basavarajappa B.S., Yalamanchili R., Cooper T.B., Mann J.J., and Arango V. (2004) Upregulation of CB1 receptors and agonist-stimulated [S-35]GTP gamma S binding in the prefrontal cortex of depressed suicide victims. *Mol. Psychiatry* 9, 184-190.

Ising M., Horstmann S., Kloiber S., Lucae S., Binder E.B., Kern N., Kunzel H.E., Pfennig A., Uhr M., and Holsboer F. (2007) Combined dexamethasone/corticotropin releasing hormone test predicts treatment response in major depression-a potential biomarker? *Biol. Psychiatry* 62, 47-54.

Jardinaud F., Crete D., Canestrelli C., Ledent C., Roques B.P., and Noble F. (2005) CB1 receptor knockout mice show similar behavioral modifications to wild-type mice when enkephalin catabolism is inhibited. *Brain Res.* 1063, 77-83.

Javitt D.C. (2004) Glutamate as a therapeutic target in psychiatric disorders. *Mol. Psychiatry* 9, 984-97, 979.

Jin W., Brown S., Roche J.P., Hsieh C., Celver J.P., Kovoor A., Chavkin C., and Mackie K. (1999) Distinct domains of the CB1 cannabinoid receptor mediate desensitization and internalization. *J. Neurosci.* 19, 3773-3780.

Johannessen M., Delghandi M.P., and Moens U. (2004) What turns CREB on? *Cell Signal.* 16, 1211-1227.

Juszczak G.R., Sliwa A.T., Wolak P., Tymosiak-Zielinska A., Lisowski P., and Swiergiel A.H. (2006) The usage of video analysis system for detection of immobility in the tail suspension test in mice. *Pharmacol. Biochem. Behav.* 85, 332-338.

Kallal L. and Benovic J.L. (2000) Using green fluorescent proteins to study G-protein-coupled receptor localization and trafficking. *Trends Pharmacol. Sci.* 21, 175-180.

Kamprath K., Marsicano G., Tang J., Monory K., Bisogno T., Di M., V, Lutz B., and Wotjak C.T. (2006) Cannabinoid CB1 receptor mediates fear extinction via habituation-like processes. *J. Neurosci.* 26, 6677-6686.

Karanth S., Linthorst A.C.E., Stalla G.K., Barden N., Holsboer F., and Reul J.M.H.M. (1997) Hypothalamic-pituitary-adrenocortical axis changes in a transgenic mouse with impaired glucocorticoid receptor function. *Endocrinology* 138, 3476-3485.

Karege F., Vaudan G., Schwald M., Perroud N., and La H.R. (2005) Neurotrophin levels in postmortem brains of suicide victims and the effects of antemortem diagnosis and psychotropic drugs. *Brain Res. Mol. Brain Res.* 136, 29-37.

Kathuria S., Gaetani S., Fegley D., Valino F., Duranti A., Tontini A., Mor M., Tarzia G., La Rana G., Calignano A., Giustino A., Tattoli M., Palmery M., Cuomo V., and Piomelli D. (2003) Modulation of anxiety through blockade of anandamide hydrolysis. *Nat. Med.* 9, 76-81.

Katz R.J. (1982) Animal model of depression: pharmacological sensitivity of a hedonic deficit. *Pharmacol. Biochem. Behav.* 16, 965-968.

Keck M.E., Ohl F., Holsboer F., and Muller M.B. (2005) Listening to mutant mice: a spotlight on the role of CRF/CRF receptor systems in affective disorders. *Neurosci. Biobehav. Rev.* 29, 867-889.

Keren O. and Sarne Y. (2003) Multiple mechanisms of CB1 cannabinoid receptors regulation. *Brain Res.* 980, 197-205.

Kessler R.C., Berglund P., Demler O., Jin R., Koretz D., Merikangas K.R., Rush A.J., Walters E.E., and Wang P.S. (2003) The epidemiology of major depressive disorder: results from the National Comorbidity Survey Replication (NCS-R). *JAMA* 289, 3095-3105.

Kessler R.C., Mcgonagle K.A., Zhao S.Y., Nelson C.B., Hughes M., Eshleman S., Wittchen H.U., and Kendler K.S. (1994) Lifetime and 12-Month Prevalence of Dsm-Iii-R Psychiatric-Disorders in the United-States - Results from the National-Comorbidity-Survey. *Arch. Gen. Psychiatry* 51, 8-19.

Khaspekov L.G., Verca M.S.B., Frumkina L.E., Hermann H., Marsicano G., and Lutz B. (2004) Involvement of brain-derived neurotrophic factor in cannabinoid receptor-dependent protection against excitotoxicity. *Eur. J. Neurosci.* 19, 1691-1698.

Kim M.S., Kim W.H., and Lee G.M. (2007) A simple analysis system for the estimation of recombination efficiency using fluorescence-activated cell sorting. *J. Biotechnol.* 127, 373-384.

Klerman G.L. and Weissman M.M. (1985) Psychiatric epidemiology and clinical psychiatry. *Am. J. Psychiatry* 142, 1123-1124.

Kondo S., Okuda A., Sato H., Tachikawa N., Terashima M., Kanegae Y., and Saito I. (2003) Simultaneous on/off regulation of transgenes located on a mammalian chromosome with Cre-expressing adenovirus and a mutant loxP. *Nucleic Acids Res.* 31, e76.

Koob G.F. (1999) Corticotropin-releasing factor, norepinephrine, and stress. *Biol. Psychiatry* 46, 1167-1180.

Korosi A., Veening J.G., Kozicz T., Henckens M., Dederen J., Groenink L., van der G.J., Olivier B., and Roubos E.W. (2006) Distribution and expression of CRF receptor 1 and 2 mRNAs in the CRF over-expressing mouse brain. *Brain Res.* 1072, 46-54.

Kouznetsova M., Kelley B., Shen M., and Thayer S.A. (2002) Desensitization of cannabinoid-mediated presynaptic inhibition of neurotransmission between rat hippocampal neurons in culture. *Mol. Pharmacol.* 61, 477-485.

Ledent C., Valverde O., Cossu C., Petitet F., Aubert L.F., Beslot F., Bohme G.A., Imperato A., Pedrazzini T., Roques B.P., Vassart G., Fratta W., and Parmentier M. (1999) Unresponsiveness to cannabinoids and reduced addictive effects of opiates in CB1 receptor knockout mice. *Science* 283, 401-404.

Lee G. and Saito I. (1998) Role of nucleotide sequences of loxP spacer region in Cre-mediated recombination. *Gene* 216, 55-65.

Leterrier C., Bonnard D., Carrel D., Rossier J., and Lenkei Z. (2004) Constitutive endocytic cycle of the CB1 cannabinoid receptor. *J. Biol. Chem.* 279, 36013-36021.

Leterrier C., Laine J., Darmon M., Boudin H., Rossier J., and Lenkei Z. (2006) Constitutive activation drives compartment-selective endocytosis and axonal targeting of type 1 cannabinoid receptors. *J. Neurosci.* 26, 3141-3153.

Levinson D.F. (2006) The genetics of depression: a review. *Biol. Psychiatry* 60, 84-92.

Lidke D.S., Nagy P., Heintzmann R., rndt-Jovin D.J., Post J.N., Grecco H.E., Jares-Erijman E.A., and Jovin T.M. (2004) Quantum dot ligands provide new insights into erbB/HER receptor-mediated signal transduction. *Nat. Biotechnol.* 22, 198-203.

Liebsch G., Landgraf R., Gerstberger R., Probst J.C., Wotjak C.T., Engelmann M., Holsboer F., and Montkowski A. (1995) Chronic infusion of a CRH1 receptor antisense oligodeoxynucleotide into the central nucleus of the amygdala reduced anxiety-related behavior in socially defeated rats. *Regul. Pept.* 59, 229-239.

Linthorst A.C., Penalva R.G., Flachskamm C., Holsboer F., and Reul J.M. (2002) Forced swim stress activates rat hippocampal serotonergic neurotransmission involving a corticotropin-releasing hormone receptor-dependent mechanism. *Eur. J. Neurosci.* 16, 2441-2452.

Lucki I. and O'Leary O.F. (2004) Distinguishing roles for norepinephrine and serotonin in the behavioral effects of antidepressant drugs. *J. Clin. Psychiatry* 65, 11-24.

Lucki I., Dalvi A., and Mayorga A.J. (2001) Sensitivity to the effects of pharmacologically selective antidepressants in different strains of mice. *Psychopharmacology* 155, 315-322.

Mackie K. (2005) Distribution of cannabinoid receptors in the central and peripheral nervous system. *Handb. Exp. Pharmacol.* 168, 299-325.
Makino S., Shibasaki T., Yamauchi N., Nishioka T., Mimoto T., Wakabayashi I., Gold P.W., and Hashimoto K. (1999) Psychological stress increased corticotropin-releasing hormone mRNA and content in the central nucleus of the amygdala but not in the hypothalamic paraventricular nucleus in the rat. *Brain Res.* 850, 136-143.

Manzanares J., Corchero J., and Fuentes J.A. (1999) Opioid and cannabinoid receptor-mediated regulation of the increase in adrenocorticotropin hormone and corticosterone plasma concentrations induced by central administration of Delta(9)-tetrahydrocannabinol in rats. *Brain Res.* 839, 173-179.

Marsicano G. and Lutz B. (1999) Expression of the cannabinoid receptor CB1 in distinct neuronal subpopulations in the adult mouse forebrain. *Eur. J. Neurosci.* 11, 4213-4225.

Marsicano G. and Lutz B. (2006) Neuromodulatory functions of the endocannabinoid system. *J. Endocrinol. Invest* 29, 27-46.

Marsicano G., Goodenough S., Monory K., Hermann H., Eder M., Cannich A., Azad S.C., Cascio M.G., Gutierrez S.O., van der Stelt M., Lopez-Rodriguez M.L., Casanova E., Schutz G., Zieglgansberger W., Di Marzo V., Behl C., and Lutz B. (2003) CB1 cannabinoid receptors and on-demand defense against excitotoxicity. *Science* 302, 84-88.

Marsicano G., Wotjak C.T., Azad S.C., Bisogno T., Rammes G., Cascio M.G., Hermann H., Tang J.R., Hofmann C., Zieglgansberger W., Di Marzo V., and Lutz B. (2002) The endogenous cannabinoid system controls extinction of aversive memories. *Nature* 418, 530-534.

Martin M., Ledent C., Parmentier M., Maldonado R., and Valverde O. (2002) Involvement of CB1 cannabinoid receptors in emotional behaviour. *Psychopharmacology* 159, 379-387.

Masand P.S. and Gupta S. (2002) Long-term side effects of newer-generation antidepressants: SSRIS, venlafaxine, nefazodone, bupropion, and mirtazapine. *Ann. Clin. Psychiatry* 14, 175-182.

Mayorga A.J. and Lucki I. (2001) Limitations on the use of the C57BL/6 mouse in the tail suspension test. *Psychopharmacology (Berl)* 155, 110-112.

Mayorga A.J., Dalvi A., Page M.E., Zimov-Levinson S., Hen R., and Lucki I. (2001) Antidepressant-like behavioral effects in 5-hydroxytryptamine (1A) and 5-hydroxytryptamine (1B) receptor mutant mice. *J. Pharmacol. Exp. Ther.* 298, 1101-1107.

McArthur R. and Borsini F. (2006) Animal models of depression in drug discovery: a historical perspective. *Pharmacol. Biochem. Behav.* 84, 436-452.

McDonald N.A., Henstridge C.M., Connolly C.N., and Irving A.J. (2007) An essential role for constitutive endocytosis, but not activity, in the axonal targeting of the CB1 cannabinoid receptor. *Mol. Pharmacol.* 71, 976-984.

McPherson P.S., Kay B.K., and Hussain N.K. (2001) Signaling on the endocytic pathway. *Traffic.* 2, 375-384.

Menzaghi F., Howard R.L., Heinrichs S.C., Vale W., Rivier J., and Koob G.F. (1994) Characterization of a novel and potent corticotropin-releasing factor antagonist in rats. *J. Pharmacol. Exp. Ther.* 269, 564-572.

Merikangas K.R., Zhang H.P., Avenevoli S., Acharyya S., Neuenschwander M., and Angst J. (2003) Longitudinal trajectories of depression and anxiety in a prospective community study - The Zurich cohort study. *Arch. Gen. Psychiatry* 60, 993-1000.

Minichiello L., Korte M., Wolfer D., Kuhn R., Unsicker K., Cestari V., Rossi-Arnaud C., Lipp H.P., Bonhoeffer T., and Klein R. (1999) Essential role for TrkB receptors in hippocampus-mediated learning. *Neuron* 24, 401-414.

Mombaerts P., Wang F., Dulac C., Chao S.K., Nemes A., Mendelsohn M., Edmondson J., and Axel R. (1996) Visualizing an olfactory sensory map. *Cell* 87, 675-686.

Monory K., Massa F., Egertova M., Eder M., Blaudzun H., Westenbroek R., Kelsch W., Jacob W., Marsch R., Ekker M., Long J., Rubenstein J.L., Goebbels S., Nave K.A., During M., Klugmann M., Wolfel B., Dodt H.U., Zieglgansberger W., Wotjak C.T., Mackie K., Elphick M.R., Marsicano G., and Lutz B. (2006) The endocannabinoid system controls key epileptogenic circuits in the hippocampus. *Neuron* 51, 455-466.

Moreira F.A., Kaiser N., Monory K., and Lutz B. (2007) Reduced anxiety-like behaviour induced by genetic and pharmacological inhibition of the endocannabinoid-degrading enzyme fatty acid amide hydrolase (FAAH) is mediated by CB1 receptors. *Neuropharmacology.* In press.

Morozov A., Kellendonk C., Simpson E., and Tronche F. (2003) Using conditional mutagenesis to study the brain. *Biol. Psychiatry* 54, 1125-1133.

Moutsimilli L., Farley S., Dumas S., El Mestikawy S., Giros B., and Tzavara E.T. (2005) Selective cortical VGLUT1 increase as a marker for antidepressant activity. *Neuropharmacology* 49, 890-900.

Muller M.B. and Holsboer F. (2006) Mice with mutations in the HPA-system as models for symptoms of depression. *Biol. Psychiatry* 59, 1104-1115.

Muller M.B., Zimmermann S., Sillaber I., Hagemeyer T.P., Deussing J.M., Timpl P., Kormann M.S., Droste S.K., Kuhn R., Reul J.M., Holsboer F., and Wurst W. (2003) Limbic corticotropin-releasing hormone receptor 1 mediates anxiety-related behavior and hormonal adaptation to stress. *Nat. Neurosci.* 6, 1100-1107.

Muntoni A.L., Pillolla G., Melis M., Perra S., Gessa G.L., and Pistis M. (2006) Cannabinoids modulate spontaneous neuronal activity and evoked inhibition of locus coeruleus noradrenergic neurons. *Eur. J. Neurosci.* 23, 2385-2394.

Murphy L.L., Munoz R.M., Adrian B.A., and Villanua M.A. (1998) Function of cannabinoid receptors in the neuroendocrine regulation of hormone secretion. *Neurobiol. Dis.* 5, 432-446.

Muyrers J.P., Zhang Y., Testa G., and Stewart A.F. (1999) Rapid modification of bacterial artificial chromosomes by ET-recombination. *Nucleic Acids Res.* 27, 1555-1557.

Nagai T., Ibata K., Park E.S., Kubota M., Mikoshiba K., and Miyawaki A. (2002) A variant of yellow fluorescent protein with fast and efficient maturation for cell-biological applications. *Nat. Biotechnol.* 20, 87-90.

Naidu P.S., Varvel S.A., Ahn K., Cravatt B.F., Martin B.R., and Lichtman A.H. (2007) Evaluation of fatty acid amide hydrolase inhibition in murine models of emotionality. *Psychopharmacology (Berl)* 192, 61-70.

Nakada C., Ritchie K., Oba Y., Nakamura M., Hotta Y., Iino R., Kasai R.S., Yamaguchi K., Fujiwara T., and Kusumi A. (2003) Accumulation of anchored proteins forms membrane diffusion barriers during neuronal polarization. *Nat. Cell Biol.* 5, 626-632.

Navarro M., Hernandez E., Munoz R.M., delArco I., Villanua M.A., Carrera M.R.A., and deFonseca F.R. (1997) Acute administration of the CB1 cannabinoid receptor antagonist SR 141716A induces anxiety-like responses in the rat. *Neuroreport* 8, 491-496.

Nemeroff C.B. (1996) The corticotropin-releasing factor (CRF) hypothesis depression: New findings and new directions. *Mol. Psychiatry* 1, 336-342.

Nemeroff C.B. and Evans D.L. (1984) Correlation between the dexamethasone suppression test in depressed patients and clinical response. *Am. J. Psychiatry* 141, 247-249.

Nemeroff C.B. and Owens M.J. (2002) Treatment of mood disorders. *Nat. Neurosci.* 5 Suppl, 1068-1070.

Nemeroff C.B., Owens M.J., Bissette G., Andorn A.C., and Stanley M. (1988) Reduced corticotropin releasing factor binding sites in the frontal cortex of suicide victims. *Arch. Gen. Psychiatry* 45, 577-579.

Nemeroff C.B., Widerlov E., Bissette G., Walleus H., Karlsson I., Eklund K., Kilts C.D., Loosen P.T., and Vale W. (1984) Elevated concentrations of CSF corticotropin-releasing factor-like immunoreactivity in depressed patients. *Science* 226, 1342-1344.

Nibuya M., Morinobu S., and Duman R.S. (1995) Regulation of BDNF and trkB mRNA in rat brain by chronic electroconvulsive seizure and antidepressant drug treatments. *J. Neurosci.* 15, 7539-7547.

Nickel T., Sonntag A., Schill J., Zobel A.W., Ackl N., Brunnauer A., Murck H., Ising M., Yassouridis A., Steiger A., Zihl J., and Holsboer F. (2003) Clinical and neurobiological effects of tianeptine and paroxetine in major depression. *J. Clin. Psychopharmacol.* 23, 155-168.

Nielsen D.M. (2006) Corticotropin-releasing factor type-1 receptor antagonists: the next class of antidepressants? *Life Sci.* 78, 909-919.

Nielsen D.M., Carey G.J., and Gold L.H. (2004) Antidepressant-like activity of corticotropin-releasing factor type-1 receptor antagonists in mice. *Eur. J. Pharmacol.* 499, 135-146.

Nishikawa H., Hata T., Itoh E., and Funakami Y. (2004) A role for corticotropin-releasing factor in repeated cold stress-induced anxiety-like behavior during forced swimming and elevated plus-maze tests in mice. *Biol. Pharm. Bull.* 27, 352-356.

Nutt D.J. (2006) The role of dopamine and norepinephrine in depression and antidepressant treatment. *J. Clin. Psychiatry* 67 Suppl 6, 3-8.

Oberto A., Acquadro E., Bus T., Sprengel R., and Eva C. (2007) Expression patterns of promoters for NPY Y(1) and Y(5) receptors in Y(5)RitTA and Y(1)RVenus BAC-transgenic mice. *Eur. J. Neurosci.* 26, 155-170.

Olschowka J.A., O'Donohue T.L., Mueller G.P., and Jacobowitz D.M. (1982) The distribution of corticotropin releasing factor-like immunoreactive neurons in rat brain. *Peptides* 3, 995-1015.

Oropeza V.C., Mackie K., and Van Bockstaele E.J. (2007) Cannabinoid receptors are localized to noradrenergic axon terminals in the rat frontal cortex. *Brain Res.* 1127, 36-44.

Pagotto U., Marsicano G., Cota D., Lutz B., and Pasquali R. (2006) The emerging role of the endocannabinoid system in endocrine regulation and energy balance. *Endocrine Rev.* 27, 73-100.

Pagotto U., Marsicano G., Fezza F., Theodoropoulou M., Grubler Y., Stalla J., Arzberger T., Milone A., Losa M., Di Marzo V., Lutz B., and Stalla G.K. (2001) Normal human pituitary gland and pituitary adenomas express cannabinoid receptor type 1 and synthesize endogenous cannabinoids: First evidence for a direct role of cannabinoids on hormone modulation at the human pituitary level. *J. Clin. Endocrinol. Metab.* 86, 2687-2696.

Patel S. and Hillard C.J. (2006) Pharmacological evaluation of cannabinoid receptor ligands in a mouse model of anxiety: further evidence for an anxiolytic role for endogenous cannabinoid signaling. *J. Pharmacol. Exp. Ther.* 318, 304-311.

Patel S., Cravatt B.F., and Hillard C.J. (2005) Synergistic interactions between cannabinoids and environmental stress in the activation of the central amygdala. *Neuropsychopharmacology* 30, 497-507.

Patel S., Roelke C.T., Rademacher D.J., Cullinan W.E., and Hillard C.J. (2004) Endocannabinoid signaling negatively modulates stress-induced activation of the hypothalamic-pituitary-adrenal axis. *Endocrinology* 145, 5431-5438.

Paxinos G., Franklin K.B.J. (2001) The mouse brain in stereotaxic coordinates. (2nd edition), *Academic Press, San Diego*.

Pertwee R.G. (2005) Inverse agonism and neutral antagonism at cannabinoid CB1 receptors. *Life Sci.* 76, 1307-1324.

Petit-Demouliere B., Chenu F., and Bourin M. (2005) Forced swimming test in mice: a review of antidepressant activity. *Psychopharmacology* 177, 245-255.

Piomelli D. (2003) The molecular logic of endocannabinoid signalling. *Nat. Rev. Neurosci.* 4, 873-884.

Pi-Sunyer F.X., Aronne L.J., Heshmati H.M., Devin J., and Rosenstock J. (2006) Effect of rimonabant, a cannabinoid-1 receptor blocker, on weight and cardiometabolic risk factors in overweight or obese patients: RIO-North America: a randomized controlled trial. *JAMA* 295, 761-775.

Porsolt R.D., Bertin A., and Jalfre M. (1978) Behavioral despair in rats and mice - Strain differences and effects of imipramine. *Eur. J. Pharmacol.* 51, 291-294.

Porsolt R.D., Lepichon M., and Jalfre M. (1977) Depression - New animal-model sensitive to antidepressant treatments. *Nature* 266, 730-732.

Raadsheer F.C., Hoogendijk W.J., Stam F.C., Tilders F.J., and Swaab D.F. (1994a) Increased numbers of corticotropin-releasing hormone expressing neurons in the hypothalamic paraventricular nucleus of depressed patients. *Neuroendocrinology* 60, 436-444.

Raadsheer F.C., Oorschot D.E., Verwer R.W., Tilders F.J., and Swaab D.F. (1994b) Age-related increase in the total number of corticotropin-releasing hormone neurons in the human paraventricular nucleus in controls and Alzheimer's disease: comparison of the disector with an unfolding method. *J. Comp. Neurol.* 339, 447-457.

Raadsheer F.C., van Heerikhuize J.J., Lucassen P.J., Hoogendijk W.J., Tilders F.J., and Swaab D.F. (1995) Corticotropin-releasing hormone mRNA levels in the paraventricular nucleus of patients with Alzheimer's disease and depression. *Am. J. Psychiatry* 152, 1372-1376.

Radulovic J., Ruhmann A., Liepold T., and Spiess J. (1999) Modulation of learning and anxiety by corticotropin-releasing factor (CRF) and stress: differential roles of CRF receptors 1 and 2. *J. Neurosci.* 19, 5016-5025.

Rinaldi-Carmona M., Le D.A., Oustric D., Barth F., Bouaboula M., Carayon P., Casellas P., and Le F.G. (1998) Modulation of CB1 cannabinoid receptor functions after a long-term exposure to agonist or inverse agonist in the Chinese hamster ovary cell expression system. *J. Pharmacol. Exp. Ther.* 287, 1038-1047.

Rodgers R.J. (1997) Animal models of 'anxiety': where next? *Behav. Pharmacol.* 8, 477-496.

Rodgers R.J., Evans P.M., and Murphy A. (2005) Anxiogenic profile of AM-251, a selective cannabinoid CB1 receptor antagonist, in plus-maze-naive and plus-maze-experienced mice. *Behav. Pharmacol.* 16, 405-413.

Rodriguez C.I., Buchholz F., Galloway J., Sequerra R., Kasper J., Ayala R., Stewart A.F., and Dymecki S.M. (2000) High-efficiency deleter mice show that FLPe is an alternative to Cre-loxP. *Nat. Genet.* 25, 139-140.

Sambrook J., Russell D.W. (2001) Molecular cloning – A laboratory manual. Cold Spring Harbor Laboratory Press.
Sanchis-Segura C., Cline B.H., Marsicano G., Lutz B., and Spanagel R. (2004) Reduced sensitivity to reward in CB1 knockout mice. *Psychopharmacology* 176, 223-232.

Santucci V., Storme J.J., Soubrie P., and Le F.G. (1996) Arousal-enhancing properties of the CB1 cannabinoid receptor antagonist SR 141716A in rats as assessed by electroencephalographic spectral and sleep-waking cycle analysis. *Life Sci.* 58, L103-L110.

Scherrer G., Tryoen-Toth P., Filliol D., Matifas A., Laustriat D., Cao Y.Q., Basbaum A.I., Dierich A., Vonesh J.L., Gaveriaux-Ruff C., and Kieffer B.L. (2006) Knockin mice expressing fluorescent delta-opioid receptors uncover G protein-coupled receptor dynamics in vivo. *Proc. Natl. Acad. Sci. U. S. A.* 103, 9691-9696.

Schmidt-Supprian M., Wunderlich F.T., and Rajewsky K. (2007) Excision of the Frt-flanked neo (R) cassette from the CD19cre knock-in transgene reduces Cre-mediated recombination. *Transgenic Res.* 16, 657-660

Seligman M.E. (1978) Learned helplessness as a model of depression. Comment and integration. *J. Abnorm. Psychol.* 87, 165-179.

Seong E., Seasholtz A.F., and Burmeister M. (2002) Mouse models for psychiatric disorders. *Trends Genet.* 18, 643-650.

Shearman L.P., Rosko K.M., Fleischer R., Wang J., Xu S., Tong X.S., and Rocha B.A. (2003) Antidepressant-like and anorectic effects of the cannabinoid CB1 receptor inverse agonist AM251 in mice. *Behav. Pharmacol.* 14, 573-582.

Shih J.C. (2004) Cloning, after cloning, knock-out mice, and physiological functions of MAO A and B. *Neurotoxicology* 25, 21-30.

Shirayama Y., Chen A.C.H., Nakagawa S., Russell D.S., and Duman R.S. (2002) Brain-derived neurotrophic factor produces antidepressant effects in behavioral models of depression. *J. Neurosci.* 22, 3251-3261.

Sillaber I., Rammes G., Zimmermann S., Mahal B., Zieglgansberger W., Wurst W., Holsboer F., and Spanagel R. (2002) Enhanced and delayed stress-induced alcohol drinking in mice lacking functional CRH1 receptors. *Science* 296, 931-933.

Singewald N. and Philippu A. (1993) Catecholamine release in the locus coeruleus is modified by experimentally induced changes in haemodynamics. *Naunyn Schmiedebergs Arch. Pharmacol.* 347, 21-27.

Singewald N., Kaehler S., Hemeida R., and Philippu A. (1997) Release of serotonin in the rat locus coeruleus: effects of cardiovascular, stressful and noxious stimuli. *Eur. J. Neurosci.* 9, 556-562.

Slattery D.A., Hudson A.L., and Nutt D.J. (2004) Invited review: the evolution of antidepressant mechanisms. *Fundam. Clin. Pharmacol.* 18, 1-21.

Smagin G.N., Swiergiel A.H., and Dunn A.J. (1995) Corticotropin-releasing factor administered into the locus coeruleus, but not the parabrachial nucleus, stimulates norepinephrine release in the prefrontal cortex. *Brain Res. Bull.* 36, 71-76.

Soriano P. (1999) Generalized lacZ expression with the ROSA26 Cre reporter strain. *Nat. Genet.* 21, 70-71.

Souery D., Papakostas G.I., and Trivedi M.H. (2006) Treatment-resistant depression. *J. Clin. Psychiatry* 67 Suppl 6, 16-22.

Sparwasser T., Gong S., Li J.Y., and Eberl G. (2004) General method for the modification of different BAC types and the rapid generation of BAC transgenic mice. *Genesis* 38, 39-50.

Stalla G.K., Stalla J., Schopohl J., von W.K., and Muller O.A. (1986) Corticotropin-releasing factor in humans. I. CRF stimulation in normals and CRF radioimmunoassay. *Horm. Res.* 24, 229-245.

Staub D.R., Evans A.K., and Lowry C.A. (2006) Evidence supporting a role for corticotropin-releasing factor type 2 (CRF2) receptors in the regulation of subpopulations of serotonergic neurons. *Brain Res.* 1070, 77-89.

Steckler T. and Holsboer F. (1999) Corticotropin-releasing hormone receptor subtypes and emotion. *Biol. Psychiatry* 46, 1480-1508.

Stenzel-Poore M.P., Cameron V.A., Vaughan J., Sawchenko P.E., and Vale W. (1992) Development of Cushing's syndrome in corticotropin-releasing factor transgenic mice. *Endocrinology* 130, 3378-3386.

Steru L., Chermat R., Thierry B., and Simon P. (1985) The tail suspension test: a new method for screening antidepressants in mice. *Psychopharmacology (Berl)* 85, 367-370.

Summers C.H., Kampshoff J.L., Ronan P.J., Lowry C.A., Prestbo A.A., Korzan W.J., and Renner K.J. (2003) Monoaminergic activity in subregions of raphe nuclei elicited by prior stress and the neuropeptide corticotropin-releasing factor. *J. Neuroendocrinol.* 15, 1122-1133.

Svoboda K. and Yasuda R. (2006) Principles of two-photon excitation microscopy and its applications to neuroscience. *Neuron* 50, 823-839.

Swanson L.W., Sawchenko P.E., Rivier J., and Vale W.W. (1983) Organization of ovine corticotropin-releasing factor immunoreactive cells and fibers in the rat brain: an immunohistochemical study. *Neuroendocrinology* 36, 165-186.

Taltavull J.F., Chefer V.I., Shippenberg T.S., and Kiyatkin E.A. (2003) Severe brain hypothermia as a factor underlying behavioral immobility during cold-water forced swim. *Brain Res.* 975, 244-247.

Tappe-Theodor A., Agarwal N., Katona I., Rubino T., Martini L., Swiercz J., Mackie K., Monyer H., Parolaro D., Whistler J., Kuner T., and Kuner R. (2007) A molecular basis of analgesic tolerance to cannabinoids. *J. Neurosci.* 27, 4165-4177.

Tezval H., Jahn O., Todorovic C., Sasse A., Eckart K., and Spiess J. (2004) Cortagine, a specific agonist of corticotropin-releasing factor receptor subtype 1, is anxiogenic and antidepressive in the mouse model. *Proc. Natl. Acad. Sci. U. S. A.* 101, 9468-9473.

Thase M.E., Entsuah A.R., and Rudolph R.L. (2001) Remission rates during treatment with venlafaxine or selective serotonin reuptake inhibitors. *Br. J. Psychiatry* 178, 234-241.

Timpl P., Spanagel R., Sillaber I., Kresse A., Reul J.M., Stalla G.K., Blanquet V., Steckler T., Holsboer F., and Wurst W. (1998) Impaired stress response and reduced anxiety in mice lacking a functional corticotropin-releasing hormone receptor 1. *Nat. Genet.* 19, 162-166.

Tronche F., Kellendonk C., Kretz O., Gass P., Anlag K., Orban P.C., Bock R., Klein R., and Schutz G. (1999) Disruption of the glucocorticoid receptor gene in the nervous system results in reduced anxiety. *Nat. Genet.* 23, 99-103.

Tsigos C. and Chrousos G.P. (2002) Hypothalamic-pituitary-adrenal axis, neuroendocrine factors and stress. *J. Psychosom. Res.* 53, 865-871.

Tzavara E.T., Davis R.J., Perry K.W., Li X., Salhoff C., Bymaster F.P., Witkin J.M., and Nomikos G.G. (2003b) The CB1 receptor antagonist SR141716A selectively increases monoaminergic neurotransmission in the medial prefrontal cortex: implications for therapeutic actions. *Br. J. Pharmacol.* 138, 544-553.

Tzavara E.T., Perry K.W., Rodriguez D.E., Bymaster F.P., and Nomikos G.G. (2001) The cannabinoid CB1 receptor antagonist SR141716A increases norepinephrine outflow in the rat anterior hypothalamus. *Eur. J. Pharmacol.* 426, R3-R4.

Tzavara E.T., Wade M., and Nomikos G.G. (2003a) Biphasic effects of cannabinoids on acetylcholine release in the hippocampus: site and mechanism of action. *J. Neurosci.* 23, 9374-9384.

Ueyama T., Kawai Y., Nemoto K., Sekimoto M., Tone S., and Senba E. (1997) Immobilization stress reduced the expression of neurotrophins and their receptors in the rat brain. *Neurosci. Res.* 28, 103-110.

Urani A., Chourbaji S., and Gass P. (2005) Mutant mouse models of depression: Candidate genes and current mouse lines. *Neurosci. Biobehav. Rev.* 29, 805-828.

Uriguen L., Perez-Rial S., Ledent C., Palomo T., and Manzanares J. (2004) Impaired action of anxiolytic drugs in mice deficient in cannabinoid CB1 receptors. *Neuropharmacology* 46, 966-973.

Valenti M., Vigano D., Casico M.G., Rubino T., Steardo L., Parolaro D., and Di Marzo V. (2004) Differential diurnal variations of anandamide and 2-arachidonoyl-glycerol levels in rat brain. *Cell. Mol. Life Sci.* 61, 945-950.

Valentino R.J., Foote S.L., and ston-Jones G. (1983) Corticotropin-releasing factor activates noradrenergic neurons of the locus coeruleus. *Brain Res.* 270, 363-367.

Van Bockstaele E.J., Colago E.E., and Valentino R.J. (1998) Amygdaloid corticotropin-releasing factor targets locus coeruleus dendrites: substrate for the co-ordination of emotional and cognitive limbs of the stress response. *J. Neuroendocrinol.* 10, 743-757.

Van Deursen J., Fornerod M., Van R.B., and Grosveld G. (1995) Cre-mediated site-specific translocation between nonhomologous mouse chromosomes. *Proc. Natl. Acad. Sci. U. S. A.* 92, 7376-7380.

Van Gaal L.F., Rissanen A.M., Scheen A.J., Ziegler O., and Rossner S. (2005) Effects of the cannabinoid-1 receptor blocker rimonabant on weight reduction and cardiovascular risk factors in overweight patients: 1-year experience from the RIO-Europe study. *Lancet* 365, 1389-1397.

Van Gaalen M.M., Stenzel-Poore M.P., Holsboer F., and Steckler T. (2002) Effects of transgenic overproduction of CRH on anxiety-like behaviour. *Eur. J. Neurosci.* 15, 2007-2015.

Van Pett K., Viau V., Bittencourt J.C., Chan R.K., Li H.Y., Arias C., Prins G.S., Perrin M., Vale W., and Sawchenko P.E. (2000) Distribution of mRNAs encoding CRF receptors in brain and pituitary of rat and mouse. *J. Comp Neurol.* 428, 191-212.

Vinod K.Y., Arango V., Xie S., Kassir S.A., Mann J.J., Cooper T.B., and Hungund B.L. (2005) Elevated levels of endocannabinoids and CB1 receptor-mediated G-protein signaling in the prefrontal cortex of alcoholic suicide. *Biol. Psychiatry* 57, 480-486.

Viveros M.P., Marco E.M., and File S.E. (2005) Endocannabinoid system and stress and anxiety responses. *Pharmacol. Biochem. Behav.* 81, 331-342.

Wade M.R., Degroot A., and Nomikos G.G. (2006) Cannabinoid CB1 receptor antagonism modulates plasma corticosterone in rodents. *Eur. J. Pharmacol.* 551, 162-167.

Wang P.S., Simon G., and Kessler R.C. (2003) The economic burden of depression and the cost-effectiveness of treatment. *Int. J. Methods Psychiatr. Res.* 12, 22-33.

Wei Q., Lu X.Y., Liu L., Schafer G., Shieh K.R., Burke S., Robinson T.E., Watson S.J., Seasholtz A.F., and Akil H. (2004) Glucocorticoid receptor overexpression in forebrain: A mouse model of increased emotional lability. *Proc. Natl. Acad. Sci. U. S. A.* 101, 11851-11856.

Weidenfeld J., Feldman S., and Mechoulam R. (1994) Effect of the brain constituent anandamide, a cannabinoid receptor agonist, on the hypothalamo-pituitary-adrenal axis in the rat. *Neuroendocrinology* 59, 110-112.

Wenger T., Fernandez-Ruiz J.J., and Ramos J.A. (1999) Immunocytochemical demonstration of CB1 cannabinoid receptors in the anterior lobe of the pituitary gland. *J. Neuroendocrinology* 11, 873-878.

Wenger T., Jamali K.A., Juaneda C., Leonardelli J., and Tramu G. (1997) Arachidonyl ethanolamide (anandamide) activates the parvocellular part of hypothalamic paraventricular nucleus. *Biochem. Biophys. Res. Commun.* 237, 724-728.

Wenger T., Ledent C., and Tramu G. (2003) The endogenous cannabinoid, anandamide, activates the hypothalamo-pituitary-adrenal axis in CB1 cannabinoid receptor knockout mice. *Neuroendocrinology* 78, 294-300.

West A.P. (1990) Neurobehavioral Studies of Forced Swimming - the Role of Learning and Memory in the Forced Swim Test. *Prog. Neuropsychopharmacol. Biol. Psychiatry* 14, 863-877.

Willner P. (1997) Validity, reliability and utility of the chronic mild stress model of depression: a 10-year review and evaluation. *Psychopharmacology (Berl)* 134, 319-329.

Witkin J.M., Tzavara E.T., and Nomikos G.G. (2005a) A role for cannabinoid CB1 receptors in mood and anxiety disorders. *Behav. Pharmacol.* 16, 315-331.

Witkin J.M., Tzavara E.T., Davis R.J., Li X., and Nomikos G.G. (2005b) A therapeutic role for cannabinoid CB1 receptor antagonists in major depressive disorders. *Trends Pharmacol. Sci.* 26, 609-617.

Wong M.L., Kling M.A., Munson P.J., Listwak S., Licinio J., Prolo P., Karp B., McCutcheon I.E., Geracioti T.D., DeBellis M.D., Rice K.C., Goldstein D.S., Veldhuis J.D., Chrousos G.P., Oldfield E.H., Mccann S.M., and Gold P.W. (2000) Pronounced and sustained central hypernoradrenergic function in major depression with melancholic features: Relation to hypercortisolism and corticotropin-releasing hormone. *Proc. Natl. Acad. Sci. U. S. A.* 97, 325-330.

Wotjak C.T. (2005) Role of endogenous cannabinoids in cognition and emotionality. *Mini-Rev. Med. Chem.* 5, 659-670.

Yamada S., Yamamoto M., Ozawa H., Riederer P., and Saito T. (2003) Reduced phosphorylation of cyclic AMP-responsive element binding protein in the postmortem orbitofrontal cortex of patients with major depressive disorder. *J. Neural Transm.* 110, 671-680.

Zambrowicz B.P., Imamoto A., Fiering S., Herzenberg L.A., Kerr W.G., and Soriano P. (1997) Disruption of overlapping transcripts in the ROSA beta geo 26 gene trap strain leads to widespread expression of beta-galactosidase in mouse embryos and hematopoietic cells. *Proc. Natl. Acad. Sci. U. S. A.* 94, 3789-3794.

Zhang Y., Buchholz F., Muyrers J.P., and Stewart A.F. (1998) A new logic for DNA engineering using recombination in Escherichia coli. *Nat. Genet.* 20, 123-128.

Zheng B., Sage M., Sheppeard E.A., Jurecic V., and Bradley A. (2000) Engineering mouse chromosomes with Cre-loxP: range, efficiency, and somatic applications. *Mol. Cell Biol.* 20, 648-655.

Zhou M.J. and PanchukVoloshina N. (1997) A one-step fluorometric method for the continuous measurement of monoamine oxidase activity. *Anal. Biochem.* 253, 169-174.

Zimmer A., Zimmer A.M., Hohmann A.G., Herkenham M., and Bonner T.I. (1999) Increased mortality, hypoactivity, and hypoalgesia in cannabinoid CB1 receptor knockout mice. *Proc. Natl. Acad. Sci. U. S. A.* 96, 5780-5785.

Zobel A.W., Nickel T., Kunzel H.E., Ackl N., Sonntag A., Ising M., and Holsboer F. (2000) Effects of the high-affinity corticotropin-releasing hormone receptor 1 antagonist R121919 in major depression: the first 20 patients treated. *J. Psychiatr. Res.* 34, 171-181.

Zorrilla E.P., Valdez G.R., Nozulak J., Koob G.F., and Markou A. (2002) Effects of antalarmin, a CRF type 1 receptor antagonist, on anxiety-like behavior and motor activation in the rat. *Brain Res.* 952, 188-199.

6 APPENDIX

6.1 Generated vectors and oligonucleotide sequences

Supplementary Table 6.1.1 List of plasmids

Plasmid	Description	Reference or source
p705-Cre	Based on the pSC101 temperature-sensitive origin which allows weak expression of Cre recombinase from the lambdaPR promoter at 30 ºC and strong expression at 37 ºC	Generous gift from Dr. Z. Zhang (Zhang et al., 1998)
pBluescript II KS+ (pBS)	General cloning vector	Stratagene, Heidelberg, Germany
pBS-3p(A) M.305	pBluescript with an integrated transcriptional STOP cassette (SV40-polyA + bGH-polyA)	Generous gift from Dr. J.H. Sitz
pcDNA3.1	General cloning vector allowing eukaryotic expression	Invitrogen, Mannheim, Germany
pcDNA3-CB1	pcDNA3.1 with the CB1 cds integrated in the multiple cloning site	Generous gift from Dr. M. Marsicano
pCRE-Luc	Luciferase reporter gene vector under a CRE element activated promoter	Clontech, Mountain View, CA, USA
pCRRH-R1-EGFP	pEGFP-C1 containing the CRH-R1 cds fused to the C-terminus of EGFP	Generous gift from Dr. J. Breul
pCS2-Venus	pCS2 expression vector containing the Venus cds	Generous gift from Dr. A. Miyawaki
pDsRed2-C1	DsRed2 cloning vector that allows fusions to the N-terminus of DsRed2 and eukaryotic expression	Clontech, Mountain View, CA, USA

pEGFP-N1	EGFP cloning vector that allows fusions to the N-terminus of EGFP and eukaryotic expression	Clontech, Mountain View, CA, USA
pEYFP-N1	EYFP cloning vector that allows fusions to the N-terminus of EGFP and eukaryotic expression	Clontech, Mountain View, CA, USA
pJ.182	pBluescript containing a Tn5-neomycin resistance cassette	Generous gift from Dr. J.H. Sitz
pMS1	pEGFP-N1 containing the CB1 cds fused N-terminal to EGFP	This study
pMS11	pCB1-EYFP-RH = pMS1 with EGFP exchanged for EYFP-RH	This study
pMS12	pJ.182-Tn5-neo-*FRT*-RH = J.182 with an inserted *FRT*-RH oligo at the 3'-end of Tn5-neo	This study
pMS14	pCB1-EYFP-*FRT* = pMS1 with EGFP exchanged for EYFP-*FRT*	This study
pMS15	pBS-3p(A) M.305 with an integrated LH-*lox2272* fragment 5' of the transcriptional STOP cassette	This study
pMS17	pMS14 with the Tn5-neo-*FRT*-RH cassette inserted at the 3' end of CB1-EYFP-*FRT* creating a CB1-EYFP-*FRT*-Tn5-neo-*FRT*-RH cassette within the vector	This study
pMS17V	pMS17 with the EYFP cds exchanged against the Venus cds	This study
pMS18	pMS11 where a *lox2272*-CB1-Intron fragment had been introduced upstream of the CB1 cds	This study
pMS19	pMS18 with the LH-*lox2272*-STOP and *FRT*-Tn5-neo-*FRT* cassettes inserted at the 3' end of *lox2272*-Intron-CB1-EYFP-RH creating a LH-*lox2272*-STOP-*FRT*-Tn5-neo-*FRT*-*lox2272*-Intron-CB1-EYFP-RH cassette within the vector	This study

pMS19V	pMS19 with the EYFP cds exchanged against the Venus cds	This study
pMS4	pEGFP-N1 containing the CB1 cds (the N-terminus of the receptor was shortened by 68 amino acids) fused N-terminal to EGFP	This study
pMS5	pEGFP-N1 containing the CB1 cds (the N-terminus of the receptor was shortened by 90 amino acids) fused to the N-terminus of EGFP	This study
pMS9	pMS1 with an integrated STOP codon and *EcoR*I site after the CB1 cds	This study

Supplementary Table 6.1.2 List of oligonucleotides

Oligonucleotide	Sequence (5'→ 3')
CB1-N1-26-Fw	GCTCAGATGAGCTCGCCGCCACCATGGAGAACGAGGACAACATCCAGTGTG
CB1-N1-52-Fp	GCTCAGATGAGCTCGCCGCCACCATGGACAACTCCCCGTTGGTTCCAGCA
CB1-N1-Fw	CCAGTAGTGAGCTCGCCGCCACCATGAAGTCGATCTTAGACGGCCTTG
CB1-N1-Rv	CCTAGTACGGTACCGTGCCGCCGCCCAGAGCCTCGGCAGACGTGTCTG
CB1-Rv	CTTGTGCAGGCAGTCTGAGT
EYFP-*FRT*-Rv	GCATAGACTGCGGCCGCGATCGGAAGTTCCTATACTTTCTAGAGAATAGGAACTTCCTCGAGTTACTTGTACAGCTCGTCCATGCCGAG
EYFP-Fw	GTGTACGGTGGGAGGTCTATATAAGCAGAG
EYFP-RH-Rv	GCTAGACTGCGGCCGCAGAGCTCTAAAAAAAAAAATTTTCTTTTTCTGGGCAGCCACAAAAGCAGCAGGCGGCGCGCCTTACTTGTACAGCTCGTCCATGCCGAG
Founder-Neo-Fw	TGCTCCTGCCGAGAAAGTATCCATCATGGC
Founder-Neo-Rv	CGCCAAGCTCTTCAGCAATATCACGGGTAG

222

LH-*lox2272*-STOP-Fw	CGCTAGCCCTAGCCACATCATCACAGATTTCTATGTACTTGATAGTAGAATCCTAGATAACTTCGTATAAAGTATCCTATACGAAGTTATACTAGTT
LH-*lox2272*-STOP-Rv	CTAGAACTAGTATAACTTCGTATAGGATACTTTATACGAAGTTATCTAGGATTCTACTATCAAGTACATAGAAATCTGTGATGATGTGGCTAGGGCTAGCGAGCT
lox2272-Intron-CB1-Fw	GTAGCTCTCGAGTGACATGTACGCGTATAACTTCGTATAAAGTATCCTATACGAAGTTATGGGCTAACTCTTCCCATGAGTTGCAC
lox2272-Intron-CB1-Rv	GAAGTATCCTAATTTGGATGCCATGTCTC
pMS17V-L-Fw	CTGTTCCTCACGGCCATC
pMS17V-L-Rv	CAGCTCCTCGCCCTTGCT
pMS17V-R-Fw	GTTCTTCTGATAAGCTTGTTTAAAC
pMS19V-L-Fw	CAGCACTGTGCCCTTGGAAAG
pMS19V-L-Rv	GATTATGATCATTACTTATCTAGAACTAGT
pMS19V-R-Fw	CACATGGTCCTGCTGGAGT
pMS19V-R-Rv	CAGATTTGGAAGCCAACGTT
pMS1-oligo-STOP codon-Fw	GGAAAGCTGCATCAAGAGCACTGTTAAGATCGCCAAGGTGACCATGTCTGTGTCCACAGACACGTCTGCCGAGGCTCTGTGAGAATTCA
pMS1-oligo-STOP codon-Rv	CCGGTGAATTCTCACAGAGCCTCGGCAGACGTGTCTGTGGACACAGACATGGTCACCTTGGCGATCTTAACAGTGCTCTTGATGCAGCTTTCCGC
Tn5-neo-*FRT*-RH-Fw	AGCTTGTTTAAACGAAGTTCCTATTCTCTAGAAAGTATAGGAACTTCACGCGTGCCTGCTGCTTTTGTGGCTGCCCAGAAAAAGAAAATTTTTTTTTTTAGCCTAGGG
Tn5-neo-*FRT*-RH-*Pvu*I-Fw	GCTAGACTAGTCAGTCGATCGTGGACAGCAAGCGAACCGGAATTG
Tn5-neo-*FRT*-RH-*Pvu*I-Rv	CACACAGGAAACAGCTATGACCATG
Tn5-neo-*FRT*-RH-Rv	GTACCCCTAGGCTAAAAAAAAAAATTTTCTTTTTCTGGGCAGCCACAAAAGCAGCAGGCACGCGTGAAGTTCCTATACTTTCTAGAGAATAGGAACTTCGTTTAAACA
Tn5-neo-Fw	TGGACAGCAAGCGAACCGGAATTGC

Tn5-neo-Rv	TCAGAAGAACTCGTCAAGAAGGCG
Venus-Fw	GTCATCGACCGGTCGCCACCATGGTGAGCAAGGGCGAGGAG
Venus-Fw	GACGTAAACGGCCACAAGT
Venus-Rv	GTACAGACTGGCGCGCCTTACTTGTACAGCTC
Venus-Rv	CTTCAGCTCGATGCGGTTC

6.2 Acknowledgements

Many people have helped me in the course of my Ph.D. thesis, and any merit in it is in large measure due to them.

6.3 Epilogue

"Far out in the uncharted backwaters of the unfashionable end of the western spiral arm of the Galaxy lies a small unregarded yellow sun.

Orbiting this at a distance of roughly ninety-two million miles is an utterly insignificant little blue green planet whose ape-descended life forms are so amazingly primitive that they still think digital watches are a pretty neat idea." … (The Hitchhikers's Guide to the Galaxy by Douglas Adams)
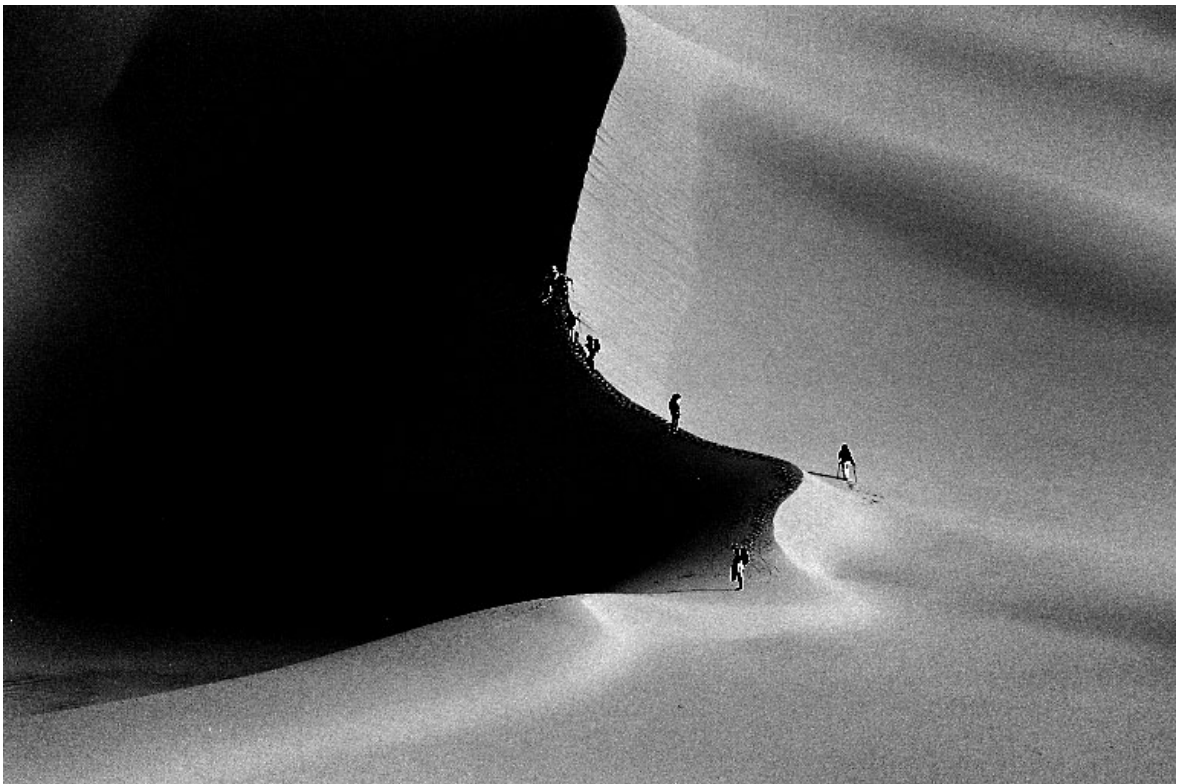
(Akakus, Libya, 2006)

Manchmal ist es gut, Dinge in die richtige Perspektive zu setzen.

6.5 Kapitel 1 und 2 aus "Das Endocannabinoid-System – Physiologie und klinische Bedeutung" (UNI-MED Science; Editor Prof. V. Schusdziarra; Erste Auflage, 2006); Mit freundlicher Genehmigung des UNI-MED Science Verlags.

Der Leser wird gebeten, darauf zu achten, dass in Abbildung 2.6 ein Fehler vorliegt: $CB1^{+/+}$ und $CB1^{-/-}$ wurden versehentlich vertauscht.

Physiologie und Pharmakologie des Endocannabinoid-Systems

(M. Steiner, B. Lutz)

1. Physiologie und Pharmakologie des Endocannabinoid-Systems

1.1. Der Ausgangspunkt der Entdeckung

Seit jeher interessierten sich die Menschen in verschiedensten Kulturkreisen für die spezifischen Wirkungen von Extrakten und Präparaten aus der Pflanzen- und Tierwelt. Viele davon hielten letztlich Einzug in die Volksmedizin, wo sie über Jahrhunderte ihren Platz als Mittel gegen unterschiedlichste kleinere und größere Leiden fanden. Die Fortschritte in der Chemie und Medizin ab Mitte des 19. Jahrhunderts förderten jedoch das Bedürfnis, die einzelnen aktiven Substanzen der Naturprodukte in reiner Form zu isolieren, um sie dann mit definiertem Wirkungsspektrum als Arzneimittel anwenden zu können. Meist beruhen die pharmakologischen Wirkungen der Reinsubstanzen darauf, dass sie in ganz bestimmte, dem Körper eigene Stoffwechselprozesse eingreifen. Das Studium dieser Stoffwechselvorgänge führte in der Vergangenheit zur Entdeckung von zahlreichen neuen, grundlegend wichtigen, körpereigenen Prozessen. Diese sind für die Aufrechterhaltung der normalen Physiologie wichtig, können jedoch unter pathologischen Zuständen des Körpers in gewissen Fällen auch außer Kontrolle geraten. Ausgangspunkte solcher Entdeckungen waren z.B. Morphin (aus der Pflanze *Papaver somniferum*), Muskarin (aus dem Fliegenpilz *Amanita muscaria*) und Cannabinoide (aus der Pflanze *Cannabis sativa*), um nur einige wenige zu nennen.

Die Geschichte der Hanfpflanze *Cannabis sativa* ist bemerkenswert. Sowohl die politischen und gesellschaftlichen Ansichten über *Cannabis* als auch die Intensität, mit der an der Aufklärung seiner Wirkmechanismen geforscht wurde, unterlagen starken Zeitströmungen. Während der letzten fünfzehn Jahre jedoch wurde ein bedeutender Erkenntnisfortschritt erreicht. Dies trifft sowohl für den Pflanzenabkömmling Δ^9-Tetrahydrocannabinol (THC), als auch für jene Cannabinoide zu, die im Körper von Mensch und Tier natürlicherweise vorkommen.

Die körpereigenen Cannabinoide (auch Endocannabinoide genannt) sind Bestandteil eines wichtigen regulatorischen Systems unseres Organismus und sind in diverse physiologische Prozesse involviert. Dieses System wird als das Endocannabinoid-System bezeichnet. Seine pharmakologische Beeinflussung - sowohl durch Stimulation als auch durch Hemmung - stellt eine viel versprechende Strategie dar, um Dysregulationen des Endocannabinoid-Systems zu normalisieren, die verschiedenen pathologischen Zuständen des Körpers zu Grunde liegen können. Solche medizinischen Anwendungen werden in den folgenden Kapiteln besprochen.

Ziel dieses Kapitels ist es zu beschreiben, wie die pflanzlichen und körpereigenen Cannabinoide wirken. Diese Erkenntnisse bilden auch die Grundlage, um später mögliche medizinische Applikationen aufzuzeigen. Eine kurze Darstellung der jahrtausend alten Geschichte der Anwendungen von *Cannabis sativa* wird vorangestellt. Es ist zweifelsfrei eine faszinierende Geschichte, die schließlich in die Entdeckung der körpereigenen Cannabinoide und deren Bindungspartner, der so genannten Cannabinoid-Rezeptoren, mündete. Die während der letzten Jahre äußerst stark ansteigende Anzahl von Publikationen über die physiologischen und pathophysiologischen Funktionen des Endocannabinoid-Systems kann als ein Abbild seiner großen Bedeutung für den Körper gesehen werden.

1.2. Die Geschichte einer alten Droge

Die Hanfpflanze *Cannabis sativa*, deren Präparationen auch als Marihuana und Haschisch bekannt sind, ist eine der ältesten Kulturpflanzen, die nicht wegen ihres Nahrungsgehaltes angebaut worden ist. Vor allem die Fasern der Pflanze waren ein beliebter Rohstoff. Sie wurden zur Produktion von Stoffen, Seilen und Papier verwendet. Aber auch die Extrakte der Pflanze wurden genutzt, vor allem als Heil- oder Genussmittel . Die ersten historischen Aufzeichnungen gehen in das 5. Jahrtausend v.Chr. in China zurück (☞ Abb. 1.1). Die Pflanze wurde in Enzyklopädien über pflanzliche Heilmittel ausführlich beschrieben, und *Cannabis*-Extrakte wurden in der Volksmedizin angewandt; indes,
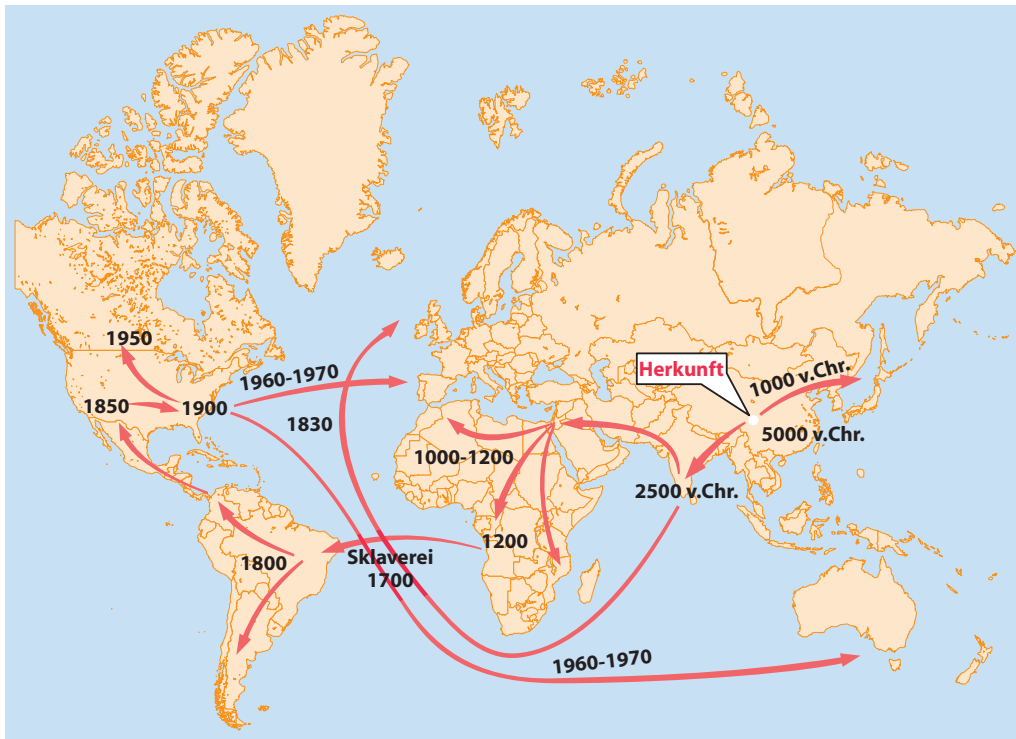
Abb. 1.1: Verbreitung der Hanfplanze *Cannabis sativa*. *Cannabis* hat eine ungewöhnlich ereignisreiche 7.000-jährige Geschichte erfahren.

der Anbau zum Zwecke der Fasergewinnung für die Textilherstellung überwog.

Von China breitete sich die Hanfpflanze nach Indien aus. Im heiligen indischen Text "Atharva Veda" (eines der heiligen Bücher der Hindu-Religion von 1.440 v.Chr.) wurde Marihuana als heiliger Pflanzenextrakt aufgelistet, mit dessen Hilfe man z.B. Stress und Angstzustände lösen könne. Typische Anwendungen waren auch die Behandlung von Schmerzen, Krämpfen und Appetitlosigkeit. Hanf war aber auch wegen seiner psychotropen Wirkungen als Vergnügungsdroge wohl bekannt.

Von Indien drang die Pflanze weiter in die westliche Welt vor. Im Zeitalter der Griechen und Römer (ca. 500 v.Chr. bis ca. 300 n.Chr.) fand Hanf vor allem wiederum als Quelle von Fasern Anwendung, um Seile und Segel herzustellen. Von wenigen medizinischen Applikationen wurde berichtet; hingegen wurde die Pflanze nicht als Vergnügungsdroge verwendet, da man Alkohol bevorzugte. Dies stand ganz im Gegensatz zur Situation im arabischen Kulturkreis. Da der Islam den Konsum

von Alkohol verbietet, wurde *Cannabis* nicht nur als eine Art Volksmedizin benutzt, sondern war auch als Vergnügungsdroge weit verbreitet. Im Zuge der arabischen Invasion von 900 bis 1200 n.Chr. wurde die Pflanze von Ägypten über Marokko auch in der westlichen, mediterranen Region bekannt. Die arabische Kultur war auch der Ausgangspunkt für dessen Verbreitung auf dem afrikanischen Kontinent. Auf dem Weg der Sklaventransporte von Afrika gelangte *Cannabis* nach Südamerika (18. Jh.), und dann später von dort in die Südstaaten der USA (19. Jh.). Während der Ära von Napoleon um 1800 n.Chr. brachten Soldaten die Hanfpflanze wegen ihrer psychotropen Wirkungen aus Ägypten nach Europa, wo sie jedoch erst nur beschränkt Verbreitung fand. Britische Ärzte im indischen Kolonialreich der ersten Hälfte des 19. Jahrhunderts berichteten über die medizinischen Anwendungen von *Cannabis* (z.B. gegen Tollwut, Rheumatismus, Epilepsie, Krämpfe und Schmerzen) und brachten die Pflanze nach Europa, wo sie dann trotz ihrer bekannten psychotropen Wirkungen als Heilmittel in der Medizin recht bekannt wurde.

Nach einem kurzen Höhepunkt Mitte des 19. Jahrhunderts nahm die Popularität schnell ab. Anfangs des 20. Jahrhunderts wurde in den USA *Cannabis* nur noch in wenigen großen Städten der Südstaaten, v.a. von Leuten mexikanischen Ursprungs und von afrikanisch-amerikanischen Jazz-Musikern konsumiert. Die Prohibition von 1932 setzte einen vorläufigen Schlussstrich unter den legalen Gebrauch von Hanf. Als Droge der Protestbewegungen in den 60er Jahren fand Marihuana dann schließlich doch große Verbreitung in den westlichen, industrialisierten Zivilisationen. Während der letzten Jahre wandelte sich *Cannabis* zu einer Lifestyledroge der Jugendlichen mit stark steigenden Prävalenzzahlen und mit sehr ernst zu nehmenden, negativen Konsequenzen für die Gesellschaft.

## 1.3. Die psychoaktive Substanz aus *Cannabis sativa* und das Endocannabinoid-System

Die Aufklärung der psychoaktiven Komponente von *Cannabis sativa* ist geprägt von mehreren fehlgeschlagenen Versuchen. Im Unterschied zu vielen anderen pflanzlichen Naturstoffen, die ebenfalls zur Klasse der Alkaloide gehören, sind Cannabinoide nicht in Wasser, sondern nur in Fetten, Ölen und organischen Lösungsmitteln gut löslich. Diese Eigenschaft verhinderte die Kristallisation eines reinen Cannabinoids und die damit verbundene recht einfache Art der Isolation. Wohl stellten Chemiker schon um 1850 angereicherte Alkoholextrakte aus *Cannabis sativa* her. Es war ein stark visköses, rotes Harz. Dieses Harz konnte auch die typischen Effekte verursachen, wie sie bei *Cannabis sativa* beobachtet wurden. Die weiteren Reinigungsschritte aber verursachten ein inaktives Abbauprodukt, das *Cannabinol* genannt wurde (☞ Abb. 1.2).
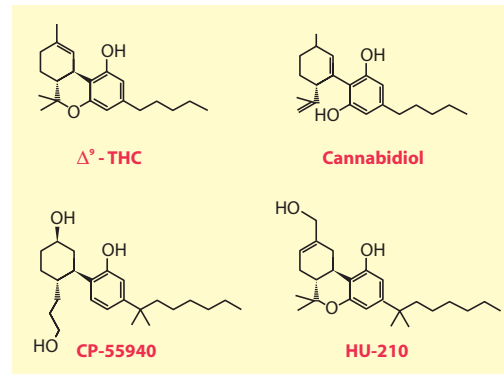
Abb. 1.2: Chemische Strukturformeln einiger Cannabinoide. **Cannabidiol** und Δ^9**-Tetrahydrocannabinol** (Δ^9**-THC**) kommen natürlicherweise in der Pflanze *Cannabis sativa* vor. Nur Δ^9-THC besitzt psychotrope Eigenschaften, da es an Cannabinoid-Rezeptoren binden kann. **CP-55490** und **HU-210** sind Cannabinoid-Rezeptor-Agonisten, dem Δ^9-THC verwandte Stoffe mit viel höherer Aktivität. Deshalb werden sie oft in der Forschung verwendet.

Es wurde in der Folge irrtümlicherweise für die psychoaktive Komponente von *Cannabis sativa* gehalten, war jedoch in Wirklichkeit mit Spuren der eigentlichen psychoaktiven Substanz verunreinigt. Um 1920 und nochmals in den 40er Jahren wurde vergeblich der Versuch unternommen, die psychoaktive Komponente von *Cannabis sativa* zu isolieren. Jedoch vergingen noch mehr als 20 Jahre, bis die Isolation 1964 endlich der israelischen Gruppe von Raphael Mechoulam mittels neuer Aufreinigungsmethoden gelang. Die begehrte Substanz wurde als Δ^9-Tetrahydrocannabinol (THC) identifiziert (☞ Abb. 1.2 und Tab. 1.1). Diese Entdeckung entfachte unter der Forschergemeinde ein reges Interesse, die Wirkungen von THC auf den Organismus im Detail aufzuklären und zu verstehen. Hier stellte sich vor allem die Frage nach den körpereigenen, zellulären Bindungspartnern für THC. Jedoch auch diese Suche gestaltete sich schwieriger als erwartet. Erst die Entwicklung von neuen, spezifischen und sehr aktiven THC-ähnlichen Substanzen wie z.B. CP-55,940 oder HU-210 (☞ Abb. 1.2) ermöglichte es, Cannabinoid-sensitive Regionen im Gehirn zu identifizieren. 1990 wurde schließlich ein spezifischer Bindungspartner, ein Rezeptor für THC charakterisiert. Er wurde Cannabinoid-Rezeptor Typ 1 (CB1-Rezeptor) getauft. Kurze Zeit später, 1992, wurde auch das erste körpereigene Cannabinoid,

Anandamid (☞ Abb. 1.3), entdeckt, und ein Jahr später sogar ein zweiter Cannabinoid-Rezeptor (CB2-Rezeptor).

Anandamid   **2-Arachidonoylglycerol**
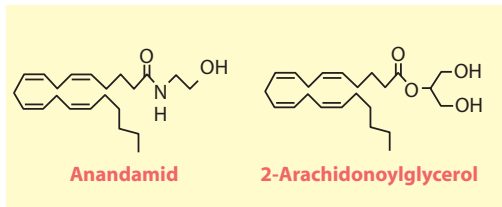
Abb. 1.3: Chemische Strukturformeln der zwei wichtigsten Endocannabinoide. Beide Verbindungen enthalten als ein Strukturelement die Fettsäure Arachidonsäure, die entweder über eine Amid-Bindung (bei **Anandamid**) oder eine Ester-Bindung (bei **2-Arachidonoylglycerol, 2-AG**) mit einem Alkohol verknüpft sind.

Geschichte des Endocannabinoid-Systems	
1964	Chemische Identifizierung von THC
1990	Klonierung des CB1-Rezeptors
1992	*Anandamid*: Identifizierung des ersten Endocannabinoids
1993	Klonierung des CB2-Rezeptors
1994	*Rimonabant*: Identifizierung des ersten CB1-Rezeptor-Blockers
1995	*2-AG*: Identifizierung des zweiten Endocannabinoids
1999	Erste Charakterisierung von transgenen Mäusen, denen der CB1-Rezeptor fehlt
2000	Erste Charakterisierung von transgenen Mäusen, denen der CB2-Rezeptor fehlt
2001	Endocannabinoide als retrograde Neurotransmitter beschrieben
2004	*Rimonabant*: Erste Ergebnisse aus klinischen Versuchen der Phase III

Tab. 1.1: Meilensteine in der Erforschung des Endocannabinoid-Systems.

Vor allem die Entdeckung der Cannabinoid-Rezeptoren stellte gewissermaßen den wissenschaftlichen Durchbruch auf dem Gebiet der Cannbinoid-Forschung dar.

Seitdem hat sich um die Erforschung des Endocannabinoid-Systems, bestehend aus

- Cannabinoid-Rezeptoren
- Endocannabinoiden und
- ihren synthetisierenden und abbauenden Enzymen

eine rasant wachsende Forschergemeinde in aller Welt geschart. Es besteht heute kein Zweifel darüber, dass gerade das Endocannabinoid-System ein höchst komplexes und äußerst wichtiges, physiologisches System des Körpers darstellt, das in mannigfaltige Stoffwechselfunktionen eingreift. Es scheint vor allem in die Aufrechterhaltung des Körpergleichgewichtes ("Homöostase") involviert zu sein und kann auch als ein System der "Stress"-Erholung betrachtet werden.

Ein Überblick über die physiologischen Funktionen wird in Tab. 1.2 gewährt; auf Details wird in den folgenden Kapiteln eingegangen werden.

Endocannabinoid-System - Physiologische Funktionen	
Entspannen	↓ Schmerzen
	↓ Körpertemperatur
	↓ Stresshormone
	↓ Muskelspannung
Ausruhen	↓ motorische Aktivität
Vergessen	↓ angsterfüllte Erinnerungen
	↓ emotionaler Stress
Schützen	↓ Erregungsleitung im Gehirn
	↓ Entzündungen
Essen	↑ Appetit
	↑ Belohnungsverhalten

Tab. 1.2: Physiologische Funktionen des Endocannabinoid-Systems.

1.4. Die Cannabinoid-Rezeptoren

Zwei verschiedene Cannabinoid-Rezeptoren wurden bisher im Menschen gefunden. Nach der Reihenfolge ihrer Entdeckung nannte man sie

- Cannabinoid-Rezeptor-Typ 1 (CB1-Rezeptor) und
- Cannabinoid-Rezeptor-Typ 2 (CB2-Rezeptor).

CB1-Rezeptoren sind evolutionär betrachtet über verschiedene Spezies stark konserviert; man findet sie z.B. nicht erst in Säugetieren, sondern bereits in niederen Spezies wie dem Manteltier. Auch Fische besitzen einen CB1 verwandten Rezeptor. Die Sequenz des CB2-Rezeptors hingegen ist weniger konserviert und divergiert zwischen verschiedenen Spezies. Erstaunlicherweise konnte bis heute ein Endocannabinoid-System weder in Insekten (z.B. in der Fruchtfliege *Drosophila melanogaster*) noch in Würmern (z.B. im Fadenwurm *Caenorhabditis elegans*), nachgewiesen werden.

Mittlerweile existiert eine ganze Reihe von Forschungsergebnissen, die nicht mit Wirkungen der klassischen Cannabinoid-Rezeptoren erklärt werden können (z.B. Effekte von Cannabinoiden in genetisch veränderten Mäusen, die keine Cannabinoid-Rezeptoren besitzen). Es häufen sich daher die Hinweise dafür, dass es eventuell noch weitere Cannabinoid-Rezeptoren geben könnte. Vor allem im Endothelgewebe und im Gehirn wären weitere Rezeptoren vorstellbar. Die Klonierung und damit der endgültige Beweis der Existenz solcher Rezeptoren steht aber bisher noch aus.

1.4.1. Vorkommen der Cannabinoid-Rezeptoren im Körper

Der CB1-Rezeptor wurde zuerst vor allem im Gehirn und Rückenmark beschrieben. Tatsächlich zählt der CB1-Rezeptor von allen bekannten Neurotransmitter- und Hormon-Rezeptoren im Gehirn zu denen, die am häufigsten vorhanden sind. Während der letzten Jahre wurde der CB1-Rezeptor auch in peripheren Organen nachgewiesen, wenn auch in viel geringeren Konzentrationen. So ist er im peripheren Nervensystem, z.B. der Spinalganglien und des Gastrointestinaltraktes, im Herz, im Hoden sowie in Fett-, Leber-, Immun- und Endothelzellen präsent (☞ Tab. 1.3).

Der CB2-Rezeptor andererseits wurde ursprünglich vor allem in Organen des Immun- und hämatopoietischen Systems gefunden. So exprimieren z.B. Immunzellen wie Makrophagen, B- und T-Zellen, Monozyten und Neutrophile sehr viele CB2-Rezeptoren. Weiterhin wird er ebenso in den Immunzellen des Gehirns, den sogenannten Mikrogliazellen exprimiert. Aber CB2 kommt auch in "Nicht-Immunzellen" vor, wie z.B. in Hautzellen und sogar – wie kürzlich entdeckt – in Neuronen des Stammhirns (☞ Tab. 1.3).

Cannabinoid-Rezeptoren - Vorkommen	
CB1	• Zentrales Nervensystem (Gehirn und Rückenmark) • Peripheres Nervensystem • Fettgewebe (Adipozyten) • Leber (Hepatozyten) • Vaskuläres System (Endothel), Herz • Zellen des Immunsystems • Hoden
CB2	• Organe des Immunsystems (Milz, Thymus, Knochenmark, Lymphsystem) • Immunzellen (Makrophagen, B-Zellen, T-Zellen, Neutrophile, Monozyten) • Gehirn (Mikrogliazellen und Neuronen des Stammhirns) • Haut (Keratinozyten)

Tab. 1.3: Vorkommen der Cannabinoid-Rezeptoren.

1.4.2. Wirkungsweise und zelluläre Effekte nach Aktivierung der Cannabinoid-Rezeptoren

Viele Signalübertragungsprozesse der Cannabinoid-Rezeptoren wurden durch deren pharmakologische Beeinflussung aufgedeckt. Nachdem man stabilere und spezifischere THC-Abkömmlinge entworfen hatte, die die Rezeptoren stärker aktivieren konnten, wurde 1994 mit Rimonabant (vormals auch als SR141716A bezeichnet) von der französischen Firma Sanofi-Synthelabo auch erstmals ein CB1-Rezeptor-Antagonist (☞ Tab. 1.1) und 1998 mit SR144528 auch ein selektiver CB2-Rezeptor-Antagonist entdeckt. Hiermit bestand die Möglichkeit, durch spezifische Blockade der Rezeptoren die daraus resultierenden Veränderungen auf zellulärer und physiologischer Ebene genau nachzuvollziehen.

Obwohl der humane CB2-Rezeptor dem CB1-Rezeptor nicht sehr ähnelt (er weist nur eine 44-prozentige Sequenzhomologie auf), sind die pharmakokinetischen Eigenschaften beider Rezeptoren doch sehr ähnlich. Die meisten endogenen sowie exogenen, d.h. die aus Hanf extrahierten Cannabinoide wie z.B. THC, binden mit vergleichbaren Affinitäten an beide Rezeptoren. In den letzten Jahren allerdings konnten Stimulatoren, soge-

nannte Agonisten, entwickelt werden, die mit einer über 100-fachen Selektivität eher an den einen oder an den anderen Cannabinoid-Rezeptor binden. Dies ermöglichte dann auch die selektive Charakterisierung der für den CB1- oder CB2-Rezeptor spezifischen Signalwege.

Zusätzlich wurde die Entdeckung vieler Mechanismen durch die Anwendung der "Gen-Knockout"-Technologie bei Mäusen erleichtert. So wurde bereits 1999 unabhängig voneinander in zwei unterschiedlichen Laboratorien eine CB1-Rezeptor-*knock-out* Maus hergestellt (☞ Tab. 1.2); im Jahr 2000 folgte die CB2-Rezeptor-*knock-out* Maus. Bei diesen Tieren wurde das entsprechende

Rezeptor-Gen in der Keimbahn ausgeschaltet, so dass sie nie das eigentliche Rezeptor-Protein besitzen. Die Tiere können ohne den jeweiligen Rezeptor zwar überleben, sie weisen jedoch verschiedenste Mängel in physiologischen Stoffwechselprozessen, sowie im Verhalten auf, auf die in späteren Kapiteln eingegangen werden wird.

Beide Cannabinoid-Rezeptoren gehören zur Klasse der sogenannten G-Protein-gekoppelten Sieben-Transmembran-Rezeptoren, so genannt, weil sie sieben Mal die Plasmamembran durchspannen, und weil sie an kleine, G-Proteine genannte, Signalmoleküle gekoppelt sind (☞ Abb. 1.4).
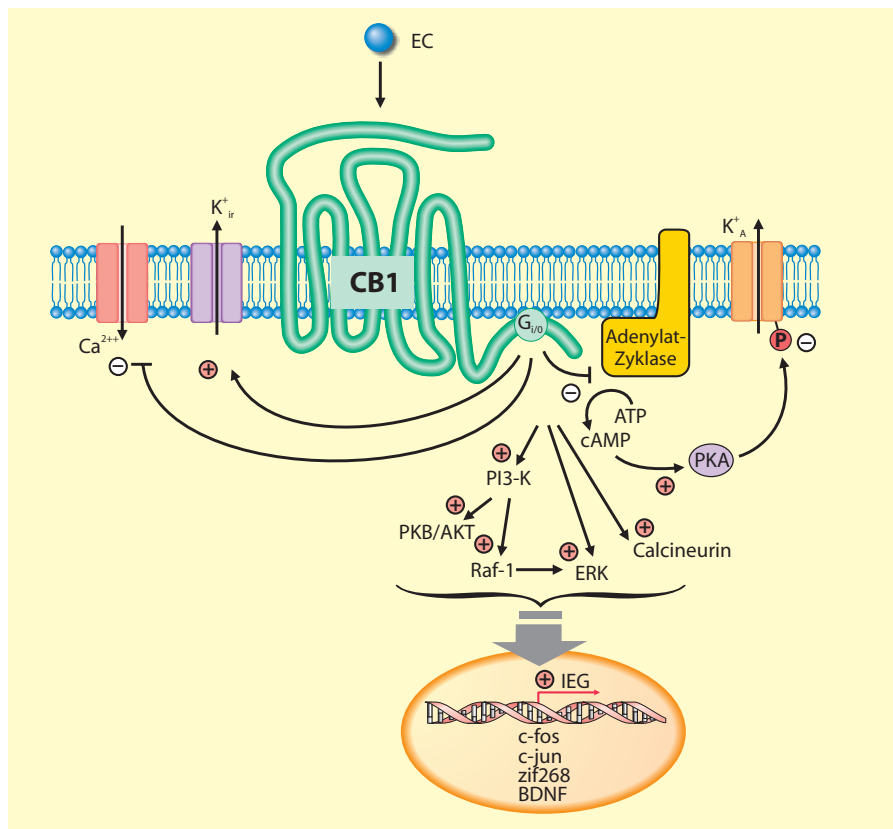
Abb. 1.4: Signaltransduktion des CB1-Rezeptors. Durch die Bindung von Cannabinoiden wird der CB1-Rezeptor aktiviert. Dies führt zu einer Vielzahl von Ereignissen, die unterschiedliche Signaltransduktionsketten in der Zelle beeinflussen können. In der Zellmembran werden verschiedene Kalzium- (Ca^{2+}) und Kaliumkanäle (K_{ir}, K_A) in ihrer Aktivität beeinflusst, was schließlich zur Verringerung der neuronalen Erregbarkeit führt. **EC**: Endocannabinoid; **CB1**: Cannabinoid-Rezeptor Typ 1; **G$_{i/o}$**: inhibitorisch wirkendes G-Protein; **cAMP**: zyklisches Adenosinmonophosphat; **PKA**: Protein-Kinase A; **PKB/AKT**: Protein-Kinase B; **PI3-K**: Phosphoinositol-3-Kinase; **Raf-1**: Raf-1-Kinase; **ERK**: Extrazellulär regulierte Kinase; **IEG**: *immediate early gene* (d.h. Gene, deren Transkription durch Signalketten schnell gesteigert wird); **c-fos, c-jun** und **zif268**: verschiedene Transkriptionsfaktoren; **BDNF**: Wachstumsfaktor *brain derived neurotrophic factor.*

Werden nun die Rezeptoren durch die Bindung von Cannabinoiden stimuliert, so verändern sie ihre räumliche Konformation und induzieren eine ganze Reihe von intrazellulären Signalen. Man kann sich dies wie eine Kettenreaktion vorstellen, die an der Zellmembran beginnt und sich wie beim Anstoßen von Dominosteinen in die ganze Zelle hinein ausbreitet, sogar bis in den Zellkern selbst. Dies passiert natürlich nicht nur an einem einzigen Rezeptor, sondern an vielen hundert bis tausend Rezeptoren, die eine einzige Zelle besitzt, gleichzeitig. Durch diese Signaltransduktion angeregt, können sich viele Eigenschaften der Zelle verändern. Es wird z.B. ihre elektrische Erregbarkeit beeinflusst, ihre Kommunikation mit anderen Zellen oder ihre Reaktion auf Reize verändert.

Die wichtigsten Vorgänge, die im Detail ablaufen, sind die Aktivierung von hemmenden G-Proteinen, damit die Hemmung des Enzyms Adenylatzyklase und die Herunterregulierung des Botenstoffes zyklisches Adenosinmonophosphat (cAMP); weiterhin das Schließen von Kalziumkanälen, die Öffnung von Kaliumkanälen und die Stimulation verschiedener phosphorylierender oder dephosphorylierender Enzyme, genannt Kinasen oder Phosphatasen, wie z.B. ERK, AKT oder Calcineurin, die letztendlich zur Veränderung verschiedenster Stoffwechselaktivitäten der Zelle führen können. Selbst die Genregulation der Zelle kann beeinflusst werden, indem Transkriptionsfaktoren aktiviert werden, die sogenannte "*immediate early genes* (IEGs)" wie c-fos oder BDNF transkribieren (☞ Abb. 1.4).

1.5. Die Endocannabinoide

1.5.1. Struktur und Eigenschaften

Die Charakterisierung der Cannabinoid-Rezeptoren ermöglichte es letztendlich erst, gezielte Experimente zu entwerfen, um deren körpereigene Bindungspartner zu isolieren. Da Endocannabinoide gleiche, oder zumindest sehr ähnliche Effekte wie THC hervorrufen sollten – so die ursprüngliche Hypothese – inkubierte man Zellen, die den CB1-Rezeptor exprimierten, in Kultur mit definierten, aus tierischen Geweben isolierten, chemischen Substanzen. Auf diese Weise wurde 1992 eine Substanz identifiziert, die THC in seiner Wirkungsweise sehr ähnelte. Das erste körpereigene Cannabinoid (Endocannabinoid) war entdeckt! Es handelte sich hierbei um ein Amid aus der Fettsäure Arachidonsäure und Ethanolamin. Es wurde Anandamid genannt, vom Sanscritwort (der heiligen Sprache der Hindus) *Ananda*, das Glückseligkeit bedeutet (☞ Abb. 1.3 und Tab. 1.1). Dieses kleine Lipid entsprach keinem bisher bekannten Neurotransmitter, obwohl es Ähnlichkeiten mit den Eicosanoiden aufwies, wie z.B. den Prostaglandinen. Drei Jahre später wurde ein zweites Endocannabinoid, 2-Arachidonoylglycerol (2-AG), gefunden, ein Ester aus Arachidonsäure und Glycerol (☞ Abb. 1.3). Beide Endocannabinoide sind in der Lage, sowohl an den CB1-Rezeptor als auch an den CB2-Rezeptor zu binden. In den letzten Jahren wurden noch weitere bioaktive Lipide identifiziert, die wie Cannabinoide wirken, so z.B. Noladinether und N-Arachidonyl-Dopamin. Sie scheinen jedoch nicht so ubiquitär verbreitet zu sein wie Anandamid und 2-AG, und über ihre spezifischen Funktionen im Körper ist wenig bekannt. Zusätzlich zu den Cannabinoid-Rezeptoren, vermag Anandamid auch an den Vanilloid-Rezeptor 1 (VR1; TRPV1) zu binden, ein nichtspezifischer Kationen-Kanal, der vor allem in inflammatorische Prozesse und Schmerzverarbeitung involviert ist.

> Wie bereits erwähnt, gehören Endocannabinoide zur Klasse der Lipide. Sie sind daher sehr fettlöslich und können nicht, wie für andere Neurotransmitter üblich, in Vesikeln gespeichert werden. Vielmehr werden sie in der Zelle bei Bedarf, d.h. erst wenn sie gebraucht werden, aus inaktiven Vorläufermolekülen, die in der Zellmembran verankert sind, synthetisiert. Eine Erhöhung der intrazellulären Kalziumkonzentration ist dabei besonders wichtig.

1.5.2. Synthese

Das Endocannabinoid Anandamid wird in zwei Schritten synthetisiert. Beim Eintreffen eines Stimulus auf die Zelle wird der Phospholipid-Vorläufer N-Archidonoyl-Phosphatidyl-Ethanolamin (N-Arachidonoyl-PE) an seiner Phosphodiesterbrücke in Anandamid und Phosphatidat gespalten (☞ Abb. 1.5).
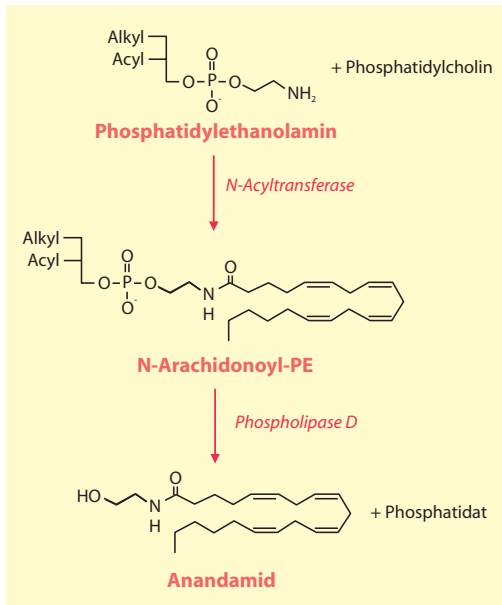
Abb. 1.5: Darstellung der Anandamid-Synthese. In zwei enzymatischen Schritten wird Anandamid aus dem Vorläufer Phosphatidylethanolamin synthetisiert, das ein Bestandteil der Zellmembran ist.

Diese Reaktion wird von dem Enzym Phospholipase D katalysiert. Zellen besitzen wahrscheinlich jedoch eine zu geringe Menge des Vorläufers N-Arachidonyl-PE, um bei länger andauernder Stimulation genügend Anandamid bereitzustellen. Daher muss auch dieses "Vorläuferlipid" bei Bedarf schnell nachgebildet werden. Dies geschieht durch das Enzym N-Acyltransferase. Es katalysiert den Transfer einer Arachidonsäuregruppe von Phosphatidylcholin an die Aminogruppe von Phosphatidyl-Ethanolamin (PE), um so N-Arachidonoyl-PE zu generieren. PE, Phosphatidylcholin und Phosphatidat sind alles häufig vorkommende Membranlipide und gleichzeitig vielseitig verwendete Zwischenprodukte des Phospholipidstoffwechsels. Die Aktivität der N-Acyltransferase ist sehr stark kalziumabhängig und wird zusätzlich durch cAMP gefördert. Weiterhin gibt es Hinweise darauf, dass auch andere G-Protein-gekoppelte Rezeptoren bei Aktivierung die Anandamid-Synthese regulieren können.

2-Arachidonoylglycerol (2-AG) ist ebenso wie andere Monoacylglycerole ein multifunktionales Zwischenprodukt des Lipidstoffwechsels. Es kann zugleich Endprodukt einer Synthesekette (wenn es z.B. als Endocannabinoid verwendet wird) als auch

Ausgangsprodukt für weitere andere Lipide sein. Daraus erklärt sich auch seine hohe Zellkonzentration verglichen mit Anandamid. Bis heute erscheinen zwei verschiedene Synthesewege von 2-AG wahrscheinlich:

- Ausgehend von Phosphatidylinositol, einem Phospholipid der Plasmamembran, werden durch das Enzym Phospholipase C (PLC) 1,2-Diacylglycerol (DGL) und Inositolphosphat gebildet (☞ Abb. 1.6). 1,2-Diacylglycerol selbst ist ein Botenstoff, der vor allem die Protein-Kinase C aktiviert; es kann jedoch auch durch das Enzym Diacyl-Glycerol-Lipase (DAGL) unter Abspaltung eines Acyl-Restes in 2-AG umgewandelt werden.
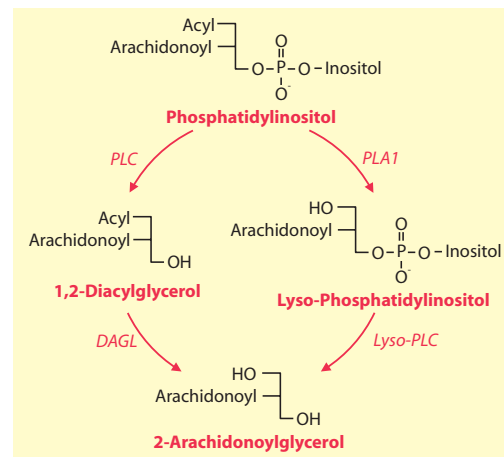
Abb. 1.6: Darstellung der 2-Arachidonoylglycerol (2-AG)-Synthese. In zwei alternativen enzymatischen Reaktionen kann 2-AG aus dem Membranvorläufer Phosphatidylinositol synthetisiert werden.

- Andererseits kann Phosphatidylinositol auch durch das Enzym Phospholipase A1 (PLA$_1$) in ein 2-Arachidonoyl-Lyso-Phospholipid umgewandelt werden, das durch die Lyso-Phospholipase C (Lyso-PLC) weiter zu 2-AG und Inositolphosphat hydrolisiert werden kann. Welcher Syntheseweg gerade angewendet wird, mag von der jeweiligen spezifischen Situation der Zelle abhängen, in der 2-AG gerade gebraucht wird. Auch die Produktion von 2-AG wird vor allem durch die freie Kalzium-Konzentration der Zelle beeinflusst.

Obgleich sowohl die Synthese von Anandamid als auch die von 2-AG primär kalziumabhängig ist,

können sie dennoch unabhängig voneinander in einer Zelle reguliert werden, denn neben Kalzium spielen noch viele weitere Signalübertragungsprozesse zusammen, die die Endocannabinoid-Synthese im Detail beeinflussen.

1.5.3. Transport zwischen Zellen

Natürlich stellt sich bei Endocannabinoiden ebenso wie bei anderen Signalmolekülen die Frage, wie sie freigesetzt werden und auf welchem Wege sie dann ihr Ziel (meist eine andere Zelle) erreichen. Interessanterweise scheint es für Endocannabinoide verschiedene Wege der Signalvermittlung zu geben. Erst kürzlich experimentell bestätigt wurde ein autokriner Mechanismus der Endocannabinoid-Signalübertragung (☞ Abb. 1.7A). Hierbei wirken Signalmoleküle auf dieselbe Zelle zurück, von der sie auch ausgeschüttet werden.

Auch eine parakrine Signalvermittlung im klassischen Sinn wurde für Endocannabinoide beschrieben (☞ Abb. 1.7B). Hierbei wirken die freigesetzten Endocannabinoide auf umgebende Nachbarzellen. Eine Zelle kann somit mehrere andere Zellen aktivieren. Leukozyten und Blutplättchen z.B. schütten Endocannabinoide aus, um damit Cannabinoid-Rezeptoren auf Endothelzellen und glatten Muskelzellen zu erreichen. Oder aber Astrozyten setzen 2-AG frei, welches auf Cannabinoid-Rezeptoren von umgebenden Neuronen und Mikrogliazellen wirkt.

Die Signalvermittlung von Endocannabinoiden als retrograder Transmitter in Nervenzellen ist ebenfalls von zentraler Bedeutung (☞ Abb. 1.7C). Während klassische Neurotransmitter wie Dopamin und Glutamat normalerweise von der Präsynapse ausgeschüttet werden und über den synaptischen Spalt zur Postsynapse diffundieren, läuft dieser Vorgang für Endocannabinoide genau umgekehrt ab. Sie werden von der Postsynapse synthetisiert und bewegen sich sozusagen rückwärts (retrograd) zur Präsynapse, wo sie an CB1-Rezeptoren binden. Dieser Weg der Signalvermittlung wird genauer in Kap. 2. beschrieben werden.

Auch eine Art endokriner Signalvermittlung scheint heute für Endocannabinoide nicht mehr ausgeschlossen (☞ Abb. 1.7D). Endocannabinoide können im Blut nachgewiesen werden, und ihre reversible Bindung an Serumalbumin, welche ihren Transport im Blut ermöglicht, wurde experimentell gezeigt. Die physiologische Bedeutung dieser Beobachtung ist heute noch ungeklärt.
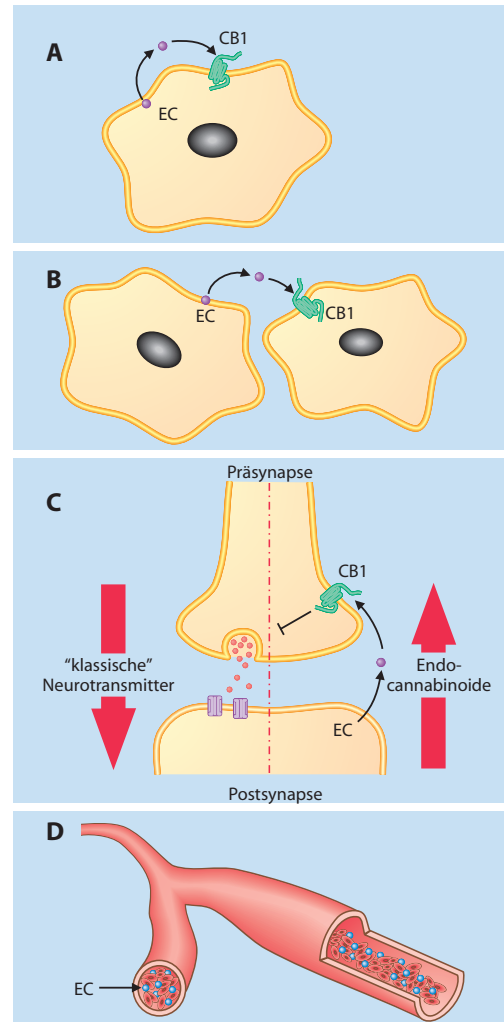
Abb. 1.7: Darstellung der möglichen Endocannabinoid-Signalübertragungen. **A**: Autokriner Mechanismus, bei dem Endocannabinoide (**EC**) an Cannabinoid-Rezeptoren Typ 1 (**CB1**) derselben Zelle binden, von der sie auch synthetisiert worden sind. **B**: Parakriner Mechanismus, bei dem das Endocannabinoid-Signal von einer zu benachbarten Zellen weitergegeben wird. **C**: Als retrograder Neurotransmitter an einer Synapse bewirken Endocannabinoide eine Erniedrigung der Neurotransmitterausschüttung. **D**: Endokriner Mechanismus über die Blutbahn, der aber noch nicht hinreichend bewiesen wurde.

Insgesamt betrachtet stehen noch viele Fragen aus, welche die Art des Transports von Endocannabi-

noiden im Extrazellärraum von einer Zelle zur nächsten betreffen. Da es sich bei den Endocannabinoiden ja um Lipide handelt, haben sie ein ureigenes Interesse daran, die membrannahe Umgebung einer Zelle nicht zu verlassen. Auf welche Weise ihre Wasserlöslichkeit heraufgesetzt wird, damit sie sich im wässrigen Milieu des Extrazellärraums bewegen können, bleibt bis heute ungeklärt. Die Hilfe von extrazellulären Lipidbindungsproteinen wie z.B. den Lipokalinen, die die Löslichkeit von vielen anderen kleinen, hydrophoben Signalmolekülen wie z.B. Retinol erhöhen, scheint wahrscheinlich.

1.5.4. Transport über die Zellmembran

Da Endocannabinoide zur Klasse der Lipide gehören, können sie die Zellmembran natürlich mittels passiver Diffusion durchqueren. Jedoch lässt gerade die Geschwindigkeit der Endocannabinoid-Aufnahme in die Zelle ein spezifisches Transportsystem vermuten, das Endocannabinoide selektiver und schneller durch die Membran schleust, als dies nur durch Diffusion machbar wäre. Im Gegensatz zu anderen Transportmechanismen, ist für den Endocannabinoid-Transport kein Energieverbrauch notwendig. Es scheint sich hierbei um eine Art erleichterte Diffusion zu handeln. Das zuständige Transportprotein allerdings wurde immer noch nicht entdeckt, obwohl in den letzten Jahren bereits verschiedene andere Lipidtransportmoleküle charakterisiert und kloniert werden konnten. Pharmakologisch jedoch gibt es bereits spezifische Substanzen, die den Endocannabinoid-Transport gezielt hemmen können (hierauf wird in Kap. 1.6. näher eingegangen); so besteht auch weiterhin die Hoffnung, das "Endocannabinoid-Transport-Protein" endlich zu identifizieren.

1.5.5. Deaktivierung und Abbau

Für den Abbau von Anandamid ist primär das Enzym Fettsäureamid-Hydrolase (FAAH) zuständig. Es handelt sich hierbei um ein intrazelluläres, in der Membran verankertes Enzym, das Anandamid zu Arachidonsäure und Ethanolamin hydrolysiert. Neben Anandamid werden auch andere bioaktive Fettsäureamide wie z.B. Oleoylethanolamid oder Palmitoylethanolamid, die nicht an Cannabinoid-Rezeptoren binden, durch die Fettsäureamid-Hydrolase abgebaut. FAAH ist im Gehirn weit ver-

breitet, vor allem in Zellkörpern und Dendriten. Die Dendriten, die FAAH enthalten, sitzen oft genau gegenüber von Axon-Enden, die CB1-Rezeptoren enthalten. Dies deutet darauf hin, dass der Abbau von Anandamid vor allem postsynaptisch stattfindet.

Das Endocannabinoid 2-AG wird ebenfalls von einem Enzym abgebaut, das jedoch im Zytosol lokalisiert ist. Hierbei handelt es sich um die Mono-Acylglycerol-Lipase (MAGL), welche 2-AG zu Arachidonsäure und Glycerol hydrolysiert. MAGL ist ebenfalls im Gehirn weit verbreitet, scheint jedoch im Gegensatz zu FAAH häufig präsynaptisch lokalisiert zu sein. Es könnte damit eine wichtige Rolle bei der Inaktivierung des retrograden Botenstoffes 2-AG spielen (☞ Kap. 2.).

Endocannabinoide - Charakteristika
• Lipide (Arachidonsäure-Abkömmlinge)
• Bei Bedarf synthetisiert aus Lipiden der Zellmembran
• Wirken als lokale "Hormone" (parakrin oder autokrin)
• Wirken als retrograde Neurotransmitter im Nervensystem
• Schneller Abbau

Tab. 1.4: Wichtige Charakteristika der Endocannabinoide.

1.6. Pharmakologische Beeinflussung des Endocannabinoid-Systems

Wie bereits dargestellt, wurden *Cannabis*-Extrakte in der Medizin schon seit sehr langer Zeit angewendet, und die Debatte darüber, ob "Marihuana als Medikament" in der medizinischen Praxis anerkannt werden sollte oder nicht, ist noch längst nicht vorüber. Ein prominentes Beispiel ist das Medikament Sativex®, entwickelt von GW Pharmaceuticals. Sativex® wurde im April 2005 von der kanadischen Gesundheitsbehörde zur begleitenden Behandlung von neuropathischen Schmerzen bei Patienten mit multipler Sklerose zugelassen. Es ist somit eines der ersten Medikamente, das die natürlichen Wirkstoffe der gesamten *Cannabis*-Pflanze beinhaltet und in Kanada vom Arzt frei verschrieben werden kann. Sativex® enthält standardisierte Mengen der beiden Cannabinoide

THC und Cannabidiol und wird als Spray auf die Mundschleimhaut appliziert. Obwohl das Medikament in den Zulassungsstudien bei den teilnehmenden Patienten zu einer signifikanten Reduktion der Schmerzen führte, traten dennoch eine Reihe von "drogenähnlichen" Nebenwirkungen wie Aufmerksamkeitsstörungen, Benommenheit, Müdigkeit, Desorientierung, euphorische Gemütszustände und veränderte Realitätswahrnehmung auf.

Dieses Beispiel zeigt also gleichsam eines der Hauptprobleme der medizinischen Anwendung von zentral wirkenden Cannabinoiden: die Präsenz von ungewollten, psychotropen Effekten. Natürlich können diese durch geschickte Rezepturen minimiert werden; die Effektivität von derartigen Arzneimitteln wird jedoch stets durch die mögliche Dosierung eingeschränkt sein.

Alternativen bestehen z.B. darin, Cannabinoid-Rezeptoren nur peripher zu aktivieren, etwa durch eine örtliche, topikale Anwendung oder aber durch die selektive Aktivierung von CB2-Rezeptoren, die kaum im Gehirn vorhanden sind. Mit beiden Möglichkeiten konnte man im Tiermodell erfolgreich schmerzmildernde Effekte erzielen.

> Grundsätzlich gibt es eine ganze Reihe von Möglichkeiten, modulierend pharmakologisch in das Endocannabinoid-System einzugreifen (☞ Abb. 1.8).
>
> - Einer Überaktivität des Systems kann man mit Antagonisten ("Blocker") wie z.B. Rimonabant für CB1-Rezeptoren oder SR144528 für CB2-Rezeptoren entgegenwirken.
>
> - Ein zu geringer Endocannabinoid-Tonus hingegen lässt sich
>   a) durch geringe THC- oder synthetische CB1- oder CB2-Agonist-Gaben oder
>   b) durch Blocker des Endocannabinoid-Transportes oder -abbaus
>   heraufregulieren.
>
> - Der CB1-Rezeptor-Blocker Rimonabant ist als verschreibungspflichtiges Medikament zur Therapie der Adipositas und begleitender Risikofaktoren wie Typ 2-Diabetes oder Dyslipidämie unter dem Namen ACOMPLIA® verfügbar.
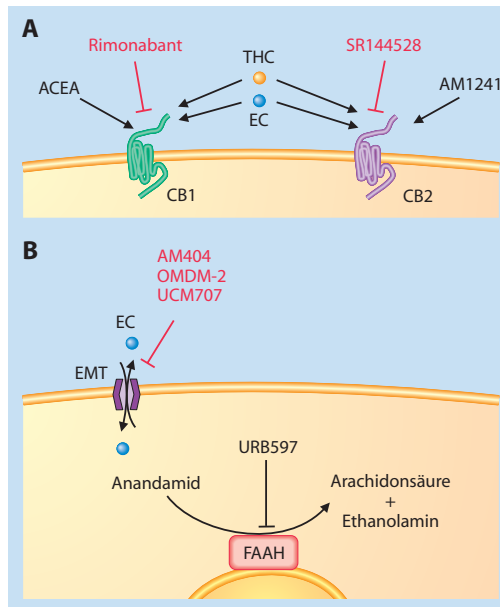
Abb. 1.8: Pharmakologische Beeinflussung des Endocannabinoid-Systems. **A**: Direkte Beeinflussung des Systems durch Stimulation mittels spezifischer CB1- und CB2-Rezeptor-Agonisten (ACEA, AM1241) oder durch Hemmung mittels spezifischer CB1- und CB2-Rezeptor-Antagonisten (Rimonabant, SR144528). **B**: Indirekte Beeinflussung durch Blockade des Endocannabinoid-Membran-Transporters (**EMT**) oder durch Inhibition des Anandamid-abbauenden Enzyms Fettsäureamid-Hydrolase (**FAAH**). Diese Art der Stimulation des Systems ist nicht mit unerwünschten psychotropen Nebeneffekten verbunden.

Eines der Hauptprobleme bei einer pharmakologischen Einflussnahme besteht immer darin, dass man nicht differenzieren kann, wo die eingesetzte Substanz im Körper hingelangt. Meist wird der ganze Körper überflutet und, wie in unserem Falle, entweder alle Cannabinoid-Rezeptoren des Körpers blockiert oder alle Rezeptoren gleichzeitig aktiviert. Dies birgt gerade bei einem solch feinabgestimmten System wie dem der Endocannabinoide ein nicht unerhebliches Risiko von Nebenwirkungen. Wenn man sich vorstellt, dass gewissen pathologischen Zuständen ja z.B. nur eine Dysregulation des Endocannabinoid-System in einer bestimmten Zellgruppe oder in einem einzelnen Organ zu Grunde liegt, so liegt der Nachteil einer solchen Behandlung auf der Hand.

Hingegen ist es bei einer Unterfunktion des Endocannabinoid-Systems eine sehr viel versprechende Strategie, den Abbau der körpereigenen Endocannabinoide zu hemmen, so dass sie vermehrt und länger verfügbar sind. Dies birgt den entscheidenden Vorteil, dass es in nicht betroffenen Regionen des Körpers durch die dann vermehrt vorhandenen Endocannabinoide wahrscheinlich nicht zu einer so starken Überaktivierung kommt, dass psychotrope Nebeneffekte auftreten, wohingegen in den betroffenen Regionen die CB-Rezeptoren durch den erhöhten Endocannabinoid-Tonus nun ausreichend aktiviert werden.

Bis heute wurden bereits einige Substanzen entwickelt, die auf diese Weise in den Endocannabinoid-Stoffwechsel eingreifen können. Zu nennen ist hier sicherlich eine Klasse von Molekülen wie z.B. AM404, OMDM-2 oder UCM707, die spezifisch den Transport der Endocannabinoide über die Zellmembran hemmen. Sie wirken hier auf den vorgeschlagenen, bisher aber nicht klonierten "Endocannabinoid-Transporter". Obwohl dieses Protein den Transport der Endocannabinoide in beide Richtungen beeinflusst, d.h. die Freisetzung und die Wiederaufnahme der Endocannabinoide erleichtern sollte, scheint dessen pharmakologische Blockierung dennoch vor allem die Wiederaufnahme zu beeinträchtigen. Pharmakologische Wirkstoffe, die selektiv die synthetisierenden Enzyme von Anandamid oder 2-AG beeinflussen, sind bisher leider noch nicht verfügbar. Auch fehlen effiziente Pharmaka, die im gesamten Organismus das Enzym MAGL spezifisch hemmen und somit die 2-AG-Konzentration erhöhen könnten.

Jedoch gibt es eine ganze Reihe von Substanzen, am bekanntesten bisher ist wohl URB597, welches das Schlüsselenzym des Anandamid-Abbaus, FAAH, hemmen kann. Somit besteht die Möglichkeit, selektiv nur die Konzentration des Endocannabinoids Anandamid zu erhöhen (im Gegensatz zu den Transport-Inhibitoren, die die Konzentration von Anandamid und 2-AG zu erhöhen scheinen). Dies könnte z.B. für die Behandlung von Angsterkrankungen in Zukunft eine Rolle spielen.

Keine der bekannten Substanzen, die in den Endocannabinoid-Stoffwechsel eingreifen, aber nicht die Rezeptoren beeinflussen, wurde bisher klinisch getestet. Jedoch wird die pharmazeutische Indu-

strie mit diesem Schritt bestimmt nicht lange auf sich warten lassen, und man darf auf die Ergebnisse gespannt sein.

Hier wurde ein Überblick über die mögliche pharmakologische Beeinflussung des Endocannabinoid-Systems gegeben; über die Chancen, durch eine Modulation desselben verbessernd auf spezifische pathologische Zustände einzuwirken, soll in den folgenden Kapiteln diskutiert werden.

1.7. Zusammenfassung

Die Beschreibung der Pflanze *Cannabis sativa* als Heilmittel geht bis ins 5. Jahrtausend v.Chr. zurück. Dennoch sollte es noch bis zum Jahr 1964 dauern, bis die psychisch aktive Komponente Δ^9-Tetrahydrocannabinol (THC) identifiziert wurde. Aber erst mit der Entdeckung des ersten Cannabinoid-Rezeptors 1990 war der entscheidende Meilenstein zur Entschlüsselung des körpereigenen Endocannabinoid-Systems erreicht. Während der letzten 15 Jahre stieg das öffentliche Interesse für dieses faszinierende Gebiet rapide an. Die weiteren Komponenten des Systems wurden in den Folgejahren identifiziert: 1993 der zweite Cannabinoid Rezeptor (CB2), 1992 und 1995 die ersten beiden körpereigenen Endocannabinoide, Anandamid und 2-Arachidonylglycerol.

Die Entdeckung von spezifischen, pharmakologisch aktiven Substanzen, vor allem von Rezeptor-Agonisten und -Antagonisten, als auch die Generierung von genetisch veränderten Mäusen, denen die Cannabinoid-Rezeptoren fehlten, ermöglichte die Erforschung des Systems im Detail.

Das Endocannabinoid-System stellt ein höchst komplexes und wichtiges physiologisches System des menschlichen Körpers dar, das vor allem für das Stoffwechselgleichgewicht zuständig ist, und als eine Art "Stress"-Erholungssystem betrachtet werden kann. Es senkt z.B. Schmerzen und Angst, Stress und Blutdruck, wirkt regulierend auf die Körpertemperatur und Muskelspannung, schützt vor Entzündungen und stimuliert Appetit und Belohungsverhalten.

Der CB1-Rezeptor kommt vor allem im zentralen Nervensystem vor, wohingegen der CB2-Rezeptor hauptsächlich in Immunzellen lokalisiert ist. Beide Rezeptoren werden sowohl durch THC als auch

durch Endocannabinoide aktiviert. Die Rezeptoren zählen zu den G-Protein-gekoppelten Sieben-Transmembran-Rezeptoren und vermitteln eine Reihe von intrazellulären Signaltransduktionsprozessen. Vor allem aktivieren sie hemmende G-Proteine, regulieren cAMP herunter, führen zum Schließen von Kalzium- und zur Öffnung von Kaliumkanälen und aktivieren verschiedenste Kinasen und Phosphatasen.

Die Endocannabinoide Anandamid und 2-AG gehören zu einer bestimmten Klasse von Lipiden, zu den Eicosanoiden. Sie werden nicht in Vesikeln gespeichert, sondern bei Bedarf von Lipidvorläufermolekülen der Zellmembran synthetisiert und durch Diffusion oder mittels "erleichterter Diffusion" durch ein Transmembran-Transporter-Protein aus der Zelle freigesetzt. Die Wiederaufnahme erfolgt ebenfalls durch diesen Transporter. Die Endocannabinoide wirken als lokale Hormone entweder auto- oder parakrin. In Nervenzellen fungieren sie als retrograder Transmitter, indem sie von der Postsynapse freigesetzt werden, "rückwärts" über den synaptischen Spalt diffundieren, und dort an präsynaptische CB1-Rezeptoren binden und diese aktivieren. Der Abbau erfolgt schnell durch Hydrolasen: Anandamid wird durch das Enzym FAAH, 2-AG durch MAGL abgebaut.

Die pharmakologische Beeinflussung des Systems für medizinische Zwecke verlangt vermehrte Beachtung. Sowohl genau definierte Extrakte aus *Cannabis sativa* als auch ein Hemmer des CB1-Rezeptors sind bereits als Arzneimittel zugelassen bzw. befinden sich in klinischen Studien der Phase III. Pharmakologische Endocannabinoid-Transport-Hemmer und Inhibitoren des Anandamid abbauenden Enzyms FAAH liefern bereits Erfolg versprechende Resultate in Tiermodellen.

1.8. Literatur

1. Bisogno T, Ligresti A, Di Marzo V (2005) The endocannabinoid signalling system: biochemical aspects. Pharmacol Biochem Behav 81:224-38.

2. Howlett AC, Barth F, Bonner TI, Cabral G, Casellas P, Devane WA, Felder CC, Herkenham M, Mackie K, Martin BR, Mechoulam R, Pertwee RG (2002) International Union of Pharmacology. XXVII. Classification of cannabinoid receptors. Pharmacol Rev 54:161-202.

3. Iversen LL (2000) The science of marijuana. Oxford University Press.

4. Lutz B (2002) Molecular biology of cannabinoid receptors. Prostaglandins Leukot Essent Fatty Acids 66: 123-42.

5. Nicoll RA, Alger BE (2005) Das Gehirn und sein Marihuana. Spektrum der Wissenschaft Juli 2005:48-55.

6. Pagotto U, Pasquali R (2005) Fighting obesity and associated risk factors by antagonising cannabinoid type 1 receptors. Lancet 365:1363-4.

7. Piomelli D (2003) The molecular logic of endocannabinoid signalling. Nat Rev Neurosci 4:873-84.

Endocannabinoid-System und zentrales Nervensystem

(M. Steiner, B. Lutz)

2. Endocannabinoid-System und zentrales Nervensystem

2.1. Exogene und endogene Cannabinoide – eine wichtige Unterscheidung

Das am meisten genutzte und bekannte exogene Cannabinoid ist ohne Zweifel die psychoaktive Komponente der Pflanze *Cannabis sativa*, bekannt als Δ^9-Tetrahydrocannabinol (THC). Die effektivste Art, um die Wirkung von THC auf das Gehirn zu erfahren, ist sicherlich das Rauchen, und erfahrene Raucher können durch ihre Inhalationsfrequenz und durch ihre Inhalationsintensität sogar die Dosierung selbst bestimmen, um gezielt die am meisten erwünschten Reaktionen hervorzurufen. THC wirkt hierbei als ein potenter Aktivator (Agonist) des CB1-Rezeptors im gesamten Gehirn und beeinflusst unter anderem Emotionen, Gedächtnisfunktion, Bewegungskoordination, Hungergefühl und Zeitwahrnehmung (☞ Tab. 2.1).

THC-Effekte beim Menschen
• Steigerung des Hungergefühls
• Veränderung des Zeitempfindens
• Beeinträchtigung der Bewegungskoordination
• Beeinträchtigung des Kurzzeit- und Arbeitsgedächtnisses
• Veränderung von Emotionszuständen (angstverstärkend oder -lösend)
• Kurzzeitige Bewegungsaktivität
• Allgemeine Beruhigung

Tab. 2.1: THC-Effekte beim Menschen.

THC-Exposition während der Embryonalentwicklung und im Kindesalter bis zur Pubertät kann zu irreversiblen, unerwünschten Veränderungen führen. In Nagern ruft die Applikation von THC dosisabhängig ein spezifisches Phänotypspektrum, die so genannte Tetrade, hervor: Es kommt

- zu einem Abfall der Körpertemperatur (Hypothermie)
- zur Schmerzunempfindlichkeit (Analgesie)
- zur Gliederstarre (Katalepsie) und
- zu verminderter Bewegungsaktivität (Hypoaktivität).

Es ist wichtig, zu beachten, dass die durch THC hervorgerufenen Wirkungen nur am Rande mit denen der im Körper synthetisierten Endocannabinoide zu vergleichen sind. Diese wirken im Gegensatz zu exogenen Cannabinoiden nur lokal, in definiertem Wirkungsspektrum und in einem genau abgestimmten Zeitrahmen. Wir wissen bereits aus dem ersten Kapitel, dass sie im Wesentlichen auf Bedarf synthetisiert und freigesetzt werden, und schnell wieder aus dem synaptischen Spalt abtransportiert und abgebaut werden können. Vergleichbar ist das Endocannabinoid-System in dieser Hinsicht z.B. mit dem schon länger bekannten Opioid-System, dessen endogene Aktivatoren wie Endorphine, Enkephaline und Dynorphine ja auch anders wirken als die exogenen Stoffe Opium oder Morphium.

Die Wirkungen des physiologisch funktionierenden Endocannabinoid-Systems sind so subtil, dass wir sie bewusst gar nicht "wahrnehmen". Erst Störungen im System-Gleichgewicht können zu Krankheitszuständen führen, die wir dann natürlich bemerken. Darauf soll in den folgenden Kapiteln eingegangen werden.

2.2. Vorkommen und Verteilung der Cannabinoid-Rezeptoren im Gehirn

Die Verteilung der Cannabinoid-Rezeptoren im Gehirn wurde erstmals 1990 mit Hilfe von Radioliganden-Bindungsstudien mit [H^3]CP-55940, einem THC-Derivat mit sehr hoher Affinität zu Cannabinoid-Rezeptoren (☞ Abb. 1.2), am Rattengehirn dargestellt. Später folgten immunhistochemische Untersuchungen mit spezifischen Antikörpern gegen die Cannabinoid-Rezeptoren, welche zwar eine verbesserte räumliche Auflösung ermöglichten, aber grundsätzlich zu den gleichen Ergebnissen führten. Im Gehirn ist fast ausschließlich der CB1-Rezeptor vorhanden. Der CB2-Rezeptor wurde im Gehirn bisher nur in Mikrogliazellen und kürzlich auch im Hirnstamm und Cerebellum nachgewiesen. Die folgenden Ausführungen beziehen sich daher vorerst nur auf den CB1-Rezeptor. Dieser ist vor allem in Axonen und Ner-

venendigungen lokalisiert, im Zellkörper jedoch nur in geringer Zahl anzutreffen. Ob CB1-Rezeptoren auch in Dendriten zu finden sind, ist bisher noch unklar. Der Rezeptor ist also hauptsächlich präsynaptisch vorzufinden, was seine Funktion als Modulator der Freisetzung von anderen Neurotransmittern unterstreicht (☞ Kap. 2.3.). Sowohl in Nagern, als auch im Menschen sind hohe Konzentrationen des Rezeptors im cerebralen Cortex zu finden (☞ Abb. 2.1).
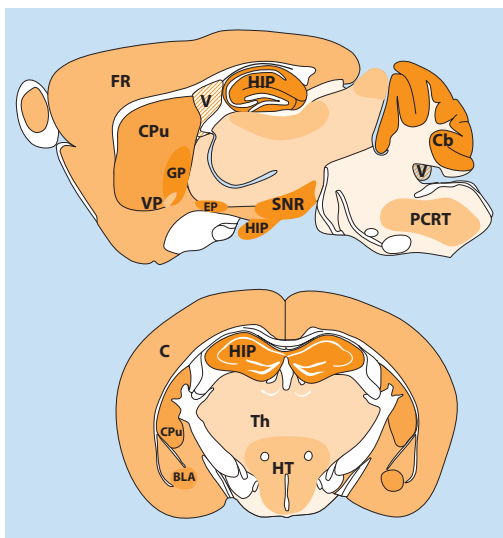

Abb. 2.1: Verteilung des CB1-Rezeptorproteins im Gehirn. **Oben**: Sagittalschnitt; **Unten**: Koronalschnitt durch ein erwachsenes Mausgehirn. Die Expressionsstärke des Proteins wird von "dunkelorange = sehr stark exprimiert" bis hin zu "hellorange = sehr schwach exprimiert" abgestuft dargestellt. **BLA**: Basolaterale Amygdala; **C**: Neocortex; **Cb**: Cerebellum; **CPu**: Caudatus Putamen; **EP**: Endopedunculärer Nukleus (homolog zum Globus pallidus interna); **FR**: Frontaler Cortex; **GP**: Globus pallidus; **HIP**: Hippocampus; **HT**: Hypothalamus; **PCRT**: Parvozellulärer Retikulärer Nucleus; **SNR**: Substantia nigra Pars Reticulata; **Th**: Thalamus; **V**: Ventrikel; **VP**: Ventroposteriorer Thalamischer Nucleus.

Eine sehr hohe Dichte trifft man in der Molekularschicht des Cerebellums und in den Basalganglien (Caudatus putamen, Globus pallidus, Substantia nigra) an. Auch Hippocampus und Amygdala enthalten viele CB1-Rezeptoren, während sie im Hypothalamus, in den Kernen des Hirnstamms und im Rückenmark geringer exprimiert sind.

Speziell die niedrige Menge im Hirnstamm wird als Erklärung dafür angeführt, dass Cannabinoide nicht toxisch sind, selbst wenn sie in sehr hoher Dosierung gegeben werden. Im Menschen sind praktisch keine Todesfälle durch eine Überdosis von THC bekannt.

In corticalen Regionen findet man CB1-Rezeptoren vor allem an den Axonenden von hemmenden Interneuronen, die den Neurotransmitter GABA (Gamma-Aminobuttersäure) ausschütten. Im Striatum z.B. findet man sie auch an schnell feuernden ("*fast-spiking*") GABA-Projektionsneuronen. In vielen Gehirnregionen sind CB1-Rezeptoren aber auch Bestandteil von stimulierenden (exzitatorischen) Neuronen, die vor allem Glutamat freisetzen (☞ Kap. 2.3.).

Die regionale Verteilung der CB1-Rezeptoren im Gehirn korreliert nicht unbedingt mit den Endocannabinoid-Konzentrationen, die in verschiedenen Bereichen gemessen wurden. Die Messung von Endocannabinoiden ist jedoch nicht einfach durchzuführen, da diese äußerst lipophil und instabil sind; außerdem erhält man bei Analysen im basalen Zustand keine Aussage darüber, wie viel bei Bedarf produziert werden würde. Besser korreliert die Verteilung des Enzyms Fettsäureamid-Hydrolase (FAAH), welches das Endocannabinoid Anandamid abbaut, mit der Expression der CB1-Rezeptoren. Obwohl FAAH auch in anderen Geweben des Körpers vorhanden ist, und somit nicht ausschließlich dem Abbau von Anandamid dient, findet man eine entsprechend hohe Dichte von FAAH gerade in jenen Gehirnregionen, die auch viele CB1-Rezeptoren enthalten. Vielfach ist FAAH vor allem in den somato-dendritischen Regionen der Neuronen zu finden, die sich postsynaptisch von CB1-Rezeptor-positiven Axonenden befinden. Hieraus ließ sich zum ersten Mal die Hypothese formulieren, dass Anandamid, nachdem es den CB1-Rezeptor auf der Präsynapse aktiviert hat, wahrscheinlich von der Postsynapse wieder aufgenommen und dort abgebaut wird. Das Endocannabinoid 2-AG hingegen wird hauptsächlich präsynaptisch durch sein abbauendes Enzym Mono-Acylglycerol-Lipase (MAGL) degradiert (☞ Abb. 2.2).
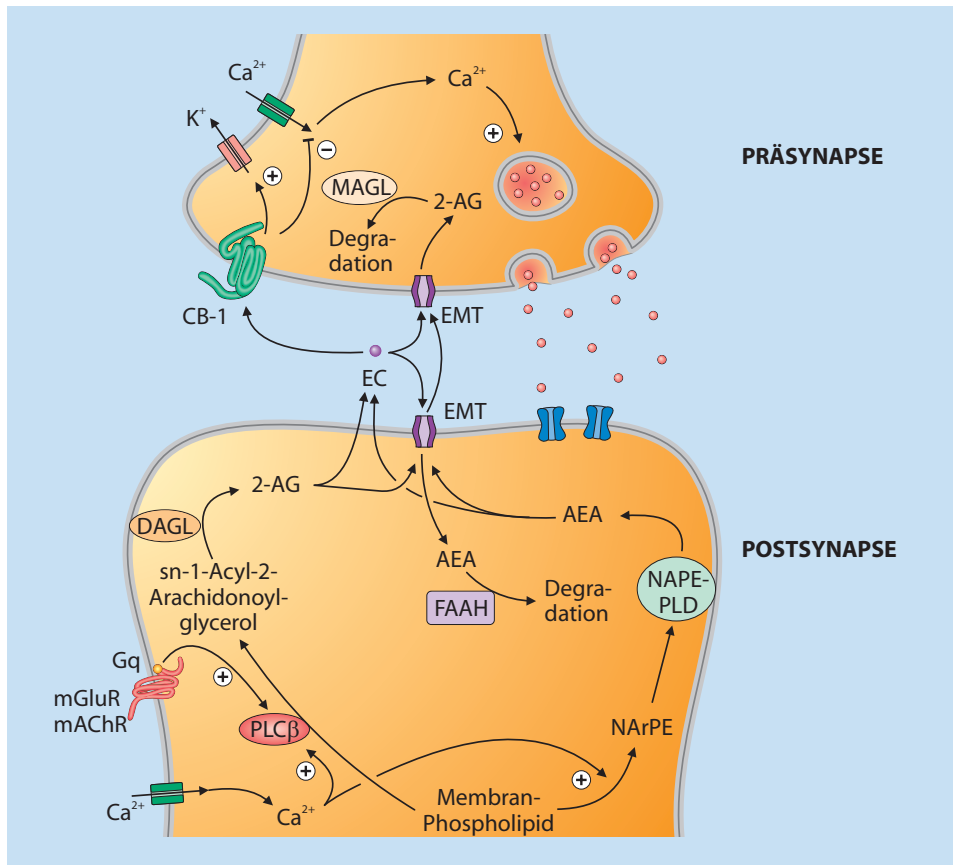
Abb. 2.2: Endocannabinoide wirken als retrograde Neurotransmitter. Darstellung von Synthese, Transport, Rezeptor-Bindung und Abbau der Endocannabinoide. **AEA**: Anandamid; **2-AG**: 2-Arachidonylglycerol; **CB1**: Cannabinoid-Rezeptor Typ 1; **DAGL**: Diacyl-Glycerol-Lipase; **EC**: Endocannabinoide; **EMT**: Endocannabinoid-Membran-Transporter; **FAAH**: Fettsäureamid-Hydrolase; **MAGL**: Mono-Acylglycerol-Lipase; **mAChR**: muscarinische Acetylcholin-Rezeptoren; **mGluR**: metabotroper Glutamat-Rezeptor; **NAPE-PLD**: N-Acyl-Phosphatidyl-Ethanolamin-Phospholipase D; **NArPE**: N-Arachidonoyl-Phosphatidyl-Ethanolamin; **PLC**$_\beta$: Phospholipase C$_\beta$; **Gq**: G-Protein q.

2.3. Endocannabinoide als retrograde Neurotransmitter

Die präsynaptische Lokalisation von CB1-Rezeptoren deutete darauf hin, dass Endocannabinoide möglicherweise die Freisetzung anderer Neurotransmitter aus den Axonenenden beeinflussen könnten. Wohl gab es eine Fülle von experimentellen Studien, die zeigten, dass THC und andere Cannabinoide die Transmission einer ganzen Reihe von Botenstoffen modulieren können; so z.B. die von Glutamat, GABA, Noradrenalin, Dopamin, Serotonin und Acetylcholin. Jedoch blieben die hier zugrunde liegenden, zellulären Mechanismen lange Zeit unbekannt.

Im Jahr 2001 wurde dann in elektrophysiologischen Studien gezeigt, dass Endocannabinoide am synaptischen Spalt als retrograde Neurotransmitter wirken können. Sie werden wahrscheinlich von der Postsynapse freigesetzt, sobald diese stark aktiviert wird. Dieser Vorgang ist meist mit einer Erhöhung der intrazellulären Kalziumionen-Konzentration verbunden, die zur Synthese von Endocannabinoiden führt. Die Endocannabinoide diffundieren wahrscheinlich aus der Postsynapse heraus und bewegen sich über den synaptischen Spalt hinweg zur Präsynapse. Dort aktivieren sie schließlich die CB1-Rezeptoren (☞ Abb. 2.2).

Angenommen, es wird ein Neurotransmittersignal von der Präsynapse zur Postsynapse übertragen

und es wird gleichzeitig aber die Postsynapse durch einen weiteren Stimulus aktiviert, führt dieser zusätzliche Stimulus zur Synthese von Endocannabinoiden in der Postsynapse, die dann im oben aufgezeigten Mechanismus die präsynaptische Ausschüttung von Neurotransmittern über das retrograde Endocannabinoid-Signal hemmt (☞ Abb. 2.3).
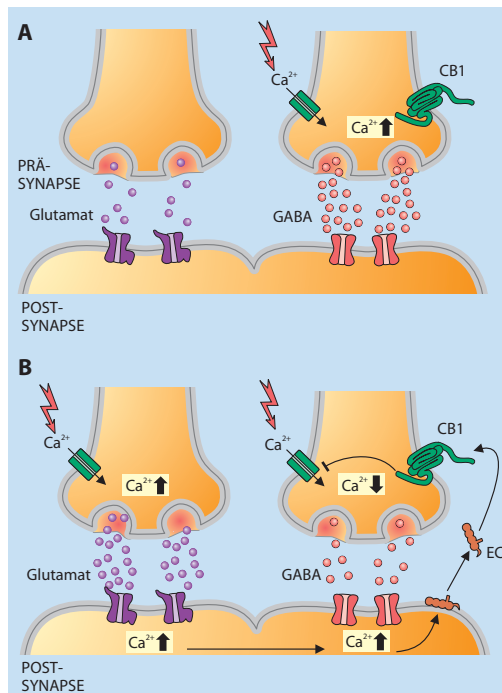
Abb. 2.3: Schematische Darstellung von DSI (Depolarisation-induzierte Suppression der Inhibition). **A**: Zustand beim Eintreffen eines Aktionspotenzials an einer GABAergen Synapse. **B**: Zustand nach zusätzlichem Eintreffen einer aktivierenden (glutamatergen) synaptischen Übertragung an der Postsynapse der GABAergen Synapse. Die Stimulation der Postsynapse löst den Einstrom von Kalzium aus, der die Endocannabinoid (EC)-Synthese stimuliert. Diese bewegen sich zurück zu einer GABAergen Präsynapse, aktivieren dort den Cannabinoid-Rezeptor Typ 1 (CB1) und unterdrücken die GABA-Freisetzung. Das gleiche Phänomen kann auch an einer glutamatergen Synapse stattfinden und würde dort als DSE (Depolarisation-induzierte Suppression der Exzitation) bezeichnet werden.

Dies führt zur Verminderung der synaptischen Signalübertragung. Hierbei sind elektrophysiologisch vor allem zwei spezifische Vorgänge gut untersucht, die analog ablaufen, sowohl an hemmen-

den, GABA ausschüttenden Synapsen (☞ Abb. 2.3), als auch an erregenden, Glutamat ausschüttenden Synapsen (in Abb. 2.3 würde rechts dann eine glutamaterge Synapse vorliegen).

2.3.1. Modulation der GABA-Freisetzung

Das prominenteste Beispiel für die Modulation der synaptischen Signalübertragung, bei der ein retrograder Transmitter involviert ist, ist ein Phänomen, welches unter dem Namen "Depolarisation-induzierte Suppression der Inhibition" (DSI) bekannt ist (☞ Abb. 2.3). Es bezieht sich auf eine experimentelle Beobachtung aus der Elektrophysiologie, bei der die Depolarisation eines postsynaptischen Neurons zur kurzzeitigen oder länger anhaltenden Unterdrückung der GABA-Freisetzung durch die Präsynapse und damit zur Unterdrückung der Inhibition der Postsynapse führt (GABA wirkt allgemein als hemmender Neurotransmitter). Mit sehr hoher Wahrscheinlichkeit sind für dieses Phänomen Endocannabinoide verantwortlich, die von der Postsynapse freigesetzt werden, retrograd zur Präsynapse diffundieren und dort über die Aktivierung von CB1-Rezeptoren die elektrochemischen Eigenschaften der Präsynapse so verändern, dass diese nun weniger GABA ausschüttet.

2.3.2. Modulation der Glutamat-Freisetzung

Ein ähnliches Beispiel, bei dem ebenso Endocannabinoide als retrograde Transmitter wirken, ist das Phänomen der "Depolarisation-induzierten Suppression der Exzitation" (DSE; ☞ Abb. 2.3). Der Vorgang läuft ebenso ab wie das soeben beschriebene DSI, mit dem einzigen Unterschied, dass Endocannabinoide nun zur Unterdrückung der Erregung der Postsynapse durch Glutamat führen. Das Phänomen läuft also diesmal an erregenden, Glutamat-ausschüttenden Synapsen ab und nicht an hemmenden, GABA-ausschüttenden Synapsen wie beim DSI. Auch hier werden bei der Stimulation der Postsynapse Endocannabinoide freigesetzt, die sich rückwärts über den synaptischen Spalt bewegen und dort wieder an CB1-Rezeptoren binden, die die Glutamat-Freisetzung der Präsynapse vermindern.

2.3.3. Endocannabinoide beeinflussen die Plastizität von Synapsen

Als synaptische Plastizität (die dynamische Anpassung der Stärke und Effizienz von synaptischen Übertragungen) bezeichnet man einen generellen Mechanismus, bei dem externe oder interne Stimuli die neuronale Antwort im Gehirn beeinflussen, wie z.B. zur Speicherung von Gedächtnisinhalten. Die Dauerhaftigkeit solcher Änderungen der synaptischen Stärke und Effizienz kann in extremen Schwankungsbreiten variieren, von Millisekunden bis hin zu Jahren. So erscheint es mehr als natürlich, dass eine Mannigfaltigkeit von zellulären und molekularen Vorgängen dabei eine Rolle spielt. Langzeit-Potenzierung (*long-term potentiation*; LTP) bezeichnet eine länger andauernde Erhöhung der synaptischen Stärke, während Langzeit-Hemmung (*long-term depression*; LTD) eine Erniedrigung beschreibt. Dies sind Vorgänge, die von Stunden bis hin zu vielen Tagen andauern können, und die experimentell sehr gut untersucht sind, besonders mit Hinblick auf ihre Bedeutung beim Lernen und Gedächtnis. Manche Prozesse, die LTP oder LTD beeinflussen, spielen sich an der Postsynapse ab, andere an der Präsynapse, und einige beruhen auf einem retrograden Transmitter, der von der Postsynapse zur Präsynapse zurückgeleitet wird. Unter diese Form fallen an vorderster Stelle die Endocannabinoide. Durch ähnlich denen oben für DSI und DSE beschriebene Mechanismen beeinflussen sie nachhaltig verschiedenste Formen von synaptischer Plastizität in den unterschiedlichsten Gehirnregionen.

Für die Synthese und Freisetzung von Endocannabinoiden an der Postsynapse sind vor allem zwei Signale wichtig: Es handelt sich einmal um die Erhöhung der intrazellulären Kalzium-Konzentration, zum anderen um die Aktivierung von metabotropen Glutamat-Rezeptoren des Typs I oder von muscarinischen Acetylcholin-Rezeptoren des Typs M1 und M3. Beide Signale alleine, aber vermehrt noch im Zusammenspiel, können eine nachhaltige Endocannabinoid-Freisetzung einleiten (☞ Abb. 2.2).

Es bleibt festzuhalten, dass Endocannabinoide sowohl bei der schnellen als auch bei der länger andauernden Modulation von synaptischer Signalübertragung im ZNS eine signifikante Rolle spielen.

Sie wirken hierbei als retrograder Neurotransmitter und üben hemmende Effekte sowohl auf die Ausschüttung von exzitatorischen als auch auf die von inhibitorischen Botenstoffen aus. Hiermit modulieren sie also eine Fülle von anderen Prozessen im Gehirn und widmen sich somit, wie auch schon im vorigen Kapitel beschrieben, vor allem der Homöostase, der Aufrechterhaltung des physiologischen Gleichgewichts im Gehirn. Sie modulieren damit sowohl überschießende als auch unterrepräsentierte Vorgänge dahingehend, dass sie diese zurück ins Gleichgewicht lenken. Neuronale Regelkreise können auf diese Weise kontrolliert werden.

Wichtig ist es, zu erkennen, dass THC oder andere exogene Cannabinoide diese physiologischen Effekte der lokal freigesetzten Endocannabinoide nicht imitieren können. Sie verursachen hingegen eine lang anhaltende Aktivierung der Cannabinoid-Rezeptoren in allen Gehirnregionen und führen zu einer insgesamten Hemmung der Neurotransmitter-Freisetzung von allen Nervenendigungen, die den CB1-Rezeptor enthalten. Sie setzen damit die örtlich und zeitlich fein aufeinander abgestimmte Einsatztätigkeit des Endocannabinoid-Systems außer Kraft.

2.4. Das Endocannabinoid-System in Gliazellen und während inflammatorischer Prozesse

Historisch betrachtet galten Gliazellen lange Zeit nur als eine Art Stützzellen für Neuronen, und ihnen wurde eine eher statische Rolle zugedacht. Inzwischen weiß man allerdings, dass Gliazellen einige entscheidende Funktionen bei der ZNS-Homöostase innehaben; so z.B. bei verschiedenen pathologischen Zuständen, bei denen es zu einer so genannten "Glia-Antwort" kommt. Es scheint daher nicht verwunderlich, dass das Endocannabinoid-System auch in Gliazellen zu finden ist. Sowohl Mikrogliazellen, die Immunzellen des Gehirns, als auch Astrozyten produzieren selbst Endocannabinoide, und deren Synthese ist ebenfalls kalziumabhängig. So wird vor allem die Produktion von 2-AG z.B. durch einen vermehrten Kalziumeinstrom durch ATP-abhängige Membranrezeptoren, die P2X$_7$-Rezeptoren, vermittelt
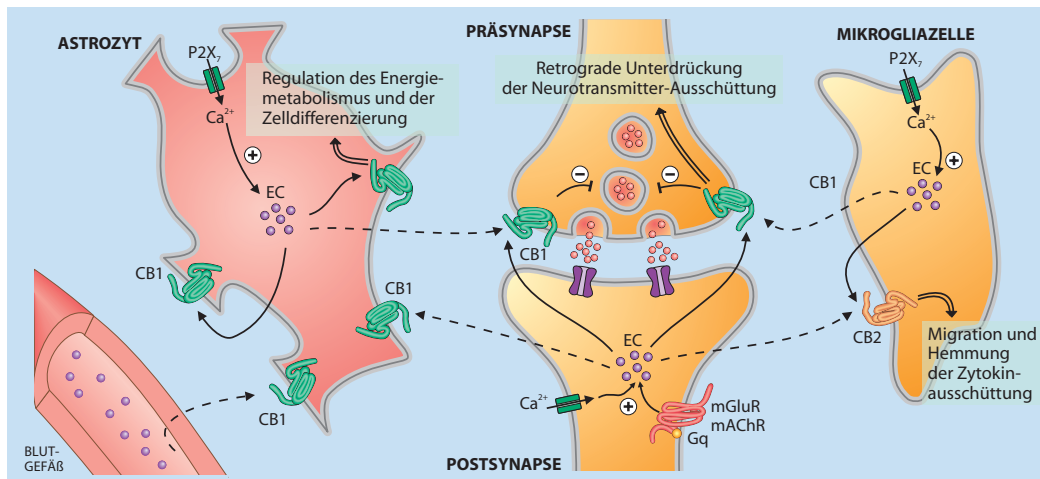
Abb. 2.4: Das Endocannabinoid-System in Gliazellen und die möglichen Interaktionen mit Neuronen und Blutgefäßen. Die gestrichelten Pfeile beziehen sich auf hypothetische Wechselwirkungen von Endocannabinoiden zwischen Glia-, Nervenzellen und Blutgefäßen. **CB1**: Cannabinoid-Rezeptor Typ 1; **CB2**: Cannabinoid-Rezeptor Typ 2; **EC**: Endocannabinoide; **mAChR**: muscarinische Acetylcholin-Rezeptoren; **mGluR**: metabotroper Glutamat-Rezeptor; **P2X7**: ATP-abhängiger Kalziumkanal.

(☞ Abb. 2.4). Auch die Endocannabinoid-degradierenden Enzyme FAAH und MAGL kann man in Gliazellen antreffen. CB1-Rezeptoren findet man vor allem auf den Endfüßen von Astrozyten, und Endocannabinoide scheinen hier die Energieversorgung vom Blut zu den Nervenzellen mitzuregulieren, als auch Einfluss auf das Überleben und die Differenzierung zu nehmen. Mikrogliazellen, besonders in aktiviertem Zustand, exprimieren vor allem CB2-Rezeptoren, die sowohl die Zellmigration, als auch die Ausschüttung von Zytokinen beeinflussen. Auch in Gliazellen gibt es eine ganze Reihe von Untersuchungen, die noch auf andere Cannabinoid-Rezeptoren bisher unbekannten Typs schließen lassen.

Das Endocannabinoid-System in Oligodendrozyten, die die elektrische Erregungsleitung an den Axonen von Neuronen maßgeblich beeinflussen, wurde bisher nur unzureichend untersucht. Jedoch findet man in Radioliganden-Bindungsstudien am menschlichen Gehirn auch ein geringes Signal in der Weißen Substanz, in den Arealen mit sehr vielen Nervenfasern, was zumindest auf eine schwache Expression der Rezeptoren schließen lässt. Während der Embryonalentwicklung hingegen scheinen CB1-Rezeptoren dort sehr stark exprimiert zu sein. Die Funktion dieser Expression ist aber noch nicht aufgeklärt.

Bei neuroinflammatorischen Zuständen, wie z.B. bei traumatischen Gehirnverletzungen, findet man oftmals eine langandauernde Erhöhung der Endocannabinoid-Konzentration. Diese wird wahrscheinlich zu einem nicht geringen Anteil durch die Produktion in Gliazellen hervorgerufen, und kann als ein Verteidigungsmechanismus gegen eine fortschreitende Entzündung und den damit verbundenen Zelltod gesehen werden. So wird durch die Aktivierung der CB2-Rezeptoren von Mikrogliazellen deren Zytokinproduktion gehemmt und eine überschießende Immunreaktion vermieden. In Maus-Modellen von Multipler Sklerose (MS) z.B. haben sich pharmakologische Substanzen, die die Wiederaufnahme und damit den Abbau von Endocannabinoiden hemmen, und so deren Konzentration und Wirksamkeit erhöhen, als therapeutisch wirksam erwiesen (☞ Tab. 2.2).

Auch in senilen Plaques bei Alzheimer-Patienten findet man Gliazellen mit veränderter Endocannabinoid-Reaktivität. Vor allem CB2-Rezeptoren sind hier hochreguliert und, ähnlich wie bei MS, könnte unter Umständen eine pharmakologisch induzierte, vermehrte Endocannabinoid-Konzentration im Gehirn hier die Zerstörung der Nervenzellen verlangsamen, indem die entzündliche Immunantwort gedrosselt wird (☞ Tab. 2.2).

Therapeutische Anwendung
• CB1-Rezeptor-Agonisten/Endocannabinoid-Wiederaufnahme-Hemmer[a]/Endocannabinoid-Abbau-Hemmer[a]
- Übelkeit, Erbrechen (z.B. nach Chemotherapie)[#]
- Appetitlosigkeit (z.B. bei Anorexia, AIDS)[#]
- Starke chronische Schmerzen (z.B. bei Krebs, Multipler Sklerose)[#]
- Muskelkrämpfe (Multiple Sklerose, Wirbelsäulenverletzung)[*]
- Tourette-Syndrom[*]
- Neuroprotektion (Schlaganfall, Epilepsie, Trauma, Hypoxie)[+]
- Inflammation (Multiple Sklerose, Alzheimer, Parkinson, Gehirnverletzungen)[+]
- Muskelkrämpfe (Chorea Huntington)[+]
- Posttraumatische Belastungsstörung, Angsterkrankungen[+]
- Autoimmunerkrankungen, Allergien[+]
• CB1-Rezeptor-Antagonisten
- Adipositas[#]
- Nikotinabstinenz[+]
- Dystonie und Dyskinesien (nach L-Dopa-Substitutionstherapie bei Parkinson)[+]
- Alkoholabstinenz[+]
- Angsterkrankungen, affektive Störungen[+]

Tab. 2.2: Therapeutische Anwendung.
Effekte klinisch etabliert
* Effekte klinisch erprobt
+ Effekte bisher hauptsächlich präklinisch erforscht
a bisher nur im Tierversuch angewendet

2.5. Kontrolle der motorischen Aktivität

Cannabinoid-Rezeptoren sind in hoher Dichte in den Basalganglien und im Cerebellum vorhanden, was auf ihre Bedeutung in der Kontrolle von Bewegungsabläufen schließen lässt. Sie sind vor allem in GABAergen, striatalen Projektionsneuronen zu finden, deren Ausläufer v.a. die Gehirnkerne Globus pallidus und Substantia nigra innervieren. Vergleichbar mit der Situation im Hippocampus kommen CB1-Rezeptoren aber auch sowohl in lokalen Schaltkreisen, d.h. in GABAergen Interneuronen im Caudatus Putamen vor, als auch auf cortico-striatalen, glutamatergen Nervenendigungen. Parallel zu der hohen Rezeptor-Dichte findet man im Globus Pallidus und der Substantia nigra auch die höchsten Konzentrationen von Endocannabinoiden im Gehirn. Es gibt sehr gute Hinweise dafür, dass die Signalübertragung durch das Endocannabinoid-System die GABA- und Glutamat-Übertragung in den Basalganglien reguliert und so z.B. die Wirkung von Dopamin beeinflusst.

Psychomotorische Effekte, die aufgrund von Marihuana-Konsum auftreten, sind gut dokumentiert. Generell beeinträchtigen THC und andere Cannabinoide die motorische Leistungsfähigkeit und haben einen sedierenden Effekt. Oftmals führen sie zuerst zu einer erhöhten motorischen Aktivität, der jedoch Bewegungsschwierigkeiten, Koordinationsstörungen, Zittrigkeit und körperliche Schwäche folgen. In Abhängigkeit von der Dosierung kann man bei Nagern Phasen der Bewegungshemmung oder aber auch der Aktivierung beobachten. Hiernach wurde z.B. auch der sogenannte "Popcorn-Effekt" von THC bei Mäusen beschrieben. Gruppen von Mäusen werden dabei durch die Droge sediert, springen jedoch als Folge von taktilen oder auditorischen Reizen unkontrolliert auf und verleiten andere Tiere, die sie aufgrund ihrer unkontrollierten Aktivität "anstupsen", wiederum auch zum Springen. Dabei ähneln

sie Popcorn, welches in der Pfanne durcheinander hüpft. Interessanter Weise konnte die motorische Aktivität von Mäusen auch durch die Gabe eines CB1-Rezeptor Antagonisten stimuliert werden, was dafür sprechen würde, dass eine tonische Aktivität des Endocannabinoid-Systems im Ruhezustand bereits zur Bewegungskontrolle beiträgt.

Obwohl CB1-Rezeptoren auch im Cerebellum reichlich vorhanden sind und auf praktisch allen, die Purkinje-Zellen innervierenden, exzitatorischen (glutamatergen) und inhibitorischen (GABAergen) Nervenendigungen zu finden sind, ist ihre physiologische Funktion hier noch weitgehend unerforscht. Man kann jedoch annehmen, dass das Endocannabinoid-System in diesem Falle bei Funktionen wie Gleichgewicht, Körperhaltung, Feinmotorik, motorischem Lernen oder Zeitempfinden eine Rolle spielt.

Da die meisten hyper- oder hypokinetischen Bewegungsstörungen durch eine Dysfunktion der neuronalen Kreisläufe zwischen Basalganglien, Thalamus und Cortex hervorgerufen werden, wurde eine Involvierung des Endocannabinoid-Systems in der Pathophysiologie entsprechender Krankheiten nicht ausgeschlossen. Während der letzten Jahre hat eine limitierte Anzahl von klinischen Versuchen gezeigt, dass die pharmakologische Beeinflussung des Systems sich als durchaus nützlich zur Behandlung von verschiedenen Bewegungsstörungen erweisen könnte.

Bei Chorea Huntington (auch Veitstanz genannt) z.B. sind vor allem striatale Projektionsneuronen betroffen, und das langsame Absterben dieser Nervenbahnen ruft die typischen psychomotorischen Störungen wie Dystonie und Chorea hervor, welche sich in plötzlich auftretenden, unwillkürlichen Bewegungen von Extremitäten oder Rumpf äußern. Viele tierexperimentelle als auch *post-mortem* Studien am menschlichen Gehirn weisen darauf hin, dass sowohl die CB1-Rezeptoren als auch die Endocannabinoide in den betroffenen Regionen schon im frühen Krankheitsverlauf rapide abnehmen, noch bevor andere Neurotransmitter-Systeme betroffen sind. Hieraus kann man folgern, dass das Endocannabinoid-System in den Basalganglien bei Chorea Huntington unzureichend funktioniert, und dies teilweise zu den beobachteten, typischen Hyperkinesien beitragen könnte. Sowohl in tierexperimentellen, als auch in ersten

klinischen Studien am Menschen hat sich die Behandlung mit THC als Erfolg versprechend erwiesen. Die schmerzhaft auftretenden Muskelkrämpfe scheinen sich unter THC-Behandlung zu verringern (☞ Tab. 2.2). Auch hier könnten sich in Zukunft "indirekte CB1-Rezeptor Agonisten", die durch eine Blockierung der Wiederaufnahme oder durch Inhibierung der abbauenden Enzyme die Endocannabinoid-Signalübertragung verstärken, als hilfreicher erweisen als direkte CB1-Agonisten wie THC.

Im Gegensatz zu Chorea Huntington, wo es zu einer Unterfunktion des Endocannabinoid-Systems kommt, ist bei Morbus Parkinson eher eine Überfunktion zu beobachten. Als Gegenregulation auf das Absterben der dopaminergen Neuronen der Substantia nigra pars compacta scheint es zu einer erhöhten Aktivität des Endocannabinoid-Systems in anderen Basalganglien-Kernen zu kommen, die mit den bei Morbus Parkinson auftretenden Hypokinesien assoziiert sein könnte. Experimentelle Daten von Studien an Mensch und Primaten deuten darauf hin, dass CB1-Rezeptor-Antagonisten sowohl die motorischen Verschleißerscheinungen als auch die nach langer L-Dopa-Substitutionstherapie auftretenden Dyskinesien verringern könnten (☞ Tab. 2.2). Der Einsatz eines CB1-Antagonisten hat hier den Vorteil der Vermeidung von ungewollten psychotropen Effekten.

Die Datenlage bei Parkinson ist jedoch nicht in jeder Hinsicht so klar wie bei Chorea Huntington, und die extreme Komplexität der beeinträchtigten neuronalen Kreisläufe stellt für die Forscher eine große Herausforderung dar.

Andere Bewegungsstörungen sind weit weniger untersucht. Allerdings erweist sich THC als hilfreich zur Verminderung von Tics und psychischen Störungen bei Patienten mit Tourette-Syndrom; und THC kann zur Verringerung von Muskelkrämpfen bei Multipler Sklerose beitragen (☞ Tab. 2.2).

2.6. Neuroprotektion

Obwohl sich die Forschung im Bereich Neuroprotektion noch auf dem Gebiet der Grundlagen bewegt, belegen eine Vielzahl von Studien inzwischen eine mögliche Schutzfunktion von Endocannabinoiden bei neurodegenerativen Erkrankungen. Neurodegeneration ist die Hauptursache

der Krankheitsverläufe von solch unterschiedlichen Leiden wie Chorea Huntington, Morbus Parkinson, Morbus Alzheimer oder Schlaganfall. Obwohl die molekularen Mechanismen, die letztendlich zum Absterben der Neuronen führen, sehr verschieden sein können, so sind die Auslöser doch ähnlich: eine vermehrte Produktion von reaktiven Sauerstoffradikalen aufgrund von mitochondrialem Versagen, eine durch Glutamat induzierte Exzitotoxizität, oder ein gestörtes Membranpotential durch schädliche Ionen-Ungleichgewichte.

Eine Aktivierung der CB1-Rezeptoren durch Endocannabinoide kann diese neurodegenerativen Effekte vermindern, indem sie einer übermäßigen Glutamat-Freisetzung und einem gefährlich erhöhten Kalziumeinstrom in die Zelle entgegenwirkt. In tierexperimentellen Versuchen, bei denen epilepsieartige Anfälle induziert werden, wirkt sich ein Verlust des CB1-Rezeptors in glutamatergen Neuronen im Vorderhirn äußerst verheerend aus. Dies wurde an sogenannten "konditionalen" *knock-out* Mäusen untersucht, bei denen das CB1-Rezeptor-Gen nur in den glutamatergen Vorderhirn-Neuronen inaktiviert wurde. Für dieses Experiment wurde ein Verhaltensmodell verwendet, bei dem den Mäusen Kainat injiziert wird – eine Substanz aus einem bestimmten Seegras –, das wie körpereigenes Glutamat an sogenannte Kainat-Rezeptoren bindet und dadurch vor allem im Hippocampus zu einer starken Überaktivierung der Neuronen führt. Diese Überaktivierung löst in den Mäusen epilepsieartige Krampfanfälle aus. In diesem Verhaltensversuch wurden sowohl Wildtyp-Mäuse als auch konditionale CB1-Rezeptor *knock-out* Mäuse mit Kainat behandelt. Dies führte in den Wildtyp-Mäusen zu Krampfanfällen mittlerer Schwere, wohingegen die *knock-out* Mäuse mit Krämpfen äußersten Schweregrades reagierten oder sogar starben (☞ Abb. 2.5A).
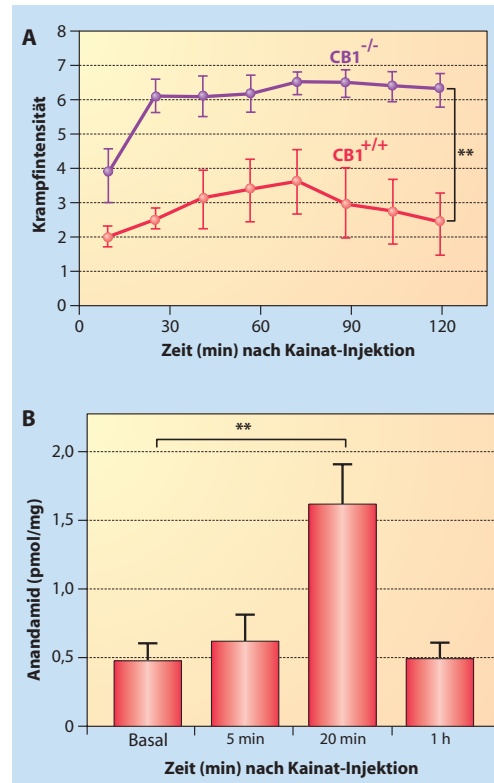
Abb. 2.5: Krampfintensität in CB1$^{+/+}$- sowie CB1$^{-/-}$ Mäusen und Endocannabinoid-Konzentrationen nach Kainat-Injektion. **A**: epileptische Krampfintensität bis zu 2 Stunden nach intraperitonealer Kainat-Injektion (30 mg/kg) in CB1-Rezeptor-Wildtyp-(CB1$^{+/+}$) und -*knock-out* Mäusen (CB1$^{-/-}$). Hohe Werte bedeuten starke Krampfintensität. **B:** Zeitlicher Verlauf der Anandamid-Konzentrationen im Hippocampus von CB1$^{+/+}$ Mäusen nach intraperitonealer Kainat-Injektion (30 mg/ kg). Signifikanz: **, p<0.01.

Zwanzig Minuten nach der Kainat-Injektion konnte im Hippocampus eine erhöhte Konzentration des Endocannabinoids Anandamid gemessen werden (☞ Abb. 2.5B), welches die Wildtyp-Mäuse augenscheinlich vor allzu schweren Krampfanfällen schützte. Wurde der Endocannabinoid-Wiederaufnahmehemmer UCM707 (vgl. Kap. 1.6.) vor der Kainat-Injektion verabreicht, so zeigten die Wildtyp-Mäuse durch die erhöhte Endocannabinoid-Konzentration geringere Krämpfe; den *knock-out* Mäusen half dies hingegen nicht, was darauf schließen lässt, dass tatsächlich die CB1-Rezeptoren hier notwendig sind, um den schützenden Effekt der Endocannabinoide zu vermitteln.

Im vorliegenden Fall scheint nicht nur die Dämpfung der neuronalen Erregbarkeit eine Rolle zu spielen, sondern auch intrazelluläre Signalübertragungsprozesse. Diese aktivieren letztendlich Transkriptionsfaktoren im Zellkern und passen so die Zellphysiologie entsprechend an, um damit für den Langzeit-Schutz zu sorgen.

So wie beim eben beschriebenen Modell kommt es fast bei jedem zerebralen Insult zu einer lokalen Erhöhung der Endocannabinoid-Konzentration, wobei sowohl Anandamid als auch 2-AG involviert zu sein scheinen. Nicht alle protektiven Effekte werden aber durch einen entsprechenden Rezeptor vermittelt. THC und Cannabidiol weisen durch ihre besondere chemische Struktur (THC z.B. durch seine phenolische Hydroxylgruppe) eine stark antioxidative Wirkung auf, die der von Vitamin C oder Alpha-Tocopherol (Vitamin E) mindestens ebenbürtig ist. Bereits auf diese Weise kann also einer starken Belastung durch Radikale bei neurodegenerativen Krankheitszuständen entgegengesteuert werden.

Ein weiterer wichtiger Aspekt der Neuroprotektion, den es zu beachten gilt, ist das oftmals gleichzeitige Auftreten von Neuroinflammation. Nach einem Schlaganfall z.B. ist eine starke Entzündung des umliegenden Nervengewebes zu beobachten, die zum Zelltod in der Penumbra, einem Gebiet der Minderdurchblutung, beiträgt. Besonders auch in Tiermodellen der Multiplen Sklerose ist der neuroinflammatorische Aspekt gut untersucht. In verschiedenen Studien hat sich gezeigt, dass eine Aktivierung des Endocannabinoid-Systems die zerebrale Immunantwort hemmt, eine übersteigerte Einwanderung von Immunzellen in das betroffene Gewebe verhindert und die Ausschüttung von inflammatorischen Zytokinen und Stickstoffmonoxid (NO) verringern kann (vgl. auch Kap. 2.4.).

Obwohl die meisten Untersuchungen einer Erhöhung der Endocannabinoid-Konzentration einen protektiven Effekt zuschreiben, gibt es auch Studien, die unter bestimmten experimentellen Bedingungen durch die Blockade des Systems einen schützenden Effekt erreichen, und bei denen eine Erhöhung hingegen zu zusätzlicher Schädigung führen kann. Auch hier tritt die Komplexität des Endocannabinoid-Systems wieder zu Tage, und in Abhängigkeit davon, welches Gehirnareal, welche Untergruppe von Nervenzellen oder welcher neuronale Kreislauf durch eine Krankheit besonders betroffen ist, könnten sich jeweils entgegengesetzte Behandlungsansätze als erfolgreich erweisen. Es gilt also, die Bedingungen und das Krankheitsstadium für eine pharmakologische Intervention genauestens festzulegen, und experimentell so gut zu untersuchen, dass sich klinische Versuche als gerechtfertigt erweisen. Auch im Falle der Neuroprotektion könnte der Einsatz von Wiederaufnahmehemmern einen gewissen Grad an Selektivität für die betroffenen Gehirnregionen bedeuten und gegenüber dem Einsatz von Agonisten wie THC von Vorteil sein (☞ Tab. 2.2; vgl. auch Kap. 1.6.).

2.7. Belohnung und Abhängigkeit

Um lebenswichtige Verhaltensweisen wie Essen, Trinken, Sexualverhalten und Elternfürsorge sicherzustellen, hat die Natur die Befriedigung dieser Bedürfnisse mit Belohnungseigenschaften ausgestattet. Hierfür ist ein als Belohnungs- oder Lustzentrum bezeichnetes System unseres Gehirns zuständig, welches aus verschiedenen Arealen und neuronalen Kreisläufen zusammengesetzt ist und auch als mesolimbisches Dopaminsystem bekannt ist. Die meisten Drogen mit Suchtpotenzial, wie z.B. Nikotin, Alkohol, *Cannabis*, Morphin, Amphetamin oder Kokain, scheinen Schlüsselstellen in diesem System zu aktivieren. Eine Stimulation geht mit einer erhöhten dopaminergen Neurotransmission einher und führt nicht nur zur Verarbeitung der erfahrenen Belohnung, sondern oftmals auch zur motorischen Aktivierung, die im Zusammenhang mit Drogenkonsum beobachtet wird. Das mesolimbische Dopaminsystem besteht vor allem aus Nervenbahnen der Area ventralis tegmentalis (VTA) im Mittelhirn, welche zu Zielregionen im Vorderhirn projizieren und dort mittels Dopaminausschüttung Kernareale wie den Nucleus accumbens oder den Präfrontalen Cortex aktivieren. Bei kontinuierlicher Verabreichung von Drogen kann es auf Dauer zu einer Abschwächung der Dopaminübertragung und damit der Drogenwirkung kommen (auch als Toleranz bezeichnet); die Effekte können sich mit der Zeit aber auch steigern (z.B. wenn Psychostimulanzien wie Amphetamin wiederholt in einer Einzeldosis verabreicht werden), ein Phänomen, welches als Sensibilisierung bezeichnet wird.

In der frühen wissenschaftlichen Literatur wurde vielfach beschrieben, dass das Phänomen der Toleranz auch nach lang andauerndem THC-Konsum zu beobachten sei. Nichts desto trotz galt *Cannabis* über viele Jahre hinweg nicht als eine Droge, die süchtig macht. Diese Einstellung hat sich jedoch gerade in den letzten Jahren gewandelt. Und wenn die DSM-IV-Kriterien (American Psychiatric Association, 1994), die nun eher die Begriffe der Substanz-Abhängigkeit und des Substanz-Missbrauchs als der Sucht definieren, auf Populationen von regelmäßigen *Cannabis*-Rauchern angewendet werden, erweist sich ein großer Anteil nach diesen Definitionen als positiv. Sorgfältig kontrollierte Studien haben inzwischen ferner nachgewiesen, dass nicht nur im Tierversuch, sondern sehr wohl auch bei *Cannabis*-Rauchern klinisch signifikante Entzugserscheinungen auftreten können. Sie beinhalten das starke Verlangen nach *Cannabis*, reduzierten Appetit, Schlafschwierigkeiten und Gewichtsverlust, verursachen manchmal auch emotionale Instabilität wie Aggression oder innere Unruhe.

Seit der Entdeckung von selektiven CB1-Rezeptor-Antagonisten ist es nun auch eher möglich, in tierexperimentellen Untersuchungen die Effekte der THC-Abhängigkeit zu erforschen. Entzugserscheinungen nach chronischer THC-Gabe lassen sich durch den Einsatz eines Antagonisten nämlich besser darstellen. In elektrophysiologischen Studien konnte gezeigt werden, dass solche *Cannabis*-assoziierten Entzugserscheinungen mit einer reduzierten Feuerrate von dopaminergen Neuronen in der Area ventralis tegmentalis einhergehen. Zusätzlich konnte man nachweisen, dass THC in der Lage ist, selektiv eine Ausschüttung von Dopamin im Nucleus accumbens hervorzurufen. Dies legt den Schluss nahe, dass THC ähnliche Effekte wie andere Drogen im Gehirn auslösen kann. Eine Reihe von Versuchen konnte weiterhin zeigen, dass ein Zusammenhang zwischen der Abhängigkeit von Cannabinoiden und der von Opiaten besteht. Zwischen beiden Systemen scheinen klare Wechselwirkungen zu bestehen, auch wenn die zugrunde liegenden neuronalen Kreisläufe noch nicht verstanden werden.

So hat in letzter Zeit das Endocannabinoid-System nicht nur wegen seiner Rolle bei *Cannabis*-Abhängigkeit aufsehen erregt, sondern vielmehr wegen seiner Interaktion und teilweisen Verstärkung von neuronalen Kreisläufen, die im Zusammenhang mit dem Suchtpotenzial anderer Drogen, wie z.B. Nikotin, stehen. Viele Untersuchungen sprechen inzwischen dafür, dass das Endocannabinoid-System via CB1-Rezeptoren vor allem die motivierenden Effekte von Nikotin vermittelt, wobei es an der Entwicklung der physischen Abhängigkeit nicht essenziell beteiligt zu sein scheint. So blockiert ein CB1-Rezeptor-Antagonist die Nikotin-abhängige Ausschüttung von Dopamin im Nucleus accumbens, interagiert jedoch hingegen nicht direkt mit den nikotinischen Acetylcholin-Rezeptoren. CB1-Rezeptor-Antagonisten blockieren aber nicht nur den motivierenden und verstärkenden Effekt von Nikotin, sondern verringern auch Umweltreiz-induziertes Verlangen nach Nikotin und damit die mögliche Rückfälligkeit nach Abstinenz.

Neurotransmitter-Veränderungen in bestimmten Gehirnarealen, wie dem mesolimbischen System, lassen sich am lebenden Tier experimentell mit Hilfe der Mikrodialyse bestimmen. Hierbei wird eine spezielle Sonde operativ in das betreffende Gehirnareal eingebracht. Diese ist mit einer semi-permeablen Membran ausgestattet und wird von außerhalb, durch Schläuche verbunden, mit artifizieller Zerebralflüssigkeit durchspült. Die im Gehirn freigesetzten Neurotransmitter diffundieren so durch die Membran in die durchspülende Flüssigkeit und können aus dieser z.B. mittels Hochdruck-Flüssigkeits-Chromatographie quantitativ bestimmt werden. So erhöht eine Ethanolinjektion z.B. die Dopamin-Konzentration im Nuclus accumbens (☞ Abb. 2.6). Dieser Effekt ist jedoch vom Endocannabinoid-System abhängig, da er in CB1-Rezeptor-*knock-out* Mäusen nicht mehr beobachtet werden kann.
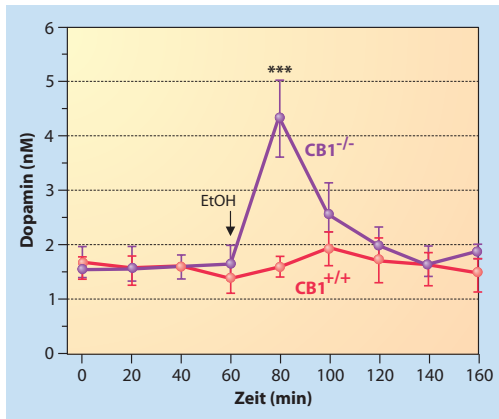
Abb. 2.6: Dopaminfreisetzung in CB1$^{+/+}$- und CB1$^{-/-}$-Mäusen im Nucleus accumbens nach Alkoholinjektion. Dopaminfreisetzung im Nucleus accumbens nach intraperitonealer Ethanol (**EtOH**)-Injektion (1,5 g/kg), gemessen über *in vivo* Mikrodialyse, in CB1-Rezeptor-Wildtyp- (**CB1**$^{+/+}$) und -*knock-out* Mäusen (**CB1**$^{-/-}$). Signifikanz: ***, p<0.001. Modif. nach Hungund et al., J Neurochem 2003 Vol 84:698.

Lang andauernde Abhängigkeit führt unausweichlich auch zu persistierenden Veränderungen der synaptischen Plastizität von neuronalen Kreisläufen. Solche Mechanismen könnten z.B. erklären, wie Nikotin-assoziierte Schlüsselreize sich zu konditionierten Verstärkern entwickeln können, die die Sucht aufrechterhalten. Auch hierbei kommt dem Endocannabinoid-System eine wichtige Rolle zu, indem es z.B. Lang-Zeit-Änderungen der synaptischen Plastizität im Striatum hervorrufen kann. Chronische Nikotin- oder Alkohol-Einnahme geht z.B. einher mit einer Erhöhung der Endocannabinoid-Konzentration im limbischen Vorderhirn.

Zusätzlich scheint die Interaktion des Endocannabinoid-Systems mit dem mesolimbischen System eine Rolle bei der Kontrolle der Nahrungsaufnahme zu spielen. Hierbei verstärken Endocannabinoide die Motivation, Nahrung zu finden und zu konsumieren durch eine Erhöhung der Anreiz-Schwelle.

Zusammenfassend kann man sagen, dass sich das Endocannabinoid-System in den letzten zehn Jahren als ein wichtiger Regulator von Motivationsprozessen herausgestellt hat, indem es in die mesolimbische Neurotransmission von Dopamin eingreift. Tierexperimentelle Studien legen den Einsatz von CB1-Rezeptor-Antagonisten als Therapie bei Nikotin-, Alkohol- und Cannabis-Abhängigkeit nahe. CB1-Rezeptor-Antagonisten könnten speziell bei der Unterstützung von Raucher-Abstinenz wirkungsvoll zum Einsatz kommen. Erste klinische Studien bestätigen dies (☞ Tab. 2.2).

2.8. Lernen und Gedächtnis

Seit der Entdeckung des Endocannabinoid-Systems hat sich die Forschung bemüht, vor allem seine endogenen, physiologischen Funktionen zu verstehen. So auch im Bereich von Lernen, Gedächtnis und Erinnerung. Vor allem die Gedächtnis-Konsolidierung (die Stabilisierung von Gedächtnisinhalten) und die Extinktion (die Auslöschung von Gedächtnisinhalten) scheinen der Kontrolle des Endocannabinoid-Systems zu unterliegen. Zudem werden auch elektrophysiologische Korrelate des Lernens, welche die synaptische Plastizität tragend beeinflussen, wie z.B. die Lang-Zeit-Potenzierung (LTP), maßgeblich von ihm moduliert.

Einer der Haupteffekte von *Cannabis* beim Menschen ist eine Einschränkung des Kurzzeit- und des Arbeitsgedächtnisses; eine Beobachtung, die vor allem dann gemacht wird, wenn die verwendeten Gedächtnistests stark von dem Aufmerksamkeitszustand des Probanden abhängen. Viele Studien bezüglich der akuten und chronischen Effekte von *Cannabis* auf kognitive Funktionen wurden in den letzten Jahren durchgeführt. Obwohl bei einer ganzen Reihe von Tests Beeinträchtigungen festgestellt wurden, sind die Effekte doch relativ subtil, und im Vergleich zur Wirkung von Alkohol z.B. wesentlich schwächer ausgeprägt. So konnte im Gegensatz zu Alkohol bei *Cannabis* bisher kein durchschlagender Effekt auf die Reaktionszeit des Probanden festgestellt werden. Auch können Menschen unter THC-Einwirkung einfache, arithmetische Tests erledigen oder einfache Listen von Wörtern immer noch lernen. Früher gemachte Erinnerungen können ohne Probleme wieder abge-

rufen werden. Hingegen traten oft Aufmerksamkeitsdefizite auf, vor allem bei länger andauernden und eintönigen Aufgaben. Weiterhin zeigen die Probanden eine verminderte Fähigkeit dazu, bestimmte Reaktionen aktiv zu verhindern, oder auch komplexe arithmetische Aufgaben und Tests, die die Reaktionszeit in komplizierter Weise abfragen, durchzuführen. Zur Frage danach, ob chronischer *Cannabis*-Missbrauch auch zu Langzeitschäden der Gedächtnisleistung führen kann, finden sich in der Literatur widersprüchliche Ergebnisse.

Obwohl man also inzwischen relativ viel über den Einfluss exogener Cannabinoide wie z.B. THC auf die Gedächtnisfunktion weiß, so ist es doch recht schwierig, die Rolle des endogenen Systems zu untersuchen. Durch die Anwendung von Agonisten kann man zwar unter Umständen darauf schließen, bei welchen Gedächtnisprozessen das Endocannabinoid-System involviert ist; über die endogenen Mechanismen des Systems, welche zusammen mit den Einwirkungen anderer Neurotransmitter-Systeme in einer orts- und zeitabhängigen Weise spezifisch integriert sind, lassen sich hingegen nur sehr schwer klare Schlüsse ziehen.

Die Hauptbeobachtung, die man in konsistenter Weise bei dem Einsatz eines Agonisten machen kann, ist auch im Tierexperiment (wie oben beim Menschen beschrieben) eine Beeinträchtigung des Kurzzeit-, und des Arbeitsgedächtnisses. Das Aufrufen gut erlernter Information aus dem Langzeitgedächtnis hingegen wird so gut wie nicht beeinflusst. Natürlich umfasst der Begriff des Arbeitsgedächtnisses mehrere unterscheidbare Aspekte des Lernens, wie Aufmerksamkeit, Assoziation, Konsolidierung, Speicherung und Wiederabrufen des Gelernten. In welche dieser Unterprozesse CB1-Agonisten genau eingreifen, wird immer noch intensiv untersucht. Hierbei muss man bedenken, dass bei tierexperimentellen Untersuchungen das Gedächtnis des Tieres ja nicht direkt abgefragt werden kann, sondern dass man aus der Art und Weise, wie das Tier den Test durchführt und auf gewisse Stimuli reagiert, auf seine Gedächtnisleistung schließen muss. Dies ist nicht unproblematisch, da auch Änderungen der Aufmerksamkeit, des Emotionszustandes oder der Sensomotorik das Verhalten der Tiere signifikant beeinflussen können. Und gerade CB1-Agonisten wirken unabhängig vom Gedächtnis auch auf viele andere Funktionen wie z.B. lokomotorische Aktivität,

Emotion oder Angst (vgl. Kap. 2.9.). Es ist also vor allem wichtig, die Versuche gegenüber diesen ungewollten Einflüssen zu kontrollieren, und das Verhalten in verschiedenen tierexperimentellen Gedächtnistests wie z.B. operanten und räumlichen Lerntests oder konditionierten Vermeidungs-Tests abzurufen. In diesem Zusammenhang sollte auch darauf hingewiesen werden, dass Cannabinoide die subjektive Wahrnehmung von Zeit signifikant verändern. Dies trifft sowohl für den Menschen, als auch für Versuchstiere zu und kann das Ergebnis von Gedächtnistests, die stark auf einer zeitlichen Komponente beruhen, indirekt beeinflussen.

Zusammenfassend lässt sich sagen, dass sowohl Cannabinoid-Agonisten verschiedener Substanzklassen als auch Endocannabinoide, exogen verabreicht, selektiv Gedächtnis-Aufgaben beeinträchtigen, die vom Kurzzeit- und Arbeitsgedächtnis abhängen; und zwar in solch geringen Dosierungen, die weder andere, ungewollte Cannabinoid-induzierte Effekte verursachen noch das Referenzgedächtnis beeinflussen. Weiterhin scheinen fast alle Agonisten über den CB1-Rezeptor auf das Gedächtnis zu wirken, da sie mit spezifischen CB1-Antagonisten wie Rimonabant aufgehoben werden konnten. Bei der Untersuchung der Effekte, die von einer chronischen Agonist-Einnahme ausgehen, bestehen jedoch weiterhin Ungereimtheiten, da sich eine Toleranz nur bei einigen spezifischen Gedächtnistests auszubilden scheint.

Um zu untersuchen, wie das Endocannabinoid-Systems unsere Gedächtnisleistung kontrolliert, untersucht man in Gedächtnistests am besten entweder CB1-Rezeptor-*knock-out* Mäuse oder Mäuse, die mit einem CB1-Antagonisten behandelt werden. Hierbei stellt sich heraus, dass das System sich im Grundzustand eher hemmend auf die Bildung und Stabilität von Gedächtnisinhalten auswirkt. So erkennen mit einem Antagonisten behandelte Tiere in einem sozialen Wiedererkennungstest die ihnen vormals unvertrauten Jungtiere bei wiederholter Präsentation besser als ihre unbehandelten Kontrollpartner. Auch in einem Objekt-Wiedererkennungstest z.B. schnitten *knock-out* Mäuse besser ab als ihre Wildtyp-Geschwister. Kürzlich allerdings wurde entdeckt, dass dieser gedächtnisverstärkende Effekt durch die genetische Inaktivierung des CB1-Rezeptors nur in jungen Tieren beobachtet wird. Bei Mäusen mittleren Al-

ters zeigen *knock-out*-Tiere, denen der CB1-Rezeptor während des gesamten Lebens gefehlt hatte, bereits Gedächtnisdefizite gegenüber den Kontrollmäusen, die sich in hohem Alter noch zunehmend verschlechtern. Dies scheint mit neurodegenerativen Prozessen im Hippocampus einher zu gehen, die durch die fehlende Funktion des CB1-Rezeptors ausgelöst werden. Das ist ein sehr interessantes Ergebnis, und es ist zu hoffen, dass diese Experimente pharmakologisch durch die chronische Blockade mit Rimonabant oder anderen CB1-Rezeptor-Antagonisten wiederholt werden. Denn es gilt zu beachten, dass bei genetischer Blockade, wie sie bei den gängigen (d.h. klassischen) *knock-out* Mäusen geschieht, das CB1-Rezeptor-Gen für die gesamte Lebensspanne ausgeschaltet ist. Es ist deshalb nicht auszuschließen, dass sich in dieser langen Zeitspanne kompensatorische Prozesse ausgebildet haben, die zum Beispiel zu den neurodegenerativen Prozessen geführt haben. Diese im Alter beobachteten Gedächtnisdefizite lassen also keine klaren Schlüsse zu, in welcher Weise das Endocannabinoid-System akut die Gedächtnisprozesse in jenem Alter beeinflusst. Ein mögliches Szenarium ist das folgende: Junge Mäuse profitieren davon, dass durch den Verlust von CB1-Rezeptoren die neuronale Erregbarkeit erhöht ist. So bewirkt diese Veränderung eine Verbesserung der Lernfähigkeit. Bei anhaltender, leicht erhöhter Erregbarkeit aber, und durch die leicht überaktivierte Stressachse (☞ Kap. 2.10.), die zu erhöhten Werten von Corticosteron führt, kann es im Alter sodann jedoch zu neurodegenerativen Prozessen kommen.

In anderen Studien wurde ebenfalls herausgefunden, dass ein Verlust des CB1-Rezeptors noch weitere negative Begleiterscheinungen mit sich führt: nämlich die verminderte Fähigkeit, unliebsame Ereignisse in adäquater Weise wieder zu vergessen. Hier greifen Endocannabinoide in einen Prozess des Lernens ein, der als Extinktion ("Auslöschen") bezeichnet wird, und einen Vorgang beschreibt, bei welchem eine gelernte Verhaltensweise, die nicht weiter verstärkt wird, mit der Zeit aktiv unterdrückt wird. In einem bestimmten Verhaltensparadigma, der sogenannten Furchtkonditionierung z.B., lernen Mäuse bei einem einzigen Trainingsdurchgang (am Tag 0), einen neutralen Stimulus (d.h. ein Tonsignal) mit einem unangenehmen Fußschock zu assoziieren (☞ Abb. 2.7). Bei

erneuter Präsentation des Tons (diesmal ohne den Schock) am darauf folgenden Tag (Tag 1), zeigen die Mäuse eine deutliche Furchtreaktion, die insbesondere durch eine ausgeprägte Körperstarre (engl. *freezing*) gekennzeichnet ist. Beim wiederholten Vorspielen des Tons an weiteren Tagen (z.B. Tag 2, 3 und 6), und gleichzeitigem Ausbleiben des furchtauslösenden Schocks, lernen die Mäuse aktiv, dass der Ton nun *per se* nicht mehr gefährlich ist, und erholen sich recht schnell von ihrer nun mehr unbegründeten Furchtstarre. CB1-Rezeptor-*knock-out* Mäuse jedoch verbleiben viel länger im Zustand der Starre, zeigen also eine unzureichende Extinktion ihrer Furchtreaktion.
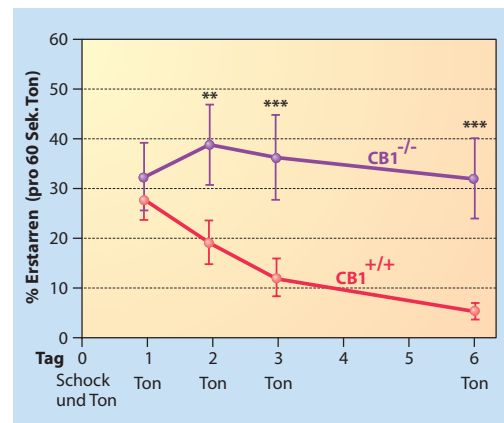
Abb. 2.7: Furchtkonditionierung und Auslöschung des Angstgedächtnis in CB1$^{+/+}$- sowie CB1$^{-/-}$ Mäusen. Einer Gruppe von CB1-Rezeptor-Wildtyp- (**CB1**$^{+/+}$) und -*knock-out* Mäusen (**CB1**$^{-/-}$) wurde am Tag 0 ein schmerzhafter Fußschock zusammen mit einem Ton verabreicht. Ihre Furchtstarre auf die erneute, alleinige Präsentation des Tons (in % Erstarren) wurde an den darauffolgenden Tagen (1, 2, 3 und 6) gemessen. Die effiziente Reduktion der Furchtreaktion ("Extinktion") hängt vom Vorhandensein des CB1-Rezeptors ab. Signifikanz: **, $p<0.01$; ***, $p<0.001$.

Offensichtlich verschlechtert sich durch das Fehlen des CB1-Rezeptors vor allem die Anpassungsfähigkeit der Tiere an potenziell bedrohliche Reize. Vielleicht lassen sich in Zukunft aus dieser Erkenntnis mögliche Therapieansätze für die Behandlung von Patienten mit inadäquater Reaktion auf potenziell bedrohliche Ereignisse ableiten, wie es z.B. bei Phobikern oder Patienten, die an Posttraumatischer Belastungsstörung leiden, der Fall ist (☞ Tab. 2.2).

Zumindest in Nagern durchgeführte Experimente konnten zeigen, dass mittels Endocannabinoid-Wiederaufnahmehemmern die Extinktion beschleunigt werden konnte. Dies weckt Optimismus, dass solche Substanzen bei klinischen Behandlungsstrategien, wie die der pharmakologisch unterstützten Expositionstherapie, zum Einsatz kommen könnten.

Als anatomische Strukturen im Gehirn, wo das Endocannabinoid-System besonderes in die Gedächtnisleistung mit eingreift, treten vor allem der Hippocampus (das Zentrum für das Gedächtnis von Raum und Fakten), der Mandelkern (die Amygdala, das Zentrum der Emotionen) und der Präfrontale Cortex (das Zentrum des Arbeitsgedächtnisses und von Prozessen, die auf Veränderungen von Verhaltensweisen hinzielen), aber auch das Striatum hervor (eine Region, die vor allem für das Lernen von Gewohnheiten und für das prozedurale Gedächtnis wichtig ist). Am weitreichendsten, vor allem elektrophysiologisch untersucht, ist sicherlich der Hippocampus. Hier treten alle gängigen Cannabinoid-vermittelten Prozesse wie Langzeit-Potenzierung (LTP) und Langzeit-Hemmung (LTD) auf, die für die Modulierung der synaptischen Plastizität von entscheidender Bedeutung sind, und damit das Verstärken oder Schwächen von "synaptischen Gedächtnisverschaltungen" entscheidend mitbestimmen (vgl. Kap. 2.3.3.).

Zusätzlich zu den elektrophysiologischen Prozessen, die dem Einfluss von Endocannabinoiden unterliegen, vermögen diese außerdem auch intrazellulär wichtige Signalketten zu aktivieren, von denen man weiß, dass sie maßgeblich an Lernen und Gedächtnis beteiligt sind. So modulieren sie z.B. die Aktivität von extrazellulären Signal-regulierten Kinasen (ERKs) oder von Phosphatasen wie Calcineurin (vgl. Kap. 1.4.2.).

Alle bisherigen Beobachtungen sprechen dafür, dass das Endocannabinoid-System maßgeblich in die physiologischen Vorgänge involviert ist, auf denen die Fähigkeit zu lernen und sich zu erinnern beruht.

2.9. Emotion und Angst

Seit vielen hundert Jahren weiß man bereits, dass das Rauchen von Marihuana den Gemütszustand des Menschen merklich verändern kann. Dass das Endocannabinoid-System aber ebenfalls die Physiologie und Pathophysiologie von Angst- und Depressionszuständen beeinflusst, erkennt man erst seit einiger Zeit, und man verspricht sich hier durch pharmakologische Interventionen bei speziellen Krankheitsbildern in Zukunft Linderung.

Der Hauptgrund für die Anwendung von *Cannabis* als Genussmittel ist seine Euphorie auslösende Wirkung. Dieses Rauscherlebnis wird oft begleitet von verminderter Ängstlichkeit, nicht selten gepaart mit erhöhter Geselligkeit. In manchen Fällen werden aber auch genau gegenteilige Effekte wie erhöhtes Angstgefühl, Dysphorie, Panik oder sogar Verfolgungswahn oder Psychosen beschrieben. Dies kann bei Personen, die in der Pubertät häufig *Cannabis* geraucht haben, sogar zu einem Risikofaktor für Schizophrenie werden. Wie der Einzelne jeweils auf *Cannabis* reagiert, scheint vor allem von seinen eigenen Vorerfahrungen und momentanem Gemütszustand, als auch von dem Umweltkontext abzuhängen. Weiterhin könnte es aber auch mit der konsumierten Menge zusammenhängen, da für *Cannabis*-Wirkungen oft Dosis-abhängig bidirektionale Effekte beschrieben werden (z.B. für Exploration und Motorik). So auch bei der Angstwahrnehmung, wo geringe Dosen eher angstlösend, hohe Dosen hingegen angstfördernd wirken. Weiter ist auch zu beachten, dass neuere Züchtungen von *Cannabis sativa* meist einen sehr hohen Gehalt von THC haben, während der Anteil des nicht-psychotrop wirkenden Cannabidiols viel geringer ist. Wie kürzlich gezeigt wurde, hat Cannabidiol anti-psychotische Wirkungen im Menschen. Diese Verschiebung im Verhältnis von THC zu Cannabidiol (☞ Abb. 1.2) verändert natürlich die Wirkungen, die das Rauchen induziert.

Eine Dosis-Abhängigkeit bei THC-Behandlungen lässt sich in Tiermodellen konsistent immer wieder beobachten, und es gibt mehrere Theorien für ihr Zustandekommen: So könnten Cannabinoide konzentrationsabhängig an verschiedenen neuroanatomischen Strukturen mit unterschiedlicher Sensitivität angreifen und damit entgegengesetzte Effekte auslösen. Vorstellbar ist auch, dass die

Cannabinoid-Rezeptoren in ein und derselben Gehirnregion, aber auf verschiedenen Neuronen-populationen, wie an GABA- oder glutamatergen Nervenendigungen, eine unterschiedliche Affini-tät aufweisen, und so bei geringer Dosis z.B. nur die Rezeptoren auf den glutamatergen, bei hoher Dosis aber zusätzlich auch die Rezeptoren auf den GABAergen Zellen, oder umgekehrt, aktiviert wer-den. Auch die Kopplung an verschiedene intrazel-luläre Signalkaskaden, abhängig von der zeitlichen oder örtlichen Rezeptoraktivierung, z.B. durch die Involvierung von inhibitorischen oder aktivieren-den G-Proteinen (vgl. Kap. 1.4.2.), ist denkbar. Nicht ausgeschlossen ist ebenso die Mitwirkung von noch nicht charakterisierten Cannabinoid-Rezeptoren. In CB1-Rezeptor-*knock-out* Mäusen lassen sich nämlich durch den Einsatz eines CB1-Rezeptor-Antagonisten noch Effekte auf das Angstverhalten nachweisen. Es könnte daher mög-lich sein, dass durch den Antagonisten zusätzlich noch andere Cannabinoid-Rezeptoren unbekann-ten Typs blockiert werden können. Aber solange ein solcher Rezeptor nicht molekular charakteri-siert wurde, sind diese Resultate noch nicht ein-deutig.

Viele tierexperimentelle Studien dokumentieren die Wichtigkeit der Umweltfaktoren für die Can-nabinoid-vermittelten Effekte auf Emotionen und Angstverhalten. CB1-Rezeptor-Agonisten können durchaus in verschieden Verhaltenstests, wie z.B. dem Sozialen Interaktionstest und dem "*elevated plus-maze*"-Test, unterschiedliche oder auch nur partielle Effekte zeigen. Dies mag damit zusam-menhängen, dass die abgefragten Verhaltenswei-sen durch unterschiedliche neurobiologische Si-gnalwege vermittelt werden, in welche das Endo-cannabinoid-System nicht in gleicher Weise ein-greift. Es scheint daher durchaus plausibel, dass das Endocannabinoid-System in unterschiedli-cher Weise in verschiedene Stadien oder Ausprä-gungen von Angst involviert sein könnte.

Nun ist Angst natürlich *per se* eine notwendige und überlebenswichtige Verhaltensweise, die dem Or-ganismus hilft, mit gefährlichen Situationen um-zugehen. Nur wenn dieser Gefühlszustand sich unangemessen verstärkt, oder in chronischer Form erhalten bleibt, können sich daraus psychia-trische Erkrankungen entwickeln. Um diese medi-kamentös zu behandeln, stehen momentan vor al-lem Benzodiazepine (z.B. Valium) und Substan-

zen, die in das Serotonin-System eingreifen, zur Verfügung. In diesem Zusammenhang scheint es interessant, dass in CB1-Rezeptor-*knock-out* Mäu-sen sowohl Anxiolytika, die auf das GABAerge Sy-stem Einfluss nehmen, viel von ihrer Wirksamkeit einbüßen. Hier scheint also eine Verknüpfung mit dem Endocannabinoid-System zu bestehen, die es bei der Behandlung von Angsterkrankungen in *Canna*bis-Konsumenten zu beachten gilt.

Knock-out Mäuse zeigen ebenso wie auch mit ei-nem CB1-Rezeptor-Antagonisten behandelte Tie-re gegenüber ihren Kontrollen ein verändertes Angstverhalten in einer ganzen Reihe von ver-schiedenen Tests. Die Ergebnisse sind nicht immer einheitlich. In Abhängigkeit von dem genetischen Hintergrund, den Haltungsbedingungen, der Ta-geszeit und den Lichtverhältnissen, bei denen die Tests durchgeführt wurden, verhielten sich die *knock-out*-Tiere entweder ängstlicher oder muti-ger. Auch in Tiermodellen für depressives Verhal-ten zeigten sich unterschiedliche Ergebnisse. In ei-nem bestimmten Test z.B., dem sogenannten "*for-ced swim test*", wird ein "Verhaltens-Unterphäno-typ" der Depression, nämlich die mangelnde Be-reitschaft, sich unangenehmen Situationen zur Wehr zu setzen, und sich sozusagen antriebslos zu ergeben, abgefragt. Hierbei werden Mäuse dazu gebracht, für sechs Minuten in einem Becherglas gefüllt mit Wasser zu schwimmen. Nach einer an-fänglichen Phase, in der sie erregt an den Wänden des Glases umher schwimmen und versuchen, aus dem Wasser herauszukommen, ergeben sie sich nach und nach der Situation und nehmen eine Körperhaltung der Immobilität an, bei welcher sie passiv auf dem Wasser treiben. Dieser Test ist äu-ßerst sensitiv gegenüber der pharmakologischen Behandlung mit den meisten gängigen Antide-pressiva, welche alle der "Immobilitätsstarre" der Maus entgegenwirken und sie länger gegen die un-liebsame Situation ankämpfen lassen. Diese "anti-depressive" Wirkung kann man bei der Maus auch nach Gabe des CB1-Rezeptor-Antagonisten Ri-monabant beobachten, wohingegen sich CB1-Rezeptor-*knock-out* Mäuse in dem Test entweder gar nicht unterschiedlich oder sogar entgegenge-setzt verhalten, indem sie wesentlich mehr "immo-bil" sind als ihre Kontrolltiere (☞ Abb. 2.8). Hier-zu sind weitere Untersuchungen notwendig, um den Einfluss der Endocannabinoide bei diesen Verhaltensweisen verstehen zu können.
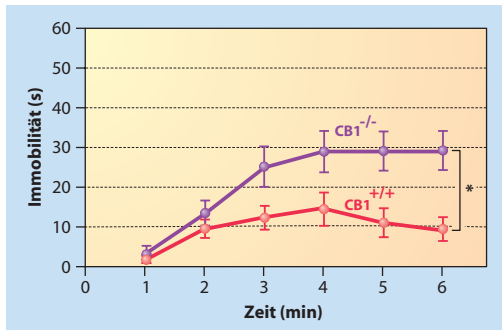
Abb. 2.8: *"Forced swim test"* in CB1$^{+/+}$- und CB1$^{-/-}$ Mäusen. CB1-Rezeptor-Wildtyp-Mäuse (**CB1$^{+/+}$**) verweilen während der sechsminütigen Schwimmphase generell eine geringere Zeitspanne in der sogenannten Immobilitätsstarre als CB1-Rezeptor-*knock-out* Mäuse (**CB1$^{-/-}$**). Signifikanz: *, p<0.05.

Gerade im Bereich der affektiven Störungen wird die Rolle des Endocannabinoid-Systems folglich noch kontrovers diskutiert. Ein Problem bei Depressions-Modellen im Tier ist, dass solche Verhaltensparadigmen zum großen Teil auf Stresskomponenten beruhen. So z.B. eine Prozedur, die "*chronic-mild-stress*" genannt wird, bei der Nager über mehrere Wochen verschiedenen Stressoren in einer für die Tiere unvorhersehbaren Weise ausgesetzt werden, um sie hiernach in verschiedenen "Emotionalitätstests" auf ihre Stressempfindlichkeit und damit auf ihre "Anfälligkeit zur Depression" hin zu untersuchen. Auch der oben genannte "*forced swim test*" ist natürlich mit einem erheblichen Stress für das Tier verbunden. Obwohl übermäßiger Stress beim Menschen zu Depressionen führen kann, besteht hier jedoch keine grundsätzliche Kausalität. Auf jeden Fall sollte man bei den Tiermodellen nicht außer Acht lassen, dass das Endocannabinoid-System auch die hormonelle Stressantwort erheblich beeinflusst, welche natürlich mit dem Verhalten rückkoppelt (☞ Kap. 2.10.). Auch die verminderte Fähigkeit der *knock-out* Mäuse, aversive Situationen in adäquater Weise wieder zu vergessen, sollte bei der Interpretation des "depressiven" Verhaltens nicht vergessen werden (vgl. Kap. 2.8.).

Als besonders viel versprechend, um pharmakologisch im Bereich der psychiatrischen Störungen einzugreifen, hat sich bisher im Tierversuch eine Substanz erwiesen, die den Abbau von Endocannabinoiden verhindert, und somit die Endocannabinoid-Konzentration im Gehirn besonders in den aktiven Gebieten erhöht. Hier handelt es sich um URB597, ein Inhibitor des Anandamid-abbauenden Enzyms FAAH (vgl. Kap. 1.6.).

URB597 wirkt bei der Ratte in verschiedenen Tests sowohl anxiolytisch als auch antidepressiv und bewirkt keine der bei Agonisten beobachteten, unerwünschten psychotropen Effekte (☞ Tab. 2.2).

Zusammenfassend lässt sich sagen, dass das Endocannabinoid-System unsere Gefühlszustände, sprich Emotionen, merklich beeinflussen kann; und zwar in Abhängigkeit von der Art und Aversivität der Umweltfaktoren, denen wir ausgesetzt sind.

CB1-Rezeptoren sind in solchen Gehirnregionen, die an der emotionalen Verarbeitung von Umweltreizen beteiligt sind, wie Amygdala, Hippocampus und Präfrontalem Cortex, reichlich vorhanden. Man könnte das Endocannabinoid-System als ein generell schützendes System betrachten, das uns nicht nur auf der neuronalen und molekularen Ebene, sondern von daher ausgehend, auch in unserem Verhalten vor emotionalen Überreaktionen bewahrt. Dysregulationen des Systems könnten zu Angst- und Depressionserkrankungen beitragen; bisher gibt es jedoch keine klinischen Studien, die dies zeigen konnten.

2.10. Neuroendokrinologie

Eine wachsende Anzahl von Untersuchungen während der letzten Jahre rückt auch die Rolle des Endocannabinoid-Systems in dem Bereich der Neuroendokrinologie ins Scheinwerferlicht. Inzwischen gilt es als gesichert, dass Endocannabinoide alle bekannten hypothalamisch-hypophysär-endokrinen Achsen mehr oder minder in ihrer Aktivität modulieren können. Obwohl CB1-Rezeptoren in den hypothalamischen Kerngebieten des Gehirns, im Vergleich zu ihrem Vorhandensein z.B. in den Basalganglien und im Hippocampus, nur meist schwach exprimiert sind, so üben

sie dennoch auch dort wichtige Kontrollfunktionen aus. Man findet CB1-Rezeptoren weiterhin auch im Vorderlappen der Hypophyse, beim Menschen vor allem in den corticotrophen und somatotrophen Zellen, und auch in den peripheren endokrinen Organen wie Nebenniere, Schilddrüse, Hoden und Eierstöcken. Vor allem die Rolle des Endocannabinoid-Systems bei der Verarbeitung der Stress-Antwort über die Hypothalamus-Hypophysen-Nebennieren-, die sogenannte HPA-Achse, als auch seine Rolle bei der Regulation der Gonadotropin-Freisetzung, und sein allgemeiner Einfluss auf die Fertilität und das Sexualverhalten sind inzwischen bekannt.

Um ein Beispiel aus der tierexperimentellen Forschung zu nennen: Blockiert man bei Mäusen den CB1-Rezeptor durch die Injektion des CB1-Antagonisten SR141716A und misst Stunden später die Konzentration des Stresshormons Corticosteron unter stressfreien (basalen) Bedingungen, so kann man gegenüber den mit Vehikel behandelten Kontroll-Tieren eine Erhöhung der Hormonausschüttung feststellen (☞ Abb. 2.9). Auch wenn man die Tiere nach der Injektion einem Stressor aussetzt und dann die Plasmakonzentration misst, so kann man einen klaren Unterschied beobachten.
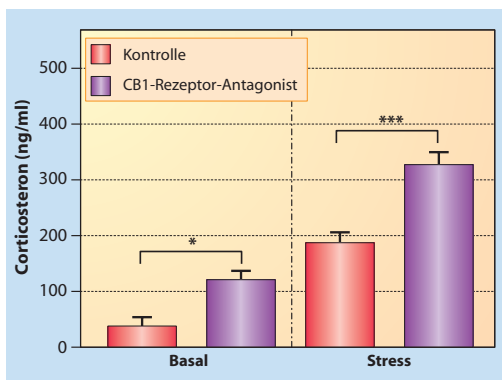
Abb. 2.9: Stresshormon-Ausschüttung in Kontroll- und CB1-Rezeptor-Antagonist-behandelten Mäusen. Plasmacorticosteron-Konzentration unter basalen Bedingungen und nach "*forced swim stress*" in kontrollbehandelten Mäusen und in CB1-Rezeptor-Antagonist-behandelten Mäusen. Signifikanz: *, p<0.05; ***, p< 0.001.

Die Ergebnisse sprechen dafür, dass die HPA-Achse, über welche letztendlich die Corticosteron-

Ausschüttung aus der Nebenniere kontrolliert wird, bereits unter basalen Bedingungen einer Hemmung durch das Endocannabinoid-System unterliegt. Sowohl basal, als auch besonders unter Stress, ist hier das System dafür da, überschießende Reaktionen zu vermeiden und die Hormonausschüttung in adäquate Bereiche zu steuern.

> Hier wird ein allgemein gültiges Prinzip des Endocannabinoid-Systems offenbar: nämlich die Modulation und damit die Regulation der Reaktionen unseres Körpers auf seine Umweltreize, um sicherzustellen, dass diese nicht unkontrolliert zu stark in die eine oder andere Richtung ausschlagen.

Das Endocannabinoid-System spielt folglich eine herausragende Rolle bei der Freisetzung von Hormonen, und dies sollte auch bei dem therapeutischen Einsatz von Pharmaka, die in das Endocannabinoid-System eingreifen, nicht außer Acht gelassen werden.

Danksagung

2.11. Literatur

1. Cohen C, Kodas E, Griebel G (2005) CB-1 receptor antagonists for the treatment of nicotine addiction. Pharmacol Biochem Beh 81:387-395.

2. De Vries TJ, Schoffelmeer AN (2005) Cannabinoid CB-1 receptors control conditioned drug seeking. Trends Pharmacol Sci 26:420-6.

3. Grotenhermen F (2005) Cannabinoids. Curr Drug Targets CNS Neurol Disord 4:507-30.

4. Leweke FM, Gerth CW, Klosterkotter J (2004) Cannabis-associated psychosis: current status of research. CNS Drugs 18:895-910.

5. Lutz B (2004) On-demand activation of the endocannabinoid system in the control of neuronal excitability and epileptiform seizures. Biochem Pharmacol 68:1691-8.

6. Mackie K (2006) Cannabinoid receptors as therapeutic targets. Annu Rev Pharmacol Toxicol 46:101-22.

7. Manzanares J, Uriguen L, Rubio G, Palomo T (2004) Role of endocannabinoid system in mental diseases. Neurotox Res 6:213-24.

8. Pagotto U, Marsicano G, Cota D, Lutz B, Pasquali R (2006) The emerging role of the endocannabinoid Ssy-

stem in endocrine regulation and energy balance. Endocr Rev 27:73-100.

9. Pertwee R; Editor; Cannabinoids. Handbook of Experimental Pharmacology. Volume 168. Springer 2005, Berlin Heidelberg New York.

10. Romero J, Lastres-Becker I, de Miguel R, Berrendero F, Ramos JA, Fernandez-Ruiz J (2002) The endogenous cannabinoid system and the basal ganglia: biochemical, pharmacological, and therapeutic aspects. Pharmacol Therap 95: 137-152

11. Schneider U, Seifert J, Karst M, Schlimme J, Cimander K, Muller-Vahl KR (2005) The endogenous cannabinoid system. Therapeutic implications for neurologic and psychiatric disorders. Nervenarzt 76:1062-72. [Article in German]

12. Stella N.(2004) Cannabinoid signaling in glial cells. Glia 48:267-77.

13. Witkin JM, Tzavara ET, Nomikos GG (2005) A role for cannabinoid CB-1 receptors in mood and anxiety disorders. Behav Pharmacol 16:315-31.

14. Wotjak CT (2005) Role of endogenous cannabinoids in cognition and emotionality. Mini Rev Med Chem 5:659-70.